

University of Alberta

**Ectromelia Virus Encodes A Novel Family Of Ankyrin/F-box Proteins
That Manipulate The SCF Ubiquitin Ligase And NF- κ B Activation**

by

Nicholas John van Buuren

A thesis submitted to the Faculty of Graduate Studies and Research
in partial fulfillment of the requirements for the degree of

Doctor of Philosophy

in

Virology

Medical Microbiology and Immunology

©Nicholas John van Buuren

Spring 2012

Edmonton, Alberta

Permission is hereby granted to the University of Alberta Libraries to reproduce single copies of this thesis and to lend or sell such copies for private, scholarly or scientific research purposes only. Where the thesis is converted to, or otherwise made available in digital form, the University of Alberta will advise potential users of the thesis of these terms.

The author reserves all other publication and other rights in association with the copyright in the thesis and, except as herein before provided, neither the thesis nor any substantial portion thereof may be printed or otherwise reproduced in any material form whatsoever without the author's prior written permission.

I dedicate this document to my amazing families! All three of them!

Abstract:

Ectromelia virus (ECTV) is the causative agent of lethal mousepox, and is highly related to the human pathogen, variola virus, the causative agent of smallpox. Poxviruses contain large dsDNA genomes that encode numerous open reading frames that manipulate cellular signalling pathways. We used bioinformatics to identify a family of four genes encoded by ECTV that contain N-terminal ankyrin repeats in conjunction with a C-terminal F-box domain. The ECTV encoded ankyrin/F-box proteins: EVM002, EVM005, EVM154 and EVM165, all interact with the cellular SCF (Skp1/Cul-1/F-box) ubiquitin ligase complex through an interaction mediated by their C-terminal F-box domain. These four proteins bind to the SCF complex in a similar manner to cellular F-box-containing substrate adaptor proteins. We hypothesize that each of the ECTV encoded ankyrin/F-box proteins recruits a unique family of target proteins to the SCF complex for ubiquitylation. The NF- κ B signalling cascade is an important mediator of innate immunity, and is tightly regulated by ubiquitylation. A critical step in the activation of NF- κ B is the ubiquitylation and degradation of the inhibitor of kappaB (I κ B α), by the cellular SCF ^{β -TRCP} ubiquitin ligase. Upon stimulation with TNF α or IL-1 β , orthopoxvirus-infected cells display an accumulation of phosphorylated I κ B α , indicating that NF- κ B activation is inhibited during poxvirus infection at the point of I κ B α degradation. Since degradation of I κ B α is catalyzed by the SCF ^{β -TRCP} ubiquitin ligase complex we investigated the role of the ECTV encoded ankyrin/F-box proteins in the regulation of NF- κ B activation. Expression of Flag-EVM005 inhibited both I κ B α degradation and p65 nuclear

translocation in response to TNF α or IL-1 β . Regulation of the NF- κ B pathway by EVM005 was dependent on the F-box domain, and interaction with the SCF complex. Additionally, we created ECTV knockout viruses devoid of each of the four ankyrin/F-box genes using a novel “Selectable and Excisable Marker” system. The EVM005 deletion virus was shown to inhibit NF- κ B activation despite lacking the EVM005 open reading frame; however, this virus was attenuated in two mouse strains. The contribution of EVM005 to virulence is therefore independent from its ability to inhibit NF- κ B activation, and is potentially linked to unique target proteins ubiquitylated through the SCF complex during infection.

Acknowledgements

First and foremost, I need to thank my supervisor, Dr. Michele Barry. For two years prior to graduate school, I had worked full time as a carpenter in BC, framing houses for Scott Ogden Construction. I was really good at pounding nails, but my lab skills were lacking and my vocabulary was atrocious. At times, I'm sure that Michele questioned what she had gotten herself into. For some unknown reason, Michele saw potential in me and therefore had the patience to allow my skills to develop within her lab. For this, I will be forever grateful! I feel that I've developed into a real scientist under her mentorship and will take the lessons learned in the Barry lab with me forever.

Next I need to thank my committee members, Dr. Luis Schang and Dr. Mike Schultz. I found these two individuals extremely challenging and thorough, yet supportive at the same time. Thanks so much for everything that you've taught me!

There have been plenty of Barry lab members to remember over the last six years. I'll start with Dr. Brienne Couturier and Dr. John Taylor aka Obiwan. These two were instrumental in teaching me all of the techniques required to be successful in the Barry lab. A big shout out to John for always believing in me and constantly picking me up when I was down. I feel incredibly fortunate to have gone through graduate school from beginning to end with Steph and Logan. These are two of the smartest people that I've ever met, and our friendship is one of the most important things I've gained while in graduate school. Kristin Burles came into the lab as my first 499 student, and has stayed on for graduate school. She continues to make huge contributions to the characterization of the ankyrin/F-box proteins. Kristin is a great friend and her passion for science and work ethic were contagious and something I've always appreciated. To the rest of the Barry lab, thanks for all of the great memories!

Over the past six years, if I wasn't at the lab, I was probably at the Phoenix Gymnastics Center and vice versa. I feel that I've learned as much about coaching trampoline and mentoring athletes as I have about Microbiology and that is a testament to Trish Quinney. What an amazing mentor! Thanks so much for keeping me sane on days I was struggling at school and providing me with such an amazing outlet!

And finally, I wouldn't have gotten this far without my family. I have two of the hardest working parents, John van Buuren and Vivien Symington, who have been the most amazing role models. They've always been there to remind me that stressful times are never as bad as they seem. I love you both and appreciate all that you've done to get me to this point. To all of my siblings, Andrew, Jess, Asia and Hannah, I love you guys and I'm proud to have each one of you in my life! To my wonder girlfriend Krystal, we make an amazing team and I can't wait to see how our future unfolds! Finally, a big thanks to Uncle Gil and Aunt Laurie for all of the ski trips, trips to Mt. Robson, and Sunday dinners! I'm going to miss you guys, stay in touch!

Table of Contents

Chapter 1: Introduction	p.1
1.1 Poxviruses	p.2
1.1.1 Viral Genome	p.6
1.1.2 Poxvirus Entry	p.7
1.1.3 Poxvirus Transcription and DNA Replication	p.10
1.1.4 Variola Virus – The Etiological Agent of Smallpox	p.11
1.1.5 Ectromelia Virus	p.14
1.1.6 Unique Poxvirus Gene Products	p.16
1.2 Ubiquitin	p.19
1.2.1 Ubiquitylation – The Conjugation of Ubiquitin	p.23
1.2.2 Ubiquitin Ligases	p.25
1.2.3 The SCF Ubiquitin Ligase Complex	p.28
1.2.4 Deubiquitylation	p.31
1.2.5 Viruses and The Ubiquitin-Proteasome System	p.33
1.2.6 Poxviruses and The Ubiquitin-Proteasome System	p.36
1.3 The NF- κ B Pathway	p.40
1.3.1 TNF α Mediated NF- κ B Activation	p.46
1.3.2 IL-1 β Mediated NF- κ B Activation	p.47
1.3.3 Alternative Pathways for IKK Activation	p.50
1.3.4 Viral Regulation of the NF- κ B Cascade	p.51
1.3.5 Poxvirus Inhibition of the NF- κ B Cascade	p.54
1.4 The ECTV Encoded Ankyrin/F-box Proteins: Hypothesis	p.57
1.5 References	p.58
Chapter 2: Materials and Methods	p.73
2.1 Cell Culture and Viruses	p.74
2.1.1 Cells	p.74
2.1.2 Viruses	p.74
2.2 Antibodies	p.76
2.3 Cell treatment – Transfection, Infection and Infection/Transfection	p.77
2.3.1 Transfections	p.77
2.3.2 Infections	p.78
2.3.3 Infection/Transfections	p.78
2.4 Bioinformatics	p.79
2.4.1 Alignments	p.79
2.5 Cloning	p.79
2.5.1 Previously Described Plasmids	p.79

2.5.2	Subcloning Vectors	p.80
2.5.2.1	Cloning into pGEMT	p.80
2.5.2.2	Gateway Subcloning Vectors	p.89
2.5.2.3	Generation of Codon Optimized Ankyrin/F-box constructs	p.90
2.5.3	Expression Vectors	p.95
2.5.4	Generation of Recombinant Vaccinia Viruses	p.96
2.5.5	pDGloxP-KO Vectors For Ectromelia Virus Recombinants	p.98
2.5.6	Generation of Recombinant Ectromelia Viruses	p.99
2.6	Assays	p.102
2.6.1	Immunoprecipitations	p.102
2.6.2	Western Blots	p.104
2.6.3	Mass Spectrometry	p.105
2.6.4	Confocal Microscopy	p.106
2.6.5	Cytoplasmic and Nuclear Extracts	p.107
2.6.6	Flow Cytometry	p.108
2.6.7	Growth Curve Analysis of Recombinant ECTVs	p.109
2.6.8	Real Time PCR	p.110
2.7	Infection of Mice with ECTV Knockout Viruses	p.110
2.8	References	p.113
Chapter 3: ECTV Encodes a Novel Family of Ankyrin/F-box Proteins That Interact with the SCF Complex		p.115
3.1	Introduction	p.116
3.2	Ectromelia Virus Encodes Four Ankyrin Repeat/F-box Proteins	p.118
3.3	EVM005 Interacts with HA-cullin-1 During Infection	p.121
3.4	EVM005 Interacts with Components of the SCF Complex in an F-box-Dependent Manner	p.127
3.5	EVM005 Associates with an Active SCF Ubiquitin Ligase Complex	p.131
3.6	EVM002 and EVM154 Contain F-box Domains and Interact with Skp1	p.135
3.7	Discussion	p.140
3.8	References	p.146
Chapter 4: Creation of ECTV Recombinant Viruses Using the Selectable and Excisable Marker System		p.150
4.1	Introduction	p.151
4.2	Deletion of EVM002 and EVM005 from ECTV Strain Moscow Using the Selectable and Excisable Marker System	p.154

4.3 Characterization of YFP Fluorescence in ECTV Recombinant Viruses	p.156
4.4 Characterization of Recombinant ECTV Genomes by PCR Analysis	p.157
4.5 Analysis of ECTV- Δ 002 and ECTV- Δ 005 Growth	p.162
4.6 Deletion of Multiple Genes from the Left End of the ECTV Genome	p.162
4.7 Discussion	p.167
4.8 References	p.172
Chapter 5: Ectromelia Virus Encoded EVM005 Inhibits NF-κB Signalling Through Manipulation of the SCF Ubiquitin Ligase Complex.	p.175
5.1 Introduction	p.176
5.2 ECTV Infection Leads to an Accumulation of Phospho-I κ B α and Inhibition of NF- κ B Activation	p.177
5.3 Flag-EVM005 Inhibits Nuclear Accumulation of p65 in an F-box Dependent Manner	p.182
5.4 EVM005 Inhibits TNF α - and IL-1 β -Induced I κ B α Degradation.	p.189
5.5 ECTV- Δ 005 Inhibits p65 Nuclear Accumulation and Synthesis of NF- κ B Regulated Transcripts	p.193
5.6 ECTV- Δ 005 Inhibits I κ B α Degradation	p.196
5.7 EVM005 is Required for Virulence	p.199
5.8 Discussion	p.202
5.9 References	p.205
Chapter 6: EVM002, EVM154 and EVM165 Encoded Ankyrin/F-box Proteins That Inhibit NF-κB Activation.	p.208
6.1 Introduction	p.209
6.2 ECTV Ankyrin/F-box Proteins Inhibit TNF α and IL-1 β Induced p65 Nuclear Accumulation in an F-box Dependent Manner	p.211
6.3 Flag-EVM002 Inhibits I κ B α Degradation in an F-box Dependent Manner	p.218
6.4 ECTV- Δ 002 Inhibits NF- κ B Activation	p.221
6.5 ECTV- Δ 002-005 Inhibits I κ B α Degradation	p.226
6.6 Discussion	p.229
6.7 References	p.233

Chapter 7: Discussion	p.236
7.1 Poxviral Ankyrin/F-box Proteins	p.237
7.2 Poxviruses Require A Functional Ubiquitin-Proteasome System For Replication	p.245
7.3 Creation of Marker-Free Recombinant Poxviruses Using SEM	p.246
7.4 Regulation of NF- κ B by Poxvirus Encoded Ankyrin/F-box Proteins	p.249
7.5 Substrate Identification for ECTV Encoded Ankyrin/F-box Proteins	p.255
7.6 Conclusion	p.260
7.7 References	p.261
Appendix A: Construction of a Large Deletion ECTV Lacking 17 ORFs at the Right-hand End of the Genome	p.268
A.1 Deletion of Multiple Genes from the Right-End of the ECTV Genome.	p.269
Appendix B: Supplementary Data	p.273

List of Tables

Chapter 2: Materials and Methods

Table 2.1 – EVM005 Construct Primers	p.81
Table 2.2 – EVM002 Construct Primers	p.82
Table 2.3 – EVM154 Construct Primers	p.83
Table 2.4 – EVM165 Construct Primers	p.84
Table 2.5 – EVM004 Construct Primers	p.84
Table 2.6 – Cellular Gene Construct Primers	p.84
Table 2.7 – EVM005 Subcloning Vectors	p.85
Table 2.8 – EVM002 Subcloning Vectors	p.86
Table 2.9 – EVM154 Subcloning Vectors	p.86
Table 2.10 – EVM165 Subcloning Vectors	p.87
Table 2.11 – EVM004 Subcloning Vectors	p.87
Table 2.12 – Subcloning Vectors for Cellular Genes	p.87
Table 2.13 – EVM005 Expression Vectors	p.91
Table 2.14 – EVM002 Expression Vectors	p.92
Table 2.15 – EVM154 Expression Vectors	p.92
Table 2.16 – EVM165 Expression Vectors	p.93
Table 2.17 – EVM004 Expression Vectors	p.93
Table 2.18 – Cellular Gene Expression Vectors	p.94
Table 2.19 – Vaccinia Virus Recombinants	p.97
Table 2.20 – Ectromelia Virus Knockout Plasmids	p.100
Table 2.21 – Ectromelia Virus Recombinants and Knockouts	p.103
Table 2.22 – Real-Time PCR Primers	p.111

List of Figures

Chapter 1: Introduction.

Figure 1.1 - Structure of the poxvirus virion and virus factory.	p.3
Figure 1.2 - Poxvirus phylogenetic tree.	p.4
Figure 1.3 - The <i>Orthopoxvirus</i> genus.	p.5
Figure 1.4 - Poxvirus life cycle.	p.8
Figure 1.5 - Structure of ubiquitin.	p.21
Figure 1.6 - Conjugation of ubiquitin.	p.22
Figure 1.7 - The cellular cullin/RING ubiquitin ligase family.	p.27
Figure 1.8 - The NF- κ B family of transcription factors.	p.41
Figure 1.9 - The inhibitor of κ B family of proteins.	p.42
Figure 1.10 - The TNF α induced NF- κ B activation signalling cascade.	p.44
Figure 1.11 - The IL-1 β induced NF- κ B activation signalling cascade.	p.45
Figure 1.12 - Intracellular inhibitors of NF- κ B activation.	p.55

Chapter 3: ECTV Encodes a Novel Family of Ankyrin/F-box Proteins That Interact with the SCF Complex.

Figure 3.1 - Ectromelia virus encodes four ankyrin-repeat/F-box proteins.	p.119
Figure 3.2 - Ectromelia virus strain Moscow encodes four ankyrin/F-box proteins.	p.120
Figure 3.3 - EVM005 associates with human cullin-1 during infection.	p.122
Figure 3.4 - EVM005 interacts with HA-cullin-1 during infection.	p.124
Figure 3.5 - Localization of ectopically expressed cullin-1 and EVM005.	p.125
Figure 3.6 - Flag-EVM005 co-localizes with HA-cullin-1 during infection.	p.126
Figure 3.7 - EVM005 interacts with endogenous components of the SCF ubiquitin ligase.	p.128
Figure 3.8 - EVM005 F-box domain required for interaction with the SCF complex.	p.130
Figure 3.9 - EVM005 fails to interact with HA-cullin-1 Δ N53.	p.132
Figure 3.10 - EVM005 associates with conjugated ubiquitin.	p.134
Figure 3.11 - EVM005 co-localizes with conjugated ubiquitin.	p.136
Figure 3.12 - EVM002 and EVM154 interact with Skp-1.	p.138
Figure 3.13 - All ECTV encoded ankyrin/F-box proteins require F-box domain to interact with Skp1.	p.139
Figure 3.14 - EVM002 and EVM154 interact with conjugated ubiquitin.	p.141
Figure 3.15 - EVM002 and EVM154 co-localize with conjugated ubiquitin.	p.142

Chapter 4: Creation of ECTV Recombinant Viruses Using the Selectable and Excisable Marker System.

Figure 4.1 - Schematic of the Selectable and Excisable Marker System for deletion of EVM002.	p.155
Figure 4.2 - Detection of ECTV expressed YFP-GPT fusion proteins by immunofluorescence.	p.158
Figure 4.3 - Detection of ECTV expressed YFP-GPT fusion proteins by flow cytometry.	p.159
Figure 4.4 - PCR analysis of viral genomes.	p.160
Figure 4.5 - Multi-step growth curve analysis of ECTV recombinant viruses.	p.163
Figure 4.6 - Schematic for construction of ECTV- Δ 002-005.	p.165
Figure 4.7 - PCR analysis of viral genomes to verify construction of ECTV- Δ 002-005.	p.166

Chapter 5: Ectromelia Virus Encoded EVM005 Inhibits NF- κ B Signalling Through Manipulation of the SCF Ubiquitin Ligase Complex.

Figure 5.1 - ECTV infection inhibits I κ B α degradation	p.179
Figure 5.2 - ECTV infection inhibits TNF α induced nuclear accumulation of p65.	p.180
Figure 5.3 - ECTV infection inhibits IL-1 β induced nuclear accumulation of p65.	p.181
Figure 5.4 - ECTV infection prevents TNF α induced p65 nuclear translocation in HeLa and MEF cells.	p.183
Figure 5.5 - ECTV infection prevents IL-1 β induced p65 nuclear translocation in HeLa and MEF cells.	p.184
Figure 5.6 - Flag-EVM005 inhibits TNF α induced p65 nuclear accumulation in an F-box dependent manner.	p.186
Figure 5.7 - Flag-EVM005 inhibits IL-1 β induced p65 nuclear accumulation in an F-box dependent manner.	p.187
Figure 5.8 - Quantification of p65 nuclear accumulation in cells transfected with Flag-EVM005 and Flag-EVM005(1-593).	p.188
Figure 5.9 - Flag-EVM005 inhibits TNF α induced I κ B α degradation.	p.190
Figure 5.10 - EVM005 requires the C-terminal F-box domain to inhibit TNF α and IL-1 β induced I κ B α degradation.	p.192
Figure 5.11 - ECTV- Δ 005 inhibits TNF α induced p65 nuclear accumulation.	p.194

Figure 5.12 - ECTV-Δ005 inhibits TNFα induced p65 nuclear accumulation.	p.195
Figure 5.13 - ECTV-Δ005 inhibits the production of NF-κB regulated transcripts.	p.197
Figure 5.14 - ECTV-Δ005 inhibits TNFα induced IκBα degradation.	p.198
Figure 5.15 - ECTV-Δ005 is attenuated in C57BL/6 and A/NCR mice.	p.200

Chapter 6: EVM002, EVM154 and EVM165 Encoded Ankyrin/F-box Proteins That Inhibit NF-κB Activation.

Figure 6.1 - All ECTV encoded ankyrin/F-box proteins inhibit TNFα induced p65 nuclear accumulation.	p.212
Figure 6.2 - All ECTV encoded ankyrin/F-box proteins inhibit IL-1β induced p65 nuclear accumulation.	p.214
Figure 6.3 - Nuclear translocation of p65 in cells expressing the ECTV encoded ankyrin/F-box proteins.	p.215
Figure 6.4 - All ECTV encoded ankyrin/F-box proteins require an F-box domain to inhibit TNFα induced p65 nuclear accumulation.	p.216
Figure 6.5 - All ECTV encoded ankyrin/F-box proteins require an F-box domain to inhibit IL-1β induced p65 nuclear accumulation.	p.217
Figure 6.6 - Nuclear translocation of p65 in cells expressing the ECTV encoded ankyrin/F-box proteins with truncated or mutated F-box domains.	p.219
Figure 6.7 - Flag-EVM002 inhibits the degradation of IκBα in an F-box dependent manner.	p.220
Figure 6.8 - ECTV-Δ002 inhibits p65 nuclear accumulation.	p.222
Figure 6.9 - ECTV-Δ002 inhibits p65 nuclear accumulation following TNFα stimulation.	p.223
Figure 6.10 – ECTV and ECTV-Δ002 inhibit the production of NF-κB regulated transcripts.	p.225
Figure 6.11 – ECTV and ECTV-Δ002 infection prevents IκBα-p65/p50 dissociation.	p.227
Figure 6.12 - ECTV-Δ002 and ECTV-Δ002-005 inhibit TNFα induced IκBα degradation.	p.230

Chapter 7: Discussion.

Figure 7.1 - The ECTV encoded ankyrin/F-box proteins function as substrate adaptors for the cellular SCF complex. p.243

Figure 7.2 - The ECTV encoded ankyrin/F-box proteins inhibit NF- κ B activation through manipulation of the SCF ubiquitin ligase. p.256

Appendix A: Construction of a Large Deletion ECTV Lacking 17 ORFs at the Right-hand End of the Genome

A.1 - Schematic for construction of ECTV large deletion virus. p.271

A.2 - PCR analysis of ECTV large deletion viral genomes. p.272

Appendix B: Supplementary Data

B.1 - Multiple proteasome inhibitors block late protein expression in vaccinia virus. p.274

List of Definitions

ABSL-3 – Animal biosafety level 3
ADP – Adenine diphosphate
ATCC – American type culture collection
BGMK – Baby green monkey kidney cell line
BME – β -mercaptoethanol
bp – Base pairs
BrdU – Bromo-deoxy-uridine
BSA – Bovine serum albumin
BSL-2 – Biosafety level 2 containment
BTB – Bric-a-brack/tram-track/broad complex protein domain
CDC – Center for disease control
CDK – Cyclin-dependent kinase
CEF – Chicken embryo fibroblast cells
CHO – Chinese hamster ovary cells
CHOhr – CHO cell host range factor encoded by CPXV
CMC – Carboxy-methyl cellulose
CMLV – Camelpox virus
CPXV – Cowpox virus strain Brighton red
CSN – COP9 signalosome
DAPI - 4',6-diamino-2-phenylindole
DIGE – Differential in gel expression
DMEM – Dulbecco's modified eagle medium
DNA – Deoxyribonucleic acid
DTT – Dithiothreitol
DUB – Deubiquitylating enzyme
E1 – Ubiquitin activating enzyme
E2 – Ubiquitin conjugating enzyme
E3 – Ubiquitin ligase
EBV – Epstein-Barr virus
ECL – Enhanced chemiluminescence
ECTV – Ectromelia virus strain Moscow
EDTA – Ethylenediaminetetraacetic acid
EGFP – Enhanced green fluorescent protein
EGTA – Ethylene glycol tetraacetic acid
FBS – Fetal bovine serum
FDA – Food and drug administration
FTICR – Fourier transform ion cyclotron resonance
GAPDH – Glyceraldehyde 3-phosphate dehydrogenase

GFP – Green fluorescent protein
GM-CSF – Granulocyte-macrophage colony-stimulating factor
GPT – Guaninine phospho-ribosyl transferase
GST – Glutathione S-transferase
HA – Hemagglutinin
HBV – Hepatitis B virus
HEK – Human embryonic kidney cell line
HIV – Human immunodeficiency virus
HPRT – Hypoxanthine-guanine phosphoribosyl transferase
HRP – Horse radish peroxidase
HSPV – Horsepox virus
HTLV-1 – Human T-lymphotrophic virus
HUL1 – Herpes virus ubiquitin ligase 1
IFN- Interferon
I κ B α – Inhibitor of kappa B alpha
IKK – Inhibitor of kappa B kinase
IL-1 β - Interleukin 1 beta
IL-1R – Interleukin 1 receptor
IL-6 – Interleukin 6
IP – Immunoprecipitate
IPTG – Isopropyl- β -D-1-thiogalactopyranoside
ITR – Inverted Terminal Repeat
IVIS – *In vivo* imaging system
JAMM - JAB1/MPN/MOV34 metalloenzymes
kDa – Kilodalton
kbp – Kilo base pairs
KLH – Keyhole limpet hemocyanin
LB – Luria-Bertani broth
LD₅₀ – Dose of virus which kills 50% of infected animals
LRR – Leucine rich repeat
MEF – Mouse embryonic fibroblast cell line
MFI – Mean fluorescence intensity
MOI – Multiplicity of infection
MPA – Mycophenolic acid
MPXV – Monkeypox virus
MVA – Modified vaccinia ankara
NBS – New born calf serum
NEMO – Nuclear factor kappa B essential modifier
NF- κ B – Nuclear factor kappa B
NK – Natural killer cells

NKC – The natural killer complex, a set of NK cell specific genes
ORF – Open reading frame
PARP – Poly(ADP-ribose) polymerase
PBS – Phosphate buffered saline
PCR – Polymerase chain reaction
PFU – Plaque forming units
PMA – Phorbol myristate acetate
RING – Really interesting new gene protein domain contains active ubiquitin
ligase activity
RNA – Ribonucleic acid
RPXV – Rabbitpox virus
RR – Ribonucleotide reductase
RT-PCR – Real time polymerase chain reaction
SCF – Skp1/Cul-1/F-box ubiquitin ligase complex
SDS – Sodium dodecyl sulphate
SDS-PAGE – SDS polyacrylamide gel electrophoresis
SEM – Selectable and excisable marker system
SILAC – Stable isotope labelling of amino acids in cell culture
SOC – Super optimal broth with catabolite repression
SOCS – Suppressor of cytokine signalling protein domain
SSC – Sterile sodium citrate
TAD – Transcriptional activation domain
TATV – Taterapox virus
TBS – Tris buffered saline
TBST – Tris buffered saline containing Tween-20
THP-1 – Human acute monocytic leukemia cell line
TIR – Toll and IL-1 receptor domain
TK – Thymidine kinase
TLR – Toll-like receptor
TNF α – Tumor necrosis factor alpha
TNFR – Tumor necrosis factor receptor
Ub – Ubiquitin
UBA – Ubiquitin associated domains
UBD – Ubiquitin binding domains
UCH – Ubiquitin C-terminal hydrolase
UIM – Ubiquitin interacting motif
USP – Ubiquitin specific protease
vIL-1R – Virally encoded interleukin 1 receptor
vTNFR – Virally encoded tumor necrosis factor receptor
VARV – Variola virus

VVCop – Vaccinia virus strain Copenhagen

WB – Western blot analysis

WD40 – Protein domain consisting of repeats that mediate protein-protein interactions

WHO – World health organization

X-gal - Bromo-chloro-indolyl-galactopyranoside

YFP – Yellow fluorescent protein

YFP-GPT – Yellow fluorescent protein (YFP) – Guanine phospho-ribosyl transferase (GPT) fusion protein

Chapter 1: Introduction

1.1 Poxviruses

Poxviruses are large double stranded DNA viruses that replicate exclusively in the cytoplasm of their host cells (114). Poxviruses genomes range in size from 134 kbp in the *Parapoxviruses* to over 350 kbp in the *Avipoxviruses*. The DNA genome is enclosed in a dumbbell-shaped capsid, a characteristic feature of poxvirus morphology (Figure 1.1A). The capsid is wrapped with one or more lipid envelopes to produce a brick-shaped virion characteristic of all poxviruses (Figure 1.1B)(114). The *Poxviridae* are classified into two subfamilies: the *Chordopoxvirinae*, which infect vertebrate hosts, and the *Entomopoxvirinae*, which infect invertebrates (Figure 1.2)(92). The *Chordopoxvirinae* are subdivided into eight genera: *Orthopoxvirus*, *Parapoxvirus*, *Avipoxvirus*, *Capripoxvirus*, *Leporipoxvirus*, *Suipoxvirus*, *Molluscipoxvirus*, and *Yatapoxvirus* (Figure 1.2)(92). Of these eight genera, the *Orthopoxviruses* are the most extensively studied (Figure 1.3A)(55). The *Orthopoxvirus* genus contains the historically important variola virus (VARV), the etiological agent of smallpox, which to this day remains one of the most lethal viruses in human history (55). Additionally, the *Orthopoxvirus* genus contains vaccinia virus (VV), the virus used to vaccinate and eventually eradicate variola virus (114), cowpox virus (CPXV), the original smallpox vaccine developed by Dr. Edward Jenner (80), as well as monkeypox virus (MPXV), the causative agent of a recent zoonosis in the United States (125), and ectromelia virus (ECTV), the causative agent of mousepox, a lethal disease of mice. With the recent outbreak of both MPXV and



Figure 1.1. Structure of the poxvirus virion and virus factory. **A.** Poxvirus dsDNA genomes are enclosed in a dumbbell-shaped capsid, characteristic of all poxviruses. **B.** Electron micrograph of the VV capsid. The capsid is wrapped in a number of membranes to produce a brick-shaped virion, a hallmark of poxvirus morphology. **C.** Poxviruses are unique amongst DNA viruses in that they replicate in the cytoplasm of infected cells in “virus factories”. Shown is a HeLa cell infected with VV for 12 hours, which was fixed and stained with DAPI and visualized by confocal microscopy.

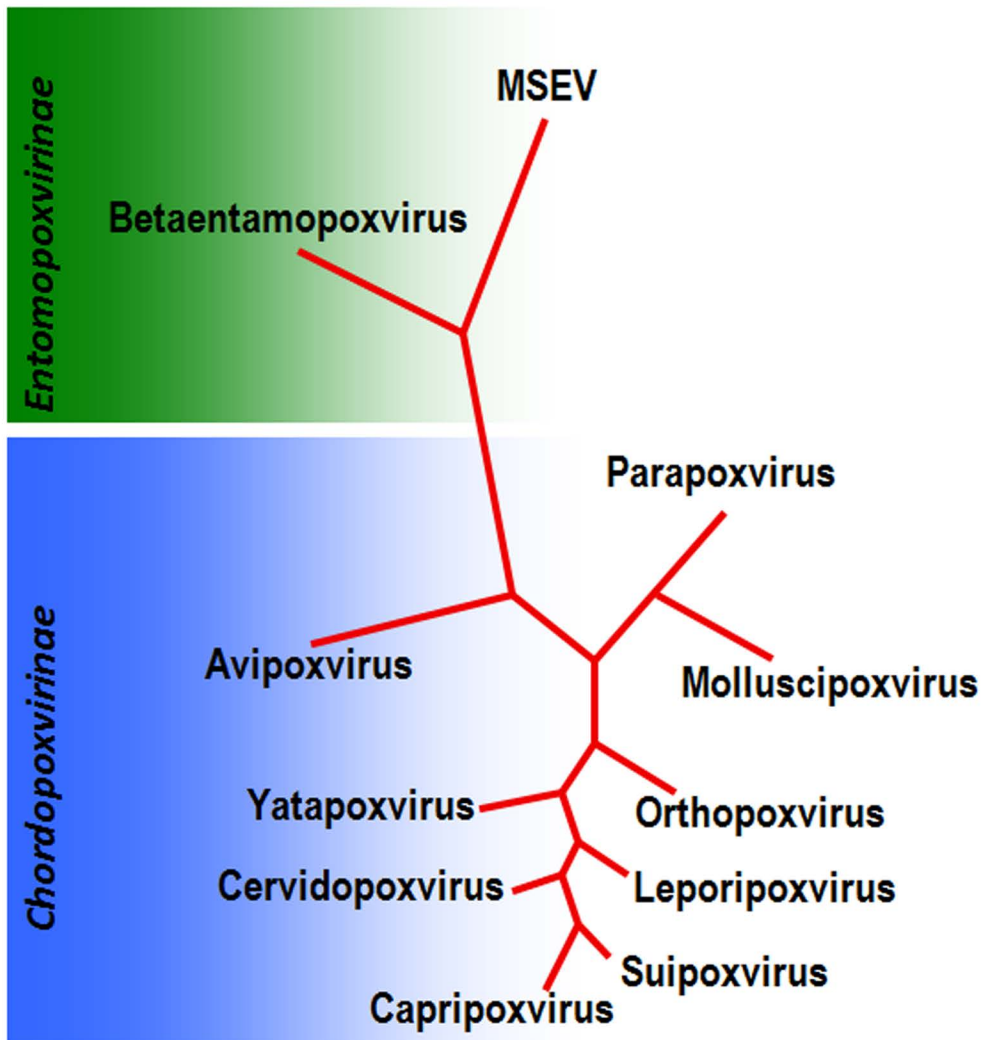


Figure 1.2. Poxvirus phylogenetic tree. Poxviruses are large dsDNA viruses that infect a variety of vertebrate and invertebrate hosts. The *Entomopoxvirinae* family is composed of viruses that specifically infect invertebrate hosts including insects. The *Chordopoxvirinae* family infect vertebrates including a large number of mammalian hosts. The *Orthopoxvirus* genus contains many poxviruses that are human pathogens including variola virus, the causative agent of smallpox, vaccinia virus, the virus used to vaccinate against smallpox, and the zoonotic viruses, monkeypox virus and cowpox virus. Additionally, ectromelia virus is in the *Orthopoxvirus* genus and causes a lethal disease in mice. Adapted from (92).

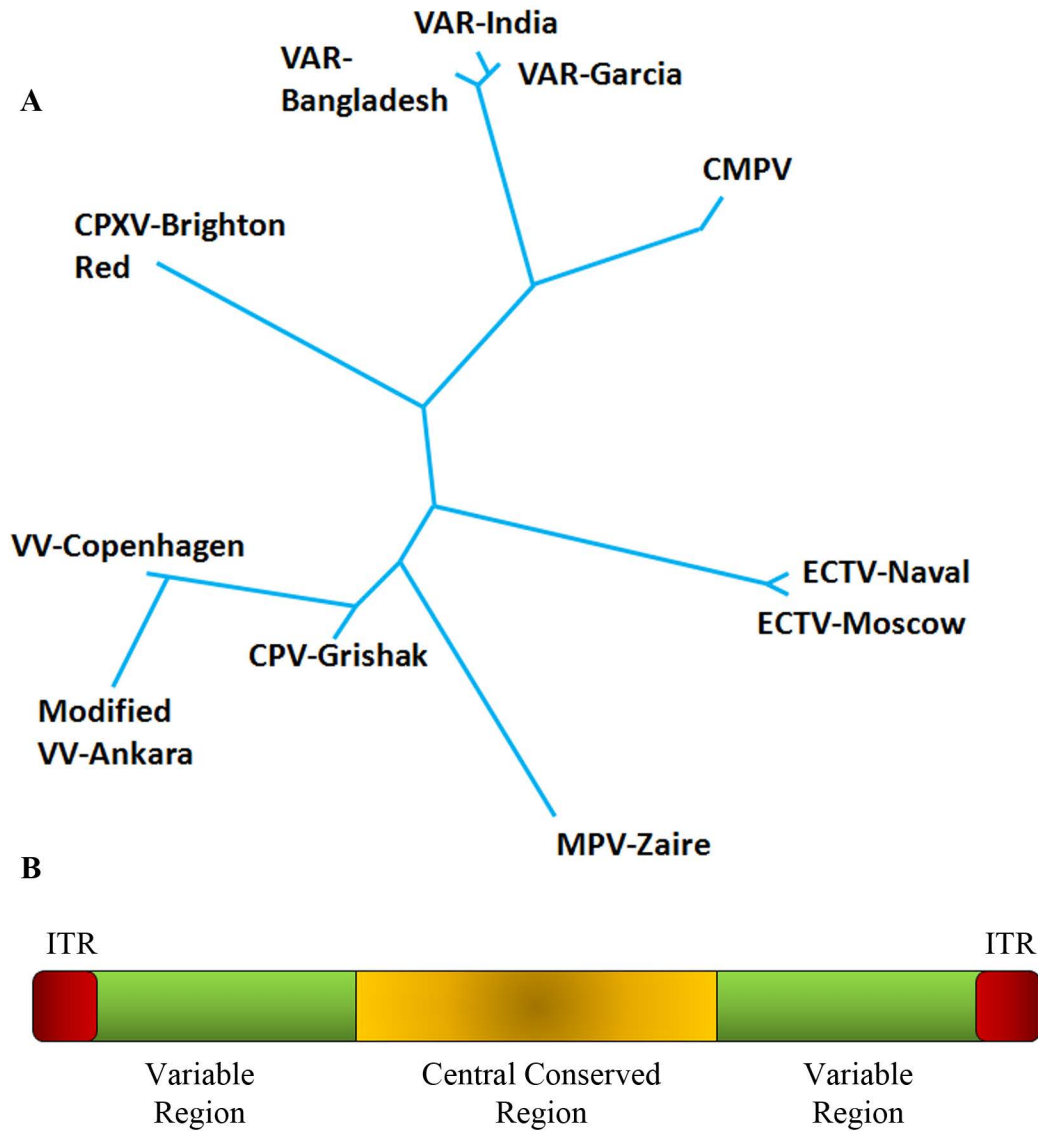


Figure 1.3. The *Orthopoxvirus* genus. **A.** The *Orthopoxviruses* are a genus of poxviruses that infect mammalian hosts. Variola virus is the causative agent of the highly lethal human disease smallpox, and vaccinia virus was used to vaccinate against smallpox. Both monkeypox virus and cowpox virus have caused recent zoonotic infections in humans. Camelpox virus is the closest relative to variola virus and causes smallpox-like symptoms in camels. Ectromelia virus is a poxvirus that causes a smallpox-like infection in susceptible mouse strains. Adapted from (55). **B.** The genome of *Orthopoxviruses* contains a central conserved region, consisting of genes essential for virus replication and virion morphology. The terminal variable regions contain many host range and immunoregulatory genes specific to each virus. The genome also contains an inverted terminal repeat (ITR) region that contains a 100bp sequence required for resolution of concatameric structures, an A/T rich closed hairpin loop region at each termini, and several open reading frames that are replicated at each end.

CPXV zoonoses in North America (125, 175) mousepox serves a good animal model for the study of anti-poxvirus drugs and poxvirus-host interactions.

1.1.1 Viral Genome

Poxvirus genomes range in size from 134 kbp to over 350 kbp of dsDNA with a closed hairpin loop of AT rich DNA at each end encoding over 320 unique gene products. Most poxvirus genes are non-overlapping and are typically arranged in clusters oriented towards the nearest end of the genome. The genome contains inverted terminal repeats (ITR) of identical DNA sequences at each end of the viral genome (Figure 1.3B)(114). The ITR region consists of an AT-rich DNA hairpin that links both strands of DNA, a highly conserved 100 bp sequence required for the resolution of concatameric structures following DNA replication, and several open reading frames (114). The genes located in the ITR are present as exact copies oriented in opposite directions at either end of the genome. All other open reading frames (ORF) within the genome tend to be organized by their degree of conservation. Poxvirus genomes contain a central conserved region within the genome that encodes the majority of transcription factors, polymerases, structural proteins and essential enzymes (Figure 1.3B)(92). This central conserved region contains almost 100 genes conserved throughout the *Orthopoxvirus* genus, of which, almost 50 are conserved in all poxviruses (55, 92). The terminal variable regions of the genome contain ORFs that are unique to each virus and drive the unique host range of each species (Figure 1.3B)(102, 150). Within the variable region are many immune-modulators, host range

factors, and other factors that mediate unique virus-host interactions. No gene located in the variable region of *Orthopoxvirus* genomes is conserved in all *Orthopoxviruses* (55, 92). The largest of the *Orthopoxvirus* genus is CPXV that encodes one copy of all variable genes encoded by other members of the *Orthopoxvirus* genus, and is likely the closest relative to the ancestral *Orthopoxvirus* (92). Other members of the *Orthopoxvirus* genus have likely arisen from gene deletion events, and the unique repertoire of host range factors that remain has generated a new species with modified host range for a new mammalian host (92).

1.1.2 Poxvirus Entry

Until recently the mechanism that poxviruses use to enter cells remained unclear and was complicated by the lack of a known poxvirus receptor. Research in this area is also complicated by the existence of two infectious forms of virus: intracellular mature virions (MV) and extracellular enveloped virions (EV)(114). EV particles contain one additional membrane with unique embedded proteins. Historically, there has been much debate about the number of membranes wrapping each type of virion. Current data support a single lipid bilayer wrapping the MV particle, while the EV is wrapped in two (Figure 1.4)(115). MV particles undergo the addition of a double membrane at either the trans-Golgi network or the endosomal cisternae to produce a wrapped virion (WV)(Figure 1.4)(146, 171). The WV particle travels along microtubules to the plasma membrane where the WV outer membrane fuses to release an EV particle (115). The EV particles

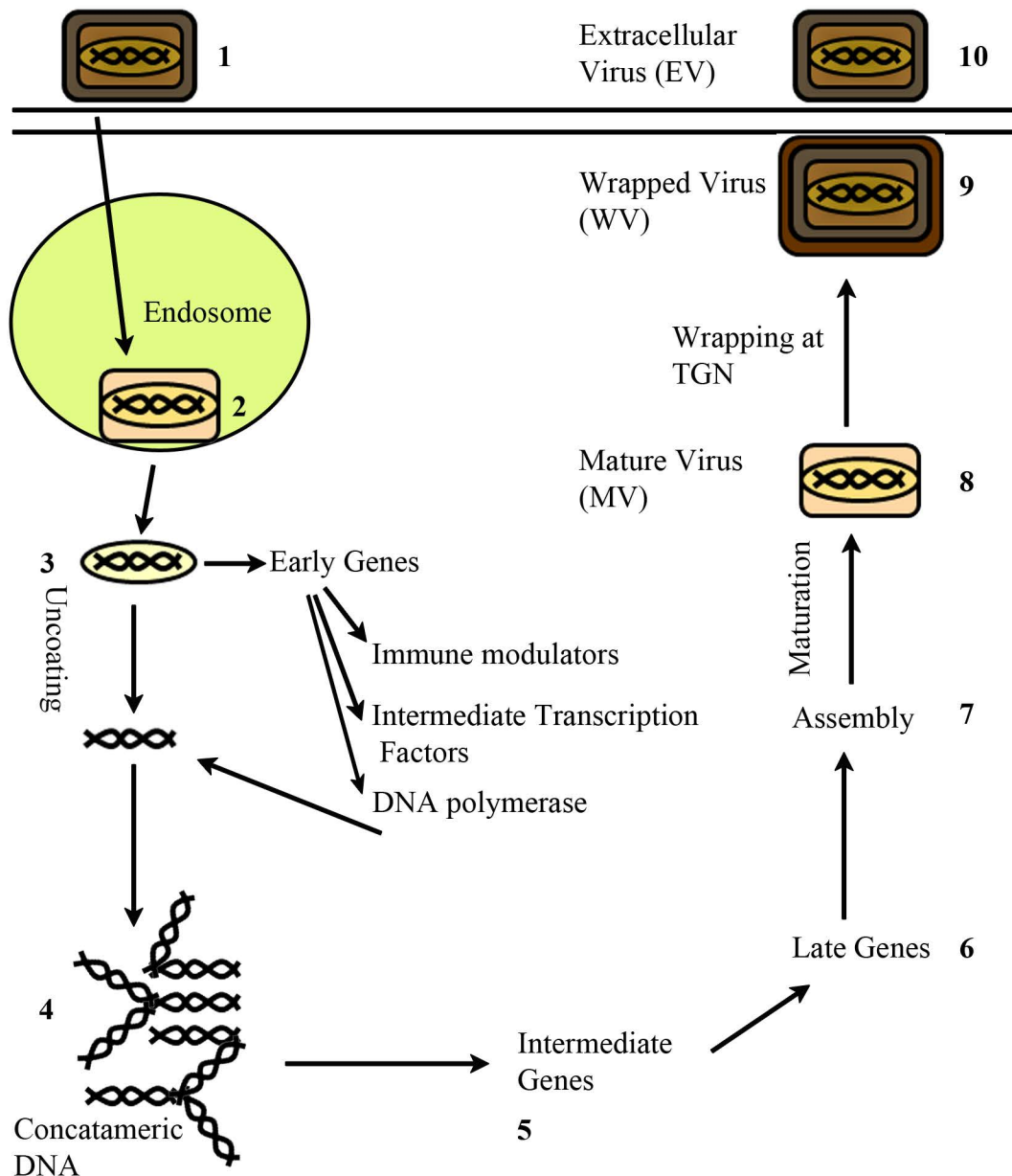


Figure 1.4. Poxvirus life cycle. 1. The poxvirus core is wrapped in two lipid bilayers, with the entry/fusion complex located on the inner membrane. Upon binding to the cell, the entry/fusion complex becomes exposed through loss of the outer membrane and the virion is taken into the cell by macropinocytosis. 2. The remaining viral membrane fuses with the endosomal membrane to release the core particle into the cytoplasm. 3. Early genes are transcribed prior to uncoating. DNA replication occurs in the cytoplasm in viral factories, and produces large concatameric DNA structures (4) which are resolved by late genes. 7. Immature virions are assembled with discrete crescent shaped membranes of unknown origin. 8/9. Following maturation, the virion is wrapped at the trans-golgi network or endosomal cisternae in an additional double membrane. 10. The outer membrane fuses with the plasma membrane to release extracellular virus particles wrapped in two membranes.

again come in two forms: virions that remain cell associated and those that are released for long distance spread (114). Cell associated EV particles are important for cell to cell spread, as these particles are pushed into neighboring cells by actin projections (114).

The majority of research on poxvirus entry has been performed using VV, the prototypical poxvirus. VV contains an entry/fusion complex on the MV outer membrane, consisting of A21, A28, H2 and L5, that mediates fusion of this membrane with host membranes (114, 115, 152). This fusion event leads to internalization of the VV core into the cytoplasm, at which point initiation of viral replication occurs. EV particles contain a distinct set of membrane proteins on their surface, and it is thought that the EV must shed its extra membrane in order to enter a new cell (115, 152). To date, the mechanism with which EV shed their outer membrane is not understood. However, the entry/fusion complex exists on the MV outer membrane, and therefore, loss of the EV outer membrane is mandatory to expose this complex, and allow poxvirus entry to take place. Whether the MV particles fuse at the plasma membrane or within endosomes has also been highly debated with evidence supporting both arguments (38, 156). Recently strong evidence supports a mechanism for VV entry involving macropinocytosis and apoptotic mimicry (106, 107)(Figure 1.4). The authors argue that VV infected cells undergo apoptosis at late times post infection, resulting in the incorporation of phosphatidylserine into MV membranes. The data suggest that VV is recognized through the phosphatidylserine receptor and

taken up by macropinocytosis, followed by fusion within endosomal membranes leading to release of the VV core into the host cytoplasm (106).

1.1.3 Poxvirus Transcription and DNA Replication

Poxvirus gene transcription is divided into three phases termed early, intermediate and late gene transcription, the DNA replication phase occurs between the early and intermediate phases (Figure 1.4)(114). In this cascade, each of the three phases encodes essential transcription factors required to initiate the next round of transcription. Upon release of the poxvirus core into the host cytoplasm, early transcription begins immediately as early transcription factors and RNA polymerases are packaged within the virion core (114). The early gene transcription phase promotes the synthesis of many immune-modulators as well as growth factors, host range factors, intermediate gene transcription factors and genes involved in DNA replication (Figure 1.4). The synthesis of early transcripts can be detected as early as 20 minutes post infection and continues for roughly 4 hours. Termination of the early transcription phase coincides with core disassembly, when exposure of viral genomes to the cytoplasm initiates the DNA replication phase.

Upon synthesis of DNA replication enzymes and disassembly of the viral core, the viral genome is copied a number of times, producing a large concatameric structure of fused viral genomes (Figure 1.4)(114). The onset of DNA replication varies depending on the virus species and cell type, but typically is detected between 1 to 2 hours post infection (114). The concatameric structures

are visible by microscopy as perinuclear DNA rich regions within the cytoplasm of infected cells that fluoresce when stained with DAPI. These areas are referred to as ‘virus factories’, and each infecting particle and corresponding genome has the capability to initiate its own factory (Figure 1.1C). The concatameric DNA structures are resolved into unit length genomes by proteins encoded by late genes. The production of progeny unit length viral genomes therefore occurs at late times post infection, coinciding with the generation of progeny virions.

The intermediate gene transcription phase includes only a small subset of genes. In VV, only five intermediate genes have been identified, of which three encode late gene transcription factors (114). Late gene transcripts can be detected as early as 3 hours post infection and continue to be detected through the end of the virus life cycle. Late gene products include structural proteins involved in virion assembly, early transcription factors, RNA polymerase, transcript capping and methylation enzymes, polyA polymerase and topoisomerases. All of these proteins are packaged into virions and required to initiate early transcription in the next host cell (114). Following the synthesis of late proteins, the concatameric DNA structures are resolved to produce unit length viral genomes that are packaged into capsids and wrapped in a membrane to complete the virus life cycle.

1.1.4 Variola Virus – The Etiological Agent of Smallpox

Poxviruses are well known due to one infamous member, variola virus, the causative agent of the human disease, smallpox. Smallpox is an ancient disease,

possibly dating back over 5000 years, as smallpox-like lesions have been found on the remains of Egyptian mummies (154). Smallpox causes a characteristic rash with the formation of pustules or “pox” on the skin. These smallpox pustules typically originate at the extremities and through the course of disease progress to the torso of infected individuals (30). Two strains of variola virus existed, variola virus major and variola virus minor, the major strain being more pathogenic (30). Although mortality rates varied, rates rose as high as 40% in certain outbreaks of variola virus major. Due to the extremely high mortality rate, it is estimated that smallpox has resulted in between 300-500 million deaths in the 20th century alone (46). It was first noticed that survivors of a variola virus infection became immune to further infections, an observation that led to the highly dangerous practice of variolation, in which dried, ground smallpox lesions were used to infect non-exposed individuals to combat infection (46). This practice typically used the less pathogenic strain, variola virus minor, in which the mortality rate was typically around 1%. Variolation resulted in severe smallpox infections in those treated, but with decreased mortality compared to variola virus major infection. In the late 18th century, Dr. Edward Jenner published that protection against smallpox infections could be established through variolation with cowpox virus lesions (80). Dr. Jenner immunized an 8 year old boy named James Phipps, the son of his gardener, with cowpox and subsequently challenged him by traditional variolation to show that the boy was cross protected against smallpox infection (80). It was thus demonstrated that variolation with cowpox provided equal protection to traditional variolation in a manner much less dangerous to

treated patients. These experiments were the first recorded demonstrations of vaccination, and led to Dr. Jenner being nicknamed “The Father of Vaccination” or “The Father of Immunology”.

Today, variola virus has been eradicated from the planet through an extensive smallpox eradication campaign, spearheaded by the World Health Organization (WHO)(46). Over time, the smallpox vaccine switched from cowpox virus to vaccinia virus, the modern vaccination agent. The origins and original host of vaccinia virus are unknown, and some hypothesize that vaccinia virus originated on vaccine farms during the eradication campaign (30, 46). Following the declaration of smallpox eradication by the WHO in 1977, there was a laboratory outbreak in the UK that led to the death of a researcher in 1978. Following this outbreak, all smallpox stocks were collected in one of two facilities with BSL4 containment: The Vector Institute in Russia and the Centers for Disease Control and Prevention (CDC) in Atlanta. At this time, a date was set for the destruction of all smallpox stocks. However, this date has continuously been pushed back to this day. Researchers argue that the smallpox stocks contribute to current insights in virology. Additionally, some fear that additional smallpox stocks were obtained by dangerous individuals who could one day use them as bioterror agents, and that maintenance of the variola virus stocks will pay dividends if/when this occurs. Alternatively, others contend that variola virus should be completely eradicated from the planet, and the money spent to maintain stocks and perform research could be better spent on modern health concerns. As these arguments continue, valuable research on variola virus and many other

poxviruses is ongoing, and only time will tell the fate of variola virus on this planet.

1.1.5 Ectromelia Virus

Ectromelia virus (ECTV) is the etiological agent of the disease mousepox, a disease specific to susceptible strains of mice. ECTV was first described in England in 1930 by Dr. J. Marchal (97). ECTV manifests as a foot lesion followed by swelling of the foot and eventual amputation. The disease was termed *infectious ectromelia*: *ectromelia* is defined as the congenital absence or marked imperfection of one or more of the limbs, the term *infectious* was used to differentiate from the congenital disease (97). However, Dr. Marchal observed lesions in the liver and spleen in addition to the foot, indicating that infectious ectromelia was a systemic infection.

It was observed during laboratory outbreaks in 1954 and 1955 in Buffalo, New York that not all strains of mice are equally susceptible to ECTV infection (18). Susceptible mouse strains include the BALB/C, A/NCR and DBA/2 mice in which ECTV is extremely lethal (39). Alternatively, C57BL/6 mice are considered resistant to ECTV infection. Many studies have been done to characterize the genetic determinants of susceptibility to ECTV infection. Through crossing the susceptible DBA/2 strain with the resistant C57BL/6 strain, the mousepox susceptibility loci were identified and termed resistance to mousepox 1 (*rmp1*) to *rmp4* (33). It was in these studies in which researchers first noticed that early innate immune responses produced by natural killer (NK)

cells mediated resistance to ECTV infections as *rmp1* is in fact part of the natural killer complex (NKC) (33). Subsequently, it was observed that depletion of NK cells in C57BL/6 mice rendered these resistant mice susceptible to ECTV challenge (44, 124). More recently published data have demonstrated that mouse CD94, an NKC encoded molecule that interacts with many of the NKG2 activating and inhibitory receptors, is essential for resistance to mousepox (45). C57BL/6 mice devoid of CD94 are rendered susceptible to ECTV infection (45). With this data in hand, the potential for an improved mouse model exists. Due to the large number of transgenic mouse strains generated on the C57BL/6 background, combined with the ability to render these mice susceptible to natural ECTV infection could drastically advance current design of ECTV animal studies.

ECTV represents a very good animal model for the study of smallpox-like infections. Although the natural route of infection between variola virus and ECTV is different, ECTV does cause some smallpox-like symptoms in susceptible mouse strains. Symptoms of ECTV can include the papular rash characteristic of smallpox infections; however, this is not always the case. Mice typically die due to extensive necrosis in the liver and spleen (39, 97). The natural route of infection for ECTV is through abrasions in the skin of the footpad, and therefore, laboratory infections have typically been through footpad injections of susceptible mouse strains. More recently, intranasal infections in the non-susceptible C57BL/6 strain have been used to simulate smallpox-like infections, which were primarily transmitted through aerosolized droplets (126). Even though higher doses of ECTV are required in this model, it remains

advantageous due to the large number of transgenic mouse lines on the C57BL/6 background, and the smallpox-like route of infection.

One historically important, but ethically questionable experiment has been performed using ECTV and has had major implications not only in poxvirology but also in the general construction of all recombinant viruses. Researchers published on a novel recombinant ECTV in which the murine IL-4 gene had been recombined into the viral genome for expression in infected cells (79). The idea was to create a virus that lead to sterility of the infected host, which could potentially lead to the use of this recombinant virus to control mouse populations in Australia. This recombinant virus ended up displaying increased lethality not only in susceptible strains, but also overcame resistance to produce a productive infection in C57BL/6 mice (79). The major controversy was due to the fact that the ECTV-IL-4 virus also overcame pre-existing immunity, resulting in productive infection of mice that had been previously immunized (79). These results had major implications in the potential use of variola virus as a bioterror weapon. The results lead to speculation that a recombinant variola virus, expressing human IL-4, could be used to infect the general population, and that this virus would infect all individuals, including those with pre-existing immunity. Subsequently, many heated debates about the “dual-use dilemma”, or research that has the potential to be used for nefarious purposes in addition to scientific advancement, have centered on this highly pathogenic ECTV “supervirus” (78).

1.1.6 Unique Poxvirus Gene Products

Due to their extremely large viral genome, poxviruses encode a plethora of unique open reading frames that promote fascinating virus-host interactions (8, 102, 111, 150). It is these virus-host interactions that remain the research focus within the Barry laboratory. The study of virus-host interactions allows us to further understand poxvirology and moreover, we may also gain insight into host immune mechanisms and essential activities and even uncover novel targets for anti-viral therapeutics. Our laboratory focuses on poxvirus interactions with the host ubiquitin-proteasome system, the NF- κ B activation cascade and cell death pathways. Here, I will outline important poxviral proteins that mediate unique interactions with the host; this is by no means a comprehensive list and serves only to demonstrate the breadth of this field.

The Barry laboratory has been a leader in the field of poxvirus-host interactions since the discovery of the VV encoded protein F1L (179). F1L is a homolog of the cellular BCL-2 family that localizes to the mitochondria through its C-terminal tail (163). At the mitochondria, F1L has been shown to interact with the BCL-2 protein Bak, and the BH3-only protein BimL to prevent apoptosis (21, 169, 178). Apoptosis is a cell death program initiated by the host in order to remove virally infected cells. F1L functions to inhibit this programmed cell death in order to promote survival of the host cell and prolong the viral life cycle. Inhibition of apoptosis appears to be a highly conserved mechanism within poxviruses as we have now characterized BCL-2 homologs that inhibit apoptosis in fowlpox virus (4, 6), deerpox virus (5), ECTV, and sheeppox virus.

VV encoded E3L is one of the most studied and fascinating poxviral proteins. E3L contains two nucleic acid binding domains, an N-terminal left-handed Z-DNA binding domain and a C-terminal dsRNA binding domain (127). The dsRNA binding domain has been shown to bind and sequester cytoplasmic viral dsRNA (24). Cytoplasmic dsRNA is an important activator of the host interferon (IFN) pathway, a component of the innate immune system, through activation of both the protein kinase R (PKR) and RIG-I pathways (29, 145). E3L has been shown to sequester dsRNA from the sensors of these pathways as well as bind to and inhibit PKR, one of the major sensors of dsRNA (142). One of the consequences of activating PKR is the induction of apoptosis, therefore, E3L also contributes to the inactivation of apoptosis during VV infection (91). Finally, E3L binds and sequesters cytoplasmic dsDNA (135). Cytoplasmic dsDNA is also a potent stimulator of the host IFN response due to recognition by the pattern recognition receptor DAI (167). Therefore, E3L binds to and sequesters both cytoplasmic dsRNA and dsDNA to inhibit the host IFN response and apoptosis.

Many poxviruses encode a variety of proteins that are secreted from the infected cell and mimic membrane receptors for a variety of cytokines. One of the first characterized proteins in this family was a soluble viral tumor necrosis factor receptor (vTNFR) in Shope fibroma virus named M-T2 (187). M-T2 is secreted from infected cells, as it lacks the membrane anchor domain present in cellular TNFRs (158). M-T2 interacts with cellular TNF α preventing its recognition by host receptors and, therefore, subverting the host innate immune response (158). Subsequently, vTNFRs have been identified in *Leporipoxviruses*,

Orthopoxviruses, and *Yatapoxviruses*, with each virus encoding between one and four homologs (114). Additionally, soluble secreted cytokine receptors that recognize interleukin (IL) -2, IL-10, IL-18 and granulocyte-macrophage colony-stimulating factor (GM-CSF) have been identified in a variety of poxviruses (111, 114).

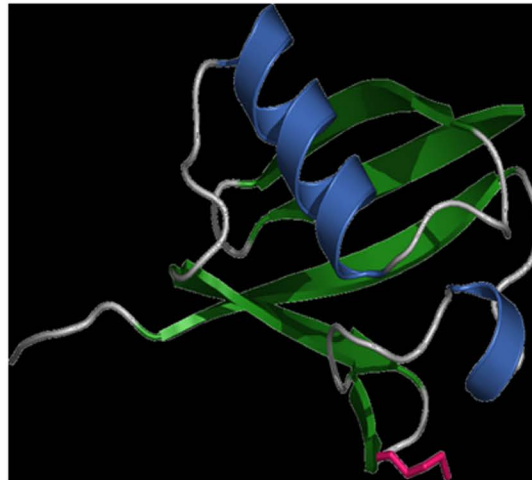
Most viruses mediate their host tropism through specific interactions with host receptors, and therefore tropism is dictated by cell types expressing these specific proteins. Poxvirus tropism does not correlate with virus entry, as poxviruses can manipulate the macropinocytic machinery to enter a variety of cell types (102). Therefore, poxvirus tropism is typically dictated by virus encoded host range factors that function intracellularly to promote a productive infection. Two VV encoded proteins, K1L and C7L, have been identified as host range factors that are essential for VV to initiate a productive replication in RK13 and HeLa cells, respectively (128, 164). Additionally, a CPXV encoded host range protein called CP77 or CHOhr, is essential for replication of CPXV in Chinese hamster ovary (CHO) cells (160). This host range factor can also substitute C7L or K1L in vaccinia virus to promote replication in both CHO and HeLa cells (139). The molecular mechanism governing the host range phenotypes instilled by these proteins is still not understood. Further characterization of host range factors and manipulation of host range phenotypes is a major component to the development of novel poxvirus-based oncolytic virus therapies.

1.2 Ubiquitin

Ubiquitin is a highly conserved 76 amino acid protein that plays a crucial role in protein regulation, as only three amino acid changes appear between yeast and humans (66, 67, 177, 180). Ubiquitin conjugation serves as a post translational modification to a large number of cellular proteins through covalent attachment to lysine residues within the target. Ubiquitin is a rigid globular protein composed of both α -helical and β -sheet structural components (Figure 1.5A). At the C-terminus, ubiquitin contains a diglycine motif, and the terminal glycine residue is critical for the formation of a covalent bond with the lysine residue on the target substrate. There are seven lysine residues within the ubiquitin molecule, K6, K11, K27, K29, K33, K48 and K63, all of which have the potential to support the formation of polyubiquitin chains (Figure 1.5B)(104). The covalent attachment of ubiquitin to target substrates can result in protein degradation via the 26S proteasome or in dramatic alterations in protein function (67, 180). The process of ubiquitylation is essential for cellular homeostasis, and tightly regulates a wide range of cellular functions, such as the cell cycle, signal transduction, transcription, protein transport and DNA repair (67, 132, 180).

The process of ubiquitylation can result in modification of targets through monoubiquitylation or the formation of polyubiquitin chains (Figure 1.6). Monoubiquitylation results in the covalent attachment of only one molecule of ubiquitin onto the target substrate. This type of modification usually results in modification of the substrate function (67). Monoubiquitylation has been shown to be involved in several functions including histone modification, protein trafficking, and retrovirus egress (67). The prototypical polyubiquitin chain is

A



B

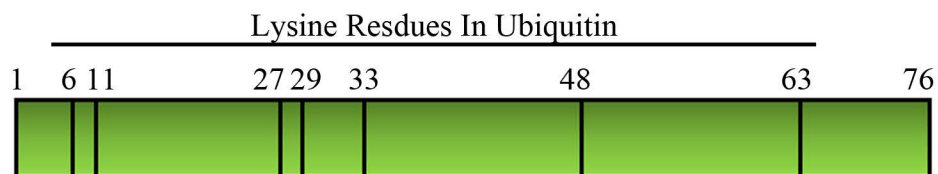


Figure 1.5. Structure of ubiquitin. **A.** Ubiquitin is a rigid globular protein of 76 amino acids that consists of both α -helical and β -sheet structural components. Shown in pink is K48, a lysine residue required for the formation of polyubiquitin chains that direct targets for degradation by the 26S proteasome (175). **B.** The C-terminal glycine residue forms a covalent attachment to lysine residues within the substrate or previously attached ubiquitin moiety. Ubiquitin contains seven lysine residues that are all surface exposed and capable of mediating polyubiquitin chain formation. K48-linked polyubiquitin chains typically direct targets for proteasomal degradation. K63-linked polyubiquitin chains serve as signalling platforms for a variety of signalling events including NF- κ B activation. Additionally, linear ubiquitin chains can be formed between the C-terminal glycine and the N-terminal methionine.

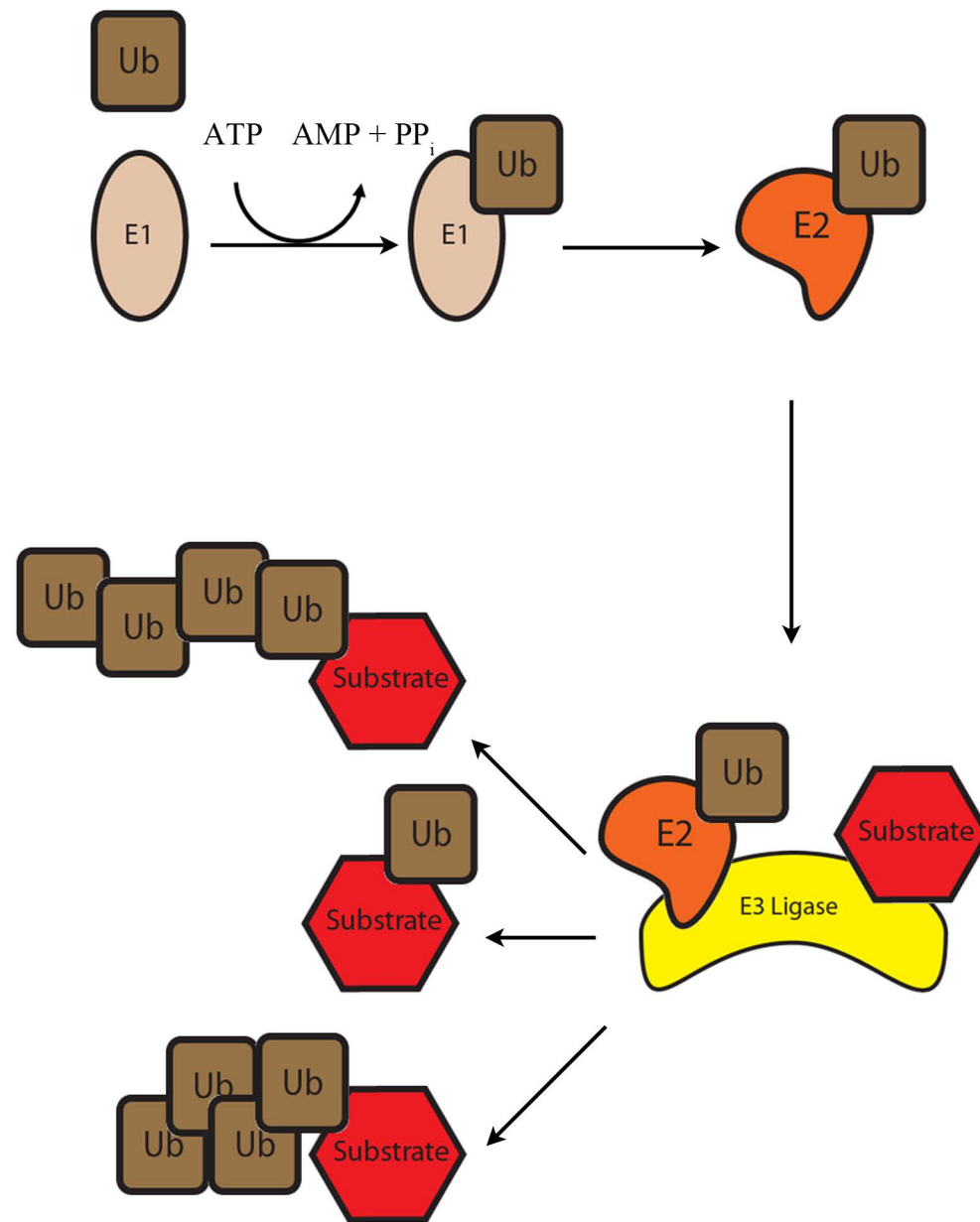


Figure 1.6. Conjugation of ubiquitin. Ubiquitylation of target substrates is catalyzed by a three step enzymatic cascade. The E1 activating enzyme first becomes covalently attached to one molecule of ubiquitin, this requires ATP hydrolysis. Next the activated ubiquitin is transferred to the E2 conjugating enzyme. The E2 determines the type of ubiquitylation reaction that occurs and chain specificity. Finally, the E3 ubiquitin ligase transfers ubiquitin from the E2 to the substrate protein. The final result is either monoubiquitylation, when only one molecule of ubiquitin is attached to the substrate, or polyubiquitylation, the formation of a polyubiquitin chain. Ubiquitin chains linked through different lysine residues within ubiquitin are structurally distinct.

formed through attachment of subsequent ubiquitin moieties onto K48 of the previous ubiquitin. K48-linked polyubiquitin chains that consist of four or more ubiquitin molecules label the substrate for destruction through the 26S proteasome (180). Additionally, polyubiquitin chains formed on K63 of ubiquitin have been demonstrated to be important in signal transduction, specifically in the activation of NF- κ B which will be covered later in this chapter (See Section 1.3)(140). In addition to K48- and K63-linked polyubiquitin chains, polyubiquitin chains consisting of linkages utilizing all seven lysine residues have been described in addition to the formation of linear chains, in which the N-terminus of one ubiquitin is linked to the C-terminal glycine of another to form head to tail chains (74, 76, 170). Finally, the formation of branched and/or mixed ubiquitin chains has been described *in vivo*, but the significance of these chain types is still unclear (74). The complexity of the ubiquitylation system is only beginning to be understood, and the signals induced by all of these chain types are only now being investigated.

1.2.1 Ubiquitylation – The Conjugation of Ubiquitin

Ubiquitin is encoded by one of four genes: two genes encode for a single molecule of ubiquitin attached to ribosomal components, while two other genes encode linear polyubiquitin chains of several ubiquitin molecules linked end to end (81, 123, 141). All of these gene products can be processed by ubiquitin specific proteases (See Section 1.2.4) to produce free monoubiquitin ready to be activated. The conjugation of ubiquitin onto a target molecule is a three step

process resulting in the covalent attachment of the C-terminal glycine residue of ubiquitin onto the ϵ -amino group of a lysine residue within the target substrate (180). The first step involves the activation of ubiquitin by an E1 activating enzyme (Figure 1.6)(61). The activation of ubiquitin requires the hydrolysis of ATP. Notably, the E1 activating enzyme is highly conserved and generally present as a single copy in most eukaryotic genomes. There are two E1 activating enzymes encoded by one gene with two translational start sites in the human genome, perhaps indicative of the additional complexity of the ubiquitin-proteasome system in higher eukaryotes (61).

The second step of ubiquitylation involves the transfer of the activated ubiquitin molecule onto an E2 ubiquitin conjugating enzyme (Figure 1.6)(47). The human genome encodes at least 25 E2 conjugating enzymes, with each molecule interacting with a distinct set of E3 ubiquitin ligases (180). Historically, it has been thought that the E2 enzyme determines the type of ubiquitylation event that occurs, such as chain type and length. This is demonstrated by the E2 conjugating enzyme, Ubc13, which is critical for the formation of K63-linked polyubiquitin chains (71). However, recent evidence indicates that this is not always the case, and the E3 ubiquitin ligase can also be a key contributor to determining chain specificity (31).

The final step is the conjugation of ubiquitin onto the target substrate by the E3 ubiquitin ligases (Figure 1.6)(180). The E3 ubiquitin ligase has both substrate and E2 binding domains, and catalyzes the ubiquitin transfer. Therefore, it is the crucial role of the E3 ligase to mediate the substrate specificity. There are

hundreds of putative E3 ubiquitin ligases encoded in the human genome, and it is predicted that each of these has a unique subset of substrates that are targeted for ubiquitylation. Substrate identification remains one of the most challenging aspects of the study of the ubiquitin-proteasome system, as proteasomal degradation occurs rapidly. However, recent advances in proteomic techniques have advanced this field, making this an exciting time to closely follow research on ubiquitylation.

1.2.2 Ubiquitin Ligases

There are three cellular protein domains that confer E3 ubiquitin ligase activity: the HECT (homologous to E6AP C-terminus) domain, the U-box domain, and the RING (really interesting new gene) domain (2, 189). The HECT domain-containing ligases are single proteins that have a cysteine residue within their active site. This cysteine initially accepts the molecule of ubiquitin from the E2 enzyme, forming a thiolester bond, prior to transferring ubiquitin to the target substrate (73). The HECT domain is responsible for recruitment of the activated E2, while an additional protein-protein interaction domain within the HECT protein, often a WW domain, is responsible for substrate recruitment. The U-box domain consists of a conserved 70 amino acid motif originally identified in yeast and appears structurally related to RING finger E3 ligases (87). The U-box ligases are single proteins that recruit both ubiquitin-charged E2 and substrates to catalyze ubiquitylation, and appear to have an extended family in plants (87). RING finger E3 ligases have a series of conserved histidine and cysteine residues

that coordinate two zinc ions. These ligases can be single proteins or part of a multiprotein complex (130). The RING domain functions to recruit the activated E2 and catalyze the transfer of ubiquitin onto the target substrate. In single subunit RING proteins, an additional protein-protein interaction domain is typically responsible for substrate recruitment. Multi-protein complexes consisting of RING proteins typically have additional protein(s) that function in substrate recruitment. RING fingers differ from HECT domain ligases in that they transfer the molecule of ubiquitin directly to the target substrate without first forming an intermediate covalent attachment to ubiquitin.

Multi-subunit ubiquitin ligases in the RING family of E3s are composed of a scaffold protein, a linker protein, and a substrate adaptor protein, the latter being responsible for recruitment of substrates to the complex for ubiquitylation (130, 182). Multi-protein ubiquitin ligases incorporate a member of the cullin family to act as the molecular scaffold for assembly of the ubiquitin ligase (Figure 1.7). Seven cullin family members have been identified, cullin-1, -2, -3, -4A, -4B, 5, and 7 (130). Each of the cullin proteins contains a cullin-homology domain at the C-terminus that binds Roc1 (Regulator of cullins, also known as Rbx1), a RING containing protein that supplies E3 ligase activity to the complex and recruits an activated E2 (84, 122). Substrate adaptor proteins associate with the N-terminus of cullin family members and contain protein-protein interaction domains that recruit the substrate to the complex. Substrate adaptor proteins can bind directly to the cullin protein, as in the case of cullin-3, or through a family of

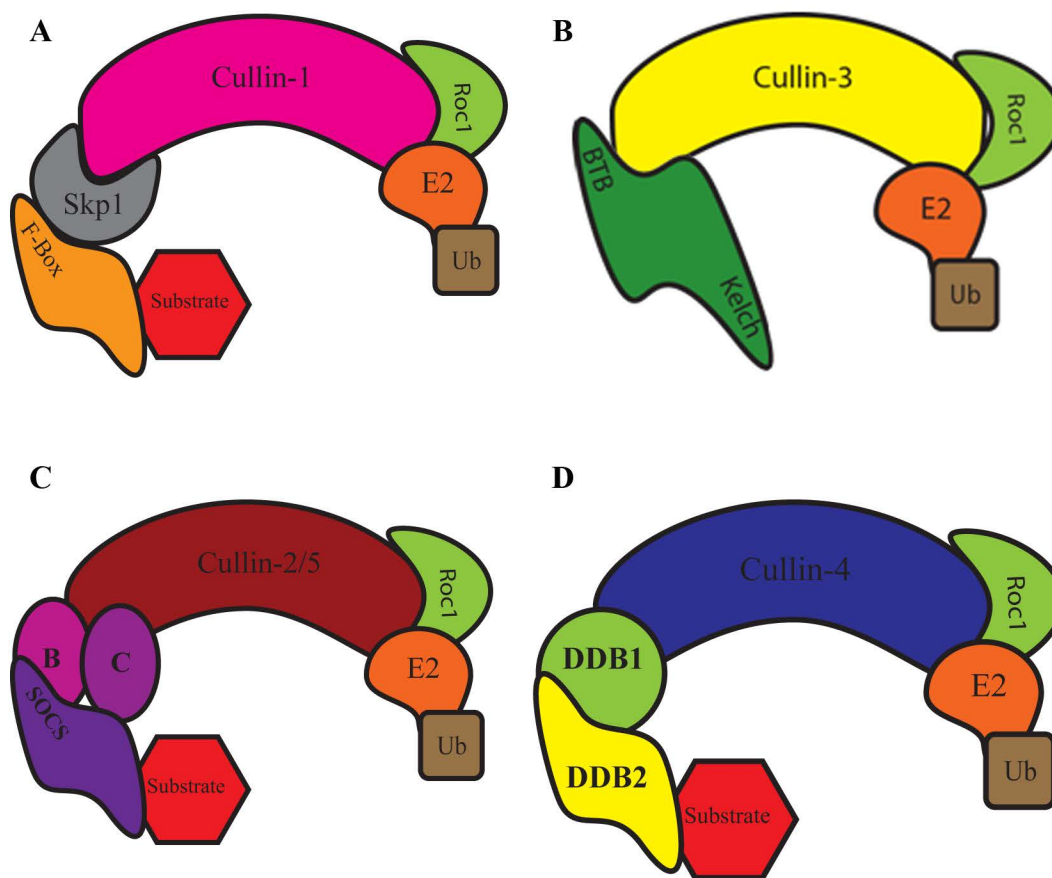


Figure 1.7. The cellular cullin/RING ubiquitin ligase family. There are seven cullin family members encoded in the human genome, six of these are typical cullins: cullin-1, cullin-2, cullin-3, cullin-4A, cullin-4B, and cullin-5. Although cullin-7 shares the cullin name, it is divergent in many regions of the protein, leaving it as an atypical cullin family member. All cullins associate at their C-terminus with Roc1, a RING finger protein that contains E3 ligase activity. **A.** The cullin-1 complex, or SCF, utilizes Skp1 as a linker protein that binds to one of many cellular F-box containing substrate adaptor proteins. **B.** Cullin-3 binds directly to substrate adaptor proteins through BTB domains. **C.** Cullin-2 and 5 utilize elongins B and C as linker proteins that bind to substrate adaptors containing SOCS boxes. **D.** Cullin-4 binds to the linker protein DDB1, which associate with a poorly characterized family of substrate adaptor proteins including DDB2.

linker proteins that are specific for each of the other cullin family members (130, 182).

The anaphase promoting complex/cyclosome (APC/C) is the largest known cellular ubiquitin ligase complex, composed of at least 12 subunits (129). It is thought that the APC/C complex has evolved from an ancestral cullin-type ubiquitin ligase as the subunits APC2 and APC11 resemble a cullin-family member and RING E3 ligase, respectively. APC2 functions as the molecular scaffold, and contains a cullin homology domain that binds to the RING-finger protein APC11 (168). APC1 recruits the E2 conjugating enzymes UbcH5 and Ubc10 to the APC/C in order to catalyze the transfer of ubiquitin onto target substrates (93). Substrates for the APC/C are recognized through the presence of D-box or KEN-box domains. These domains are recognized by a variety of APC/C components including Cdh1 and Doc1 (53, 131). The APC/C plays a major role in regulation of the cell cycle at several points, and is best known for its ability to degrade securin, a protein that regulates the separation of sister chromatids during anaphase (118, 193).

1.2.3 The SCF Ubiquitin Ligase Complex

The SCF (Skp1/Cull1/E-box) complex is a highly conserved ubiquitin ligase involved in regulation of the cell cycle, DNA repair, and innate immunity (3, 89, 109, 116, 117). The complex consists of cullin-1 (86), which serves as the molecular scaffold, Roc1 (84, 122), a RING finger ubiquitin ligase, Skp1 (S-phase kinase associated protein)(108), the linker protein, and one of 69 known

human F-box proteins which function in substrate recruitment (130, 192)(Figure 1.7A). Cellular F-box proteins consist of N-terminal F-box domains in conjunction with C-terminal protein binding domains such as WD40 repeats or leucine-rich repeats (LRR)(23). The N-terminal F-box domain consists of a highly conserved 50 amino acid sequence, folding into three α -helices, which function to bind the linker protein, Skp1 (149, 159). The WD40 repeats, LRRs, or other domains present at the C-terminus of the cellular F-box domain function to bind substrates that are subsequently ubiquitylated through the E3 ligase activity of Roc1. Substrates of the SCF ubiquitin ligase complex usually require a phosphorylation event prior to recognition by the substrate adaptor, which is followed by K48-linked polyubiquitylation and protein degradation via the 26S proteasome (157).

The SCF complex is regulated itself by a variety of mechanisms. A ubiquitin-like molecule called NEDD8 (neuronal precursor cell-expressed and developmentally down-regulated) becomes conjugated to the C-terminus of cullin-1, which requires a ubiquitin-like E1, E2, and E3 cascade (185). Both NEDD8 and its associated E1 are located in the nucleus. Cullin-1 must first bind Roc1 in the cytoplasm to induce nuclear translocation of cullin-1 followed by neddylation, and the subsequent activation of SCF complexes (49). The mechanism whereby NEDD8 activates SCF complexes has been related to its ability to dissociate an inhibitor of the SCF complex called CAND1 (cullin-associated and neddylation-dissociated) (94). CAND1 binds to unneddylated cullins and functions to dissociate the linker protein, Skp1, and therefore inhibit

substrate recruitment (94). Upon neddylation, CAND1 dissociates from cullin-1, allowing recruitment of Skp1, an F-box protein, and substrates and therefore protein ubiquitylation. Finally, the COP9 signalosome (CSN) is responsible for the deneddylation of cullins. The CSN is a multiprotein complex with metalloprotease activity. Recent evidence suggests that the CSN binds to the SCF complex in the absence of bound substrates (147). F-box proteins are subject to autoubiquitylation in the absence of substrates, leading to their degradation. The CSN is recruited to the SCF complex in the absence of bound substrates and deneddylates these complexes, inhibiting autoubiquitylation of the F-box proteins. These SCF complexes bound to CAND1 require reactivation before further ubiquitylation can occur.

Of the 69 cellular F-box proteins currently known, only nine have identified target proteins (48). The cellular F-box proteins have been classified into three subfamilies based on the type of protein-protein interaction domains located at the C-terminus. The Fbw (F-box with WD40 repeats) and Fbl (F-box with Leucine rich repeats) families are the largest groups composed of proteins with WD40 or LRR repeat domains located at their C-terminus, respectively (23). The third family is called Fbx, as these proteins contain a variety of different protein-protein interaction domains at their C-terminus. Several human Fbx proteins have been identified with C-terminal cyclin box, CASH (carbohydrate binding), CH (calponin homology), sec7, proline rich and zinc-finger domains (23). Substrate identification is a major challenge due to the rapid turnover of ubiquitylated proteins. Additionally, many of the substrates form weak and/or

transient interactions with their corresponding F-box proteins, making protein-protein interaction studies difficult. Of the nine cellular F-box proteins with known substrates, the substrates have been classified into two subfamilies: direct regulators of cyclin dependent kinases (CDKs) and regulators of gene transcription (48). Many of these substrates are phosphorylated prior to recognition by the F-box proteins, adding an additional layer of complexity to this regulatory process (157). The F-box protein family appears to be even larger in plants, as over 700 putative F-box proteins were identified in *Arabidopsis* using bioinformatics (51). This has led to the hypothesis that not all F-box proteins function as substrate adaptors for the SCF ubiquitin ligase complex, but many may have evolved to exert novel functions (65).

1.2.4 Deubiquitylation

Similar to phosphorylation, the process of ubiquitylation is reversible. In this case, deubiquitylation enzymes (DUB) play the role of phosphatases in removal of the post-translational modification. The human genome encodes at least 100 DUBs (88). Each DUB has specificity for chain type in addition to specificity for the ubiquitin moiety that it cleaves (88). Additionally, many DUBs possess substrate specificity. There are five different domains with known DUB activity, including, ubiquitin C-terminal hydrolases (UCH), ubiquitin specific proteases (USP), ovarian tumour proteases (OTU), Josephins, and JAB1/MPN/MOV34 metalloenzymes (JAMM)(88). The largest family is the USP enzymes, of which the human genome encodes over 50 (88). DUBs are essential for a variety of

cellular processes including USPs that cleave ubiquitin precursors to produce free ubiquitin molecules that can be activated by E1s. A second function is the removal of unwanted polyubiquitin chains, as a regulatory mechanism for ubiquitin chain synthesis. Additionally, substrates that are targeted for degradation at the 26S proteasome become deubiquitylated by DUBs located in the 19S cap of the proteasome prior to degradation, to recycle the ubiquitin molecules. Finally, DUBs are involved in chain editing. The cellular DUB, A20, deubiquitylates K63-linked polyubiquitin chains on signaling molecules in order to shut off signaling (181). During NF- κ B signaling events, A20 replaces K63-linked polyubiquitin chains with K48-linked polyubiquitin chains on two separate signaling molecules to induce their degradation and ensure signaling is completely turned off.

In addition to containing a DUB enzymatic domain, all DUBs contain a variety of ubiquitin binding domains (UBD) (34). The three major classes of UBDs are ubiquitin interacting motifs (UIMs), ubiquitin associated domains (UBAs) and ubiquitin-specific protease domains (ZnF-UBP)(34). Most of these UBDs recognize a specific patch on the surface of ubiquitin molecules centered on I44, and bind free ubiquitin with low affinity (34). However, in each DUB, the coordination of several UBDs increases the affinity for a specific chain type. Each ubiquitin chain type forms a unique structure that differs greatly from other linkage types. UBDs also contribute to the location of proteolysis. Cleavage can occur at the distal ubiquitin moiety or internally within the chain. In addition to the UBDs, many DUBs confer substrate specificity that is typically determined by

unique protein-protein interaction domains incorporated into the individual DUBs.

1.2.5 Viruses and The Ubiquitin-Proteasome System

It has become apparent that many viruses have evolved to exploit the host ubiquitylation machinery, including HIV (12, 14, 40, 149, 190), adenoviruses (36, 134), herpes viruses (15, 16), and poxviruses (7, 83, 105, 119). The viral proteins can serve as novel substrate adaptors for multi-protein cellular ubiquitin ligases, or possess their own ubiquitin ligase activity (7, 75). Many viral proteins also inhibit the cellular ubiquitylation machinery, or are targeted themselves for ubiquitylation by cellular or viral ubiquitin ligases. Finally, recent studies have demonstrated DUB activity in a variety of viral proteins, suggesting that viruses can mediate the addition and removal of ubiquitin moieties during infection (75).

The first identified target of virus mediated ubiquitylation was the cellular oncoprotein p53, which was shown to be degraded during infection with human papillomavirus (HPV) and subsequently by adenoviruses (13, 144). HPV is a small dsDNA virus that causes cervical cancer in some infected individuals. During infection, the viral dsDNA genome is replicated in the nucleus. It is essential for the virus to activate the cell cycle in order for DNA replication to occur. Activation of the cell cycle results in an increase in free nucleotide pools and cellular DNA replication enzymes that are required for the synthesis of progeny viral genomes. The HPV encoded E6 protein associates with a cellular E3 ligase from HECT family called E6AP (E6 associated protein)(10). E6

redirects the substrate specificity for E6AP, leading to the ubiquitylation and proteasomal degradation of p53 (144). This constitutes one of many examples in which a virus redirects the target specificity for a cellular ubiquitin ligase. p53 is a cellular transcription factor that functions as a tumour suppressor, and its degradation leads to uncontrolled cellular replication, which in some HPV infections can lead to cervical cancer (10).

The replication and pathogenicity of the human immunodeficiency virus (HIV) is also tightly linked to the ubiquitin-proteasome system. HIV encoded Vif mediates the degradation of a cellular cytidine deaminase with anti-viral activity called APOBEC3G, through association with a cellular cullin-based E3 ubiquitin ligase (190). It had been previously known that replication of Vif-deficient HIV was non-permissive in certain cell types (50). Eventually, it was determined that expression of the cellular protein APOBEC3G, controlled HIV replication in the absence of Vif. APOBEC3G has been shown to be packaged in progeny viral genomes. During infection of new cells, APOBEC3G deaminates cytosine residues in newly synthesized DNA during reverse transcription of the HIV RNA genome. This leads to the presence of uracil moieties in the proviral dsDNA molecule, which are recognized by cellular DNA excision and repair enzymes, leading to destruction of proviral dsDNA. HIV encoded Vif counteracts this anti-viral mechanism by associating with a cellular ubiquitin ligase composed of cullin-5, Roc1, and the linker proteins elongin B and C (Figure 1.7C)(190). Vif replaces the cellular substrate adaptors by binding to the elongin proteins, and redirecting the cullin-5 based ubiquitin ligase to target APOBEC3G.

APOBEC3G is subsequently polyubiquitylated with a K48-linked polyubiquitin chain and targeted for destruction via the 26S proteasome. Therefore, Vif counteracts the cellular anti-viral response leading to productive infection of cells infected with virus produced in cells expressing APOBEC3G (54). In addition to Vif, there exists a large family of viral proteins that function as virally encoded substrate adaptors for a variety of cullin family ubiquitin ligases, each mediating the ubiquitylation of a unique subset of substrates that contributes to viral fitness (7).

Herpes simplex virus encodes its own ubiquitin ligase called infected-cell protein 0 (ICP0). ICP0 has two ubiquitin ligase domains: a RING domain, and a HUL1 (herpes virus ubiquitin ligase) domain (41, 57). Both of these domains are functional ubiquitin ligases as demonstrated by *in vitro* ubiquitylation assays. Early in infection, ICP0 localizes to nuclear bodies called ND10s (42). At these sites, ICP0 induces the ubiquitylation and degradation of ND10 structural proteins called PML (promyelocytic leukemia) and SP100; this degradation is dependent on the RING domain (42, 98, 99). Disruption of ND10s supports viral replication as ND10 components interact with viral genomes early in infection to inhibit viral DNA replication (100). Additionally, the HUL1 domain of ICP0 has been shown to mediate the ubiquitylation of the cellular E2 protein, UbcH3 (57, 58). UbcH3 is the E2 constituent of a cellular SCF ubiquitin ligase complex that promotes the degradation of cyclins D1 and D3. Therefore, ICP0 upregulates cyclins D1 and D3 through the ubiquitylation and degradation of the E2 component of the ubiquitin ligase that down-regulates these proteins. The dual ubiquitin ligase

domains and activity of ICP0 appears to be unique feature amongst virally encoded ubiquitin ligases (59).

In addition to regulating the ubiquitylation of virus specific substrates, many viruses encode their own DUBs in order to induce deubiquitylation of virus and/or host proteins (75). This was first described in herpes viruses as the viral protein UL36 was reported to contain DUB activity (85). UL36 has a cysteine protease domain and catalyzes the deubiquitylation of an unknown substrate. Notably, UL36 contains no homology with any cellular DUBs, and therefore constitutes a novel catalytic domain. Although it is clear that UL36 is capable of functioning on artificial polyubiquitin chains, the relevance of this enzymatic activity *in vivo* remains unclear. UL36 is a major component of the herpes simplex virus tegument, recently shown to associate with VP16 potentially function in scaffolding for the regulated assembly of the tegument (165), and therefore, the DUB activity may contribute to the formation of progeny virions.

1.2.6 Poxviruses and The Ubiquitin-Proteasome System

Poxviruses encode a wide variety of unique gene products that regulate host machinery, and many of these specifically target the ubiquitin-proteasome system. Many poxviruses encode an ortholog of the ECTV encoded RING protein p28. p28 contains a C-terminal RING domain that has demonstrated ubiquitin ligase activity during *in vitro* ubiquitylation assays (72, 151, 152). Additionally, p28 contains a Kila-N domain at its N-terminus. The Kila-N domain is a DNA binding domain that localizes p28 to virus factories during infection (77, 153).

The identity of p28 substrates remains unknown, but these could potentially be cellular or viral proteins located within viral factories. ECTV devoid of p28 demonstrated decreased virulence in infected mice (151). Attenuation is may be linked to a modified host range, as ECTV- Δ p28 is incapable of productively infecting macrophages, a cell line essential for systemic spread of ECTV (153). Notably, the variola virus ortholog of p28 has been shown to associate with Ubc13, an E2 enzyme specific for the formation of K63-linked polyubiquitin chains (72). Therefore, p28 potentially mediates the synthesis of K63-linked polyubiquitin chains on substrates located within the virus factory.

A second family of poxvirus encoded ubiquitin ligases are the membrane associate RING-CH (MARCH) proteins (8). These proteins contain a modified RING domain and localize to intracellular membranes. These proteins are among the few viral ubiquitin ligases with known substrates. The myxoma virus encoded MARCH protein M153R is essential for the down-regulation of the cell surface protein MHC class I (56, 96). Down-regulation of MHC class I prevents the presentation of viral peptides to the cytotoxic T cells, and therefore suppresses the adaptive immune response. Additionally, M153R down-regulates cell surface expression of CD4, CD95, and ALCAM1 (96).

Many *Orthopoxviruses*, including ECTV, encode a family of proteins that contain BTB and Kelch domains and regulate the ubiquitin-proteasome system. A former member of the Barry laboratory, Dr. Brianne Couturier, identified four BTB/Kelch proteins encoded by ECTV, named EVM018, EVM027, EVM150 and EVM167. These proteins interact with the cellular cullin-3 ubiquitin ligase

complex and conjugated ubiquitin molecules (183). Like cellular BTB/Kelch proteins, the poxviral BTB/Kelch proteins may function as substrate adaptor molecules for the cellular cullin-3 ubiquitin ligase (Figure 1.7B). The ECTV encoded BTB/Kelch proteins likely each have their own subset of substrates that are recruited for ubiquitylation during infection. These substrates are potentially involved in regulation of NF- κ B signaling, as EVM150 has been shown to suppress TNF α induced NF- κ B activation (Brienne Couturier, Qian Wang and Michele Barry, unpublished data). Future studies that determine the identification of these substrates will provide essential insight into the roles of these proteins *in vivo*.

A family of poxvirus RING-finger proteins was recently identified that contains sequence similarity with the RING domain of the APC/C subunit APC11 (110). These APC11 homologs were identified in the *Parapoxviruses*, *Molluscipoxviruses*, as well as the crocodilepox and squirrelpox viruses. The only homolog studied is the Orf virus-encoded APC11 homolog, which has been named PACR (poxvirus APC/cyclosome regulator)(110). PACR was shown to coprecipitate with APC/C subunits APC2, APC3 and APC4, and interact with the APC/C complex in a similar manner to APC11. Upon sequence analysis, however, it was shown that PACR and the other poxvirus orthologs contain mutations within the RING domain that inhibit the binding of E2 ubiquitin-conjugating enzymes to the complex, and therefore inhibit substrate ubiquitylation. It is thought that inhibition of APC/C may prompt cells into S-phase, a stage within the cell cycle where cellular factors may be present that

contribute to virus replication. Additionally, two of the targets of the APC/C are cellular ribonucleotide reductase (RR) and thymidine kinase (TK) proteins, proteins that contribute to the free nucleotide pools required for DNA synthesis (129). Typically, poxviruses encode their own TK and RR genes, however, the TK gene is absent from Orf virus (110). In contrast, many viruses that encode their own TK genes lack PACR orthologs. Perhaps one of the main reasons for encoding APC/C inhibitors is to upregulate cellular TK and RR genes to enhance free nucleotide pools in poxviruses that lack the ability to promote this themselves.

One of the more fascinating findings was that several poxviruses encode their own molecule of ubiquitin, highlighting the importance of the relationship between poxviruses and the ubiquitin-proteasome pathway. Virus encoded ubiquitin was first identified in two *Entomopoxviruses*: *Melanoplus sanguinipes entomopoxvirus* (MSEV) and *Amsacta moorei entomopoxvirus* (AMEV)(9). The ubiquitin orthologs in MSEV and AMEV encode proteins of 80 and 81 amino acids in length, which share 86% and 89% identity with human ubiquitin, respectively (8). Subsequently, a ubiquitin homolog was identified in the *Avipoxvirus*, canaraypox virus, that encodes a protein of 85 amino acids that shares 98% identity with human ubiquitin (172). There is currently no biochemical data characterizing these ubiquitin homologs, or evidence that they can be incorporated into polyubiquitin chains. It would be interesting to determine the contribution of these molecules to poxvirus virulence. Whether

these ubiquitin homologs are essential or not, their mere presence highlights the important link between poxviruses and the ubiquitin-proteasome system.

1.3 The NF- κ B Pathway

Nuclear factor κ B (NF- κ B) is a family of transcription factors activated by a variety of signaling pathways to activate proinflammatory and anti-viral immune responses (64, 174). The family of NF- κ B transcription factors consists of five members, p50, p52, p65 (RelA), RelB, and c-Rel, which function as homo- or heterodimers to activate transcription of specific genes (Figure 1.8)(64). The NF- κ B dimers recognize ~10bp κ B binding sites within promoter regions of the genome to activate transcription (70). Three members of the NF- κ B family, p65, RelB and c-Rel, contain a transcriptional activation domain (TAD) required for induction of transcription. Therefore, p50 and p52 function as inhibitors of transcription as homodimers. However, they activate a unique set of genes as heterodimers with a TAD-containing NF- κ B family member. The prototypical NF- κ B dimer consists of p65 and p50 and will be the focus of research to be described in later chapters. p105 and p100 are processed by the 26S proteasome to produce the NF- κ B transcription factors, p50 and p52, leading to activation of the canonical and non-canonical NF- κ B pathways, respectively (Figure 1.8).

NF- κ B transcription factors are predominantly cytoplasmic prior to activation due to association with a member of the inhibitor of κ B (I κ B) family of proteins (Figure 1.9)(64, 174). The I κ B family is composed of three prototypical members, I κ B α , I κ B β , and I κ B ϵ , which function to sequester NF- κ Bs in the

p65 (RelA) - 551 amino acids



RelB - 579 amino acids



c-Rel - 619 amino acids



NF- κ B2 (p100/p52) - 899 amino acids



NF- κ B1 (p105/p50) - 969 amino acids

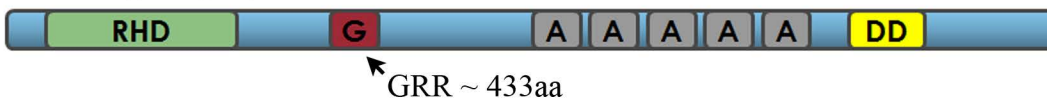


Figure 1.8. The NF- κ B family of transcription factors. There are five members of the NF- κ B family of transcription factors. These include p65, RelB, c-Rel, p50 and p52. These proteins function as dimers, and binding is mediated by the conserved Rel-homology domain (RHD) located at the N-terminus of these proteins. RelB, c-Rel and p65 all contain C-terminal transcriptional activation domains (TAD) that function to recruit transcription machinery to κ B promoter regions on the DNA. p52 and p50 are processed from larger proteins of the I κ B family, p100 and p105, respectively. p100 and p105 are processed by the 26S proteasome up to the GRR regions resulting in proteins of 447aa and 433aa, respectively. DD - death domain, GRR - glycine-rich region, A - ankyrin repeat, LZ - leucine zipper.

I κ B α - 317 amino acids



I κ B β - 356 amino acids



I κ B ϵ - 361 amino acids



I κ B γ - 607 amino acids



BCL-3 - 446 amino acids



I κ B ζ - 718 amino acids



Figure 1.9. The inhibitor of κ B family of proteins. There are eight proteins that function as I κ Bs: I κ B α , I κ B β , I κ B ϵ , I κ B γ , BCL-3, I κ B ζ , and the p50 and p52 precursor proteins, p105 and p100, respectively. These proteins all contain a series of ankyrin repeats that function to sequester NF- κ B dimers in the cytoplasm. I κ B α , I κ B β and I κ B ϵ are all phosphorylated by the IKK complex in response to external stimuli, resulting in their ubiquitylation by the SCF ^{β -TRCP} ubiquitin ligase, and the subsequent nuclear translocation of their bound NF- κ B dimer. A - ankyrin repeat, DD - death domain, PEST - rich in proline (P), glutamate (E), serine (S), and threonine (T).

cytoplasm (64). The I κ Bs contain a series of ankyrin repeat domains that function to bind NF- κ B dimers and hide their corresponding nuclear localization signals sequestering them in the cytoplasm. I κ B family members are phosphorylated by the I κ B kinase (IKK) complex in response to a variety of stimuli, leading to their degradation by the 26S proteasome and subsequent nuclear translocation of NF- κ B dimers. Of all I κ Bs, I κ B α is the major contributor to the cytoplasmic retention of the p65/p50 heterodimer. Additionally, two proteins, p105 and p100, contain ankyrin domains at their C-termini and can function as I κ Bs. A third set of inducible-expressed atypical I κ Bs called BCL3, I κ B ζ , and I κ B γ . These atypical I κ Bs may function to bind inhibitory NF- κ B dimers such as p50/p50 or p52/p52, to allow TAD-containing dimers access to κ B binding sites on DNA to initiate transcription.

The canonical NF- κ B activation pathways, such as those activated by tumor necrosis factor α (TNF α)(Figure 1.10) and interleukin 1 β (IL-1 β)(Figure 1.11), trigger the activation of a set of kinases known as the I κ B kinase (IKK) complex. The IKK complex consists of IKK α , IKK β and IKK γ (NEMO)(174). Phosphorylation of IKK β is required to transmit canonical NF- κ B signals. In contrast, the non-canonical activation of NF- κ B requires phosphorylation of IKK α . Phospho-IKK β in turn phosphorylates I κ B α on serines 32 and 36, which targets I κ B α for polyubiquitination and degradation by the 26S proteasome (64, 174). The SCF ^{β -TRCP} ubiquitin ligase complex recruits phospho-I κ B α through the adaptor molecule, β -TRCP (β transducin repeat-containing protein), which is a

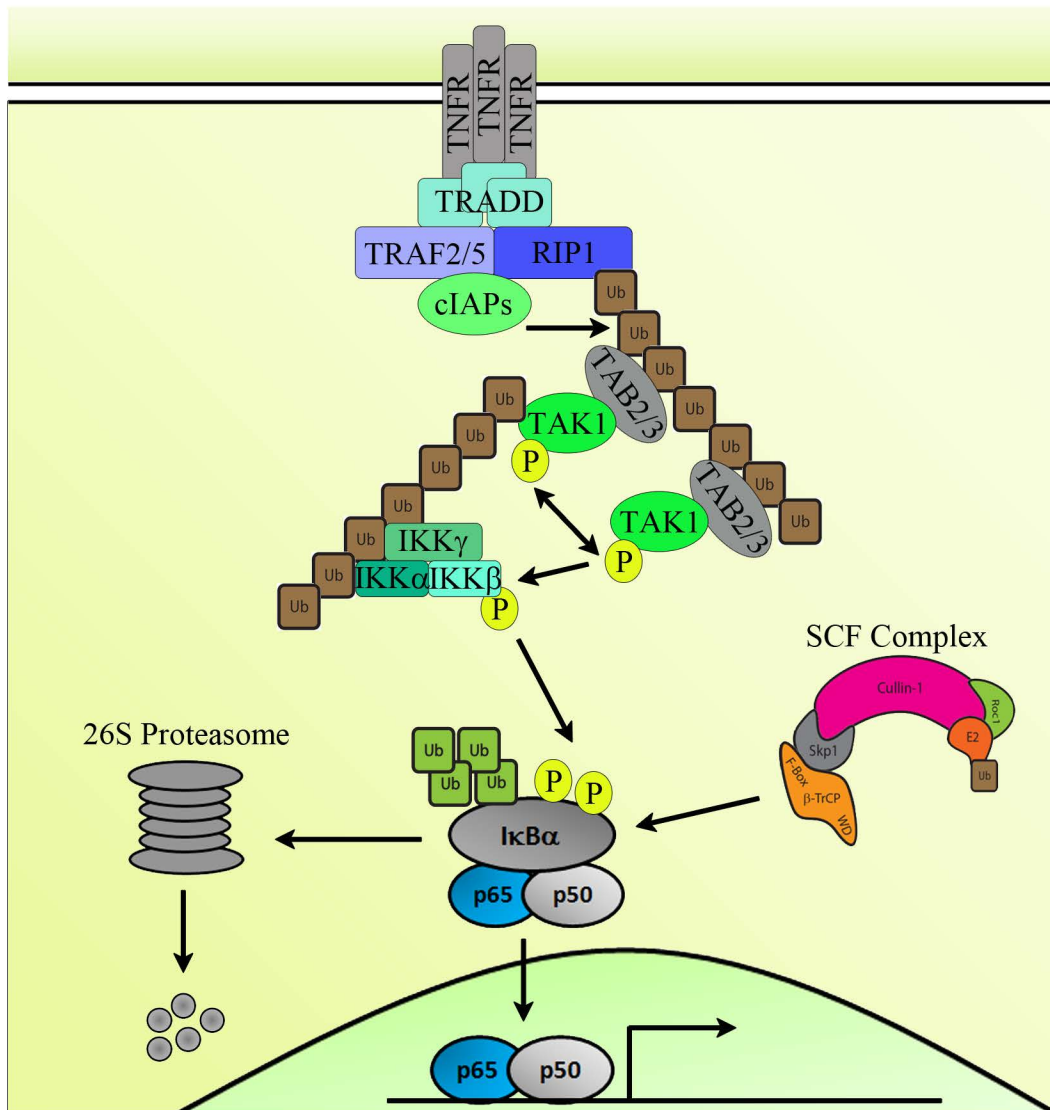


Figure 1.10. The TNF α induced NF- κ B activation signalling cascade. TNF α is a membrane bound cytokine that can be cleaved to produce a soluble form. Upon binding of TNF α to the TNFR, TNRF trimerizes and recruits several proteins to induce signalling. Molecules recruited to the TNFR include TRAF2/5, cIAP1/2, RIP1, and TRADD. Upon recruitment of these proteins, RIP1 becomes K63 polyubiquitylated, leading to further recruitment of proteins. TAB2/3 contain UBD domains that bind the K63-linked polyubiquitin chain on RIP1, and recruit TAK1 to the TNFR. TAK1 molecules autophosphorylate each other leading to TAK1 activation. The mechanism of IKK recruitment to the TNFR is not clearly understood. Potentially IKK γ binds to the K63-linked polyubiquitin chain on RIP1, or another molecule such as TAK1 is K63 polyubiquitylated leading to IKK recruitment and IKK β phosphorylation by TAK1. Phospho-IKK β phosphorylates I κ B α , leading to its ubiquitylation by the SCF $^{\beta\text{-TRCP}}$ ubiquitin ligase, and its proteasomal degradation. I κ B α degradation releases the p65/p50 heterodimer, which translocates to the nucleus to induce NF- κ B regulated transcriptional activity.

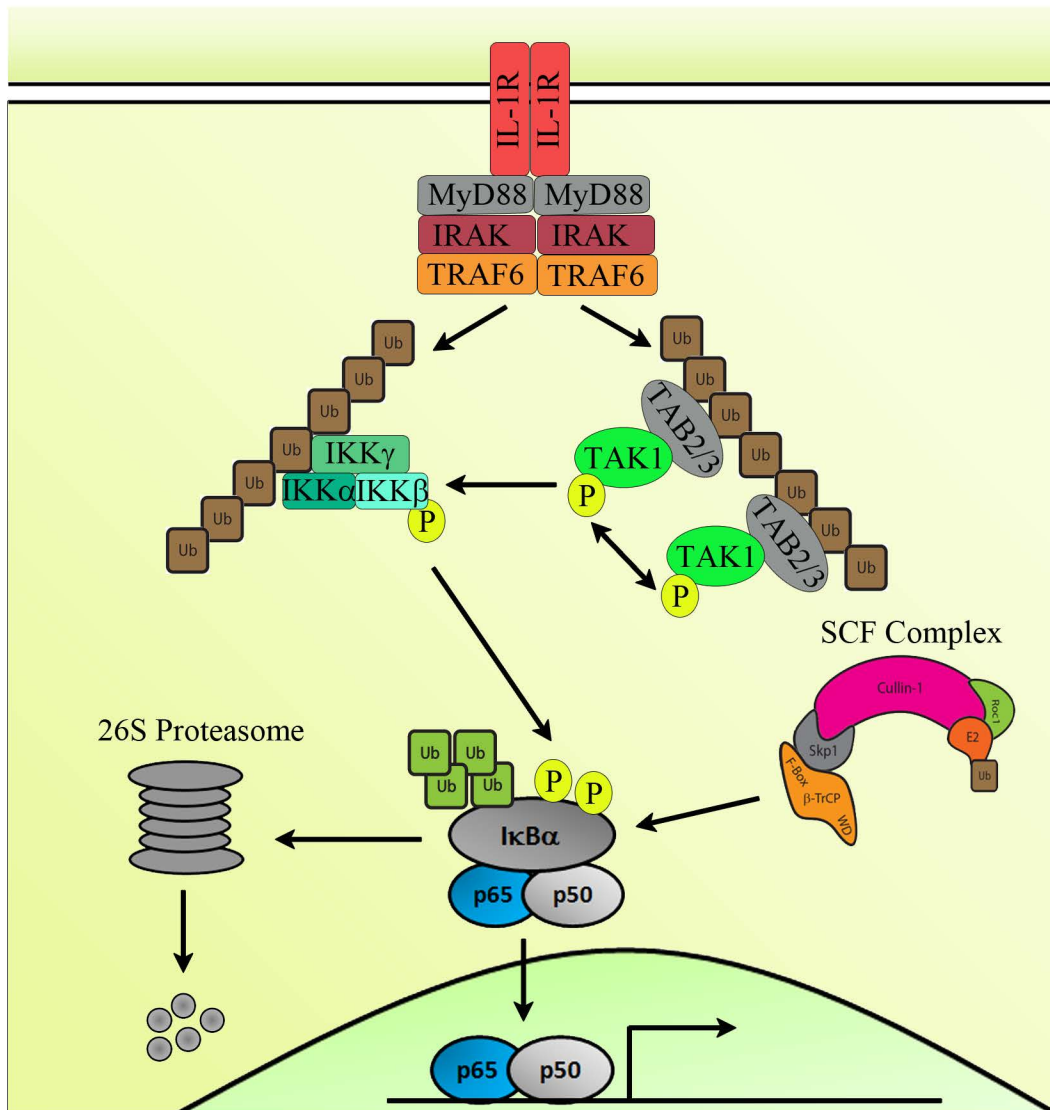


Figure 1.11. The IL-1 β induced NF- κ B activation signaling cascade. Upon binding of IL-1 β to the IL-1R, the adaptor molecule MyD88 is recruited to the IL-1R complex to initiate signalling. MyD88 interacts with the IL-1R through homotypic interactions mediated by TIR domains on both proteins. MyD88 recruits additional signalling molecules including IRAK1/4 and TRAF6. TRAF6 contains a RING domain and catalyzes the formation of K63-linked polyubiquitin chains that are essential for the propagation of IL-1 β induced NF- κ B activation. It is unclear what molecules are K63 polyubiquitylated following IL-1 β stimulation, however, free K63-linked polyubiquitin chains can induce NF- κ B activation. TAB2/3 and IKK γ contain UBDs and bind to K63-linked polyubiquitin chains and are recruited to the TRAF6 constructed chains. TAK1 becomes autophosphorylated, activating TAK1 allowing TAK1 to phosphorylate IKK β to induce activation of the IKK complex. Phospho-IKK β then phosphorylates I κ B α twice. Phospho-I κ B α is a substrate of the SCF $^{\beta$ -TRCP ubiquitin ligase complex, leading to its proteasomal degradation, the nuclear translocation of p50/p65, and induction of NF- κ B regulated transcription.

cellular F-box protein. SCF ^{β -TRCP} catalyzes the synthesis of a K48-linked polyubiquitin chain on I κ B α resulting in its degradation via the 26S proteasome, and subsequent translocation of the p50/p65 heterodimer to the nucleus to activate transcription of immune regulatory genes (64, 174).

Activation of the IKK complex varies depending on the origin of the NF- κ B activating signal. The following sections will compare and contrast the activation of the IKK complex following stimulation with TNF α (Section 1.3.1 and Figure 1.10), IL-1 β (Section 1.3.2 and Figure 1.11), or alternative mechanisms (Section 1.3.3). These pathways rely heavily on a series of proteasome-independent ubiquitylation reactions and kinases that converge at the IKK complex, resulting in the phosphorylation and activation of IKK β .

1.3.1 TNF α Mediated NF- κ B Activation

TNF α is expressed as a membrane protein that is processed and released as a soluble cytokine. Both membrane bound and soluble forms of TNF α function as trimers to activate an NF- κ B signaling cascade at the TNF receptor (TNFR). Upon binding trimeric TNF α , the TNFR trimerizes leading to the activation of TNF α induced signaling (Figure 1.10)(95). The trimeric TNFR recruits a variety of signaling molecules including TNFR associated death domain protein (TRADD), cellular inhibitors of apoptosis (cIAP1 and cIAP2), the receptor interacting protein kinase (RIP1), and the TNFR associated factors (TRAF2 and TRAF5)(95). Recent evidence suggests that cIAP1 and cIAP2 can induce the formation of K63-linked polyubiquitin chains on RIP1 through their RING

domains (11). These K63-linked polyubiquitin chains recruit the TGF β activated kinase (TAK1) through the adaptor proteins, TAK1 binding proteins (TAB2 and TAB3) (37). TAB2 and TAB3 contain UBDs that interact with K63-linked polyubiquitin chains, and function to recruit TAK1 to the K63-linked polyubiquitin chain on RIP1. Recruitment of TAK1 leads to the autophosphorylation of TAK1 molecules at the receptor, leading to activation of TAK1 kinase activity. Activated TAK1 is responsible for phosphorylating IKK β and activation of the IKK complex (37).

Recruitment of the IKK complex to the TNFR remains incompletely understood, but requires proteasome-independent ubiquitylation events. IKK γ contains UBDs that bind to both K63-linked and linear polyubiquitin chains (28, 136, 184). IKK γ may bind the same K63-linked polyubiquitin chain on RIP1 as the TAK1/TAB complex. The ubiquitin chain length on RIP1 is not known. Alternatively, TRAF2 contains a RING domain that mediates the formation of K63-linked polyubiquitin chains on phospho-TAK1 (43). Ubiquitylation of TAK1 may be required for the recruitment of the IKK complex to the TNFR followed by phosphorylation of IKK β by TAK1. Further complexity was revealed when the ubiquitin ligase complex consisting of HOIP/HOIL was shown to form linear polyubiquitin chains on IKK γ (170). It is currently unclear how the linear polyubiquitylation of IKK γ contributes to TNF α induced NF- κ B activation.

1.3.2 IL-1 β Mediated NF- κ B Activation

Activation of the IKK complex by IL-1 β or the toll-like receptor (TLR) family of proteins share similar mechanisms. Both the IL-1 β receptor (IL-1R) and TLRs contain Toll/IL-1R (TIR) domains on their cytoplasmic tails. Upon ligand binding, the TIR domains of these receptors recruit the TIR containing adaptor molecule myeloid differentiation primary gene 88 (MyD88)(Figure 1.11). MyD88 functions to recruit additional signaling molecules, including the IL-1R associated kinases (IRAK 1 and IRAK4), and TRAF6, which contains a RING domain (95). TRAF6, in conjunction with the E2 enzyme, Ubc13, catalyzes the formation of K63-linked polyubiquitin chains, leading to the recruitment of the TAK1/TAB and IKK complexes, as they do during TNF α stimulation. The primary target of TRAF6 mediated K63-linked polyubiquitylation is still unclear. It has been suggested that TRAF6 autoubiquitylation or IRAK1 ubiquitylation by TRAF6 may contribute to IL-1 β induced NF- κ B activation. However, free K63-linked polyubiquitin chains have also been implicated in IL-1 β induced NF- κ B activation, leaving this a highly controversial area of research (27, 176, 186).

Until recently it was thought that K63-linked polyubiquitin chains were essential for both IL-1 β and TNF α induced activation of IKK. However, recent evidence suggests that TNF α signaling occurs in the absence of Ubc13 (E2 enzyme specializing in K63 chains), and in cells expressing a K63R mutation in ubiquitin. K63-linked polyubiquitin chains may therefore not be essential for TNF α induced NF- κ B activation (95, 188). These results indicate that an E2 other than Ubc13 may generate K63-linked polyubiquitin chains to promote TNF α induced NF- κ B activation. Alternatively, linear polyubiquitin chains may

contribute to IKK activation in the absence of K63-linked polyubiquitin chains. However, disrupting the formation of K63-linked polyubiquitin chains does completely inhibit IL-1 β induced NF- κ B activation, highlighting a significant difference between the two signaling pathways.

Due to the requirement for a large number of proteasome-independent ubiquitylation reactions in the activation of NF- κ B by both TNF α and IL-1 β , it is no surprise that DUBs have been shown to negatively regulate NF- κ B activation (62). Two cellular DUBs, A20 and the cylindromatosis tumor suppressor (CYLD), are involved in the deubiquitylation of NF- κ B signaling molecules, contributing to shut off of these signaling pathways. A20 is a cellular DUB containing an OTU domain, which is upregulated by NF- κ B signaling in a negative feedback loop (62). A20 inhibits TNF α induced NF- κ B activation by removing K63-linked polyubiquitin chains from RIP1 (181). Additionally, A20 contains a unique zinc-finger domain with ubiquitin ligase activity that catalyzes the formation of K48-linked polyubiquitin chains on RIP1, therefore functioning as a ubiquitin chain editing enzyme (181). The K48-linked polyubiquitin chain on RIP1 targets RIP1 for proteasomal degradation. Mice deficient in A20 die due to chronic inflammation and uncontrolled apoptosis, highlighting the importance of A20 as a negative regulator of NF- κ B activation (90). CYLD is a DUB containing USP activity (62). CYLD has also been implicated in the deubiquitylation of RIP1, as a mechanism of regulating NF- κ B activation (19). CYLD may inhibit NF- κ B through a variety of mechanisms. Further characterization of this protein will likely unveil novel mechanisms of NF- κ B

activation and inhibition. Many cancers and inflammatory diseases are associated with disrupted function of these two DUBs, highlighting the importance of DUB activity in the regulation of NF- κ B and its inherent prosurvival and inflammatory properties.

1.3.3 Alternative Pathways for IKK Activation

In addition to the TNF α and IL-1 β /TLR signaling pathways, IKK β phosphorylation can be induced by signaling initiated by the RIG-I, the T-cell receptor and NOD receptors (95). All of these events converge on the IKK complex leading to the phosphorylation and degradation of I κ Bs and the nuclear translocation of NF- κ B transcription factors. Upstream of IKK β phosphorylation, all three of these pathways also involve members of the TRAF family to regulate the synthesis of K63-linked polyubiquitin chains that induce the recruitment of the TAK1/TAB and IKK complexes, and their subsequent activation (95). In addition to activating IKK β , RIG-I signaling activates an IKK-related kinase called TBK1. TBK1 phosphorylates and activates IRF-3, a transcription factor that activates the interferon response. TBK1 phosphorylation requires TRAF molecules and K63-linked polyubiquitin chains, similar to the activation of IKK β .

In addition to the canonical activation of NF- κ B through the activation of IKK β , non-canonical activation of NF- κ B represents an important transcriptional program in B-cells through activation of IKK α (95). The non-canonical NF- κ B signaling pathway is triggered in B-cells via a variety of cell surface receptors including B-cell activating factor receptor (BAFF-R), lymphotoxin β receptor

(LT- β R) and CD40 (64). Signaling events downstream of these receptors all lead to activation of the NF- κ B inducing kinase (NIK). NIK phosphorylates IKK α , which in turn phosphorylates p100. Phospho-p100 is recognized by the SCF ^{β -TRCP} ubiquitin ligase complex leading to proteasomal processing which generates the NF- κ B subunit p52. The p52/RelB heterodimer is then free to enter the nucleus to induce transcription in B-cells.

1.3.4 Viral Regulation of the NF- κ B Cascade

Regulation of NF- κ B signaling is a common trait amongst most viruses, with each virus employing a combination of specifically tailored strategies (68, 69, 111). For example, viruses such as human immunodeficiency virus (HIV), human T-lymphotropic virus type 1 (HTLV-1), hepatitis B virus (HBV), and Epstein-Barr virus (EBV) activate the NF- κ B signaling pathway (69). Virus activation of the NF- κ B pathway could serve several roles. For instance, viruses that lack anti-apoptotic mechanisms may activate NF- κ B to prolong the life of the infected cell in order to complete the viral replication cycle. In the case of EBV, constitutive activation of NF- κ B leads to the upregulation of NF- κ B-regulated pro-survival proteins, which contributes to EBV associated malignancies (20). Alternatively, HIV-1 contains κ B binding sites in the long terminal repeat (LTR) region of the genome that activate HIV-1 gene expression (143).

In contrast to activating the NF- κ B pathway, many other viruses encode proteins that specifically inhibit NF- κ B signaling (68, 69, 111, 137). Inhibiting NF- κ B activation is beneficial for a large number of viruses due to the strong

early innate immune response generated by NF- κ B. For example, the V and C proteins within the paramyxovirus family associate with the STAT family of transcription factors in order to inhibit the interferon response and NF- κ B activation (138). Influenza and Ebola virus encode proteins that bind and inhibit the activity of viral dsRNA, which is an important activator of the interferon response and NF- κ B (22, 60).

Poliovirus encodes two proteins that have been shown to inhibit the activation of NF- κ B. The poliovirus non-structural protein 3A has been shown to down-regulate TNFR from the cell surface through manipulation of the host protein trafficking machinery (121). Promoting removal of TNFR from the cell surface decreases sensitivity to TNF α induced NF- κ B activation. At this time, the mechanism by which 3A effects trafficking to down-regulate cell surface expression of the TNFR is unknown. However, 3A effects not only TNFR expression, but cell surface expression of a number of cellular proteins including peptide loaded MHC class I (32). Additionally the poliovirus 3C protease has been shown to specifically cleave p65 following the activation of NF- κ B in poliovirus infected cells (120). Cleaved p65 is incapable of promoting transcription of anti-viral and early innate immune genes. Poliovirus 3C induced cleavage of p65 begins early post infection, and cellular p65 is completely cleaved by 4 hours post infection. In a related mechanism, Coxsackie virus 3C^{pro} was shown to cleave I κ B α (191). At first glance, it appears that this mechanism may actually activate NF- κ B, as degradation of I κ B α should release NF- κ B dimers for nuclear translocation. However, in this case, the I κ B α cleavage

product translocates to the nucleus with the p65 transcription factor and inhibits transcriptional activation within the nucleus (191).

African swine fever virus (ASFV), a large dsDNA virus, encodes a homologue to cellular I κ B α (133). ASFV, like members of the *Poxviridae*, has a genome of roughly 200 kbps and encodes a large number of unique proteins that regulate host machinery. The A238L open reading frame is a homologue of cellular I κ B α that functions to inhibit NF- κ B activation (133). A38L has 21% identity and 40% homology to porcine I κ B α at the amino acid level. Following signaling induced degradation of I κ B α by the SCF ^{β -TRCP} ubiquitin ligase complex, A238L has been shown to bind the NF- κ B transcription factors p65 and p50, and functions to retain these proteins in the cytoplasm to prevent their nuclear transcriptional activity (166).

The HIV encoded protein, Vpu, functions to regulate the cellular SCF ^{β -TRCP} ubiquitin ligase complex and in turn, inhibit NF- κ B activation (12, 14). Vpu contains a phosphorylation motif that becomes dually phosphorylated in a similar fashion to SCF substrate proteins. Phosphorylation of Vpu leads to binding by the cellular F-box protein β -TRCP (12). Vpu functions to sequester β -TRCP and inhibits β -TRCP induced degradation of β -catenin and I κ B α amongst others (12). This manipulation of the SCF ^{β -TRCP} ubiquitin ligase leads to inhibition of NF- κ B activation in cells transfected with Vpu as well as cells infected with Vpu-expressing HIV (14). Data demonstrate that Vpu has no effect on the upstream activation of the IKK complex, but clearly inhibits the proteasomal degradation of I κ B α (14).

1.3.5 Poxvirus Inhibition of the NF- κ B Cascade

The inhibition of NF- κ B by poxviruses has become a growing area of interest (111). Poxviruses are renowned for the plethora of immune evasion mechanisms they encode including mechanisms that regulate NF- κ B (82, 111, 150). One of the first identified mediators of NF- κ B activation was M-T2, which encodes a soluble version of the tumor necrosis factor receptor (vTNFR)(158, 173). The myxoma virus encoded protein binds to rabbit TNF α to inhibit its association with the rabbit TNFR. Myxoma virus devoid of M-T2 is attenuated in rabbits demonstrating the importance of regulating NF- κ B during poxvirus infection (103). Additionally, a large family of poxvirus encoded cytokine receptors have been identified in the *Orthopoxviruses* called the cytokine response modifiers (Crm) (150). Crm proteins associate with TNF α from a variety of species. All *Orthopoxviruses* encode between one and four Crm proteins. Finally, a soluble IL-1 β receptor is encoded by VV and CPXV demonstrating the importance of inhibiting both IL-1 β and TNF α induced NF- κ B activation during poxvirus infection (1, 161).

The focus has more recently shifted to the identification of intracellular inhibitors of NF- κ B encoded by poxviruses (Figure 1.12)(111). VV encodes three proteins, A46, A52, and K7R which contain TIR domains and disrupt NF- κ B activation triggered through the IL-1R and TLR4 (17, 63, 148, 162). These proteins inhibit recruitment of MyD88 to the IL-1R and TLR4, therefore inhibiting recruitment of signaling molecules to the receptor complex.

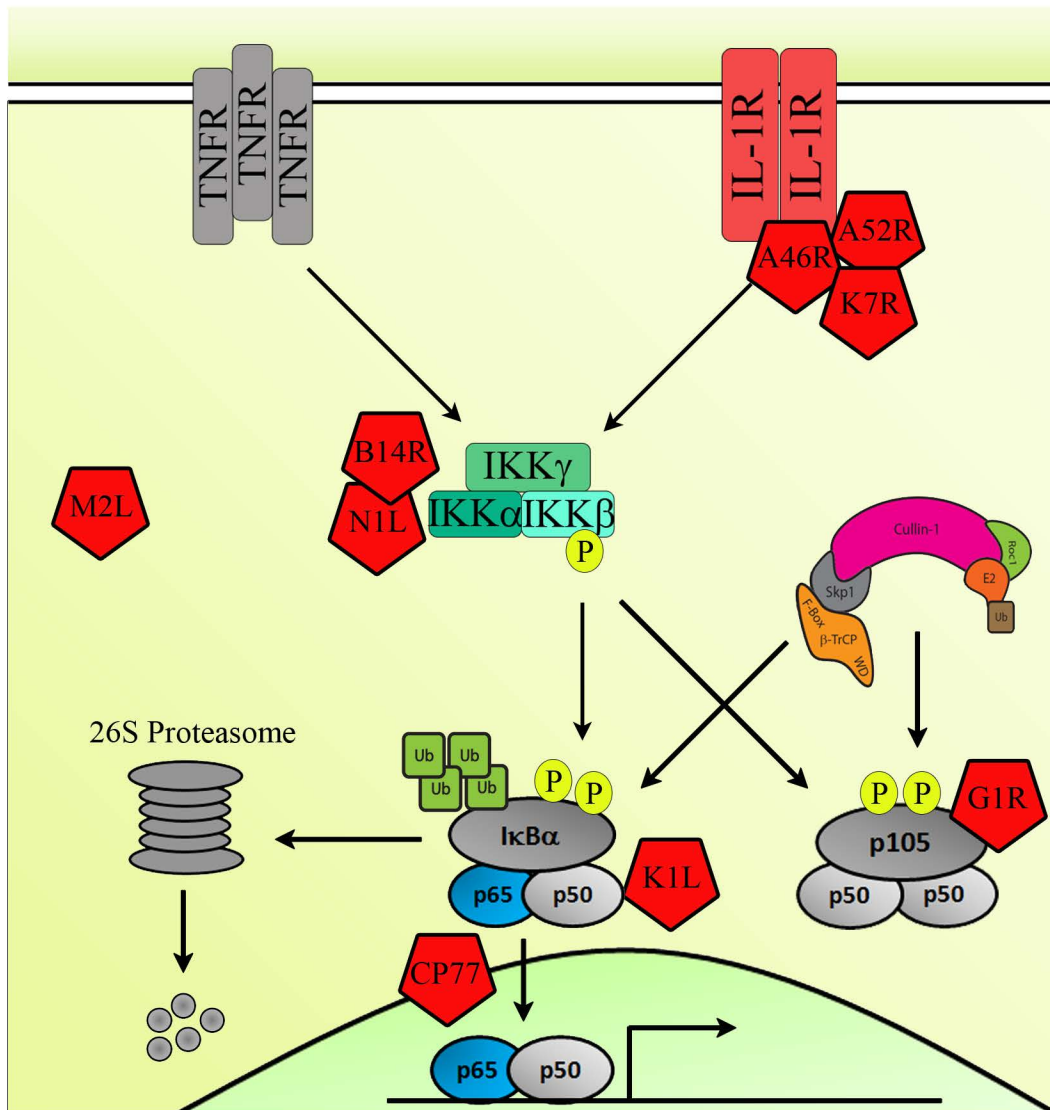


Figure 1.12. Intracellular inhibitors of NF- κ B activation. VV encodes A46R, K7R and A52R, three TIR containing proteins that inhibit recruitment of signalling adaptors to the IL-1R. VV also encodes N1L and B14R that inhibit NF- κ B signalling at the IKK complex. These proteins have unique functions that inhibit the phosphorylation of IKK β . K1L is also a VV encoded protein that consists of a series of ankyrin repeats. K1L inhibits I κ B α degradation through an unknown mechanism. Finally, VV encodes M2L, a protein that inhibits NF- κ B activation through the MEK/ERK pathway. CPXV encodes two proteins that have been shown to inhibit TNF α induced NF- κ B activation. G1R and CP77 are ankyrin/F-box proteins that have been shown to bind Skp1. G1R also binds p105, a member of the I κ B family of proteins that sequesters the p50/p50 homodimer in the cytoplasm. G1R is able to inhibit TNF α induced p105 degradation. Finally, CP77 is a known host range factor for CPXV containing the shortest known F-box domain at only 13 amino acids in length. CP77 has been shown to bind p65 through its ankyrin repeat domains. It is thought that CP77 binds p65 following I κ B α degradation to inhibit p65 nuclear translocation.

Additionally, four VV encoded proteins, B14R, M2L, K1L, and N1L, disrupt NF- κ B activation triggered through the TNFR pathway (26, 35, 52, 155). These proteins function at different points in the signaling cascade, clearly highlighting the importance of NF- κ B inhibition during poxvirus infection. B14R has been shown to associate with the IKK complex and specifically inhibit the phosphorylation of IKK β , therefore inhibiting canonical NF- κ B activation triggered through both TNF α and IL-1 β (26, 101). M2L has been shown to inhibit NF- κ B activation mediated by the mitogen activated protein kinase kinase (MEK) and extracellular signal regulated kinase (ERK) pathway (52). The K1L protein encoded by VV inhibits the degradation of I κ B α via unknown mechanisms (155). Finally, the N1L protein inhibits I κ B α degradation. N1L inhibits NF- κ B activation stimulated by TNF α , IL-1 β and lymphotoxin receptors by binding the IKK-like kinase TBK1 (35). TBK1 is also important for the activation of the IRF3 transcription factor following RIG-I activation. N1L also inhibits IRF3 activation during VV infection (35). Of interest to the Barry laboratory, ECTV does not encode orthologs to all of these VV encoded NF- κ B inhibitors. The M2L, K7R, A52R, and B14R genes in ECTV are either missing or truncated, suggesting that ECTV is either more susceptible to NF- κ B activation than VV or that ECTV encodes novel NF- κ B inhibitors.

CPXV encodes two ankyrin/F-box proteins that inhibit NF- κ B activation. These proteins are the host range factor CP77 and CPXV006, an ortholog of VARV encoded G1R (Figure 1.12). CP77 contains a very short, 13 amino acid F-box domain that is required to inhibit NF- κ B activation (25). Additionally, it

appears that CP77 binds to cellular p65 through its ankyrin repeat domains to inhibit nuclear translocation following degradation of I κ B α (25). Notably, this interaction was only demonstrated *in vitro*, as *in vivo* binding assays were inconclusive. The VARV encoded ortholog of CPXV006, G1R bound the NF- κ B inhibitory protein p105, as well as the SCF linker protein Skp1 in a large scale yeast-two-hybrid screen (112). Data demonstrate that G1R, CPXV006 and additional orthologs (including ECTV encoded EVM002) binding to p105 to inhibit its TNF α -induced degradation (112). p105 is a member of the I κ B family of inhibitory proteins, and inhibition of its degradation inhibits NF- κ B activation. Additionally, it was shown CPXV006 and G1R inhibit p65 nuclear translocation following TNF α stimulation (112, 113). Interestingly, neither CP77 nor CPXV006 require their F-box domains to inhibit NF- κ B activation.

1.4 The ECTV Encoded Ankyrin/F-box Proteins: Hypothesis

Using bioinformatics, we identified a family of four ankyrin/F-box proteins encoded by ECTV named EVM002, EVM005, EVM154 and EVM165. The ECTV proteins contain N-terminal ankyrin repeats in conjunction with a C-terminal F-box domain. This family of viral ankyrin/F-box proteins have been found in a wide range of poxviruses (105). To date, no cellular F-box proteins have been found in conjunction with ankyrin repeats, suggesting that poxviruses including ECTV have evolved a novel set of genes to regulate the cellular SCF complex. Multiple orthologs for EVM002, EVM154, and EVM165 exist in the *Orthopoxvirus* genus, however EVM005 has only one ortholog, CPXV-BR011,

encoded by cowpox virus strain Brighton Red. EVM005 and CPXV-BR011 may therefore play an important role specific to ECTV and CPXV. Following TNF α and IL-1 β stimulation, the degradation of I κ B α is catalyzed by the cellular SCF ^{β} -TRCP ubiquitin ligase. We investigate the role of EVM005 and the other ECTV encoded ankyrin/F-box proteins in the regulation of NF- κ B activation. We hypothesized that the ECTV encoded ankyrin/F-box proteins function to recruit novel virus-specific substrates to the cellular SCF complex for ubiquitylation and that regulation of the SCF complex can lead to the inhibition of I κ B α degradation and NF- κ B transcriptional activity.

1.5 References

1. **Alcami, A., and G. L. Smith.** 1992. A soluble receptor for interleukin-1 beta encoded by vaccinia virus: a novel mechanism of virus modulation of the host response to infection. *Cell* **71**:153-67.
2. **Ardley, H. C., and P. A. Robinson.** 2005. E3 ubiquitin ligases. *Essays Biochem* **41**:15-30.
3. **Bai, C., P. Sen, K. Hofmann, L. Ma, M. Goebel, J. W. Harper, and S. J. Elledge.** 1996. SKP1 connects cell cycle regulators to the ubiquitin proteolysis machinery through a novel motif, the F-box. *Cell* **86**:263-74.
4. **Banadyga, L., J. Gerig, T. Stewart, and M. Barry.** 2007. Fowlpox virus encodes a Bcl-2 homologue that protects cells from apoptotic death through interaction with the proapoptotic protein Bak. *J Virol* **81**:11032-45.
5. **Banadyga, L., S. C. Lam, T. Okamoto, M. Kvensakul, D. C. Huang, and M. Barry.** 2011. Deerpox virus encodes an inhibitor of apoptosis that regulates Bak and Bax. *J Virol* **85**:1922-34.
6. **Banadyga, L., K. Veugelers, S. Campbell, and M. Barry.** 2009. The fowlpox virus BCL-2 homologue, FPV039, interacts with activated Bax and a discrete subset of BH3-only proteins to inhibit apoptosis. *J Virol* **83**:7085-98.
7. **Barry, M., and K. Fruh.** 2006. Viral modulators of cullin RING ubiquitin ligases: culling the host defense. *Sci STKE* **2006**:pe21.
8. **Barry, M., N. van Buuren, K. Burles, K. Mottet, Q. Wang, and A. Teale.** 2010. Poxvirus exploitation of the ubiquitin-proteasome system. *Viruses* **2**:2356-80.

9. **Bawden, A. L., K. J. Glassberg, J. Diggans, R. Shaw, W. Farmerie, and R. W. Moyer.** 2000. Complete genomic sequence of the Amsacta moorei entomopoxvirus: analysis and comparison with other poxviruses. *Virology* **274**:120-39.
10. **Beaudenon, S., and J. M. Huibregtse.** 2008. HPV E6, E6AP and cervical cancer. *BMC Biochem* **9 Suppl 1**:S4.
11. **Bertrand, M. J., S. Milutinovic, K. M. Dickson, W. C. Ho, A. Boudreault, J. Durkin, J. W. Gillard, J. B. Jaquith, S. J. Morris, and P. A. Barker.** 2008. cIAP1 and cIAP2 facilitate cancer cell survival by functioning as E3 ligases that promote RIP1 ubiquitination. *Mol Cell* **30**:689-700.
12. **Besnard-Guerin, C., N. Belaidouni, I. Lassot, E. Segeal, A. Jobart, C. Marchal, and R. Benarous.** 2004. HIV-1 Vpu sequesters beta-transducin repeat-containing protein (betaTrCP) in the cytoplasm and provokes the accumulation of beta-catenin and other SCFbetaTrCP substrates. *J Biol Chem* **279**:788-95.
13. **Blanchette, P., C. Y. Cheng, Q. Yan, G. Ketner, D. A. Ornelles, T. Dobner, R. C. Conaway, J. W. Conaway, and P. E. Branton.** 2004. Both BC-box motifs of adenovirus protein E4orf6 are required to efficiently assemble an E3 ligase complex that degrades p53. *Mol Cell Biol* **24**:9619-29.
14. **Bour, S., C. Perrin, H. Akari, and K. Strebel.** 2001. The human immunodeficiency virus type 1 Vpu protein inhibits NF-kappa B activation by interfering with beta TrCP-mediated degradation of Ikappa B. *J Biol Chem* **276**:15920-8.
15. **Boutell, C., A. Orr, and R. D. Everett.** 2003. PML residue lysine 160 is required for the degradation of PML induced by herpes simplex virus type 1 regulatory protein ICP0. *J Virol* **77**:8686-94.
16. **Boutell, C., S. Sadis, and R. D. Everett.** 2002. Herpes simplex virus type 1 immediate-early protein ICP0 and its isolated RING finger domain act as ubiquitin E3 ligases in vitro. *J Virol* **76**:841-50.
17. **Bowie, A., E. Kiss-Toth, J. A. Symons, G. L. Smith, S. K. Dower, and L. A. O'Neill.** 2000. A46R and A52R from vaccinia virus are antagonists of host IL-1 and toll-like receptor signaling. *Proc Natl Acad Sci U S A* **97**:10162-7.
18. **Briody, B. A., T. S. Hauschka, and E. A. Mirand.** 1956. The role of genotype in resistance to an epizootic of mouse pox (ectromelia). *Am J Hyg* **63**:59-68.
19. **Brummelkamp, T. R., S. M. Nijman, A. M. Dirac, and R. Bernards.** 2003. Loss of the cylindromatosis tumour suppressor inhibits apoptosis by activating NF-kappaB. *Nature* **424**:797-801.
20. **Cahir McFarland, E. D., K. M. Izumi, and G. Mosialos.** 1999. Epstein-barr virus transformation: involvement of latent membrane protein 1-mediated activation of NF-kappaB. *Oncogene* **18**:6959-64.
21. **Campbell, S., B. Hazes, M. Kvensakul, P. Colman, and M. Barry.** 2010. Vaccinia virus F1L interacts with Bak using highly divergent Bcl-2

- homology domains and replaces the function of Mcl-1. *J Biol Chem* **285**:4695-708.
22. **Cardenas, W. B., Y. M. Loo, M. Gale, Jr., A. L. Hartman, C. R. Kimberlin, L. Martinez-Sobrido, E. O. Saphire, and C. F. Basler.** 2006. Ebola virus VP35 protein binds double-stranded RNA and inhibits alpha/beta interferon production induced by RIG-I signaling. *J Virol* **80**:5168-78.
 23. **Cardozo, T., and M. Pagano.** 2004. The SCF ubiquitin ligase: insights into a molecular machine. *Nat Rev Mol Cell Biol* **5**:739-51.
 24. **Chang, H. W., J. C. Watson, and B. L. Jacobs.** 1992. The E3L gene of vaccinia virus encodes an inhibitor of the interferon-induced, double-stranded RNA-dependent protein kinase. *Proc Natl Acad Sci U S A* **89**:4825-9.
 25. **Chang, S. J., J. C. Hsiao, S. Sonnberg, C. T. Chiang, M. H. Yang, D. L. Tzou, A. A. Mercer, and W. Chang.** 2009. Poxvirus host range protein CP77 contains an F-box-like domain that is necessary to suppress NF-kappaB activation by tumor necrosis factor alpha but is independent of its host range function. *J Virol* **83**:4140-52.
 26. **Chen, R. A., G. Ryzhakov, S. Cooray, F. Randow, and G. L. Smith.** 2008. Inhibition of IkappaB kinase by vaccinia virus virulence factor B14. *PLoS Pathog* **4**:e22.
 27. **Conze, D. B., C. J. Wu, J. A. Thomas, A. Landstrom, and J. D. Ashwell.** 2008. Lys63-linked polyubiquitination of IRAK-1 is required for interleukin-1 receptor- and toll-like receptor-mediated NF-kappaB activation. *Mol Cell Biol* **28**:3538-47.
 28. **Cordier, F., O. Grubisha, F. Traincard, M. Veron, M. Delepierre, and F. Agou.** 2009. The zinc finger of NEMO is a functional ubiquitin-binding domain. *J Biol Chem* **284**:2902-7.
 29. **D'Acquisto, F., and S. Ghosh.** 2001. PACT and PKR: turning on NF-kappa B in the absence of virus. *Sci STKE* **2001**:re1.
 30. **Damon, I. K.** 2007. Poxviruses. *In* D. a. P. H. Knipe (ed.), *Field's Virology*, 5 ed. Lippincott Williams & Wilkins.
 31. **David, Y., N. Ternette, M. J. Edelmann, T. Ziv, B. Gayer, R. Sertchook, Y. Dadon, B. M. Kessler, and A. Navon.** 2011. E3 Ligases Determine the Ubiquitination Site and Conjugate Type by Enforcing Specificity on E2 Enzymes. *J Biol Chem*.
 32. **Deitz, S. B., D. A. Dodd, S. Cooper, P. Parham, and K. Kirkegaard.** 2000. MHC I-dependent antigen presentation is inhibited by poliovirus protein 3A. *Proc Natl Acad Sci U S A* **97**:13790-5.
 33. **Delano, M. L., and D. G. Brownstein.** 1995. Innate resistance to lethal mousepox is genetically linked to the NK gene complex on chromosome 6 and correlates with early restriction of virus replication by cells with an NK phenotype. *J Virol* **69**:5875-7.
 34. **Dikic, I., S. Wakatsuki, and K. J. Walters.** 2009. Ubiquitin-binding domains - from structures to functions. *Nat Rev Mol Cell Biol* **10**:659-71.

35. **DiPerna, G., J. Stack, A. G. Bowie, A. Boyd, G. Kotwal, Z. Zhang, S. Arvikar, E. Latz, K. A. Fitzgerald, and W. L. Marshall.** 2004. Poxvirus protein N1L targets the I-kappaB kinase complex, inhibits signaling to NF-kappaB by the tumor necrosis factor superfamily of receptors, and inhibits NF-kappaB and IRF3 signaling by toll-like receptors. *J Biol Chem* **279**:36570-8.
36. **Dobner, T., N. Horikoshi, S. Rubenwolf, and T. Shenk.** 1996. Blockage by adenovirus E4orf6 of transcriptional activation by the p53 tumor suppressor. *Science* **272**:1470-3.
37. **Ea, C. K., L. Deng, Z. P. Xia, G. Pineda, and Z. J. Chen.** 2006. Activation of IKK by TNFalpha requires site-specific ubiquitination of RIP1 and polyubiquitin binding by NEMO. *Mol Cell* **22**:245-57.
38. **Earp, L. J., S. E. Delos, H. E. Park, and J. M. White.** 2005. The many mechanisms of viral membrane fusion proteins. *Curr Top Microbiol Immunol* **285**:25-66.
39. **Esteban, D. J., and R. M. Buller.** 2005. Ectromelia virus: the causative agent of mousepox. *J Gen Virol* **86**:2645-59.
40. **Estrabaud, E., E. Le Rouzic, S. Lopez-Verges, M. Morel, N. Belaidouni, R. Benarous, C. Transy, C. Berlioz-Torrent, and F. Margottin-Goguet.** 2007. Regulated degradation of the HIV-1 Vpu protein through a betaTrCP-independent pathway limits the release of viral particles. *PLoS Pathog* **3**:e104.
41. **Everett, R. D., P. Barlow, A. Milner, B. Luisi, A. Orr, G. Hope, and D. Lyon.** 1993. A novel arrangement of zinc-binding residues and secondary structure in the C3HC4 motif of an alpha herpes virus protein family. *J Mol Biol* **234**:1038-47.
42. **Everett, R. D., and G. G. Maul.** 1994. HSV-1 IE protein Vmw110 causes redistribution of PML. *EMBO J* **13**:5062-9.
43. **Fan, Y., Y. Yu, Y. Shi, W. Sun, M. Xie, N. Ge, R. Mao, A. Chang, G. Xu, M. D. Schneider, H. Zhang, S. Fu, J. Qin, and J. Yang.** 2010. Lysine 63-linked polyubiquitination of TAK1 at lysine 158 is required for tumor necrosis factor alpha- and interleukin-1beta-induced IKK/NF-kappaB and JNK/AP-1 activation. *J Biol Chem* **285**:5347-60.
44. **Fang, M., L. L. Lanier, and L. J. Sigal.** 2008. A role for NKG2D in NK cell-mediated resistance to poxvirus disease. *PLoS Pathog* **4**:e30.
45. **Fang, M., M. T. Orr, P. Spee, T. Egebjerg, L. L. Lanier, and L. J. Sigal.** 2011. CD94 is essential for NK cell-mediated resistance to a lethal viral disease. *Immunity* **34**:579-89.
46. **Fenner, F., DA Henderson, I Arita, Z Jezek, and ID Ladnyi.** 1988. Smallpox and its Eradication. World Health Organization.
47. **Finley, D., A. Ciechanover, and A. Varshavsky.** 1984. Thermolability of ubiquitin-activating enzyme from the mammalian cell cycle mutant ts85. *Cell* **37**:43-55.
48. **Frescas, D., and M. Pagano.** 2008. Deregulated proteolysis by the F-box proteins SKP2 and beta-TrCP: tipping the scales of cancer. *Nat Rev Cancer* **8**:438-49.

49. **Furukawa, M., Y. Zhang, J. McCarville, T. Ohta, and Y. Xiong.** 2000. The CUL1 C-terminal sequence and ROC1 are required for efficient nuclear accumulation, NEDD8 modification, and ubiquitin ligase activity of CUL1. *Mol Cell Biol* **20**:8185-97.
50. **Gabuzda, D. H., K. Lawrence, E. Langhoff, E. Terwilliger, T. Dorfman, W. A. Haseltine, and J. Sodroski.** 1992. Role of vif in replication of human immunodeficiency virus type 1 in CD4+ T lymphocytes. *J Virol* **66**:6489-95.
51. **Gagne, J. M., B. P. Downes, S. H. Shiu, A. M. Durski, and R. D. Vierstra.** 2002. The F-box subunit of the SCF E3 complex is encoded by a diverse superfamily of genes in Arabidopsis. *Proc Natl Acad Sci U S A* **99**:11519-24.
52. **Gedey, R., X. L. Jin, O. Hinthong, and J. L. Shisler.** 2006. Poxviral regulation of the host NF-kappaB response: the vaccinia virus M2L protein inhibits induction of NF-kappaB activation via an ERK2 pathway in virus-infected human embryonic kidney cells. *J Virol* **80**:8676-85.
53. **Glotzer, M., A. W. Murray, and M. W. Kirschner.** 1991. Cyclin is degraded by the ubiquitin pathway. *Nature* **349**:132-8.
54. **Goila-Gaur, R., and K. Strebel.** 2008. HIV-1 Vif, APOBEC, and intrinsic immunity. *Retrovirology* **5**:51.
55. **Gubser, C., S. Hue, P. Kellam, and G. L. Smith.** 2004. Poxvirus genomes: a phylogenetic analysis. *J Gen Virol* **85**:105-17.
56. **Guerin, J. L., J. Gelfi, S. Boullier, M. Delverdier, F. A. Bellanger, S. Bertagnoli, I. Drexler, G. Sutter, and F. Messud-Petit.** 2002. Myxoma virus leukemia-associated protein is responsible for major histocompatibility complex class I and Fas-CD95 down-regulation and defines scrapins, a new group of surface cellular receptor abductor proteins. *J Virol* **76**:2912-23.
57. **Hagglund, R., and B. Roizman.** 2002. Characterization of the novel E3 ubiquitin ligase encoded in exon 3 of herpes simplex virus-1-infected cell protein 0. *Proc Natl Acad Sci U S A* **99**:7889-94.
58. **Hagglund, R., and B. Roizman.** 2003. Herpes simplex virus 1 mutant in which the ICPO HUL-1 E3 ubiquitin ligase site is disrupted stabilizes cdc34 but degrades D-type cyclins and exhibits diminished neurotoxicity. *J Virol* **77**:13194-202.
59. **Hagglund, R., C. Van Sant, P. Lopez, and B. Roizman.** 2002. Herpes simplex virus 1-infected cell protein 0 contains two E3 ubiquitin ligase sites specific for different E2 ubiquitin-conjugating enzymes. *Proc Natl Acad Sci U S A* **99**:631-6.
60. **Hale, B. G., R. E. Randall, J. Ortin, and D. Jackson.** 2008. The multifunctional NS1 protein of influenza A viruses. *J Gen Virol* **89**:2359-76.
61. **Handley-Gearhart, P. M., A. G. Stephen, J. S. Trausch-Azar, A. Ciechanover, and A. L. Schwartz.** 1994. Human ubiquitin-activating enzyme, E1. Indication of potential nuclear and cytoplasmic

- subpopulations using epitope-tagged cDNA constructs. *J Biol Chem* **269**:33171-8.
62. **Harhaj, E. W., and V. M. Dixit.** 2011. Deubiquitinases in the regulation of NF-kappaB signaling. *Cell Res* **21**:22-39.
 63. **Harte, M. T., I. R. Haga, G. Maloney, P. Gray, P. C. Reading, N. W. Bartlett, G. L. Smith, A. Bowie, and L. A. O'Neill.** 2003. The poxvirus protein A52R targets Toll-like receptor signaling complexes to suppress host defense. *J Exp Med* **197**:343-51.
 64. **Hayden, M. S., and S. Ghosh.** 2008. Shared principles in NF-kappaB signaling. *Cell* **132**:344-62.
 65. **Hermant, D.** 2006. F-box proteins: more than baits for the SCF? *Cell Div* **1**:30.
 66. **Hershko, A., and A. Ciechanover.** 1998. The ubiquitin system. *Annu Rev Biochem* **67**:425-79.
 67. **Hicke, L.** 2001. Protein regulation by monoubiquitin. *Nat Rev Mol Cell Biol* **2**:195-201.
 68. **Hiscott, J., H. Kwon, and P. Genin.** 2001. Hostile takeovers: viral appropriation of the NF-kappaB pathway. *J Clin Invest* **107**:143-51.
 69. **Hiscott, J., T. L. Nguyen, M. Arguello, P. Nakhaei, and S. Paz.** 2006. Manipulation of the nuclear factor-kappaB pathway and the innate immune response by viruses. *Oncogene* **25**:6844-67.
 70. **Hoffmann, A., G. Natoli, and G. Ghosh.** 2006. Transcriptional regulation via the NF-kappaB signaling module. *Oncogene* **25**:6706-16.
 71. **Hofmann, R. M., and C. M. Pickart.** 1999. Noncanonical MMS2-encoded ubiquitin-conjugating enzyme functions in assembly of novel polyubiquitin chains for DNA repair. *Cell* **96**:645-53.
 72. **Huang, J., Q. Huang, X. Zhou, M. M. Shen, A. Yen, S. X. Yu, G. Dong, K. Qu, P. Huang, E. M. Anderson, S. Daniel-Issakani, R. M. Buller, D. G. Payan, and H. H. Lu.** 2004. The poxvirus p28 virulence factor is an E3 ubiquitin ligase. *J Biol Chem* **279**:54110-6.
 73. **Huibregtse, J. M., M. Scheffner, S. Beaudenon, and P. M. Howley.** 1995. A family of proteins structurally and functionally related to the E6-AP ubiquitin-protein ligase. *Proc Natl Acad Sci U S A* **92**:2563-7.
 74. **Ikeda, F., N. Crosetto, and I. Dikic.** 2010. What determines the specificity and outcomes of ubiquitin signaling? *Cell* **143**:677-81.
 75. **Isaacson, M. K., and H. L. Ploegh.** 2009. Ubiquitination, ubiquitin-like modifiers, and deubiquitination in viral infection. *Cell Host Microbe* **5**:559-70.
 76. **Iwai, K., and F. Tokunaga.** 2009. Linear polyubiquitination: a new regulator of NF-kappaB activation. *EMBO Rep* **10**:706-13.
 77. **Iyer, L. M., E. V. Koonin, and L. Aravind.** 2002. Extensive domain shuffling in transcription regulators of DNA viruses and implications for the origin of fungal APSES transcription factors. *Genome Biol* **3**:RESEARCH0012.

78. **Jackson, R., and I. Ramshaw.** 2010. The mousepox experience. An interview with Ronald Jackson and Ian Ramshaw on dual-use research. Interview by Michael J. Selgelid and Lorna Weir. *EMBO Rep* **11**:18-24.
79. **Jackson, R. J., A. J. Ramsay, C. D. Christensen, S. Beaton, D. F. Hall, and I. A. Ramshaw.** 2001. Expression of mouse interleukin-4 by a recombinant ectromelia virus suppresses cytolytic lymphocyte responses and overcomes genetic resistance to mousepox. *J Virol* **75**:1205-10.
80. **Jenner, E.** 1798. An enquiry into the causes and effects of variolae vaccinae, a disease discovered in some of the western counties of England, particularly Gloucestershire, and known by the name of cowpox.
81. **Jentsch, S., W. Seufert, and H. P. Hauser.** 1991. Genetic analysis of the ubiquitin system. *Biochim Biophys Acta* **1089**:127-39.
82. **Johnston, J. B., and G. McFadden.** 2003. Poxvirus immunomodulatory strategies: current perspectives. *J Virol* **77**:6093-100.
83. **Johnston, J. B., G. Wang, J. W. Barrett, S. H. Nazarian, K. Colwill, M. Moran, and G. McFadden.** 2005. Myxoma virus M-T5 protects infected cells from the stress of cell cycle arrest through its interaction with host cell cullin-1. *J Virol* **79**:10750-63.
84. **Kamura, T., M. N. Conrad, Q. Yan, R. C. Conaway, and J. W. Conaway.** 1999. The Rbx1 subunit of SCF and VHL E3 ubiquitin ligase activates Rub1 modification of cullins Cdc53 and Cul2. *Genes Dev* **13**:2928-33.
85. **Kattenhorn, L. M., G. A. Korbel, B. M. Kessler, E. Spooner, and H. L. Ploegh.** 2005. A deubiquitinating enzyme encoded by HSV-1 belongs to a family of cysteine proteases that is conserved across the family Herpesviridae. *Mol Cell* **19**:547-57.
86. **Kipreos, E. T., L. E. Lander, J. P. Wing, W. W. He, and E. M. Hedgecock.** 1996. cul-1 is required for cell cycle exit in *C. elegans* and identifies a novel gene family. *Cell* **85**:829-39.
87. **Koegl, M., T. Hoppe, S. Schlenker, H. D. Ulrich, T. U. Mayer, and S. Jentsch.** 1999. A novel ubiquitination factor, E4, is involved in multiubiquitin chain assembly. *Cell* **96**:635-44.
88. **Komander, D., M. J. Clague, and S. Urbe.** 2009. Breaking the chains: structure and function of the deubiquitinases. *Nat Rev Mol Cell Biol* **10**:550-63.
89. **Latres, E., D. S. Chiaur, and M. Pagano.** 1999. The human F box protein beta-Trcp associates with the Cul1/Skp1 complex and regulates the stability of beta-catenin. *Oncogene* **18**:849-54.
90. **Lee, E. G., D. L. Boone, S. Chai, S. L. Libby, M. Chien, J. P. Lodolce, and A. Ma.** 2000. Failure to regulate TNF-induced NF-kappaB and cell death responses in A20-deficient mice. *Science* **289**:2350-4.
91. **Lee, S. B., and M. Esteban.** 1994. The interferon-induced double-stranded RNA-activated protein kinase induces apoptosis. *Virology* **199**:491-6.
92. **Lefkowitz, E. J., C. Wang, and C. Upton.** 2006. Poxviruses: past, present and future. *Virus Res* **117**:105-18.

93. **Leverson, J. D., C. A. Joazeiro, A. M. Page, H. Huang, P. Hieter, and T. Hunter.** 2000. The APC11 RING-H2 finger mediates E2-dependent ubiquitination. *Mol Biol Cell* **11**:2315-25.
94. **Liu, J., M. Furukawa, T. Matsumoto, and Y. Xiong.** 2002. NEDD8 modification of CUL1 dissociates p120(CAND1), an inhibitor of CUL1-SKP1 binding and SCF ligases. *Mol Cell* **10**:1511-8.
95. **Liu, S., and Z. J. Chen.** 2011. Expanding role of ubiquitination in NF-kappaB signaling. *Cell Res* **21**:6-21.
96. **Mansouri, M., E. Bartee, K. Gouveia, B. T. Hovey Nerenberg, J. Barrett, L. Thomas, G. Thomas, G. McFadden, and K. Fruh.** 2003. The PHD/LAP-domain protein M153R of myxomavirus is a ubiquitin ligase that induces the rapid internalization and lysosomal destruction of CD4. *J Virol* **77**:1427-40.
97. **Marchal, J.** 1930. Infectious Ectromelia. *J. Pathol. Bacteriol.* **33**:713-28.
98. **Maul, G. G., and R. D. Everett.** 1994. The nuclear location of PML, a cellular member of the C3HC4 zinc-binding domain protein family, is rearranged during herpes simplex virus infection by the C3HC4 viral protein ICP0. *J Gen Virol* **75 (Pt 6)**:1223-33.
99. **Maul, G. G., H. H. Guldner, and J. G. Spivack.** 1993. Modification of discrete nuclear domains induced by herpes simplex virus type 1 immediate early gene 1 product (ICP0). *J Gen Virol* **74 (Pt 12)**:2679-90.
100. **Maul, G. G., A. M. Ishov, and R. D. Everett.** 1996. Nuclear domain 10 as preexisting potential replication start sites of herpes simplex virus type-1. *Virology* **217**:67-75.
101. **McCoy, L. E., A. S. Fahy, R. A. Chen, and G. L. Smith.** 2010. Mutations in modified virus Ankara protein 183 render it a non-functional counterpart of B14, an inhibitor of nuclear factor kappaB activation. *J Gen Virol* **91**:2216-20.
102. **McFadden, G.** 2005. Poxvirus tropism. *Nat Rev Microbiol* **3**:201-13.
103. **McFadden, G., M. Schreiber, and L. Sedger.** 1997. Myxoma T2 protein as a model for poxvirus TNF receptor homologs. *J Neuroimmunol* **72**:119-26.
104. **Meierhofer, D., X. Wang, L. Huang, and P. Kaiser.** 2008. Quantitative analysis of global ubiquitination in HeLa cells by mass spectrometry. *J Proteome Res* **7**:4566-76.
105. **Mercer, A. A., S. B. Fleming, and N. Ueda.** 2005. F-box-like domains are present in most poxvirus ankyrin repeat proteins. *Virus Genes* **31**:127-33.
106. **Mercer, J., and A. Helenius.** 2008. Vaccinia virus uses macropinocytosis and apoptotic mimicry to enter host cells. *Science* **320**:531-5.
107. **Mercer, J., S. Knebel, F. I. Schmidt, J. Crouse, C. Burkard, and A. Helenius.** 2010. Vaccinia virus strains use distinct forms of macropinocytosis for host-cell entry. *Proc Natl Acad Sci U S A* **107**:9346-51.

108. **Michel, J. J., and Y. Xiong.** 1998. Human CUL-1, but not other cullin family members, selectively interacts with SKP1 to form a complex with SKP2 and cyclin A. *Cell Growth Differ* **9**:435-49.
109. **Minella, A. C., and B. E. Clurman.** 2005. Mechanisms of tumor suppression by the SCF(Fbw7). *Cell Cycle* **4**:1356-9.
110. **Mo, M., S. B. Fleming, and A. A. Mercer.** 2009. Cell cycle deregulation by a poxvirus partial mimic of anaphase-promoting complex subunit 11. *Proc Natl Acad Sci U S A* **106**:19527-32.
111. **Mohamed, M. R., and G. McFadden.** 2009. NFkB inhibitors: strategies from poxviruses. *Cell Cycle* **8**:3125-32.
112. **Mohamed, M. R., M. M. Rahman, J. S. Lanchbury, D. Shattuck, C. Neff, M. Dufford, N. van Buuren, K. Fagan, M. Barry, S. Smith, I. Damon, and G. McFadden.** 2009. Proteomic screening of variola virus reveals a unique NF-kappaB inhibitor that is highly conserved among pathogenic orthopoxviruses. *Proc Natl Acad Sci U S A* **106**:9045-50.
113. **Mohamed, M. R., M. M. Rahman, A. Rice, R. W. Moyer, S. J. Werden, and G. McFadden.** 2009. Cowpox virus expresses a novel ankyrin repeat NF-kappaB inhibitor that controls inflammatory cell influx into virus-infected tissues and is critical for virus pathogenesis. *J Virol* **83**:9223-36.
114. **Moss, B.** 2007. Poxviridae: The Viruses and Their Replication. *In* D. a. P. H. Knipe (ed.), *Fields Virology*, 5 ed. Lippincott Williams & Wilkins.
115. **Moss, B.** 2006. Poxvirus entry and membrane fusion. *Virology* **344**:48-54.
116. **Nakayama, K. I., S. Hatakeyama, and K. Nakayama.** 2001. Regulation of the cell cycle at the G1-S transition by proteolysis of cyclin E and p27Kip1. *Biochem Biophys Res Commun* **282**:853-60.
117. **Nakayama, K. I., and K. Nakayama.** 2006. Ubiquitin ligases: cell-cycle control and cancer. *Nat Rev Cancer* **6**:369-81.
118. **Nasmyth, K.** 2001. Disseminating the genome: joining, resolving, and separating sister chromatids during mitosis and meiosis. *Annu Rev Genet* **35**:673-745.
119. **Nerenberg, B. T., J. Taylor, E. Bartee, K. Gouveia, M. Barry, and K. Fruh.** 2005. The poxviral RING protein p28 is a ubiquitin ligase that targets ubiquitin to viral replication factories. *J Virol* **79**:597-601.
120. **Neznanov, N., K. M. Chumakov, L. Neznanova, A. Almasan, A. K. Banerjee, and A. V. Gudkov.** 2005. Proteolytic cleavage of the p65-RelA subunit of NF-kappaB during poliovirus infection. *J Biol Chem* **280**:24153-8.
121. **Neznanov, N., A. Kondratova, K. M. Chumakov, B. Angres, B. Zhumabayeva, V. I. Agol, and A. V. Gudkov.** 2001. Poliovirus protein 3A inhibits tumor necrosis factor (TNF)-induced apoptosis by eliminating the TNF receptor from the cell surface. *J Virol* **75**:10409-20.
122. **Ohta, T., J. J. Michel, A. J. Schottelius, and Y. Xiong.** 1999. ROC1, a homolog of APC11, represents a family of cullin partners with an associated ubiquitin ligase activity. *Mol Cell* **3**:535-41.

123. **Ozkaynak, E., D. Finley, M. J. Solomon, and A. Varshavsky.** 1987. The yeast ubiquitin genes: a family of natural gene fusions. *EMBO J* **6**:1429-39.
124. **Parker, A. K., S. Parker, W. M. Yokoyama, J. A. Corbett, and R. M. Buller.** 2007. Induction of natural killer cell responses by ectromelia virus controls infection. *J Virol* **81**:4070-9.
125. **Parker, S., A. Nuara, R. M. Buller, and D. A. Schultz.** 2007. Human monkeypox: an emerging zoonotic disease. *Future Microbiol* **2**:17-34.
126. **Parker, S., A. M. Siddiqui, C. Oberle, E. Hembrador, R. Lanier, G. Painter, A. Robertson, and R. M. Buller.** 2009. Mousepox in the C57BL/6 strain provides an improved model for evaluating anti-poxvirus therapies. *Virology* **385**:11-21.
127. **Perdiguero, B., and M. Esteban.** 2009. The interferon system and vaccinia virus evasion mechanisms. *J Interferon Cytokine Res* **29**:581-98.
128. **Perkus, M. E., S. J. Goebel, S. W. Davis, G. P. Johnson, K. Limbach, E. K. Norton, and E. Paoletti.** 1990. Vaccinia virus host range genes. *Virology* **179**:276-86.
129. **Peters, J. M.** 2006. The anaphase promoting complex/cyclosome: a machine designed to destroy. *Nat Rev Mol Cell Biol* **7**:644-56.
130. **Petroski, M. D., and R. J. Deshaies.** 2005. Function and regulation of cullin-RING ubiquitin ligases. *Nat Rev Mol Cell Biol* **6**:9-20.
131. **Pfleger, C. M., and M. W. Kirschner.** 2000. The KEN box: an APC recognition signal distinct from the D box targeted by Cdh1. *Genes Dev* **14**:655-65.
132. **Pickart, C. M., and D. Fushman.** 2004. Polyubiquitin chains: polymeric protein signals. *Curr Opin Chem Biol* **8**:610-6.
133. **Powell, P. P., L. K. Dixon, and R. M. Parkhouse.** 1996. An IkappaB homolog encoded by African swine fever virus provides a novel mechanism for downregulation of proinflammatory cytokine responses in host macrophages. *J Virol* **70**:8527-33.
134. **Querido, E., R. C. Marcellus, A. Lai, R. Charbonneau, J. G. Teodoro, G. Ketner, and P. E. Branton.** 1997. Regulation of p53 levels by the E1B 55-kilodalton protein and E4orf6 in adenovirus-infected cells. *J Virol* **71**:3788-98.
135. **Quyen, D. V., S. C. Ha, K. Lowenhaupt, A. Rich, K. K. Kim, and Y. G. Kim.** 2007. Characterization of DNA-binding activity of Z alpha domains from poxviruses and the importance of the beta-wing regions in converting B-DNA to Z-DNA. *Nucleic Acids Res* **35**:7714-20.
136. **Rahighi, S., F. Ikeda, M. Kawasaki, M. Akutsu, N. Suzuki, R. Kato, T. Kensche, T. Uejima, S. Bloor, D. Komander, F. Randow, S. Wakatsuki, and I. Dikic.** 2009. Specific recognition of linear ubiquitin chains by NEMO is important for NF-kappaB activation. *Cell* **136**:1098-109.
137. **Rahman, M. M., and G. McFadden.** 2011. Modulation of NF-kappaB signalling by microbial pathogens. *Nat Rev Microbiol* **9**:291-306.

138. **Ramachandran, A., and C. M. Horvath.** 2009. Paramyxovirus disruption of interferon signal transduction: STATus report. *J Interferon Cytokine Res* **29**:531-7.
139. **Ramsey-Ewing, A. L., and B. Moss.** 1996. Complementation of a vaccinia virus host-range K1L gene deletion by the nonhomologous CP77 gene. *Virology* **222**:75-86.
140. **Ravid, T., and M. Hochstrasser.** 2004. NF-kappaB signaling: flipping the switch with polyubiquitin chains. *Curr Biol* **14**:R898-900.
141. **Redman, K. L., and M. Rechsteiner.** 1989. Identification of the long ubiquitin extension as ribosomal protein S27a. *Nature* **338**:438-40.
142. **Romano, P. R., F. Zhang, S. L. Tan, M. T. Garcia-Barrio, M. G. Katze, T. E. Dever, and A. G. Hinnebusch.** 1998. Inhibition of double-stranded RNA-dependent protein kinase PKR by vaccinia virus E3: role of complex formation and the E3 N-terminal domain. *Mol Cell Biol* **18**:7304-16.
143. **Roulston, A., R. Lin, P. Beauparlant, M. A. Wainberg, and J. Hiscott.** 1995. Regulation of human immunodeficiency virus type 1 and cytokine gene expression in myeloid cells by NF-kappa B/Rel transcription factors. *Microbiol Rev* **59**:481-505.
144. **Scheffner, M., J. M. Huibregtse, R. D. Vierstra, and P. M. Howley.** 1993. The HPV-16 E6 and E6-AP complex functions as a ubiquitin-protein ligase in the ubiquitination of p53. *Cell* **75**:495-505.
145. **Schlee, M., E. Hartmann, C. Coch, V. Wimmenauer, M. Janke, W. Barchet, and G. Hartmann.** 2009. Approaching the RNA ligand for RIG-I? *Immunol Rev* **227**:66-74.
146. **Schmelz, M., B. Sodeik, M. Ericsson, E. J. Wolffe, H. Shida, G. Hiller, and G. Griffiths.** 1994. Assembly of vaccinia virus: the second wrapping cisterna is derived from the trans Golgi network. *J Virol* **68**:130-47.
147. **Schmidt, M. W., P. R. McQuary, S. Wee, K. Hofmann, and D. A. Wolf.** 2009. F-box-directed CRL complex assembly and regulation by the CSN and CAND1. *Mol Cell* **35**:586-97.
148. **Schroder, M., M. Baran, and A. G. Bowie.** 2008. Viral targeting of DEAD box protein 3 reveals its role in TBK1/IKKepsilon-mediated IRF activation. *EMBO J* **27**:2147-57.
149. **Schulman, B. A., A. C. Carrano, P. D. Jeffrey, Z. Bowen, E. R. Kinnucan, M. S. Finnin, S. J. Elledge, J. W. Harper, M. Pagano, and N. P. Pavletich.** 2000. Insights into SCF ubiquitin ligases from the structure of the Skp1-Skp2 complex. *Nature* **408**:381-6.
150. **Seet, B. T., J. B. Johnston, C. R. Brunetti, J. W. Barrett, H. Everett, C. Cameron, J. Sypula, S. H. Nazarian, A. Lucas, and G. McFadden.** 2003. Poxviruses and immune evasion. *Annu Rev Immunol* **21**:377-423.
151. **Senkevich, T. G., E. V. Koonin, and R. M. Buller.** 1994. A poxvirus protein with a RING zinc finger motif is of crucial importance for virulence. *Virology* **198**:118-28.

152. **Senkevich, T. G., S. Ojeda, A. Townsley, G. E. Nelson, and B. Moss.** 2005. Poxvirus multiprotein entry-fusion complex. *Proc Natl Acad Sci U S A* **102**:18572-7.
153. **Senkevich, T. G., E. J. Wolffe, and R. M. Buller.** 1995. Ectromelia virus RING finger protein is localized in virus factories and is required for virus replication in macrophages. *J Virol* **69**:4103-11.
154. **Shchelkunov, S. N.** 2009. How long ago did smallpox virus emerge? *Arch Virol* **154**:1865-71.
155. **Shisler, J. L., and X. L. Jin.** 2004. The vaccinia virus K1L gene product inhibits host NF-kappaB activation by preventing IkappaBalpha degradation. *J Virol* **78**:3553-60.
156. **Sieczkarski, S. B., and G. R. Whittaker.** 2005. Viral entry. *Curr Top Microbiol Immunol* **285**:1-23.
157. **Skowyra, D., K. L. Craig, M. Tyers, S. J. Elledge, and J. W. Harper.** 1997. F-box proteins are receptors that recruit phosphorylated substrates to the SCF ubiquitin-ligase complex. *Cell* **91**:209-19.
158. **Smith, C. A., T. Davis, J. M. Wignall, W. S. Din, T. Farrah, C. Upton, G. McFadden, and R. G. Goodwin.** 1991. T2 open reading frame from the Shope fibroma virus encodes a soluble form of the TNF receptor. *Biochem Biophys Res Commun* **176**:335-42.
159. **Sonnberg, S., S. B. Fleming, and A. A. Mercer.** 2009. A truncated two-alpha-helix F-box present in poxvirus ankyrin-repeat proteins is sufficient for binding the SCF1 ubiquitin ligase complex. *J Gen Virol* **90**:1224-8.
160. **Spehner, D., S. Gillard, R. Drillien, and A. Kirn.** 1988. A cowpox virus gene required for multiplication in Chinese hamster ovary cells. *J Virol* **62**:1297-304.
161. **Spriggs, M. K., D. E. Hraby, C. R. Maliszewski, D. J. Pickup, J. E. Sims, R. M. Buller, and J. VanSlyke.** 1992. Vaccinia and cowpox viruses encode a novel secreted interleukin-1-binding protein. *Cell* **71**:145-52.
162. **Stack, J., I. R. Haga, M. Schroder, N. W. Bartlett, G. Maloney, P. C. Reading, K. A. Fitzgerald, G. L. Smith, and A. G. Bowie.** 2005. Vaccinia virus protein A46R targets multiple Toll-like-interleukin-1 receptor adaptors and contributes to virulence. *J Exp Med* **201**:1007-18.
163. **Stewart, T. L., S. T. Wasilenko, and M. Barry.** 2005. Vaccinia virus FIL protein is a tail-anchored protein that functions at the mitochondria to inhibit apoptosis. *J Virol* **79**:1084-98.
164. **Sutter, G., A. Ramsey-Ewing, R. Rosales, and B. Moss.** 1994. Stable expression of the vaccinia virus K1L gene in rabbit cells complements the host range defect of a vaccinia virus mutant. *J Virol* **68**:4109-16.
165. **Svobodova, S., S. Bell, and C. M. Crump.** 2012. Analysis of the Interaction between the Essential Herpes Simplex Virus 1 Tegument Proteins VP16 and VP1/2. *J Virol* **86**:473-83.
166. **Tait, S. W., E. B. Reid, D. R. Greaves, T. E. Wileman, and P. P. Powell.** 2000. Mechanism of inactivation of NF-kappa B by a viral homologue of I kappa b alpha. Signal-induced release of i kappa b alpha

- results in binding of the viral homologue to NF-kappa B. *J Biol Chem* **275**:34656-64.
167. **Takaoka, A., Z. Wang, M. K. Choi, H. Yanai, H. Negishi, T. Ban, Y. Lu, M. Miyagishi, T. Kodama, K. Honda, Y. Ohba, and T. Taniguchi.** 2007. DAI (DLM-1/ZBP1) is a cytosolic DNA sensor and an activator of innate immune response. *Nature* **448**:501-5.
 168. **Tang, Z., B. Li, R. Bharadwaj, H. Zhu, E. Ozkan, K. Hakala, J. Deisenhofer, and H. Yu.** 2001. APC2 Cullin protein and APC11 RING protein comprise the minimal ubiquitin ligase module of the anaphase-promoting complex. *Mol Biol Cell* **12**:3839-51.
 169. **Taylor, J. M., D. Quilty, L. Banadyga, and M. Barry.** 2006. The vaccinia virus protein F1L interacts with Bim and inhibits activation of the pro-apoptotic protein Bax. *J Biol Chem* **281**:39728-39.
 170. **Tokunaga, F., S. Sakata, Y. Saeki, Y. Satomi, T. Kirisako, K. Kamei, T. Nakagawa, M. Kato, S. Murata, S. Yamaoka, M. Yamamoto, S. Akira, T. Takao, K. Tanaka, and K. Iwai.** 2009. Involvement of linear polyubiquitylation of NEMO in NF-kappaB activation. *Nat Cell Biol* **11**:123-32.
 171. **Tooze, J., M. Hollinshead, B. Reis, K. Radsak, and H. Kern.** 1993. Progeny vaccinia and human cytomegalovirus particles utilize early endosomal cisternae for their envelopes. *Eur J Cell Biol* **60**:163-78.
 172. **Tulman, E. R., C. L. Afonso, Z. Lu, L. Zsak, G. F. Kutish, and D. L. Rock.** 2004. The genome of canarypox virus. *J Virol* **78**:353-66.
 173. **Upton, C., J. L. Macen, M. Schreiber, and G. McFadden.** 1991. Myxoma virus expresses a secreted protein with homology to the tumor necrosis factor receptor gene family that contributes to viral virulence. *Virology* **184**:370-82.
 174. **Vallabhapurapu, S., and M. Karin.** 2009. Regulation and function of NF-kappaB transcription factors in the immune system. *Annu Rev Immunol* **27**:693-733.
 175. **Vorou, R. M., V. G. Papavassiliou, and I. N. Pierroutsakos.** 2008. Cowpox virus infection: an emerging health threat. *Curr Opin Infect Dis* **21**:153-6.
 176. **Walsh, M. C., G. K. Kim, P. L. Maurizio, E. E. Molnar, and Y. Choi.** 2008. TRAF6 autoubiquitination-independent activation of the NFKappaB and MAPK pathways in response to IL-1 and RANKL. *PLoS One* **3**:e4064.
 177. **Wang, C., J. Xi, T. P. Begley, and L. K. Nicholson.** 2001. Solution structure of ThiS and implications for the evolutionary roots of ubiquitin. *Nat Struct Biol* **8**:47-51.
 178. **Wasilenko, S. T., L. Banadyga, D. Bond, and M. Barry.** 2005. The vaccinia virus F1L protein interacts with the proapoptotic protein Bak and inhibits Bak activation. *J Virol* **79**:14031-43.
 179. **Wasilenko, S. T., T. L. Stewart, A. F. Meyers, and M. Barry.** 2003. Vaccinia virus encodes a previously uncharacterized mitochondrial-

- associated inhibitor of apoptosis. *Proc Natl Acad Sci U S A* **100**:14345-50.
180. **Weissman, A. M.** 2001. Themes and variations on ubiquitylation. *Nat Rev Mol Cell Biol* **2**:169-78.
 181. **Wertz, I. E., K. M. O'Rourke, H. Zhou, M. Eby, L. Aravind, S. Seshagiri, P. Wu, C. Wiesmann, R. Baker, D. L. Boone, A. Ma, E. V. Koonin, and V. M. Dixit.** 2004. De-ubiquitination and ubiquitin ligase domains of A20 downregulate NF-kappaB signalling. *Nature* **430**:694-9.
 182. **Willems, A. R., M. Schwab, and M. Tyers.** 2004. A hitchhiker's guide to the cullin ubiquitin ligases: SCF and its kin. *Biochim Biophys Acta* **1695**:133-70.
 183. **Wilton, B. A., S. Campbell, N. Van Buuren, R. Garneau, M. Furukawa, Y. Xiong, and M. Barry.** 2008. Ectromelia virus BTB/kelch proteins, EVM150 and EVM167, interact with cullin-3-based ubiquitin ligases. *Virology* **374**:82-99.
 184. **Wu, C. J., D. B. Conze, T. Li, S. M. Srinivasula, and J. D. Ashwell.** 2006. Sensing of Lys 63-linked polyubiquitination by NEMO is a key event in NF-kappaB activation [corrected]. *Nat Cell Biol* **8**:398-406.
 185. **Wu, J. T., H. C. Lin, Y. C. Hu, and C. T. Chien.** 2005. Neddylation and deneddylation regulate Cull1 and Cul3 protein accumulation. *Nat Cell Biol* **7**:1014-20.
 186. **Xia, Z. P., L. Sun, X. Chen, G. Pineda, X. Jiang, A. Adhikari, W. Zeng, and Z. J. Chen.** 2009. Direct activation of protein kinases by unanchored polyubiquitin chains. *Nature* **461**:114-9.
 187. **Xu, X., P. Nash, and G. McFadden.** 2000. Myxoma virus expresses a TNF receptor homolog with two distinct functions. *Virus Genes* **21**:97-109.
 188. **Yamamoto, M., T. Okamoto, K. Takeda, S. Sato, H. Sanjo, S. Uematsu, T. Saitoh, N. Yamamoto, H. Sakurai, K. J. Ishii, S. Yamaoka, T. Kawai, Y. Matsuura, O. Takeuchi, and S. Akira.** 2006. Key function for the Ubc13 E2 ubiquitin-conjugating enzyme in immune receptor signaling. *Nat Immunol* **7**:962-70.
 189. **Yee, D., and D. R. Goring.** 2009. The diversity of plant U-box E3 ubiquitin ligases: from upstream activators to downstream target substrates. *J Exp Bot* **60**:1109-21.
 190. **Yu, X., Y. Yu, B. Liu, K. Luo, W. Kong, P. Mao, and X. F. Yu.** 2003. Induction of APOBEC3G ubiquitination and degradation by an HIV-1 Vif-Cul5-SCF complex. *Science* **302**:1056-60.
 191. **Zaragoza, C., M. Saura, E. Y. Padalko, E. Lopez-Rivera, T. R. Lizarbe, S. Lamas, and C. J. Lowenstein.** 2006. Viral protease cleavage of inhibitor of kappaBalpha triggers host cell apoptosis. *Proc Natl Acad Sci U S A* **103**:19051-6.
 192. **Zheng, N., B. A. Schulman, L. Song, J. J. Miller, P. D. Jeffrey, P. Wang, C. Chu, D. M. Koepp, S. J. Elledge, M. Pagano, R. C. Conaway, J. W. Conaway, J. W. Harper, and N. P. Pavletich.** 2002.

Structure of the Cul1-Rbx1-Skp1-F boxSkp2 SCF ubiquitin ligase complex. *Nature* **416**:703-9.

193. **Zur, A., and M. Brandeis.** 2001. Securin degradation is mediated by fzy and fzr, and is required for complete chromatid separation but not for cytokinesis. *EMBO J* **20**:792-801.

Chapter 2: Materials and Methods

2.1 Cell Culture and Viruses

2.1.1 Cells

CV-1, HeLa and HEK293T cells were obtained from the American Type Culture Collection (ATCC) and cultured in Dulbecco's Modified Eagle Medium (DMEM) supplemented with 10% fetal bovine serum (FBS), 50U/ml of penicillin, 50µg/ml of streptomycin and 200µM glutamine (Invitrogen Corporation). MEF cells were obtained from the ATCC and cultured in DMEM supplemented with 10% FBS, 50U/ml of penicillin, 50µg/ml of streptomycin, 200µM glutamine, and 10µM non-essential amino acids (Invitrogen Corporation). Baby Green Monkey Kidney (BGMK) cells were cultured in DMEM supplemented with 10% newborn calf serum, 50U/ml of penicillin, 50µg/ml of streptomycin and 200µM glutamine. HuTk^{143B} cells were obtained from the ATCC and cultured in DMEM supplemented with 10% FBS, 50U/ml of penicillin, 50µg/ml of streptomycin, 200µM glutamine and 25 µg/ml bromodeoxyuridine (BrdU)(Sigma Aldrich). U20S-Cre cells were generously provided by Dr. John Bell (University of Ottawa, Ottawa, Canada)(15). U20S-Cre cells were cultured in DMEM supplemented with 10% FBS, 50U/ml of penicillin, 50µg/ml of streptomycin and 200µM glutamine (Invitrogen Corporation).

2.1.2 Viruses

Vaccinia virus strain Copenhagen (VVCop), ectromelia virus strain Moscow (ECTV) and cowpox virus strain Brighton Red (CPXV) were propagated in BGMK cells and harvested as previously described (18). Low passage ECTV

(P2) was a gift from Dr. Mark Buller (St. Louis University). Creation of VV-Flag-EVM004 (20), VV-Flag-EVM150 (20) and VV-Flag-FPV039 (1) have been previously described.

Viral titers were measured by plaque assay. VV and CPXV stocks were titered by performing serial 10-fold dilutions of the virus in BGMK cell culture media. A 450 μ l volume of the dilutions (10^{-3} to 10^{-8}) were plated onto confluent BGMK cells in 6-well plates and plates were rocked every 10 minutes at 37°C for 1 hour. At 1 hour post infection, 1ml of BGMK cell culture media was added to each well and plates were incubated at 37°C for 24 hours. At 24 hours post infection, plates were washed with 1ml of warm PBS, fixed with 1ml of neutral buffered formalin (4% formaldehyde, 145mM NaCl, 55mM Na₂HPO₄, 30mM NaH₂PO₄) at room temperature for 5 minutes, and stained with 1ml of crystal violet (0.1% crystal violet, 2% ethanol). Wells containing 20-200 plaques were counted and used to calculate the concentration of the viral stocks.

Calculation of the concentration of ECTV stocks required a separate protocol since ECTV does not form plaques on BGMK cells at 24 hours post infection (4). In order to titer stocks of ECTV, virus was serially diluted 10-fold in PBS. A 450 μ l volume of the dilutions (10^{-3} to 10^{-8}) was then plated onto BGMK cells in 6-well plates and rocked every 10 minutes at 37°C for 1 hour. At 1 hour post infection 2ml of DMEM supplemented with 50U/ml of penicillin, 50 μ g/ml of streptomycin, 1% (w/v) carboxymethylcellulose (CMC), and 5% FBS was added to each well. Formation of plaques on BGMK cells required incubation for 3-5 days at 37°C. The CMC overlay has a high viscosity and prevents the formation

of secondary plaques due to prevention of progeny virus diffusion in the culture dish. Upon formation of plaques as determined through visualization under a light microscope, BGMK monolayers were stained by adding 2ml of crystal violet stain composed of 0.13% crystal violet, 4.75% ethanol, and 11.1% formaldehyde directly to the CMC containing media. The plates were rocked at room temperature for 1 hour to fix and stain monolayers. The plates were then washed and air dried. Plaques were counted on the well containing between 20-200 plaques, and the number of plaques was used to calculate the concentration of our viral stocks.

2.2 Antibodies

Mouse and rabbit anti-Flag (M2) were purchased from Sigma-Aldrich. Mouse anti-HA (clone 12CA5) was purchased from Roche Applied Science. Mouse anti-T7 was purchased from Novagen. Mouse anti-Myc (clone 9E10) was a gift from Dr. T. Hobman, University of Alberta. Antibodies specific for cullin-1, cullin-3, Skp1 and Roc1 were obtained from the laboratory of Dr. Yue Xiong and have been previously described (11, 12). Anti-ubiquitin (clone FK2) was purchased from Biomol International (6). Anti-poly(ADP-ribose) polymerase (PARP) was purchased from BD Biosciences. Anti- β -tubulin was purchased from ECM Biosciences. Antibodies recognizing $\text{I}\kappa\text{B}\alpha$, phospho- $\text{I}\kappa\text{B}\alpha$, and NF- κB 1 p50/105 were purchased from Cell Signalling Technologies. Anti-NF- κB p65 was purchased from Santa Cruz Biotechnology. Antibodies recognizing the early poxvirus protein I3L were generously donated by Dr. David Evans (University of

Alberta). An antibody specific to I5L was generated by immunizing rabbits with 500µg of peptide (TYVKSLLMKS) conjugated to KLH as previously described (3, 19).

2.3 Cell treatment – Transfection, Infection and Infection/Transfection

2.3.1 Transfections

HeLa or 293T cells were seeded into 6-well plates or onto coverslips in 12-well plates. Following adherence, cells were transfected once cells reached ~75% confluence. Cells were washed with 1ml of warm PBS and 900µl of warm Opti-MEM (Invitrogen Corporation) was added to each well of a 6-well plate, or 400µl to each coverslip, that was to be transfected.

Two 1.5ml eppendorf tubes were set up for each transfection. The first tube contained 50µl of Opti-MEM (Invitrogen Corporation) per well to be transfected along with 2µl of Lipofectamine 2000 (Invitrogen Corporation) per well. The second tube contained 50µl of Opti-MEM per well along with 1 to 5µg of the expression vector. Tubes were incubated at room temperature for 5 minutes, at which time tubes containing Lipofectamine 2000 were mixed with tubes containing DNA to allow formation of liposomes around the plasmid DNA, followed by an additional incubation at room temperature for 15 minutes. Finally, 100µl of the liposome/DNA mixture was added to each well of the 6-well plate or coverslip and incubated at 37°C. At 2 hours post transfection, 1ml of DMEM supplemented with 20% FBS and 400µM glutamine was added to each well or 500µl to each coverslip.

2.3.2 Infections

HeLa, HEK293T, BGMK or MEF cells were seeded onto 6-well plates ($\sim 1 \times 10^6$ cells per well), 10cm dishes ($\sim 7 \times 10^6$ cells per plate) or onto coverslips in 12-well plates ($\sim 5 \times 10^5$ cells were coverslip). Media was removed from coverslips and replaced with 400 μ l of fresh media. In 6-well plates, media was removed and replaced with 500 μ l of fresh media. In 10cm dishes, media was removed and replaced with 5ml of fresh media. Cells were typically infected at a MOI of either 5 or 10 pfu/cell, unless noted otherwise and incubated at 37°C with 5% CO₂. The cell/virus mixture was rocked every 10 minutes during the first hour of infection to promote infection. At one hour post infection, 500 μ l of cell culture media was added to each coverslip, 1ml to each well of a 6-well plate, or 5ml to each 10cm dish. Infections were incubated for 12 hours at 37°C unless noted otherwise.

2.3.3 Infection/Transfections

HeLa, HEK293T, or BGMK cells were seeded into 6-well plates or onto coverslips in 12-well plates. Cells were washed with 1ml of warm PBS and replaced with either 400 μ l of warm Opti-MEM for coverslips, or 900 μ l of Opti-MEM for 6-well plates. Cells were then infected at a MOI of 5. Infected plates were rocked every 10 minutes during the first hour to promote infection. Also during the first hour on infection, the liposome/DNA mixture was generated as described in section 2.3.1. The experiment was timed so that 100 μ l of the liposome/DNA mixture was added to the infected cells at 1 hour post infection.

At 1 hour post transfection 1ml of DMEM supplemented with 20% FBS and 400 μ M glutamine was added to each well of a 6-well plate or 500 μ l was added to each coverslip.

2.4 Bioinformatics

2.4.1 Alignments

Protein alignments for the ankyrin/F-box proteins were created with the AlignX program (Invitrogen Corporation). Skp2, a known cellular F-box containing protein, was included in the alignments (16). Predicted secondary structures included in the alignment were previously described for the Skp1/Skp2 interface (16).

2.5 Cloning

2.5.1 Previously Described Plasmids

pcDNA3-Myc-cullin-1, pcDNA3-Myc-cullin-2, pcDNA3-Myc-cullin-3, pcDNA3-Myc-cullin-4A, and pcDNA3-Myc-cullin-5 were obtained from Dr. Yue Xiong (University of North Carolina), and have been previously described (11). pcDNA3-hemagglutinin(HA)-cullin-1, pcDNA3-HA-cullin-1 Δ 610-615, and pcDNA3-HA-cullin-1 Δ N53, were also obtained from Dr. Yue Xiong (University of North Carolina) and have been previously described (7, 11). pcDNA3-T7-Skp1 was obtained from Dr. Manabu Furukawa (University of Nebraska, Medical Center) and has been previously described (11). pGEX-4T3-Skp1 was obtained from Dr. Brenda Schulman (St. Jude Children's Hospital) and has been previously described (16).

2.5.2 Subcloning Vectors

2.5.2.1 Cloning Into pGEMT

The majority of expression plasmids created for this study were created by PCR followed by TA cloning into the pGEMT vector (Promega). Constructs were then subcloned from pGEMT into the expression vector of choice using cut sites incorporated into the PCR primers to flank the gene of interest. The pGEMT vector allows for blue/white screening of transformants through use of the *lac* operon and bromo-chloro-indolyl-galactopyranoside (X-gal)(Rose Scientific). Briefly, plasmids that contain a ligated PCR product have an interrupted *lacZ* ORF and are unable to produce β -galactosidase. Therefore, colonies that appear blue contain no PCR insert, while colonies that appear white contain a PCR insert.

Primers used to create PCR products are outlined in Tables 2.1 to 2.6. PCR products were amplified with the polymerase outlined in Tables 2.7 to 2.12. PCR products generated with the *taq* polymerase (Invitrogen Corporation) or LongAmp *taq* (Invitrogen Corporation) contain 3'-A overhangs and were directly ligated into the pGEMT vector. PCR products generated with either *Pfu* (Stratagene) or *Pwo* (Invitrogen Corporation) polymerases were first subjected to an A-addition (Qiagen) prior to ligation into the pGEMT vector. Ligation into pGEMT was carried out at room temperature for 1 hour using 1 Weiss unit of the T4 ligase as outlined in the manufacturer's protocol.

Following ligation, plasmid DNA was transformed into competent *E. coli* (DH5 α) using heat shock. Five μ l of each ligation reaction was mixed with 50 μ l

Table 2.1 EVM005 Construct Primers

Primer #	Primer Name	Sequence (5' to 3')	Cut Site
2.1.1	EVM005 Flag Fwd	<u>AAGCTT</u> ATGGACTACAAAGACGATGAC GACAAGGAAAGATATTCATTACATAAA	<i>Hin</i> dIII
2.1.2	EVM005 Rvs	GCGGCCGCTTCTCAATGTGTCTGTGTTT GGAC	<i>Not</i> I
2.1.3	EVM005 Fwd	<u>AAGCTT</u> GAAAGATATTCATTACATAAA	<i>Hin</i> dIII
2.1.4	EVM005 Rvs	<u>GGATCC</u> TTCATTCATGTGTCTGTGTTTG	<i>Bam</i> HI
2.1.5	EVM005 Internal	CAGATATAATTATGCCTA	N/A
2.1.6	EVM005 Flag Fwd	<u>GTCGAC</u> ATGGACTACAAAGACGATGAC GACAAGGAAAGATATTCATTACATAAA	<i>Sal</i> I
2.1.7	EVM005 Gateway Fwd	<u>CACCGAA</u> AGATATTCATTACATAAA	N/A
2.1.8	EVM005(1-380) Rvs	GCGGCCGCTCAATTATTATAAGTTCGT AACGT	<i>Not</i> I
2.1.9	EVM005(381-650) Flag Fwd	<u>GTCGAC</u> AGTACTACAAAGACGATGAC GACAAGAAAATATTTTCTATTTGGCA	<i>Sal</i> I
2.1.10	EVM005(1-345) Rvs	GCGGCCGCTCAATAACCGTCATAATAT TT	<i>Not</i> I
2.1.11	EVM005(346-650) Flag Fwd	<u>GTCGAC</u> ATGGACTACAAAGACGATGAC GACAAGACGCCGTTACATTATGCC	<i>Sal</i> I
2.1.12	EVM005(1-231) Rvs	GCGGCCGCTCAATGGCGTTTATATCGTT T	<i>Not</i> I
2.1.13	EVM005(232-650) Flag Fwd	<u>GTCGAC</u> ATGGACTACAAAGACGATGAC GACAAGACTCCGTTGGGAACA	<i>Sal</i> I
2.1.14	EVM005(1-593) Rvs	GCGGCCGCTCACAAGTAAGTTGGTTGA TC	<i>Not</i> I
2.1.15	CO EVM005 Flag Fwd	<u>GGATCC</u> ATGGACTACAAAGACGATGAC GACAAGGAGCGGTACAGCCTGCAC	<i>Bam</i> HI
2.1.16	CO EVM005(1-593) Rvs	GCGGCCGCTCACAGGTAGGTGGGCTGG TC	<i>Not</i> I
2.1.17	CO EVM005 Gateway Fwd	<u>CACCGAG</u> CGGTACAGCCTGCAC	N/A
2.1.18	CO EVM005 Rvs	<u>CTCGAG</u> TCACTCGTGGGTCTGGGT	<i>Xho</i> I
2.1.19	EVM005 3'(150bp) Fwd	<u>GCGGCCG</u> CTCGTACCCGCGAACAAAAT AG	<i>Not</i> I
2.1.20	EVM005 3'(150bp) Rvs	<u>GAATCC</u> TTTTTTATAAACGATATTGTT	<i>Bam</i> HI
2.1.21	EVM005 5'(150bp) Fwd	<u>AAGCTT</u> TCTCTACAAAGTATAATATATT	<i>Hin</i> dIII
2.1.22	EVM005 5'(150bp) Rvs	<u>CTCGAG</u> ATATTATACATATTAGATGTG	<i>Xho</i> I
2.1.23	EVM005 Rev (400bp) Fwd	AAGAAACAAGATACAAGA	N/A
2.1.24	EVM005 Rev (400bp) Rvs	ATCAATGGCCGTCTCGAT	N/A

Table 2.2 EVM002 Construct Primers

Primer #	Primer Name	Sequence (5' to 3')	Cut Site
2.2.1	EVM002 Flag Fwd	<u>GGTACCATGGACTACAAAGACGATGAC</u> GACAAGGGCGAGATGGACGAGATT	<i>Kpn</i> I
2.2.2	EVM002 Rvs	<u>GCTAGCTTATGAATAATATTTGTA</u>	<i>Nhe</i> I
2.2.3	EVM002 Fwd	<u>GAATTCTCGGCGAGATGGACGAGATT</u>	<i>Eco</i> RI
2.2.4	EVM002 Rvs	<u>GCGGCCGCTTATGAATAATATTTGTA</u>	<i>Not</i> I
2.2.5	EVM002 Rvs	<u>GGATCCTTATGAATAATATTTGTA</u>	<i>Bam</i> HI
2.2.6	EVM002(1-554) Rvs	<u>GCTAGCTCACGATAGTCTAGATTGACC</u>	<i>Nhe</i> I
2.2.7	EVM002(1-554) Rvs	<u>GCGGCCGCTCACGATAGTCTAGATTGA</u> CC	<i>Not</i> I
2.2.8	CO EVM002 Flag Fwd	<u>AAGCTTATGGACTACAAAGACGATGAC</u> GACAAGGGCGAGATGGACGAGATC	<i>Hin</i> dIII
2.2.9	CO EVM002(1-554) Rvs	<u>GGATCCGCTCAGTCTGCTCTGGCC</u>	<i>Bam</i> HI
2.2.10	CO EVM002 Flag Fwd	<u>GTCGACATGGACTACAAAGACGATGAC</u> GACAAGGGCGAGATGGACGAGATC	<i>Sal</i> I
2.2.11	CO EVM002 Rvs	<u>CTCGAGTCAGCTGTAGTACTTGTA</u>	<i>Xho</i> I
2.2.12	EVM002 3'(150bp) Fwd	<u>GCGGCCGCGGTGCTATATCTTTTCCGTT</u> T	<i>Not</i> I
2.2.13	EVM002 3'(150bp) Rvs	<u>GGATCCTAGAAAGAAAATATTTAAAAA</u>	<i>Bam</i> HI
2.2.14	EVM002 5'(150bp) Fwd	<u>AAGCTTCTCATAATGATTTACTTTTTTC</u>	<i>Hin</i> dIII
2.2.15	EVM002 5'(150bp) Rvs	<u>CTCGAGCGATTCCGTCCAAGATGATAA</u>	<i>Xho</i> I
2.2.16	MPXV003 Flag Fwd	<u>GGATCCATGGACTACAAAGACGATGAC</u> GACAAGAAAATGGACGAGATTGTG	<i>Bam</i> HI
2.2.17	MPXV003 Rvs	<u>GCGGCCGCTCATGGATAATATTTGTAA</u> TG	<i>Not</i> I
2.2.18	CPXV006 Flag Fwd	<u>GAATTCATGGACTACAAAGACGATGAC</u> GACAAGTCAACCATTACTAAAAAA	<i>Eco</i> RI
2.2.19	CPXV006 Rvs	<u>GCGGCCGCTCACTAGTATGGATAATGT</u> TT	<i>Not</i> I

Table 2.3 EVM154 Construct Primers

Primer #	Primer Name	Sequence (5' to 3')	Cut Site
2.3.1	EVM154 Flag Fwd	<u>GTCGAC</u> ATGGACTACAAAGACGATGAC	<i>Sal</i> I
2.3.2	EVM154 Rvs	GCGGCCGCTTATATTTTAATAGTGTT	<i>Not</i> I
2.3.3	EVM154 Fwd	<u>GAATTCAAGATTTTTTTTAAAAA</u> AGGAA	<i>Eco</i> RI
2.3.4	EVM154 Rvs	<u>GGATCCTTATATTTTAATAGTGTT</u>	<i>Bam</i> HI
2.3.5	EVM154 Flag Fwd	<u>GGATCC</u> ATGGACTACAAAGACGATGAC GACAAGGATTTTTTTTAAAAAAGGAA	<i>Bam</i> HI
2.3.6	EVM154 Rvs	<u>GAATTCTTATATTTTAATAGTGTT</u>	<i>Eco</i> RI
2.3.7	CO EVM154 Flag Fwd	<u>AAGCTT</u> ATGGACTACAAAGACGATGAC GACAAGGACTTCTTCAAGAAAGAG	<i>Hin</i> dIII
2.3.8	CO EVM154(1-532) Rvs	<u>GGATCCTCACC</u> ACTTGTCGCCGGCGTC	<i>Bam</i> HI
2.3.9	CO EVM154 FP/AA Fwd	GACAAGTGGAGCTGC*GCC*GCCAACG AGATCAAG	N/A
2.3.10	CO EVM154 FP/AA Rvs	CTTGATCTCGTT*GGC*GGCGCAGCTCC ACTTGTC	N/A
2.3.11	EVM154 3'(200bp) Fwd	<u>GGATCCAATCTAAGTAGGATA</u> AAAA	<i>Bam</i> HI
2.3.12	EVM154 3'(200bp) Rvs	<u>GCGGCCGCAAACGATGTTTCGGT</u> AGA	<i>No</i> tI
2.3.13	EVM154 5'(200bp) Fwd	<u>CTCGAGATCATATAGACAATA</u> ACT	<i>Xho</i> I
2.3.14	EVM154 5'(200bp) Rvs	<u>AAGCTTGACATATAATTTATATTCTGT</u>	<i>Hin</i> dIII

Table 2.4 EVM165 Construct Primers

Primer #	Primer Name	Sequence (5' to 3')	Cut Site
2.4.1	EVM165 Flag Fwd	<u>GTCGACATGGACTACAAAGACGATGAC</u> GACAAGAATATTAACAATTAACAAT	<i>Sal</i> I
2.4.2	EVM165 Rvs	<u>GCGGCCGCTCACTATACTTTGGTAGAT</u> GGATA	<i>Not</i> I
2.4.3	EVM165 Flag Fwd	<u>AAGCTTATGGACTACAAAGACGATGAC</u> GACAAGAATATTAACAATTAACAAT	<i>Hin</i> dIII
2.4.4	EVM165 Fwd	<u>AAGCTTATGAATATTAACAATTAAC</u> AAT	<i>Hin</i> dIII
2.4.5	EVM165 Rvs	<u>GGATCCTCACTATACTTTGGTAGATGG</u> ATA	<i>Bam</i> HI
2.4.6	CO EVM165 Flag Fwd	<u>GGATCCATGGACTACAAAGACGATGAC</u> GACAAGAACATCAAGCAGCTGAAC	<i>Bam</i> HI
2.4.7	CO EVM165(1-566) Rvs	<u>GAATTCTCATCACAGGGTCAGCAGACA</u> GTT	<i>Eco</i> RI
2.4.8	EVM165 3'(200bp) Fwd	<u>GGATCCTTGTATTTTTATCATGTG</u>	<i>Bam</i> HI
2.4.9	EVM165 3'(200bp) Rvs	<u>GCGGCCGCGTATCTCTCATTTTATTG</u>	<i>Not</i> I
2.4.10	EVM165 5'(200bp) Fwd	<u>CTCGAGACTATAGTATTCTGGACT</u>	<i>Xho</i> I
2.4.11	EVM165 5'(200bp) Rvs	<u>AAGCTTTATTATAAACGAGTCCCA</u>	<i>Hin</i> dIII

Table 2.5 EVM004 Construct Primers

Primer #	Primer Name	Sequence (5' to 3')	Cut Site
2.5.1	EVM004 Gateway Fwd	<u>CACCATGAGTGATTACTATTTTGTT</u>	N/A
2.5.2	EVM004 Rvs	GGATCCTTAATAATACCTAGAAAATAT	<i>Bam</i> HI
2.5.3	EGFP Fwd	<u>GTCGACATGGTGAGCAAGGGCGAGGAG</u> CTG	<i>Sal</i> I

Table 2.6 Cellular Gene Construct Primers

Primer #	Primer Name	Sequence (5' to 3')	Cut Site
2.6.1	T7 Fwd	<u>GCGGCCGCAATACGACTCACTATAGGG</u> A	<i>Not</i> I
2.6.2	Cullin1 Rvs	<u>CCCGGGTTAAGCCAAGTAACTGTAGGT</u> GTC	<i>Xma</i> I
2.6.3	HA-Skp1 Fwd	<u>GTCGACATGTACCCATACGACGTCCCA</u> GACTACGCTCCTTCAATTAAGTTGCAG AGT	<i>Sal</i> I
2.6.4	Skp1 Rvs	<u>GCGGCCGCTCACTTCTTTCACACCACT</u> G	<i>Not</i> I

Table 2.7 EVM005 Subcloning Vectors

Plasmid Name	Fwd	Rvs	Temp	Pol	Seq	Dest
pGEMT-Flag-EVM005	2.1.1	2.1.2	ECTV DNA	<i>Pwo</i>	Yes	pcDNA3
pGEMT-EVM005	2.1.3	2.1.4	pGEMT-Flag-EVM005	<i>Pwo</i>	Yes	pEGFP
pGEMT-Flag-EVM005	2.1.2	2.1.2	pGEMT-Flag-EVM005	<i>Pwo</i>	Yes	pSC66
pGEMT-Flag-EVM005(1-593)	2.1.6	2.1.14	pGEMT-Flag-EVM005	<i>Pwo</i>	Yes	pSC66
pGEMT-Flag-EVM005(346-650)	2.1.11	2.1.2	pSC66-Flag-EVM005	<i>Pwo</i>	Yes	pSC66
pGEMT-Flag-EVM005(1-345)	2.1.6	2.1.10	pSC66-Flag-EVM005	<i>Pwo</i>	Yes	pSC66
pGEMT-Flag-EVM005(232-650)	2.1.13	2.1.2	pSC66-Flag-EVM005	<i>Pwo</i>	Yes	pSC66
pGEMT-Flag-EVM005(1-231)	2.1.6	2.1.12	pSC66-Flag-EVM005	<i>Pwo</i>	Yes	pSC66
pGEMT-Flag-EVM005(381-650)	2.1.9	2.1.2	pSC66-Flag-EVM005	<i>Pwo</i>	Yes	pSC66
pGEMT-Flag-EVM005(1-380)	2.1.6	2.1.8	pSC66-Flag-EVM005	<i>Pwo</i>	Yes	pSC66
pGEMT-EGFP-EVM005	2.13.3	2.1.2	pEGFP-	<i>Pwo</i>	Yes	pSC66
pGA15-EVM005 (CO)	N/A	N/A	GeneArt©	N/A	N/A	pcDNA3/ pEGFP
pGEMT-CO-Flag-EVM005 (1-593)	2.1.15	2.1.16	pGA15-EVM005 (CO)	<i>Taq</i>	Yes	pcDNA3
pENTR-EVM005	2.1.17	2.1.2	pGEMT-Flag-EVM005	<i>Pwo</i>	No	pDEST15
pENTR-EVM005(1-231)	2.1.17	2.1.12	pGEMT-Flag-EVM005	<i>Pwo</i>	No	pDEST15

N/A - Not applicable

Pwo - High Fidelity Polymerase (Roche Applied Science)

Pfu - High Fidelity Polymerase (Promega)

Taq - Polymerase (Invitrogen Corporation)

Table 2.8 EVM002 Subcloning Vectors

Plasmid Name	Fwd	Rvs	Template	Pol	Seq	Dest
pGEMT-Flag-EVM002	2.2.1	2.2.2	ECTV DNA	<i>Pwo</i>	Yes	pSC66
pGEMT-Flag-EVM002	2.2.1	2.2.4	pGEMT-Flag-EVM002	<i>Pwo</i>	Yes	pcDNA3
pGEMT-EVM002	2.2.3	2.2.5	pGEMT-Flag-EVM002	<i>Pwo</i>	Yes	pEGFP
pGEMT-Flag-EVM002(1-554)	2.2.1	2.2.6	pSC66-Flag-EVM002	<i>Pfu</i>	Yes	pSC66
pMK-RQ-EVM002(CO)	N/A	N/A	GeneArt©	N/A	No	pcDNA3/ pEGFP
pGEMT-CO-Flag-EVM002(1-554)	2.2.8	2.2.9	pMK-RQ-EVM002(CO)	<i>Pwo</i>	Yes	pcDNA3
pDONR-CPXV006	N/A	N/A	McFadden Lab	N/A	No	N/A
pDONR-MPXV003	N/A	N/A	McFadden Lab	N/A	No	N/A
pGEMT-Flag-CPXV006	2.2.18	2.2.19	pDONR-CPXV006	<i>Pfu</i>	No	pcDNA3
pGEMT-Flag-MPXV003	2.2.16	2.2.17	pDONR-MPXV003	<i>Pfu</i>	No	pcDNA3

N/A - Not applicable

Pwo - High Fidelity Polymerase (Roche Applied Science)

Pfu - High Fidelity Polymerase (Promega)

Table 2.9 EVM154 Subcloning Vectors

Plasmid Name	Fwd	Rvs	Template	Pol	Seq	Dest
pGEMT-Flag-EVM154	2.3.1	2.3.2	ECTV DNA	<i>Pwo</i>	Yes	pSC66
pGEMT-EVM154	2.3.3	2.3.4	pGEMT-Flag-EVM154	<i>Taq</i>	Yes	pEGFP
pGEMT-Flag-EVM154	2.3.5	2.3.6	pGEMT-Flag-EVM154	<i>Taq</i>	Yes	pcDNA3
pMK-RQ-EVM154 (CO)	N/A	N/A	GeneArt©	N/A	N/A	pcDNA3/ pEGFP
pGEMT-Flag-CO-EVM154(1-532)	2.3.7	2.3.8	pMK-RQ-EVM154 (CO)	<i>Pwo</i>	Yes	pcDNA3

N/A - Not applicable

Pwo - High Fidelity Polymerase (Roche Applied Science)

Taq - Polymerase (Invitrogen Corporation)

Table 2.10 EVM165 Subcloning Vectors

Plasmid Name	Fwd	Rvs	Template	Pol	Seq	Dest
pGEMT-Flag-EVM165	2.4.1	2.4.2	pGEMT-EVM165	<i>Pwo</i>	Yes	pSC66
pGEMT-Flag-EVM165	2.4.3	2.4.5	ECTV DNA	<i>Pfu</i>	Yes	pcDNA3
pGEMT-EVM165	2.4.4	2.4.5	ECTV DNA	<i>Pfu</i>	Yes	pEGFP
pMA-RQ-EVM165(CO)	N/A	N/A	GeneArt©	N/A	N/A	pcDNA3/
pGEMT-Flag-CO-EVM165 (1-566)	2.4.6	2.4.7	pMA-RQ-EVM165(CO)	<i>Pwo</i>	Yes	pcDNA3

N/A - Not applicable

Pwo - High Fidelity Polymerase (Roche Applied Science)

Pfu - High Fidelity Polymerase (Promega)

Table 2.11 EVM004 Subcloning Vectors

Plasmid Name	Fwd	Rvs	Template	Pol	Seq	Dest
pENTR-EVM004	2.5.1	2.5.2	pGEMT-EVM004	<i>Taq</i>	Yes	pDEST15

N/A - Not applicable

Taq - Polymerase (Invitrogen Corporation)

Table 2.12 Subcloning Vectors for Cellular Genes

Plasmid Name	Fwd	Rvs	Template	Pol	Seq	Dest
pGEMT-HA-Skp1	2.6.3	2.6.4	pGEX-4T3-Skp1	<i>Taq</i>	Yes	pSC66
pGEMT-Myc-Cullin1	2.6.1	2.6.2	pcDNA3-Myc-Cullin1	<i>Pwo</i>	Yes	pSC66
pGEMT-HA-Cullin1	2.6.1	2.6.2	pcDNA3-HA-	<i>Pwo</i>	Yes	pSC66
pGEMT-HA-Cullin1ΔN53	2.6.1	2.6.2	pcDNA3-HA-Cullin1ΔN53	<i>Pwo</i>	Yes	pSC66
pGEMT-HA-Cullin1Δ610-615	2.6.1	2.6.2	pcDNA3-HA-Cullin1Δ610-	<i>Pwo</i>	Yes	pSC66

Taq - Polymerase (Invitrogen Corporation)

Pwo - High Fidelity Polymerase (Roche Applied Science)

of competent *E. coli* (DH5 α) on ice for 30 minutes. Cells were then incubated at 42°C for 1 minute to induce uptake of plasmid DNA into competent cells. Five hundred μ l of SOC media was added to each tube of transformed cells and incubated at 37°C for 1 hour with shaking. The transformed cell mixture was then plated on Luria-Bertani (LB) agar plates containing 50 μ g/ml ampicillin (Sigma Aldrich), 80 μ g/ml X-gal and 0.5mM isopropyl- β -D-1-thiogalactopyranoside (IPTG)(Rose Scientific) and incubated overnight at 37°C.

White colonies were picked and inoculated into 5ml of LB broth containing 50 μ g/ml ampicillin and incubated at 37°C with shaking overnight. Plasmid DNA was harvested by mini-prep the following morning. To produce mini-prep DNA, 1.5ml of cultured bacteria was centrifuged at 10,000rpm on a bench top Becton Dickinson rotor for 1 minute. The pelleted bacteria cells were then resuspended in 100 μ l of Solution A (50mM glucose, 25mM Tris pH 8.0, 10mM EDTA). The resuspended bacteria were then lysed with 200 μ l of Solution B (1% SDS, 0.2M NaOH) on ice for 5 minutes. Proteins and lipids were removed from the lysate by precipitation with 150 μ l of Solution C (3M potassium acetate, 11.5% glacial acetic acid) on ice for 5 minutes. The lysates were then centrifuged at 10,000rpm on a Becton Dickinson bench top rotor for 15 minutes. The supernatant was collected and subjected to phenol-chloroform extraction, to purify plasmid DNA. The plasmid DNA was then precipitated with ice cold ethanol at -20°C for 30 minutes and centrifuged at 10,000rpm in a Becton Dickinson bench top rotor for 15 minutes. Plasmid DNA pellets were air dried for 5 minutes at room temperature and resuspended in 50 μ l of TE buffer (10mM

Tris pH 8.0, 1mM EDTA). Verification of PCR product was accomplished by restriction digest analysis on the resulting mini-prep DNA, using the restriction enzymes present in the PCR primers. Finally, sequencing the gene of interest was completed using the T7 and SP6 primer sites flanking the pGEMT multiple cloning site to ensure that no mutations had arisen during cloning (The Applied Genomics Center, University of Alberta).

2.5.2.2 Gateway Subcloning Vectors

To express GST-tagged versions of EVM005 and EVM004, these genes were first cloned into the pENTR directional topo cloning vector (Invitrogen Corporation). Forward primers for EVM005 and EVM004 (Tables 2.1 and 2.5) were designed with a four nucleotide extension composed of CACC at the 5' end of the forward primer. The EVM004 and EVM005 genes were then amplified by PCR using Gateway specific forward primers and gene specific reverse primers. Additionally, EVM005(1-231) was amplified by PCR using the gateway specific EVM005 forward primer and the EVM005(1-231) reverse primer (Table 2.1). The pENTR vector provided in the kit contained a GTGG overhang on one end and a blunt end on the other; both ends are covalently linked to topoisomerases. The GTGG overhang allows directional ligation of the 5' end of the gene of interest into the pENTR subcloning vector. Following the ligation reaction, DNA was transformed into competent *E. coli* (DH5 α) as described in section 2.5.2.1. Transformed *E. coli* was subjected to mini prep to harvest plasmid DNA (section

2.5.2.1) and assessed for the presence of inserted EVM004 or EVM005 DNA by PCR.

The pENTR plasmids were used to introduce the EVM004, EVM005, and EVM005(1-231) constructs into the pDEST15 vector (Invitrogen Corporation). Through recombination these constructs were inserted into the pDEST15 vector in order to express these genes as GST-fusion proteins in *E. coli*. Unfortunately, no pDEST15-GST-fusion constructs were positive for protein expression. However, there is a vast assortment of pDEST vectors available (Invitrogen Corporation), and the pENTR vectors created here could be used to create other tagged versions of EVM004, EVM005 or EVM005(1-231) for expression in a wide array of systems in the future.

2.5.2.3 Generation of Codon Optimized Ankyrin/F-box Constructs

Unfortunately initial attempts to express EVM002, EVM005, EVM154 and EVM165 during transient transfection failed. We subcloned the wild type sequences of these ORFs into both pcDNA3.1 and pEGFP in an attempt to express Flag-tagged and EGFP-tagged constructs, respectively (Tables 2.13 to 2.16). An inability to transiently express poxvirus proteins is not uncommon. Due to the cytoplasmic replication of poxviruses none of the poxvirus ORFs are subject to the RNA processing that occurs in the nucleus, such as removal of introns. Many poxvirus ORFs contain cryptic splice sites, which are recognized by the RNA processing machinery, and are therefore degraded upon transient expression from the nucleus (2). To counteract this, we employed GeneArt® to

Table 2.13 EVM005 Expression Vectors

Plasmid Name	Subcloning Vector	5' site	3' site	Express
pcDNA3-Flag-EVM005	pGEMT-Flag-EVM005	<i>Hin dIII</i>	<i>Not I</i>	No
pEGFP-EVM005	pGEMT-EVM005	<i>Hin dIII</i>	<i>Bam HI</i>	No
pSC66-Flag-EVM005	pGEMT-Flag-EVM005	<i>Sal I</i>	<i>Not I</i>	Yes
pSC66-Flag-EVM005(1-593)	pGEMT-Flag-EVM005 (1-593)	<i>Sal I</i>	<i>Not I</i>	Yes
pGEX-4T3-EVM005	pGEMT-Flag-EVM005	<i>Sal I</i>	<i>Not I</i>	Yes
pGEX-4T3-EVM005(1-593)	pGEMT-Flag-EVM005 (1-593)	<i>Sal I</i>	<i>Not I</i>	Yes
pGEX-4T3-EVM005(1-231)	pGEMT-Flag-EVM005 (1-231)	<i>Sal I</i>	<i>Not I</i>	Yes
pDEST15-EVM005	pENTR-EVM005	Topo	Topo	No
pDEST15-EVM005(1-231)	pENTR-EVM005(1-231)	Topo	Topo	No
pcDNA3-Flag-CO-EVM005(1-593)	pGEMT-Flag-CO-EVM005 (1-593)	<i>Bam HI</i>	<i>Not I</i>	Yes
pEGFP(C2)-CO-EVM005	pGA15-EVM005	<i>Eco RI</i>	<i>Bam HI</i>	Yes
pcDNA3-Flag-CO-EVM005	pGA15-EVM005	<i>Hind III</i>	<i>Bam HI</i>	Yes
pSC66-Flag-EVM005(346-650)	pGEMT-Flag-EVM005(346-650)	<i>Sal I</i>	<i>Not I</i>	Yes
pSC66-Flag-EVM005(1-345)	pGEMT-Flag-EVM005 (1-345)	<i>Sal I</i>	<i>Not I</i>	Yes
pSC66-Flag-EVM005(232-650)	pGEMT-Flag-EVM005 (232-650)	<i>Sal I</i>	<i>Not I</i>	Yes
pSC66-Flag-EVM005(1-231)	pGEMT-Flag-EVM005 (1-231)	<i>Sal I</i>	<i>Not I</i>	Yes
pSC66-Flag-EVM005(381-650)	pGEMT-Flag-EVM005 (381-650)	<i>Sal I</i>	<i>Not I</i>	Yes
pSC66-Flag-EVM005(1-380)	pGEMT-Flag-EVM005 (1-380)	<i>Sal I</i>	<i>Not I</i>	Yes
pSC66-EGFP-EVM005	pGEMT-EGFP-EVM005	<i>Sal I</i>	<i>Not I</i>	Yes

Topo - Cloned using recombination Gateway System (Invitrogen Corporation)

Table 2.14 EVM002 Expression Vectors

Plasmid Name	Subcloning Vector	5' site	3' site	Express
pSC66-Flag-EVM002	pGEMT-Flag-EVM002	<i>Kpn</i> I	<i>Nhe</i> I	Yes
pcDNA3-Flag-EVM002	pGEMT-Flag-EVM002	<i>Kpn</i> I	<i>Not</i> I	No
pEGFP(C2)-EVM002	pGEMT-EVM002	<i>Eco</i> RI	<i>Bam</i> HI	No
pSC66-Flag-EVM002(1-554)	pGEMT-Flag-EVM002 (1-554)	<i>Kpn</i> I	<i>Nhe</i> I	Yes
pcDNA3-Flag-CO-EVM002	pMK-RQ-EVM002	<i>Hin</i> dIII	<i>Bam</i> HI	Yes
pEGFP(C2)-CO-EVM002	pMK-RQ-EVM002	<i>Eco</i> RI	<i>Bam</i> HI	Yes
pcDNA3-Flag-CO-EVM002(1-554)	pGEMT-Flag-CO-EVM002 (1-554)	<i>Hin</i> dIII	<i>Bam</i> HI	Yes
pcDNA3-Flag-MPXV003	pGEMT-Flag-MPXV003	<i>Bam</i> HI	<i>Not</i> I	No
pcDNA3-Flag-CPXV006	pGEMT-Flag-CPXV006	<i>Eco</i> RI	<i>Not</i> I	No

Table 2.15 EVM154 Expression Vectors

Plasmid Name	Subcloning Vector	5' site	3' site	Express
pSC66-Flag-EVM154	pGEMT-Flag-EVM154	<i>Sal</i> I	<i>Not</i> I	Yes
pEGFP-EVM154	pGEMT-EVM154	<i>Eco</i> RI	<i>Bam</i> HI	No
pcDNA3-Flag-EVM154	pGEMT-Flag-EVM154	<i>Bam</i> HI	<i>Eco</i> RI	No
pEGFP(C2)-CO-EVM154*	pMK-RQ-EVM154	<i>Eco</i> RI	<i>Bam</i> HI	Yes
pcDNA3-Flag-CO-EVM154*	pMK-RQ-EVM154	<i>Hin</i> dIII	<i>Bam</i> HI	Yes
pcDNA3-Flag-CO-EVM154(1-532)*	pGEMT-Flag-CO-EVM154 (1-532)	<i>Hin</i> dIII	<i>Bam</i> HI	No
pcDNA3-Flag-CO-EVM154(F534A/P535A)*	pcDNA3-Flag-EVM154	SD	SD	Yes

* - cloned by Kristin Burles

SD - Site-directed mutagenesis

Table 2.16 EVM165 Expression Vectors

Plasmid Name	Subcloning Vector	5' site	3' site	Express
pSC66-Flag-EVM165	pGEMT-Flag-EVM165	<i>Sal</i> I	<i>Not</i> I	Yes
pcDNA3-Flag-EVM165	pGEMT-Flag-EVM165	<i>Hin</i> dIII	<i>Bam</i> HI	No
pEGFP-EVM165	pGEMT-EVM165	<i>Hin</i> dIII	<i>Bam</i> HI	No
pcDNA3-Flag-CO-EVM165	pMA-RQ-EVM165	<i>Hin</i> dIII	<i>Bam</i> HI	Yes
pEGFP-CO-EVM165	pMA-RQ-EVM165	<i>Eco</i> RI	<i>Bam</i> HI	Yes
pcDNA3-Flag-CO-EVM165(1-566)*	pGEMT-Flag-EVM165(1-566)	<i>Bam</i> HI	<i>Eco</i> RI	Yes

* - cloned by Megan Edwards

Table 2.17 EVM004 Expression Vectors

Plasmid Name	Subcloning Vector	5' site	3' site	Express
pSC66-EGFP-EVM004*	pGEMT-EGFP-EVM004	<i>Sal</i> I	<i>Bam</i> HI	Yes
pSC66-Flag-EVM004*	pGEMT-Flag-EVM004			
pcDNA3-Flag-EVM004*	pGEMT-Flag-EVM004			No
pEGFP-EVM004*	pGEMT-EVM004	<i>Not</i> I	<i>Sal</i> I	Yes
pDEST15-EVM004	pENTR-EVM004	Topo	Topo	No

* - Cloned by Dr. Stephanie Campbell

Topo - Cloned using recombination Gateway System (Invitrogen Corporation)

Table 2.18 Cellular Gene Expression Vectors

Plasmid Name	Subcloning Vector	5' site	3' site	Express
pGEX-4T3-Skp1	N/A ^a	N/A	N/A	ND
pcDNA3-T7-Skp1	N/A ^b	N/A	N/A	Yes
pcDNA3-Skp1	N/A ^c	N/A	N/A	ND
pSC66-HA-Skp1	pGEMT-HA-Skp1	<i>Sal</i> I	<i>Not</i> I	ND
pcDNA3-Myc-Cullin1	N/A ^c	N/A	N/A	Yes
pcDNA3-Myc-Cullin2	N/A ^c	N/A	N/A	ND
pcDNA3-Flag-Cullin3	N/A ^c	N/A	N/A	Yes
pcDNA3-Myc-Cullin3	N/A ^c	N/A	N/A	Yes
pcDNA3-Myc-Cullin4A	N/A ^c	N/A	N/A	ND
pcDNA3-Myc-Cullin5	N/A ^c	N/A	N/A	ND
pcDNA3-HA-Cullin1	N/A ^c	N/A	N/A	Yes
pcDNA3-HA-Cullin1 Δ 610-615	N/A ^c	N/A	N/A	Yes
pcDNA3-HA-Cullin1 Δ N53	N/A ^c	N/A	N/A	Yes
pSC66-Myc-Cullin1	pGEMT-Myc-Cullin1	<i>Not</i> I	<i>Xma</i> I	Yes
pSC66-HA-Cullin1	pGEMT-HA-Cullin1	<i>Not</i> I	<i>Xma</i> I	Yes
pSC66-HA-Cullin1 Δ 610-615	pGEMT-HA-Cullin1 Δ 610-615	<i>Not</i> I	<i>Xma</i> I	Yes
pSC66-HA-Cullin1 Δ N53	pGEMT-HA-Cullin1 Δ N53	<i>Not</i> I	<i>Xma</i> I	Yes

N/A - not applicable

ND - not determined

^a - plasmid obtained from Dr. Brenda Schulman (St. Jude Childrens Hospital)

^b - plasmid obtained from Dr. Manabu Furukawa (University of Nebraska, Medical Center)

^c - plasmids obtained from Dr. Yue Xiong (Univeristy of North Carolina)

produce codon optimized versions of EVM002, EVM005, EVM154, and EVM165 (2). The constructs were designed to remove all cryptic splice sites, and optimize codon usage for expression in *Homo sapiens*. Additionally, the constructs obtained from GeneArt were designed for easy subcloning into both pcDNA3.1 and pEGFP, to produce Flag-tagged and EGFP-tagged versions of EVM002, EVM005, EVM154 and EVM165 during transient transfection (Tables 2.13 to 2.16).

2.5.3 Expression Vectors

A variety of expression vectors were used in this study for the expression of tagged-constructs in transfected cells: pEGFP (Clontech), pcDNA3.1 (Invitrogen Corporation); poxvirus infected cells: pSC66; or transformed bacteria: pGEX-4T3 (GE Healthcare). All expression vectors used in these experiments are listed in Tables 2.13 to 2.18.

Genes of interest were cloned by PCR and ligated into a subcloning vector as described in 2.5.2. Once our subcloning vectors were constructed and sequenced, we subcloned the gene into our expression vector of choice using restriction digest followed by ligation with T4 DNA ligase (Invitrogen Corporation). The standard ratios of insert to vector DNA for ligations was 4:1 and 8:1. Ligated DNA was transformed in to competent *E. coli* (DH5 α) as described in 2.5.2.1, and transformations were plated on LB agar containing the appropriate antibiotic (100 μ g/ml kanamycin (Sigma) or 50 μ g/ml ampicillin). Antibiotic resistant colonies were amplified in 5ml cultures and plasmid DNA

was isolated by mini-prep (described in Section 2.5.2.1). The resulting mini-prep DNA samples were analyzed by restriction digest analysis. In order to check for expression of our tagged constructs, plasmids were transfected into HEK293T cells (pEGFP, pcDNA3.1), or into poxvirus infected cells (pSC66), or transformed into *E. coli* (pGEX-4T3) and whole cell lysates were analyzed by western blot for the presence of appropriately sized and tagged proteins.

2.5.4 Generation of Recombinant Vaccinia Viruses

Generation of recombinant VVs was used to gain expression of tagged-proteins during VV infection. A gene of interest were recombined into the VV thymidine kinase (TK or J2R) locus, to produce viruses that were deficient in TK, but expressed the gene of interest with a synthetic early/late poxvirus promoter (pE/L)(9). A list of all recombinant VVs generated for this study is found in Table 2.19.

BGMK cells were seeded in 6-well plates and 2 wells were used per recombination reaction. BGMKs were infected at a MOI of 0.01 with a wild type strain of VVCop that was absent of any drug resistant or fluorescent markers. BGMKs were then transfected with pSC66 expression vectors containing the gene of interest as outlined in section 2.3.3. The pSC66 vector contains left-hand and right-hand regions of homology with the J2R ORF. BGMK cells infected with VVCop and transfected with a pSC66 construct will undergo recombination at a rate near 1:1000 (1 recombinant virus per 1000 pfu) due to recombinase activity of VV (13). The infected/transfected BGMKs were harvested at 24 hours post

Table 2.19 Vaccinia Virus Recombinants

Virues Name	Parental Strain	Recombination Plasmid	Expression
VV-Flag-EVM004	VVCop(White)	pSC66-Flag-EVM004	Yes
VV-Flag-EVM005	VVCop(White)	pSC66-Flag-EVM005	Yes
VV-Flag-EVM002	VVCop(White)	pSC66-Flag-EVM002	Yes
VV-Flag-EVM154	VVCop(White)	pSC66-Flag-EVM154	Yes
VV-Flag-EVM165	VVCop(White)	pSC66-Flag-EVM165	Yes
VV-Flag-EVM005(1-593)	VVCop(White)	pSC66-Flag-EVM005 (1-593)	Yes
VV-Flag-EVM005(1-380)	VVCop(White)	pSC66-Flag-EVM005 (1-380)	Yes
VV-Flag-EVM005(381-650)	VVCop(White)	pSC66-Flag-EVM005 (381-650)	Yes
VV-Flag-EVM002(1-554)	VVCop(White)	pSC66-Flag-EVM002 (1-554)	Yes
VV-HA-Cullin1 Δ 610-615	VVCop(White)	pSC66-HA-Cullin1 Δ 610-615	Yes

infection and lysed in swelling buffer (10mM Tris pH 8.0, 2mM MgCl₂) via three rounds of freezing at -80°C and thawing at 37°C. Recombinant VVs were selected using a combination of drug selection and blue/white screening. Due to the absence of the J2R ORF in our recombinant VVs, we were able to select for recombinants by growth on HuTk⁻143B cells in the presence of 25µg/ml BrdU (5). Additionally, due to the presence of the *lacZ* ORF in the pSC66 vector, our recombinants formed blue plaques when overlaid with agar containing X-gal. Purification of recombinant VVs was generally accomplished within 4-7 rounds of plaque purification using X-gal overlays on a combination of BGMK or HuTK⁻143B cells. Purified VVs were amplified and isolated in BGMK cells grown in roller bottles as previously described (18). A list of all constructed VV recombinants is outlined in Table 2.19.

2.5.5 pDGloxP-KO Vectors for Ectromelia Virus Recombinants

The pDGloxP-KO vector was created through collaboration between the laboratories of Dr. David Evans (University of Alberta) and Dr. John Bell (University of Ottawa)(15). This vector expresses a yellow fluorescent protein (YFP)-guanine phosphoribosyl transferase (GPT) fusion protein for selection of recombinant viruses. The *yfp-gpt* cassette is flanked by loxP sites for Cre-mediated excision following purification of recombinants. The concept for creation of this vector was to enable the construction of recombinant poxviruses that lacked drug resistant or fluorescent markers for the use in viral therapeutics and is highlighted in Chapter 4 of this document. We collaborated with these two

laboratories to extend their protocol to other poxviruses, in this case ECTV strain Moscow. We amplified 150bp or 200bp regions of homology from the ECTV genome that corresponded to regions flanking the 5' or 3' ends of the EVM002, EVM005, EVM154 or EVM165 ORFs, using *taq* polymerase (Invitrogen Corporation). These DNA fragments were then directly ligated into the pGEMT vector as outlined in section 2.5.2.1, and screened for the presence of our PCR insert using restriction digest analysis. These fragments were subcloned into the pDGloxP-KO vector, one at a time, to produce pDGloxP-EVM002-KO, pDGloxP-EVM005-KO, pDGloxP-EVM154-KO and pDGloxP-EVM165-KO (Table 2.20). Proper construction was assessed by PCR and restriction digest analysis prior to use in ECTV recombination reactions.

2.5.6 Generation of Recombinant Ectromelia Viruses

BGMK cells were infected with low passage ECTV (P5) at a MOI of 0.01 and transfected with 10 μ g of linearized pDGloxP-KO using Lipofectamine 2000 (Invitrogen Corporation)(8, 15). A combination of drug resistance and YFP fluorescence was used to select recombinant viruses. Recombinant ECTV was selected in BGMK media containing 250 μ g/ml xanthine (Sigma Aldrich), 15 μ g/ml hypoxanthine (Sigma Aldrich), and 25 μ g/ml mycophenolic acid (MPA)(Sigma Aldrich). The MPA containing media selects for recombinant viruses expressing GPT. GPT positive virus was then screened for YFP fluorescence using a fluorescent microscope with a FITC filter (Leica). ECTV foci that were resistant to MPA selection and were YFP positive were generally

Table 2.20 Ectromelia Virus Knockout Plasmids

Plasmid Name	Fwd	Rvs	Temp	Pol	Seq
pDG-loxP-KO V1 (wrong loxP site)	N/A	N/A	GeneArt©	N/A	N/A
pDG-loxP-KO	N/A	N/A	N/A	N/A	N/A
pGEMT-EVM005-5'-150bp	2.1.21	2.1.22	ECTV DNA	<i>Taq</i>	Yes
pGEMT-EVM005-3'-150bp	2.1.19	2.1.20	ECTV DNA	<i>Taq</i>	Yes
pDGloxP-EVM005-KO-5'-150bp	N/A	N/A	N/A	N/A	N/A
pDGloxP-EVM005-KO	N/A	N/A	N/A	N/A	N/A
pGEMT-EVM002-5'-150bp	2.4.14	2.4.15	ECTV DNA	<i>Taq</i>	Yes
pGEMT-EVM002-3'-150bp	2.4.12	2.4.13	ECTV DNA	<i>Taq</i>	Yes
pDGloxP-EVM002-KO-5'-150bp	N/A	N/A	N/A	N/A	N/A
pDGloxP-EVM002-KO	N/A	N/A	N/A	N/A	N/A
pGEMT-EVM165-5'-200bp	2.10.10	2.10.11	ECTV DNA	<i>Taq</i>	Yes
pGEMT-EVM165-3'-200bp	2.10.8	2.10.9	ECTV DNA	<i>Taq</i>	Yes
pDGloxP-EVM165-KO-5'-200bp	N/A	N/A	N/A	N/A	N/A
pDGloxP-EVM165-KO	N/A	N/A	N/A	N/A	N/A
pGEMT-EVM005-Revertant (150bp)	2.1.19	2.1.22	ECTV DNA	<i>Pwo</i>	Yes
pGEMT-EVM005-Revertant (400bp)	2.1.23	2.1.24	ECTV DNA	LAT	Yes
pGEMT-EVM002-Revertant	2.4.12	2.4.15	ECTV DNA	<i>Pwo</i>	No
pGEMT-EVM165-Revertant	2.10.10	2.10.9	ECTV DNA	<i>Pwo</i>	No

N/A - Not applicable

LAT - LongAmp *Taq* polymerase (Invitrogen Corporation)

Taq - Polymerase (Invitrogen Corporation)

Pwo - High Fidelity Polymerase (Roche Applied Science)

purified between 3-6 rounds of foci picks. The purity of the recombinant virus preps was assessed by PCR of viral genomes before removal of the *yfp-gpt* cassette.

Removal of the *yfp-gpt* cassette from recombinant ECTVs was performed using U20S cells stably expressing a cytoplasmic mutant of the Cre recombinase (15). White ECTV foci, lacking the *yfp-gpt* cassette, were selected and purified to create marker-free recombinant ECTVs. Marker-free recombinant viruses were isolated in 2-5 rounds of foci picks on U20S-Cre cells and purity of the virus stock was assessed by PCR of viral genomes. ECTV-005-rev was cloned by infecting BGMK cells with ECTV- Δ 005-YFP-GPT at a MOI of 0.01 followed by transfection with pGEMT-EVM005-revertant (400bp) plasmid. Infected cells were harvested at 48 hours post infection and recombinant ECTV-005-rev was selected through lack of YFP fluorescence using a fluorescent inverted microscope and a FITC filter (Leica).

PCR analysis of viral genomes verified insertion and deletion of the *yfp-gpt* cassette. Viral genomes were isolated by infecting BGMK cells with the indicated recombinant ECTV. At 24 hours post infection, infected cells were washed with 1ml of warm PBS, followed by lysis with buffer containing 1.2% SDS, 50mM Tris pH 8.0, 4mM EDTA, 4mM CaCl₂. The resulting lysate was subjected to phenol-chloroform extraction to isolate viral genomes. The viral genomes were precipitated by adding 1ml ice cold 95% ethanol and 50 μ l 3M sodium acetate to 300 μ l of phenol-chloroform extracted DNA and incubating at -70°C for 15 minutes. Viral genomes were centrifuged at 14,000rpm in a Becton

Dickinson bench top rotor for 15 minutes. The pellets were air dried at room temperature for 5 minutes and resuspended in 100µl of ddH₂O. *Taq* polymerase (Invitrogen Corporation) was used to amplify the locus of interest (EVM002, EVM005, EVM154 or EVM165) using primers flanking each loci as indicated in Tables 2.1 to 2.4. Purity of our recombinant ECTVs was assessed by the presence of a lone band on an agarose gel that corresponded to the recombination event. A list of all ECTV recombinant and knockout viruses constructed is listed in Table 2.21.

2.6 Assays

2.6.1 Immunoprecipitations

HeLa or HEK293T cells were left untreated or treated as described in sections 2.3.1, 2.3.2 or 2.3.3. Each sample was produced from either one 10cm dish or two wells of a 6-well dish. Cells were lysed at 12 hours post infection or 18 hours post transfection in either 1ml (10cm dish) or 750µl (2 wells of 6-well plate) of NP40 lysis buffer containing 1% NP40, 150mM NaCl, 50mM Tris (pH 8.0), and Complete Mini protease inhibitors (Roche Diagnostics). Samples were passed through a 22G needle 5 times to shear DNA, followed by incubation at 4°C on a rocker for 2 hours.

Following lysis, samples were centrifuged at 10,000rpm in a Becton Dickinson bench top rotor for 15 minutes to separate membranes and DNA from the cytosol. One hundred µl of the corresponding supernatant was added to 500µl of ice cold acetone and incubated at -20°C for 1 hour to produce lysate samples;

Table 2.21 Ectromelia Virus Recombinants and Knockouts

Virues Name	Parental Strain	Recombination Plasmid	Expression
ECTV-Δ005-YFP	ECTV wt (P5)	pDG-loxP-KO-EVM005	N/A
ECTV-Δ005	ECTV-Δ005-YFP	N/A	N/A
ECTV-005-Revertant	ECTV-Δ005-YFP	pGEMT-EVM005-Revertant (400bp)	N/A
ECTV-Δ002-YFP	ECTV wt (p5)	pDG-loxP-KO-EVM002	N/A
ECTV-Δ002	ECTV-Δ002-YFP	N/A	N/A
ECTV-Δ002/005-YFP	ECTV-Δ002-Cre	pDG-loxP-KO-EVM005	N/A
ECTV-Δ002-005	ECTV-Δ002/005- YFP	N/A	N/A
ECTV-Δ002-005/Δ154- YFP	ECTV-Δ002/005- Cre	pDG-loxP-KO-EVM154	N/A
ECTV-Δ002-005/154-Cre	ECTV-Δ002- 005/Δ154-YFP	N/A	N/A
ECTV-Δ002-005/Δ154-171	ECTV-Δ002- 005/Δ154-YFP	N/A	N/A
ECTV-Δ005-Flag-EVM005	ECTV-Δ005-Cre	pSC66-Flag-EVM005	Yes
ECTV-Δ005-Flag- EVM005(1-593)	ECTV-Δ005-Cre	pSC66-Flag-EVM005 (1-593)	Yes
ECTV-Δ002-Flag-EVM002	ECTV-Δ002-Cre	pSC66-Flag-EVM002	Yes
ECTV-Δ002-Flag- EVM002(1-554)	ECTV-Δ002-Cre	pSC66-Flag-EVM002 (1-554)	Yes

N/A - Not Applicable

the remainder of the supernatant was subjected to immunoprecipitation. Antibody was added to the remaining supernatant and incubated at 4°C for 2 hours on a rocker. Finally, protein G sepharose beads (GE Healthcare) that had been washed and resuspended in NP40 lysis buffer were added to the immunoprecipitation and incubated at 4°C for 1 hour. The protein G beads were washed three times with NP40 lysis buffer and finally resuspended in SDS sample buffer containing 62.5mM Tris pH 6.8, 10% glycerol, 2% SDS, 50mM β-mercaptoethanol (BME)(Bioshop).

Lysates were centrifuged at 10,000rpm in a Becton Dickinson bench top rotor for 15 minutes. Protein pellets were air dried for 5 minutes and resuspended in SDS sample buffer. Finally, all lysate and immunoprecipitation samples were boiled for 10 minutes and stored at -20°C.

2.6.2 Western Blots

Protein samples were generated by collecting whole cell lysates in SDS sample buffer containing 62.5mM Tris pH 6.8, 10% glycerol, 2% SDS, 50mM β-mercaptoethanol (BME) or via immunoprecipitation as outlined in 2.6.1. All samples were boiled for 15 minutes, prior to separation by SDS poly-acrylamide gel electrophoresis (SDS-PAGE). SDS gels containing 10-15% poly-acrylamide were run at 200V until optimal protein separation had occurred.

Proteins were then transferred from the SDS gels to nitrocellulose membranes (BioRad) using a semi-dry transfer apparatus (Tyler Research). Semi-dry transfer was achieved at 450mA for 2 hours. Nitrocellulose membranes

were then blocked in 5% milk or 1% bovine serum albumin (BSA - only for anti-ubiquitin-FK2 blots)(Roche Diagnostics) for at least 1 hour at room temperature.

Nitrocellulose membranes were incubated with primary antibodies on a rocker at 4°C overnight. Antibodies used are outlined in section 2.2. Antibodies were diluted in 10ml of TBST (50mM Tris, 150mM NaCl, pH 7.6, 0.1% Tween-20). Membranes were washed three times with TBST following incubation with the primary antibody. Membranes were then incubated with anti-mouse or anti-rabbit HRP-conjugated secondary antibodies (Jackson Laboratories) diluted 1:25000 in TBST at room temperature for 1 hour. Membranes were then washed three times in TBST and developed using enhanced chemiluminescence (ECL)(GE Healthcare).

2.6.3 Mass Spectrometry

HEK293T cells (2×10^7 , two 10cm dishes) were infected with VVCop or VV-Flag-EVM005 at a MOI of 5 for 12 hours. Following infection, cells were harvested and subjected to immunoprecipitation using the anti-Flag (M2) antibody as outlined in 2.6.1. Samples were separated by SDS-PAGE on a 12% polyacrylamide Hoeffler gel at low voltage overnight, and proteins were visualized by silver staining (17). The silver stain protocol involves fixing the gel in 50% methanol/5% acetic acid for 20 minutes, then incubating in 50% methanol for 15 minutes. The gel was then incubated in 0.2% thiosulfate (Sigma Aldrich) for 1 minute, washed in ddH₂O, and further incubated in 0.1% silver nitrate (ice cold)(Sigma Aldrich) for 25 minutes. The gel was then developed by incubating

in 187mM sodium carbonate anhydrous/0.015% formaldehyde three times for 3 minutes each round. The development step was stopped at the appropriate darkness by adding 5% acetic acid and incubating for 10 minutes. Finally, the gel was washed with H₂O, scanned and analyzed for unique banding patterns present in the VV-Flag-EVM005 lane. Bands that were unique to the VV-Flag-EVM005 immunoprecipitation were excised, trypsin digested, and analyzed by mass spectrometry at the Institute for Biomolecular Design (University of Alberta) using a FITCR Apex Q mass spectrometer (Bruker).

2.6.4 Confocal microscopy

HeLa cells were transfected, infected or infected and transfected as outlined in 2.3.1, 2.3.2, and 2.3.3. Following treatment outlined in the corresponding figure legends, cells were washed with PBS and fixed with 2% paraformaldehyde for 10 minutes at room temperature. Cells were permeabilized using 1% NP40 (Sigma Aldrich) for 5 minutes at room temperature, and blocked with 30% goat serum (Invitrogen Corporation) for 15 minutes at room temperature. Coverslips were stained with antibodies outlined in section 2.2 by diluting them in 100µl of PBS per coverslip. One hundred µl of primary antibody mixture was placed on parafilm, the coverslips were then placed on top of the antibody, cells down, and incubated in the dark at room temperature for 1 hour. Coverslips were washed three times in PBS containing 1% FBS. The secondary antibodies used were anti-rabbit or mouse conjugated with Alexafluor 546 or Alexafluor 488 (Invitrogen Corporation), diluted 1:400 in PBS. One hundred µl of the secondary antibody

mixture was placed on parafilm and coverslips were placed on top, cells down, and incubated in the dark at room temperature for 1 hour. Coverslips were washed three times with PBS containing 1% FBS, mounted onto slides using mounting media containing 50% glycerol containing 4mg/ml N-propyl-gallate (Sigma Aldrich), and 250 μ g/ml 4',6-diamino-2-phenylindole (DAPI)(Invitrogen Corporation) to visualize nuclei and viral factories. Cells were visualized using a Zeiss Axiovert laser scanning confocal microscope.

To quantify the percentage of cells expressing EVM005, EVM002 or EVM154 that co-localizing with cullin-1 or conjugated ubiquitin, greater than 100 cells were counted.

For NF- κ B p65 translocation experiments, cells were visualized using the 40x oil immersion objective of a Ziess Axiovert 200M fluorescent microscope outfitted with an ApoTome 10 optical sectioning device (Ziess). To quantify the number of cells displaying a nuclear localization of p65 greater than 50 cells were counted in triplicate.

2.6.5 Cytoplasmic and Nuclear Extracts

HeLa or MEF cells were mock infected or infected as outlined in section 2.3.2 for 12 hours then stimulated with either 10ng/ml TNF α (Roche) or 10ng/ml IL-1 β (PeproTech Inc) for 20 minutes at 37°C. Cells were harvested and lysed in 150 μ l of cytoplasmic extract buffer containing 10mM HEPES, 10mM KCl, 0.1mM EDTA (pH 8.0), 0.1mM EGTA (pH 8.0), 1mM dithiothreitol (DTT) and 0.05% NP40. Samples were centrifuged at 1000Xg for 5 minutes to remove nuclei.

Supernatants were collected and resuspended in 4x SDS sample buffer containing 50% glycerol, 1% SDS, 312.5mM Tris pH 8.0, 5mg/ml Bromophenol Blue (BioRad) and 20% BME. The nuclear pellets were washed and resuspended in 50 μ l of nuclear extract buffer containing 20mM HEPES, 25% glycerol, 0.4M NaCl, 1mM EDTA (pH 8.0), 1mM EGTA (pH 8.0), and 1mM DTT and lysis was performed on ice for 30 minutes. Samples were centrifuged at 1000Xg for 5 minutes. Supernatants were collected as nuclear extracts and mixed with 4x SDS sample buffer. Protein samples were separated by SDS-PAGE and western blotted with anti-NF- κ B p65, anti- β -tubulin (cytoplasmic control) and anti-PARP (nuclear control).

2.6.6 Flow Cytometry

HeLa cells were infected or transfected as indicated in the corresponding figure legends and as outlined in 2.3.1 and 2.3.2. At 24 hours post transfection or 12 hours post infection, mock infected cells were stimulated with 10 μ M MG132 (Sigma Aldrich) for 1 hour at 37°C. Samples were left unstimulated or stimulated with 10ng/ml TNF α (Roche) or 10ng/ml IL-1 β (PeproTech Inc) for 20 minutes at 37°C. Cells were then harvested with trypsin (Invitrogen Corporation) and fixed in 0.5% paraformaldehyde (Sigma-Aldrich) for 15 minutes at 37°C. Cells were permeablized with ice cold 90% methanol for 30 minutes on ice. Transfected cells were co-stained with rabbit anti-Flag M2 (1:200) and anti-I κ B α (1:400) diluted in 100 μ l of PBS. Cells were stained with anti-rabbit phycoerythrin (1:1000) and anti-mouse-AlexaFluor488 (1:400)(Jackson Laboratories) secondary

antibodies diluted in 200 μ l of PBS. Samples were washed with 1ml of PBS containing 1% FBS and resuspended in 500 μ l of PBS. Infected cells were stained with anti-I3L (1:100) or anti-I κ B α (1:400) diluted in 100 μ l of PBS, followed by anti-mouse-phycoerythrin (1:1000) diluted in 200 μ l of PBS. Infected samples were then washed with 1ml of PBS containing 1% FBS and resuspended in 500 μ l of PBS. Data were collected on a Becton Dickinson FACScan or FACS Calibur flow cytometers, and analyzed with CellQuest software (Becton Dickinson).

2.6.7 Growth Curve Analysis of Recombinant ECTVs

A multi-step growth curve was used to analyze the growth of ECTV- Δ 002, ECTV- Δ 005 and ECTV-005-rev on BGMK cells. BGMK cells were infected with ECTV, ECTV- Δ 005 or ECTV-005-rev at an MOI of 0.05, or ECTV and ECTV- Δ 002 at a MOI of 0.01 to perform the multi-step growth curve. Samples were collected at indicated time points post infection up to 72 hours. To collect samples, 1ml of sterile sodium citrate (SSC)(0.15M NaCl, 0.015M tri-sodium citrate) was added to each well and incubated at 37°C for 5 minutes. Cells were harvested into 1.5ml eppendorf tubes and centrifuged at 4000rpm for 5 minutes in a Becton Dickinson bench top rotor. Cell pellets were lysed in 50 μ l of swelling buffer by three rounds of freezing at -80°C and thawing at 37°C. Following the three freeze/thaw cycles, 50 μ l of 2x DMEM was added to each sample and all samples were sonicated (550 Sonic Dismembrator, Fisher Scientific, 20 seconds at level 3, 0.5 second pulses). Viral titers for each time point were obtained by diluting 10 μ l of each cell lysate with serial 10-fold dilutions in PBS and plating

onto BGMK cells as outlined in section 2.1.2. The resulting concentrations of virus in each sample were used to calculate the total number of virus particles at each time point.

2.6.8 Real Time PCR

HeLa cells were mock infected or infected with ECTV, ECTV- Δ 005 or ECTV- Δ 002. At 12 hours post infection cells were stimulated with 10ng/ml TNF α and RNA was harvested using Trizol according to the manufacturer's protocol (Invitrogen Corporation). Superscript II reverse transcriptase (Invitrogen Corporation) and Oligo-dT primers (Invitrogen Corporation) were then used for conversion of poly-adenylated mRNA into cDNA. Real time PCR was performed using the Sybr-Green master mix (Promega) and a MyIQ thermocycler (BioRad). Data analysis was performed with IQ-5 software (BioRad) and the relative changes in transcripts levels were calculated using the $2^{-\Delta\Delta C_t}$ algorithm (10). A list of all RT-PCR primers used for these analyses is found in Table 2.22.

2.7 Infection of Mice with ECTV Knockout Viruses

To determine the role of the ECTV encoded ankyrin/F-box proteins in virulence we infected female C57BL/6 mice. Four to six week old female C57BL/6 mice were obtained from the National Cancer Institute (Frederick, MD). Mice were infected via the intranasal route with 10-fold escalating doses of wild type ECTV or ECTV- Δ 002, ECTV- Δ 005, ECTV- Δ 154, ECTV- Δ 165, or ECTV-005-rev. Groups of five mice with similar body mass were housed in separate cages. Mice

Table 2.22 Real-Time PCR Primers

Primer #	Primer Name	Sequence (5' to 3')	Cut Site
2.22.1	GAPDH Fwd	AGCCTTCTCCATGGTGGTGAAGAC	N/A
2.22.2	GAPDH Rvs	CGGAGTCA ACGGATTTGGTCG	N/A
2.22.3	TNF α Fwd	GGCGTGGAGCTGAGAGATAAC	N/A
2.22.4	TNF α Rvs	GGTGTGGGTGAGGAGCACAT	N/A
2.22.5	IL-1 β Fwd	TTCCCAGCCCTT TTGTTGA	N/A
2.22.6	IL-1 β Rvs	TTAGAACCAAATGTGGCCGTG	N/A
2.22.7	IL-6 Fwd	GGCACTGGCAGAAAACAACC	N/A
2.22.8	IL-6 Rvs	GCAAGTCTCCTCATCGAATCC	N/A

were anesthetized with 0.1ml/10g body weight with ketamine HCL (9mg/ml) and xylazine (1mg/ml) by intraperitoneal injection. Anesthetized mice were laid on their dorsal side with their bodies angled so that the anterior end was raised 45° from the surface; a plastic mouse holder was used to ensure conformity. ECTV was diluted in PBS without Ca²⁺ and Mg²⁺ to the required concentration and slowly loaded into each naris (5µl/naris). Mice were subsequently left *in situ* for 2 to 3 minutes before being returned to their cages. Mice were monitored for body weight daily for up to 21 days. Mice that demonstrated a drop in body weight to 70% of their original mass, or signs of severe morbidity were euthanized. Mortality of mice was then used to calculate the LD₅₀ for each strain of ECTV using the Reed-Muench analysis (14).

Alternatively, we infected the susceptible A/NCR strain of mice to determine the role of the ECTV encoded ankyrin/F-box proteins in virulence. Five to ten week old female A/NCR mice were obtained from the National Cancer Institute (Frederick, MD). Groups of five mice with similar body mass were arranged into separate cages. These mice were anesthetized with CO₂/O₂ prior to infection. ECTV was diluted in PBS without Ca²⁺ and Mg²⁺ to the required concentration and 10µl was used to infect mice via footpad injection. Mice were monitored for body weight daily for up to 21 days. Mice that demonstrated a drop in body weight to 70% of their original mass, or signs of severe morbidity were euthanized. Mortality of mice was then used to calculate the LD₅₀ for each strain of ECTV using the Reed-Muench analysis (14). All animal studies described in this document have been performed in ABSL-3 containment at Saint Louis

University in collaboration with Dr. Mark Buller and have been approved by the University of Alberta Animal Ethics Committee.

2.8 References

1. **Banadyga, L., J. Gerig, T. Stewart, and M. Barry.** 2007. Fowlpox virus encodes a Bcl-2 homologue that protects cells from apoptotic death through interaction with the proapoptotic protein Bak. *J Virol* **81**:11032-45.
2. **Barrett, J. W., Y. Sun, S. H. Nazarian, T. A. Belsito, C. R. Brunetti, and G. McFadden.** 2006. Optimization of codon usage of poxvirus genes allows for improved transient expression in mammalian cells. *Virus Genes* **33**:15-26.
3. **Barry, M., S. Hnatiuk, K. Mossman, S. F. Lee, L. Boshkov, and G. McFadden.** 1997. The myxoma virus M-T4 gene encodes a novel RDEL-containing protein that is retained within the endoplasmic reticulum and is important for the productive infection of lymphocytes. *Virology* **239**:360-77.
4. **Chen, W., R. Drillien, D. Spehner, and R. M. Buller.** 1992. Restricted replication of ectromelia virus in cell culture correlates with mutations in virus-encoded host range gene. *Virology* **187**:433-42.
5. **Earl, P. L., B. Moss, L. S. Wyatt, and M. W. Carroll.** 2001. Generation of recombinant vaccinia viruses. *Curr Protoc Mol Biol* **Chapter 16**:Unit16 17.
6. **Fujimuro, M., and H. Yokosawa.** 2005. Production of antipolyubiquitin monoclonal antibodies and their use for characterization and isolation of polyubiquitinated proteins. *Methods Enzymol* **399**:75-86.
7. **Furukawa, M., Y. Zhang, J. McCarville, T. Ohta, and Y. Xiong.** 2000. The CUL1 C-terminal sequence and ROC1 are required for efficient nuclear accumulation, NEDD8 modification, and ubiquitin ligase activity of CUL1. *Mol Cell Biol* **20**:8185-97.
8. **Gammon, D. B., B. Gowrishankar, S. Duraffour, G. Andrei, C. Upton, and D. H. Evans.** 2010. Vaccinia virus-encoded ribonucleotide reductase subunits are differentially required for replication and pathogenesis. *PLoS Pathog* **6**:e1000984.
9. **Hammond, J. M., P. G. Oke, and B. E. Coupar.** 1997. A synthetic vaccinia virus promoter with enhanced early and late activity. *J Virol Methods* **66**:135-8.
10. **Livak, K. J., and T. D. Schmittgen.** 2001. Analysis of relative gene expression data using real-time quantitative PCR and the 2(-Delta Delta C(T)) Method. *Methods* **25**:402-8.

11. **Michel, J. J., and Y. Xiong.** 1998. Human CUL-1, but not other cullin family members, selectively interacts with SKP1 to form a complex with SKP2 and cyclin A. *Cell Growth Differ* **9**:435-49.
12. **Ohta, T., J. J. Michel, A. J. Schottelius, and Y. Xiong.** 1999. ROC1, a homolog of APC11, represents a family of cullin partners with an associated ubiquitin ligase activity. *Mol Cell* **3**:535-41.
13. **Piccini, A., M. E. Perkus, and E. Paoletti.** 1987. Vaccinia virus as an expression vector. *Methods Enzymol* **153**:545-63.
14. **Reed, L. J., and Muench, H.** 1938. A simple method of estimating fifty percent endpoints. *The American Journal of Hygiene* **27**:493-497.
15. **Rintoul, J. L., J. Wang, D. B. Gammon, N. J. van Buuren, K. Garson, K. Jardine, M. Barry, D. H. Evans, and J. C. Bell.** 2011. A selectable and excisable marker system for the rapid creation of recombinant poxviruses. *PLoS One* **6**:e24643.
16. **Schulman, B. A., A. C. Carrano, P. D. Jeffrey, Z. Bowen, E. R. Kinnucan, M. S. Finnin, S. J. Elledge, J. W. Harper, M. Pagano, and N. P. Pavletich.** 2000. Insights into SCF ubiquitin ligases from the structure of the Skp1-Skp2 complex. *Nature* **408**:381-6.
17. **Shevchenko, A., M. Wilm, O. Vorm, and M. Mann.** 1996. Mass spectrometric sequencing of proteins silver-stained polyacrylamide gels. *Anal Chem* **68**:850-8.
18. **Stuart, D., K. Graham, M. Schreiber, C. Macaulay, and G. McFadden.** 1991. The target DNA sequence for resolution of poxvirus replicative intermediates is an active late promoter. *J Virol* **65**:61-70.
19. **van Buuren, N., B. Couturier, Y. Xiong, and M. Barry.** 2008. Ectromelia virus encodes a novel family of F-box proteins that interact with the SCF complex. *J Virol* **82**:9917-27.
20. **Wilton, B. A., S. Campbell, N. Van Buuren, R. Garneau, M. Furukawa, Y. Xiong, and M. Barry.** 2008. Ectromelia virus BTB/kelch proteins, EVM150 and EVM167, interact with cullin-3-based ubiquitin ligases. *Virology* **374**:82-99.

Chapter 3: ECTV Encodes a Novel Family of Ankyrin/F-box Proteins That Interact with the SCF Complex

A version of this chapter has been published in the Journal of Virology:
van Buuren, N, B. Couturier, Y. Xiong and M. Barry. 2008. J. Virol. 82(20): 9917-27.

All of the experiments included within this chapter were performed by N. van Buuren. The original manuscript was written by N. van Buuren with a major editorial contribution by M. Barry.

3.1 Introduction

Ubiquitin is a 76 amino acid protein that plays a crucial role in protein regulation (12, 37). The covalent attachment of ubiquitin to target substrates results in protein degradation or dramatic alterations in protein function (12, 37). The process of ubiquitylation is essential for cellular homeostasis, and tightly regulates a wide range of cellular functions, such as the cell cycle, signal transduction, transcription, and DNA repair (12, 29, 37).

A large family of ubiquitin ligases is responsible for transferring ubiquitin to specific substrates. Ubiquitin ligases exist as either single subunit ligases or as part of a multi-subunit ubiquitin ligase complex (1). Multi-subunit ubiquitin ligases are composed of a scaffold protein, a linker protein, and a substrate adaptor protein that is responsible for recruiting substrates to the complex for ubiquitylation (28, 38). Multi-protein ubiquitin ligases incorporate a member of the cullin family to act as the molecular scaffold for the ubiquitin ligase and support the recruitment of substrates to the complex. Seven cullin family members have been identified, each containing a cullin-homology domain at the C-terminus that binds Roc1, which is responsible for conferring the ubiquitin ligase activity (28). Substrate adaptor proteins contain protein-protein interaction domains that recruit the substrate to the complex and bind either directly to the cullin protein or through a linker protein (28, 38).

The cellular SCF (Skp1/Cul-1/E-box) complex is the best characterized of the multi-protein ubiquitin ligases and regulates a wide range of cellular processes (2, 17, 22, 24, 25). Substrate adaptors are recruited to the SCF complex through

interactions with the linker protein Skp1 (5, 21, 41). Substrate recruitment relies upon a highly conserved F-box domain that is typically found at the N-terminus of substrate adaptor proteins and required for interaction with the linker protein Skp1 (6, 14, 33, 40). The majority of cellular F-box proteins also possess C-terminal leucine rich repeats (LRR) or WD40 repeats that are responsible for recognizing and recruiting substrates (6, 14, 33, 40). There are 69 F-box proteins that exist in the human genome indicating that a wide range of substrates are recruited to the SCF complex for ubiquitylation (5, 6, 11, 14, 18, 33, 40).

Poxviruses encode an array of proteins that interfere with cellular signaling pathways including ubiquitylation (15, 32). Several proteins encoded by ectromelia virus strain Moscow (ECTV), the causative agent of mousepox, have been shown to specifically regulate the ubiquitin-proteasome system (8). The protein p28, is highly conserved in *Orthopoxviruses*, and contains a RING domain that functions as a ubiquitin ligase (13, 26). Also ECTV encodes a family of four proteins, EVM018, EVM027, EVM150, and EVM167, that contain BTB and Kelch domains and interact with cullin-3, likely regulating ubiquitylation of currently unknown substrates (39). More recently a bioinformatics study suggested that poxviruses also regulate the SCF complex through the expression of multiple proteins that contain N-terminal ankyrin repeat domains and putative C-terminal F-box domains (20, 35). Intriguingly, this combination is unique to poxviruses and to date has not been found within cellular proteins. Using bioinformatics, we identified seven ectromelia virus genes predicted to encode ankyrin repeats: EVM002, EVM005, EVM010, EVM021, EVM022, EVM154,

and EVM165. Of these seven genes, four contain putative C-terminal F-box domains. The data in this chapter demonstrate that EVM002, EVM005, EVM154, and EVM165 contain a C-terminal F-box domain that is necessary for interaction with components of the SCF complex. These results suggest that ECTV has evolved multiple proteins that function to modulate the activity of SCF ubiquitin ligases upon infection.

3.2 Ectromelia Virus Encodes Four Ankyrin Repeat/F-box Proteins

Members of the poxvirus family have recently been shown to modulate the ubiquitin-proteasome system (4, 13, 16, 26, 39). Prompted by these recent findings and the identification of putative F-box domain containing proteins in Orf virus, a poxvirus that infects sheep (20), we used bioinformatics to identify potential F-box proteins in the ECTV strain Moscow (EVM) genome. This approach identified seven ECTV encoded ankyrin repeat containing proteins. Four of these, EVM002, EVM005, EVM154, and EVM165, contained putative C-terminal F-box-like domains. An alignment of EVM002, EVM005, EVM154, and EVM165 with the F-box from the cellular protein Skp2 demonstrated the conservation of key residues (Figure 3.1A). Moreover, many of the contact points between the F-box of Skp2 and the linker protein Skp1 were maintained in the ECTV encoded F-box domains (Figure 3.1A) (30, 41). In contrast to cellular F-box proteins, the ECTV F-boxes were located at the C-terminus in combination with a series of N-terminal ankyrin repeats (Figure 3.2). To date, no cellular F-box proteins have been found in conjunction with ankyrin repeats, suggesting that

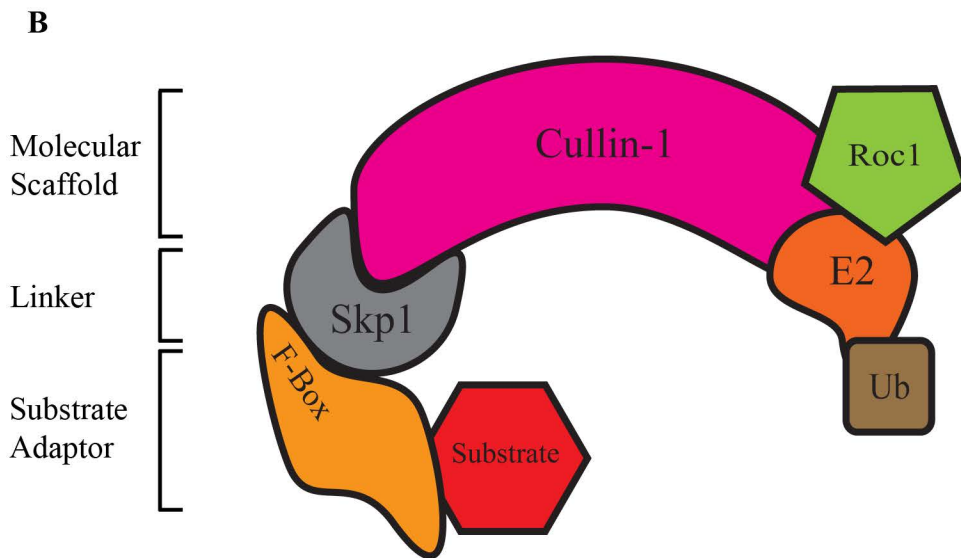
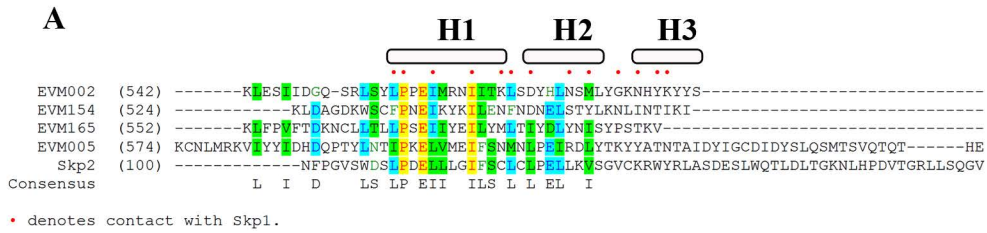


Figure 3.1. Ectromelia virus encodes four ankyrin-repeat/F-box proteins. A. AlignX was used to align the C-terminus of EVM002, EVM005, EVM154, and EVM165 with the F-box domain of Skp2, a cellular F-box protein. The dots denote known contact points between Skp2 and the linker protein Skp1. H1, H2, and H3 represent α -helical secondary structure. **B.** Cullin-1 is a scaffold protein for the cellular SCF ubiquitin ligase complex. Roc1, which supplies the ubiquitin ligase activity, binds to the C-terminus of cullin-1, and the linker protein Skp1 interacts with the N-terminus of cullin-1. Substrates are recruited for ubiquitylation through substrate adaptors containing F-box domains.

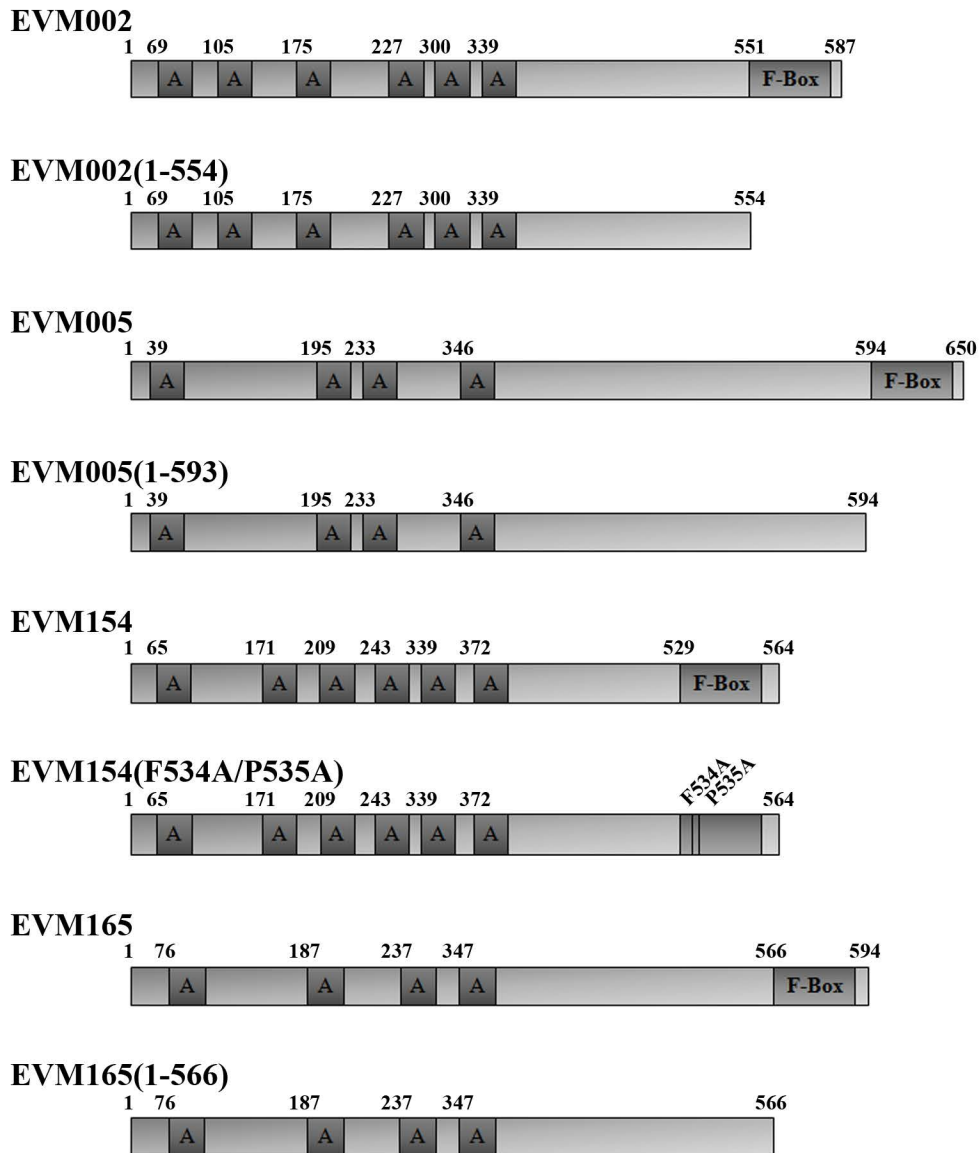


Figure 3.2. Ectromelia virus strain Moscow encodes four ankyrin/F-box proteins. Schematic representation of EVM002, EVM005, EVM154, and EVM165 containing C-terminal F-boxes and N-terminal ankyrin repeat domains (denoted as A in the diagram). The F-box deletion mutants for each of the four ankyrin/F-box proteins are also displayed. Notably, we were unable to express EVM154(1-532), even upon codon optimization. Therefore, using site-directed mutagenesis, we mutated two key residues within the F-box domain, F534 and P535, to alanine. These residues are predicted to form contact points with Skp1 in the SCF complex.

ECTV has evolved a novel set of genes to regulate the ubiquitin-proteasome pathway. Bioinformatics further indicated that multiple orthologs for EVM002, EVM154, and EVM165 were present in a variety of poxviruses. Notably, bioinformatics indicated that EVM005 had only one ortholog, CPXV011, in CPXV strain Brighton Red, suggesting that EVM005 and CPXV011 may play a role specific to ECTV and CPXV.

3.3 EVM005 Interacts with HA-cullin-1 During Infection

The presence of a putative F-box domain in EVM005 suggested that EVM005 interacted with components of the SCF ubiquitin ligase complex (Figure 3.1B). To test this possibility, we generated a Flag-tagged version of EVM005 and constructed a recombinant vaccinia virus, VV-Flag-EVM005, that expresses EVM005 during infection. To identify cellular binding partners for EVM005, HEK293T cells were infected with wild type VVCop or VV-Flag-EVM005, and protein samples were subjected to immunoprecipitation with the anti-Flag antibody followed by mass spectrometry. Mass spectrometry identified both EVM005 and cullin-1 in VV-Flag-EVM005 infected cells via immunoprecipitation, but not in cells infected with VVCop (Figure 3.3). The interaction between EVM005 and cullin-1, an essential component of the SCF ubiquitin ligase, suggested that EVM005 modulates the activity of the SCF complex in a similar manner to cellular F-box proteins (5, 41).

To confirm the mass spectrometry interaction between Flag-EVM005 and cullin-1, HEK293T cells were infected with VV-Flag-EVM005, VVCop or VV-

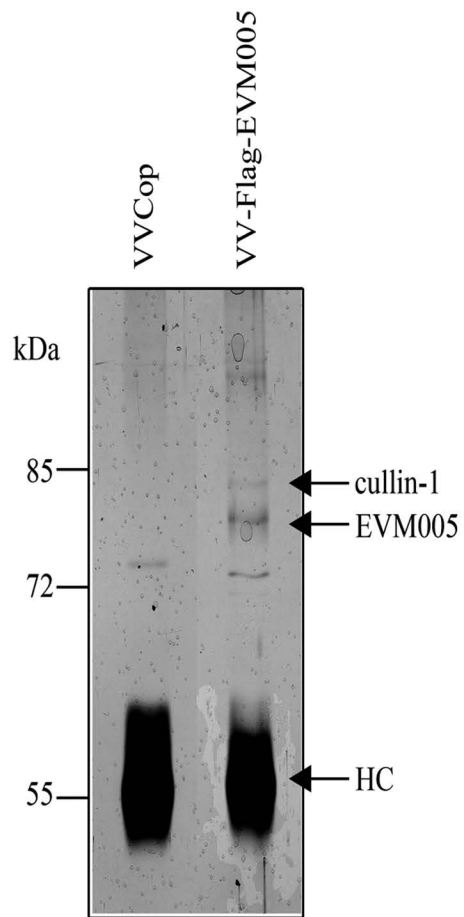


Figure 3.3. EVM005 associates with human cullin-1 during infection. HEK293T cells were infected with VVCop or VV-Flag-EVM005 at MOI of 5 for 12 hours. Cell lysates were subjected to immunoprecipitation with anti-Flag and samples were separated by SDS-PAGE and silver stained. Bands were excised and analyzed by mass spectrometry. Peptides were identified that corresponded to cullin-1 and EVM005. Antibody heavy chain is denoted by HC.

Flag-EVM004, which expresses a Flag-tagged BTB-only protein as a negative control (39). To express HA-cullin-1 during infection, cells were infected and subsequently transfected with pSC66-HA-cullin-1, to express cullin-1 from a poxvirus specific promoter (7, 19). Immunoprecipitation with anti-HA clearly demonstrated that over expressed HA-cullin-1 interacted with Flag-EVM005 during infection but not Flag-EVM004 (Figure 3.4). Western blotting lysates with anti-Flag and anti-HA indicated that HA-cullin-1, Flag-tagged EVM005, and Flag-tagged EVM004 were expressed.

Since co-immunoprecipitation data indicated that cullin-1 interacted with EVM005, we next investigated the subcellular localization of Flag-EVM005 and HA-cullin-1 during infection. As previously described, ectopic expression of HA-cullin-1 in uninfected HeLa cells produced three different expression patterns with the most prominent being nuclear accumulation (Figure 3.5 panels a-c)(10). Transient expression of Flag-EVM005 demonstrated a unique punctate staining pattern throughout the cytoplasm of the cell (Figure 3.5 panels d-f). HeLa cells infected with VV-Flag-EVM005 and stained with anti-Flag displayed a similar punctate staining pattern for EVM005 as that observed in the absence of infection (Figures 3.5 panels d-f and 3.6 panels a-d). Expression of HA-cullin-1 during infection was detected using an antibody specific for cullin-1. Although the cullin-1 antibody detected ectopically expressed HA-cullin-1, the antibody failed to detect endogenous cullin-1 in this assay likely due to low levels of cullin-1 (Figure 3.6 panel a). The cullin-1 antibody, however, clearly demonstrated that HA-cullin-1 localized throughout the infected cell to discrete punctate structures

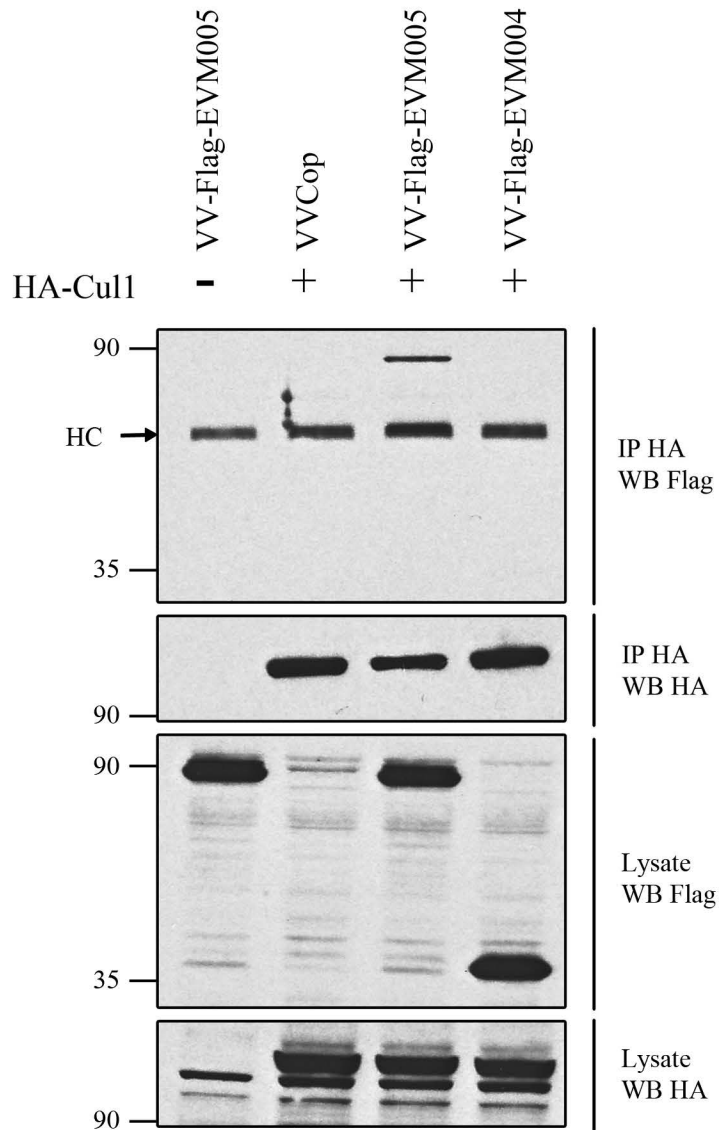


Figure 3.4. EVM005 interacts with HA-cullin-1 during infection. HEK293T cells were infected with VVCop, VV-Flag-EVM005, or VV-Flag-EVM004 and mock transfected or transfected with pSC66-HA-cullin-1. At 12 hours post infection cells were lysed in NP40 lysis buffer, subjected to immunoprecipitation with anti-HA to precipitate cullin-1, and western blotted with anti-Flag to detect EVM005. HC denotes antibody heavy chain.

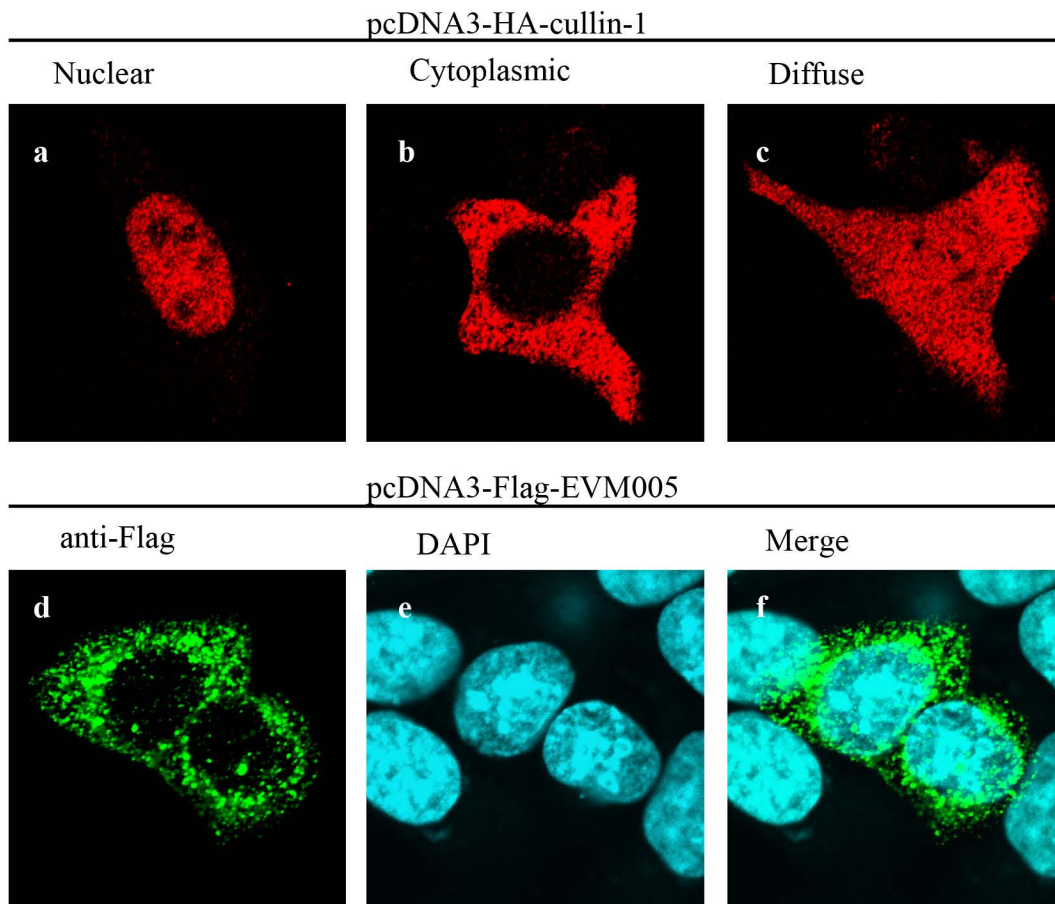


Figure 3.5. Localization of ectopically expressed cullin-1 and EVM005. HeLa cells were transfected with pcDNA3-HA-cullin-1 or pcDNA3-Flag-EVM005 for 16 hours, cullin-1 was visualized by anti-HA (a-c) and EVM005 was visualized with anti-Flag (d-f).

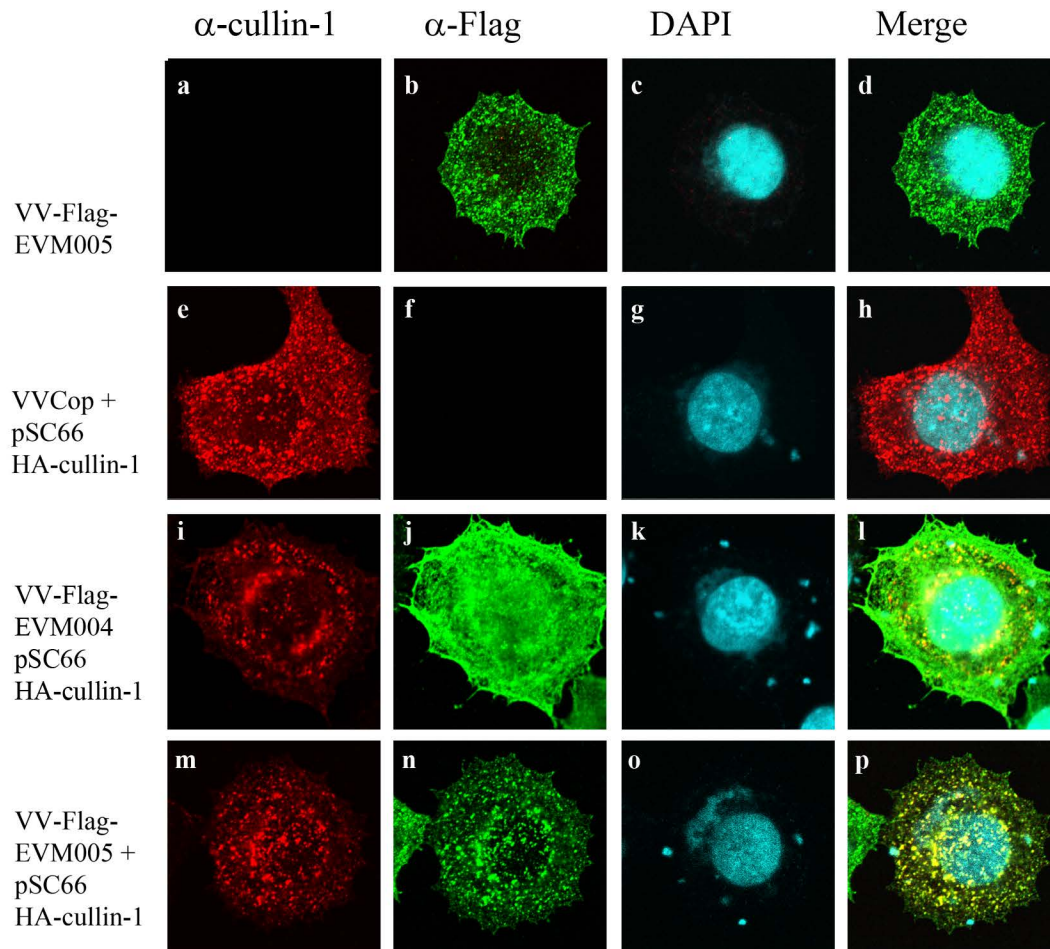


Figure 3.6. Flag-EVM005 co-localizes with HA-cullin-1 during infection. HeLa cells were infected and transfected with pSC66-HA-cullin-1. Cells were co-stained with anti-cullin-1, anti-Flag and DAPI to detect viral factories and the nucleus. (a-d) HeLa cells infected with VV-Flag-EVM005. (e-h) HeLa cells infected with VVCop and transfected with pSC66-HA-cullin-1. (i-l) HeLa cells infected with VV-Flag-EVM004 and transfected with pSC66-HA-cullin-1. (m-p) HeLa cells infected with VV-Flag-EVM005 and transfected with pSC66-HA-cullin-1. Approximately 77% of infected/transfected cells displayed co-localization between Flag-EVM005 and HA-cullin1.

(Figure 3.6 panels e-h). Furthermore, co-expression of Flag-EVM005 and HA-cullin-1 indicated co-localization (Figure 3.6 panel i-l) supporting our previous results demonstrating that HA-cullin-1 and Flag-EVM005 interact during infection (Figure 3.4). Approximately 77% of cells expressing Flag-EVM005 and HA-cullin-1 demonstrated co-localization to cytoplasmic punctate structures.

3.4 EVM005 Interacts with Components of the SCF Complex in an F-box-Dependent Manner

In order to determine whether the F-box domain of EVM005 was responsible for the interaction observed between Flag-EVM005 and cullin-1, three truncation mutants of Flag-EVM005 were created. Flag-EVM005(1-380) is composed of amino acids 1-380 and contains all four ankyrin repeats, whereas Flag-EVM005(381-650) lacks the ankyrin domains and contains the C-terminal F-box domain of EVM005 (Figure 3.7A). Flag-EVM005(1-593) lacked only the C-terminal 57 amino acids encompassing the F-box domain (Figure 3.2). HEK293T cells were mock infected or infected with VVCop, VV-Flag-EVM004, as a negative control, or recombinant VVs expressing full-length EVM005, EVM005(1-380) or EVM005(381-650). Cell lysates were subjected to immunoprecipitation with anti-Flag and western blotted with anti-cullin-1 to detect interaction with endogenous cullin-1 (Figure 3.7B). The data demonstrate that only full-length Flag-EVM005 interacts with endogenous cullin-1, reaffirming our initial mass spectrometry data (Figure 3.3). Neither Flag-EVM005(1-380), which lacks the F-box domain, nor Flag-EVM005(381-650),

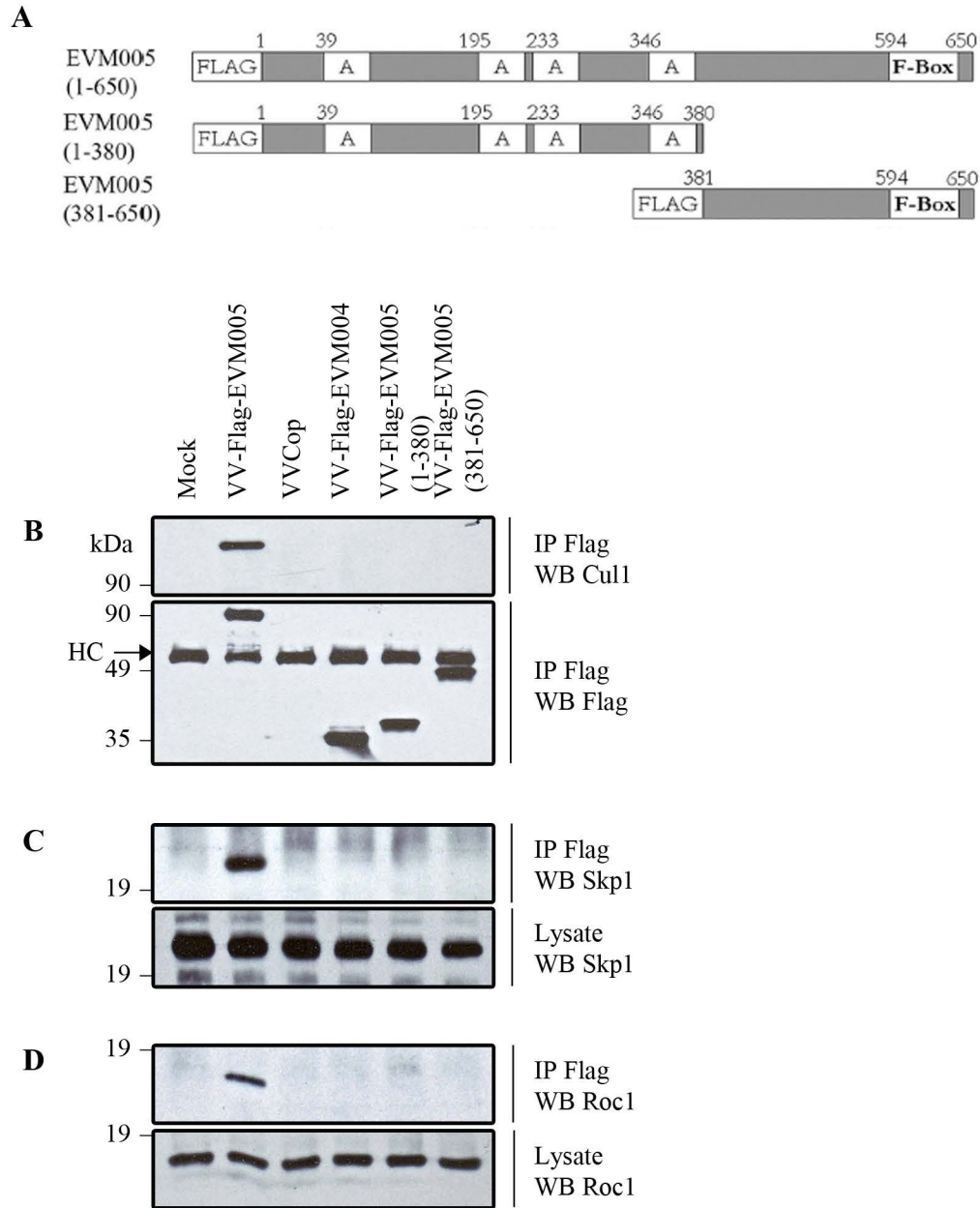


Figure 3.7. EVM005 interacts with endogenous components of the SCF ubiquitin ligase. Recombinant vaccinia viruses expressing full length and truncated versions of Flag-EVM005 were constructed. HEK293T cells were mock infected or infected with VVCop, VV-Flag-EVM005, VV-Flag-EVM004, VV-Flag-EVM005(1-380), or VV-Flag-EVM005(381-650) at a MOI of 5. At 12 hours post infection, cells were lysed in NP40 lysis buffer, immunoprecipitated with anti-Flag, and western blotted with anti-Flag or anti-Cul1, anti-Skp1 or anti-Roc1. Full-length EVM005 interacted with endogenous Skp1, Cul1 and Roc1.

which lacks the ankyrin domains but contains the F-box domain, interacted with cullin-1, suggesting that the C-terminal F-box was necessary but not sufficient for interaction with cullin-1 (Figure 3.7B). Samples were additionally subjected to western blot with antibodies specific for the linker protein Skp1 and the ubiquitin ligase Roc1 to determine if EVM005 co-precipitated with endogenous Skp1 or Roc1 (Figure 3.7C and D). Full length Flag-EVM005 interacted with both endogenous Skp1 and Roc1, suggesting that EVM005 interacted with an intact ubiquitin ligase and may serve as a unique substrate adaptor for the SCF complex (Figure 3.7C and D).

To further demonstrate that the F-box domain of EVM005 was necessary for interaction with Skp-1 and cullin-1, we generated a third EVM005 mutant, Flag-EVM005(1-593) that lacked only the C-terminal 57 amino acids encompassing the F-box domain. HEK293T cells were co-transfected with pcDNA3-Flag-EVM005, pcDNA3-Flag-EVM005(1-593) and pcDNA3-Myc-cullin-1. Immunoprecipitation with anti-Myc to pull down cullin-1 demonstrated a clear interaction with EVM005, but not with EVM005(1-593) which lacked the F-box domain (Figure 3.8A). Additionally, cells co-transfected with either pcDNA3-Flag-EVM005 or pcDNA3-Flag-EVM005(1-593) and pcDNA3-T7-Skp1 also displayed interaction between Skp1 and EVM005, but not EVM005(1-593) reaffirming that the F-box domain was necessary for interaction with the SCF complex (Figure 3.8B).

To elucidate the region of cullin-1 necessary for interaction with EVM005, we used two cullin-1 mutant constructs, HA-cullin-1 Δ 610-615 and HA-

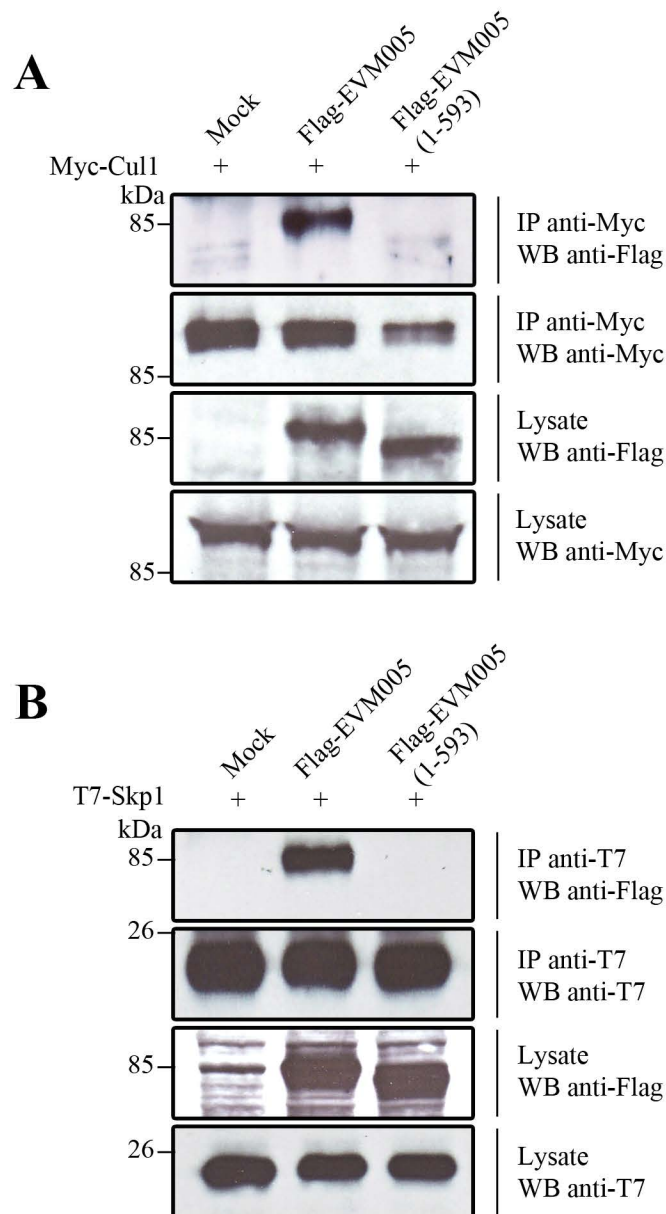


Figure 3.8. The F-box domain of EVM005 is required for interaction with the SCF complex. **A.** HEK293T cells were co-transfected with pcDNA3-T7-Skp1 and either pcDNA3-Flag-EVM005 or pcDNA3-Flag-EVM005(1-593). Cellular lysates were immunoprecipitated with anti-T7 and western blotted with anti-T7 to detect Skp1 or anti-Flag to detect EVM005. **B.** HEK293T cells were co-transfected with pcDNA3-Myc-cullin-1 and either pcDNA3-Flag-EVM005 or pcDNA3-Flag-EVM005(1-593). Cellular lysates were immunoprecipitated with anti-Myc and western blotted with anti-Myc to detect cullin-1 or anti-Flag to detect EVM005.

cullin-1 Δ N53, which are missing the C-terminal Roc1 binding domain and the N-terminal Skp1 binding domain, respectively (10). Deletion of amino acids 610-615 in cullin-1, which are critical for Roc1 interaction with cullin-1, retained the ability to interact with EVM005 as expected (Figure 3.9A). In fact, more EVM005 was immunoprecipitated with HA-cullin-1 Δ 610-615 due to increased immunoprecipitation of HA-cullin-1 Δ 610-615 in this particular assay, further supporting the interaction between cullin-1 Δ 610-65 and EVM005 (Figure 3.9A). Deletion of the N-terminal 53 amino acids of cullin-1, which has previously been shown to be necessary for Skp1 interaction, dramatically affected the ability of EVM005 to interact with cullin-1 (Figure 3.9A). Additionally, Skp-1 failed to interact with HA-cullin-1 Δ N53, indicating the possibility that Skp-1 acts as a linker between cullin-1 and EVM005 (Figure 3.9B). These data indicate that EVM005 is interacting with the cellular SCF complex in a similar fashion to cellular F-box containing substrate adaptor proteins.

3.5 EVM005 Associates with an Active SCF Ubiquitin Ligase Complex

Given that Flag-EVM005 interacted with components of the SCF complex, we hypothesized that EVM005 either interacted with a functional SCF complex to recruit novel substrates, or functioned as an inhibitor of cellular ubiquitylation. To test these possibilities, we used the anti-ubiquitin (clone FK2) antibody, which recognizes conjugated, but not free ubiquitin, to determine an association between EVM005 and conjugated ubiquitin (9). HEK293T cells were mock infected or infected with VVCop, VV-Flag-EVM005, or VV-Flag-EVM004. We also used

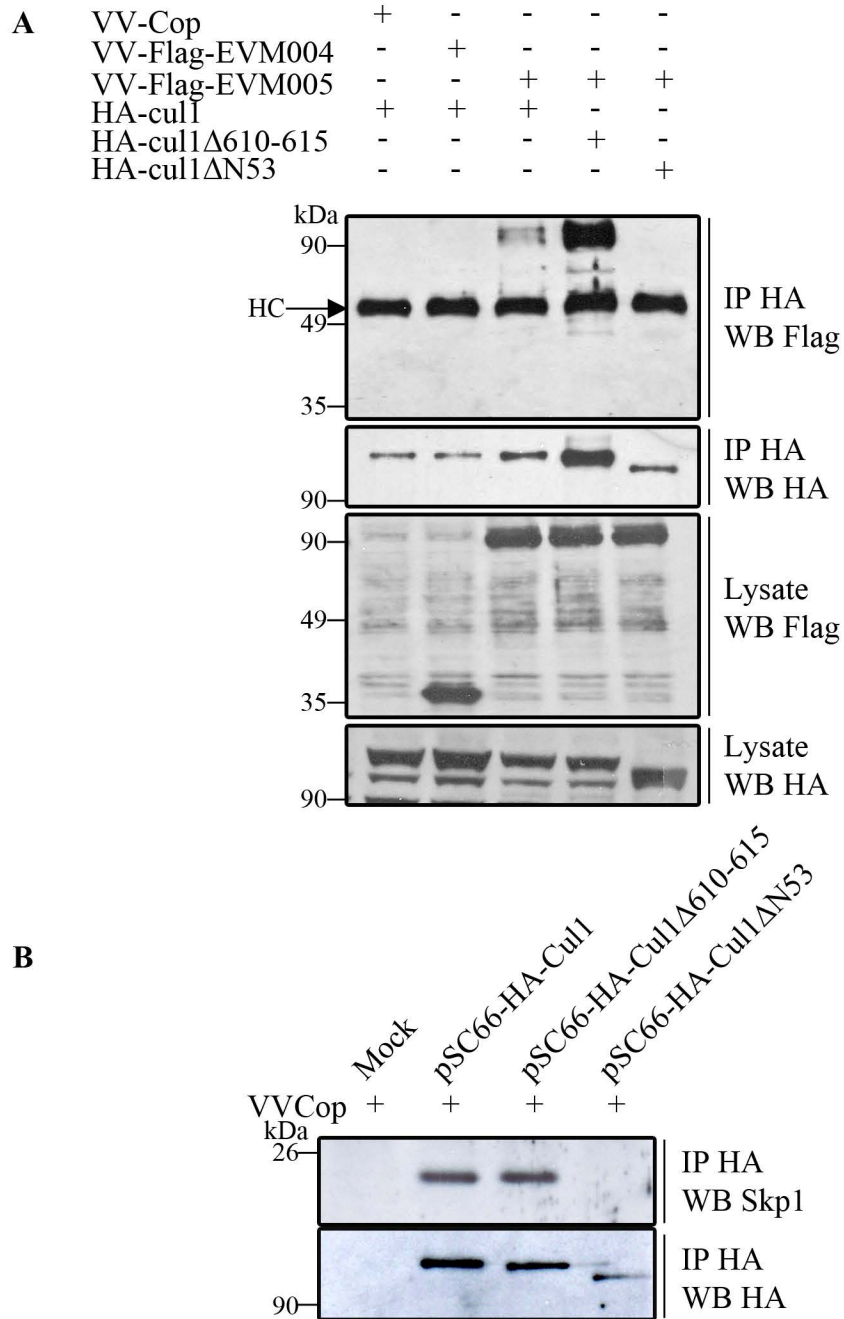


Figure 3.9. EVM005 fails to interact with HA-cullin-1ΔN53. **A.** HEK293T cells were infected with VVCop, VV-Flag-EVM004, or VV-Flag-EVM005 and transfected with either HA-cullin-1, HA-cullin-1Δ610-615, or HA-cullin-1ΔN53. Cellular lysates were immunoprecipitated with anti-HA to precipitate cullin-1 and western blotted with anti-HA or anti-Flag to detect cullin-1 or EVM005, respectively. **B.** HEK293T cells were infected with VVCop at a MOI of 5 and transfected with HA-cullin-1, HA-cullin-1Δ610-615, or HA-cullin-1ΔN53. Cells were harvested at 12 hours post infection and subjected to immunoprecipitation with anti-HA. Protein samples were separated by SDS-PAGE and western blotted with anti-HA and anti-Skp1 to detect cullin-1 and Skp1, respectively.

two viruses that served as positive controls, VV-Flag-EVM150, which expresses a BTB/kelch protein that we previously showed interacted with cullin-3 and conjugated ubiquitin, and VV-Flag-FPV039, a Bcl-2 homolog encoded by fowlpox virus that is regulated by ubiquitylation (Figure 3.10)(3, 39). Infected cells were lysed and subjected to immunoprecipitation with anti-Flag followed by western blotting with either anti-ubiquitin (FK2), anti-Flag, or anti-I5L, which detects a late protein expressed by VV (Figure 3.10)(39). The expression of I5L indicated that all recombinant VVs replicated equally in HEK293T cells (Figure 3.10). Western blotting the immunoprecipitations with anti-Flag clearly indicated that EVM005, EVM004, EVM150 and FPV039 were expressed and that Flag-FPV039 was subjected to heavy ubiquitylation resulting in the presence of multiple Flag-positive bands (Figure 3.10). Western blotting of the Flag immunoprecipitations with anti-FK2 confirmed that both Flag-EVM150 and Flag-FPV039 associate with conjugated ubiquitin due to the presence of high molecular weight ubiquitin adducts, whereas Flag-EVM004 did not as previously described (Figure 3.10)(39). Significantly, Flag-EVM005 also associated with conjugated ubiquitin, suggesting that Flag-EVM005 interacted with an active SCF complex (Figure 3.10).

To confirm the co-immunoprecipitation results, we used confocal microscopy. HeLa cells were mock infected or infected with VVCop, VV-Flag-EVM005, or VV-Flag-EVM004 and co-stained with anti-Flag, to detect EVM005 and EVM004, and anti-ubiquitin (FK2), to detect conjugated ubiquitin. In uninfected HeLa cells, the majority of conjugated ubiquitin was located in the

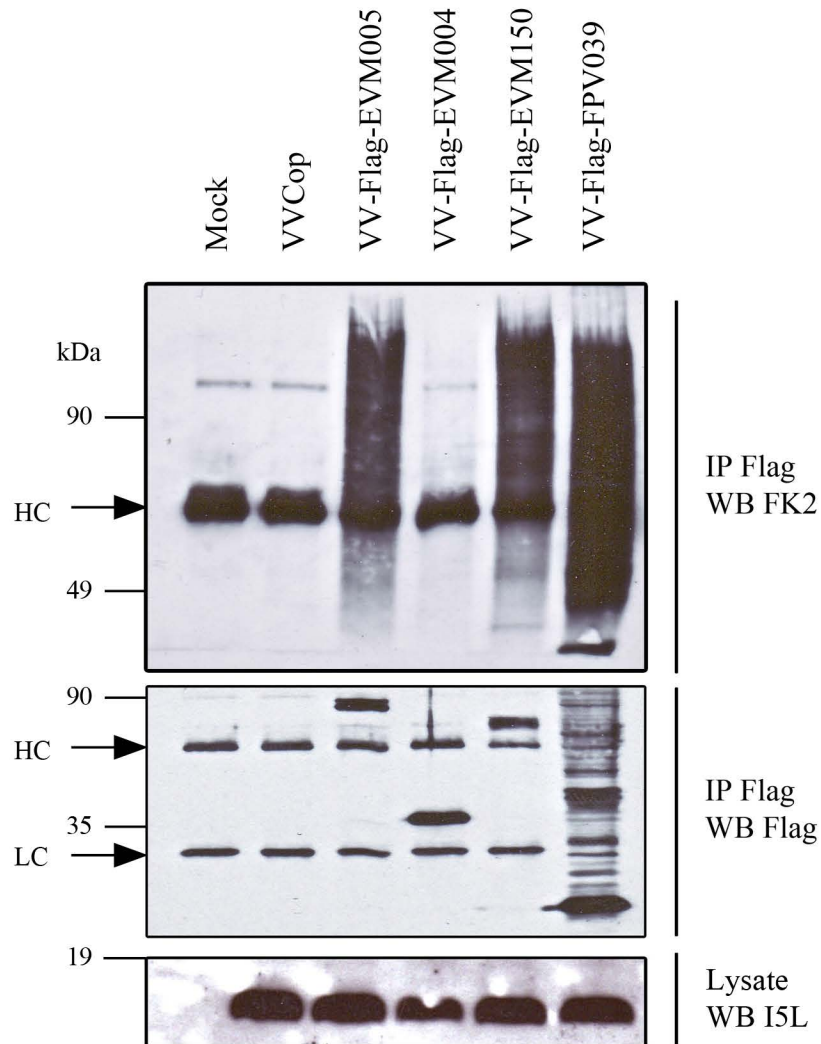


Figure 3.10. EVM005 associates with conjugated ubiquitin. HEK293T cells were mock infected or infected with VVCop, VV-Flag-EVM005, VV-Flag-EVM004, VV-Flag-EVM150, or VV-Flag-FPV039 at a MOI of 5. At 12 hours post infection, cells were lysed in NP40 lysis buffer, immunoprecipitated with anti-Flag, and western blotted with anti-ubiquitin (clone FK2) to detect conjugated ubiquitin, anti-Flag, to detect Flag-tagged proteins, or anti-I5L, to detect the vaccinia virus protein I5L. HC and LC denote antibody heavy and light chains, respectively.

nucleus (Figure 3.11 panels a-d). Upon infection with VVCop the subcellular localization of conjugated ubiquitin changed and the majority of conjugated ubiquitin was not found in the nucleus, but instead localized to punctate structures throughout the infected cell, indicating that conjugated ubiquitin was present in infected cells (Figure 3.11 panels e-h). Infection with VV-Flag-EVM004 demonstrated Flag-EVM004 localized diffusely throughout the infected cell and did not co-localize with conjugated ubiquitin (Figure 3.11 panels i-l). In contrast, HeLa cells infected with VV-Flag-EVM005 demonstrated that Flag-EVM005 localized to punctate structures throughout the infected cell, and staining with anti-ubiquitin (FK2) determined that the punctate EVM005 structures co-localized with conjugated ubiquitin (Figure 3.11 panels m-p). The co-localization of Flag-EVM005 with conjugated ubiquitin lends further support to our hypothesis that EVM005 interacts with a functional SCF ubiquitin ligase complex that is actively ubiquitylating cellular or viral proteins during infection. Greater than 80% of HeLa cells infected with VV-Flag-EVM005 displayed co-localization with conjugated ubiquitin.

3.6 EVM002 and EVM154 Contain F-box Domains and Interact with Skp1

Bioinformatics indicated that ECTV encoded three other proteins containing putative F-box domains: EVM002, EVM154, and EVM165, all of which contain N-terminal ankyrin domains in combination with C-terminal F-box domains (Figures 3.1 and 3.2). The recent demonstration that a modified vaccinia virus Ankara (MVA) ortholog of EVM165 interacts with Skp-1 clearly suggested that

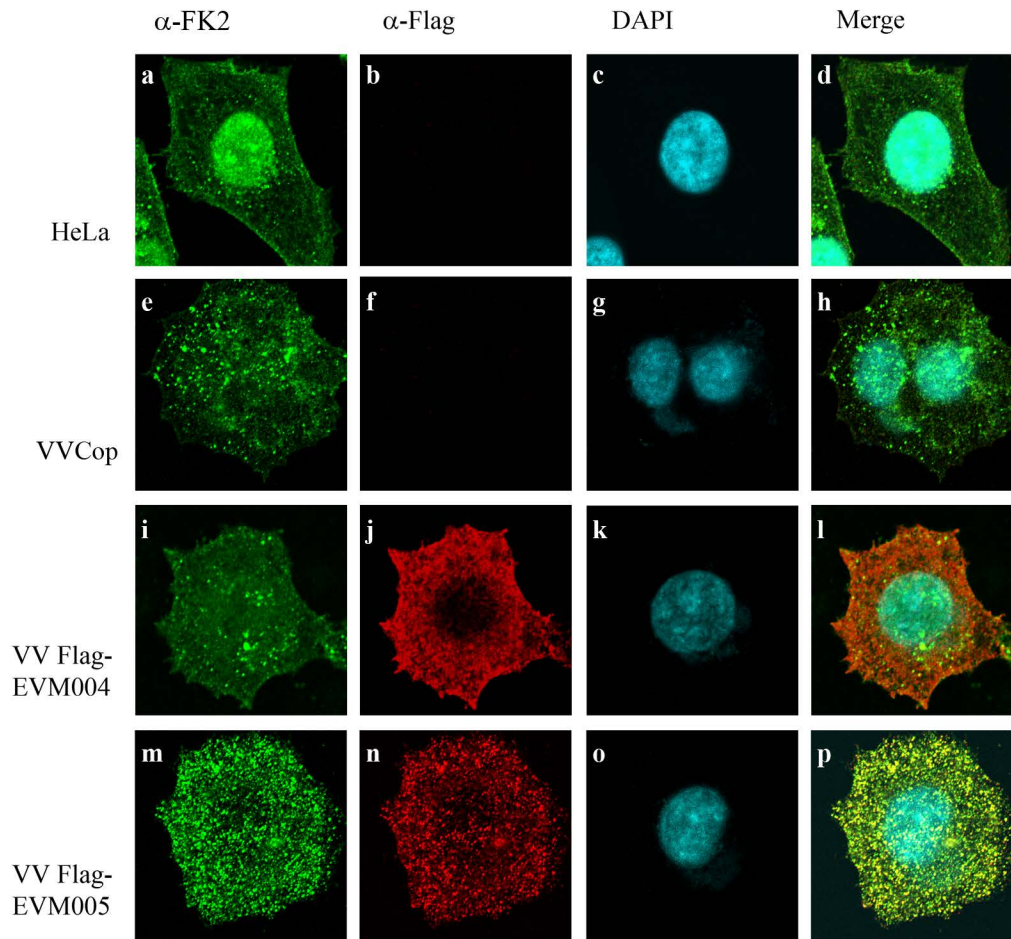


Figure 3.11. EVM005 co-localizes with conjugated ubiquitin. HeLa cells were mock infected or infected with VVCop, VV-Flag-EVM004, or VV-Flag-EVM005 at a MOI of 5 and co-localization with conjugated ubiquitin was visualized by confocal microscopy. Twelve hours post infection cells were fixed and co-stained with anti-ubiquitin (FK2), anti-Flag-Cy3, to detect the virus proteins, and DAPI, to visualize the nucleus and viral factories. (a-d) Mock infected cells. (e-h) Cells infected with VVCop. (i-l) Cells infected with VV-Flag-EVM004. (m-p) Cells infected with VV-Flag-EVM005. Greater than 80% of HeLa cells infected with VV-Flag-EVM005 displayed co-localization with conjugated ubiquitin.

EVM165 also interacts with the SCF complex (36). Prompted by this observation and our bioinformatics data, we sought to determine if EVM002 and EVM154 also interacted with the SCF complex. HeLa cells were infected with VVCop, VV-Flag-EVM004, VV-Flag-EVM005, VV-Flag-EVM002 or VV-Flag-EVM154. Cellular lysates were immunoprecipitated with anti-Flag and western blotted with anti-Skp1 to determine interaction with endogenous Skp1 (Figure 3.12). Similar to EVM005 both EVM154 and EVM002 interacted with Skp1 (Figure 3.12). Interestingly, EVM002 reproducibly demonstrated a reduced ability to interact with Skp-1 suggesting that perhaps differences in amino acid composition within the F-box domain may account for this observation.

To determine if the C-terminal F-box domains of EVM002, EVM154 and EVM165 mediated the interaction with the Skp1, we constructed F-box deletion constructs for all three proteins (Figure 3.2). Notably, we were unable to express the truncation mutant EVM154(1-532), and therefore, resorted to site-directed mutagenesis of two amino acids, F534 and P535, predicted to mediate contact with Skp1 (Figure 3.1). HEK293T cells were co-transfected with pcDNA3-T7-Skp1 and pcDNA3-Flag-EVM002, EVM005, EVM154, EVM165, or the F-box deletion mutants of EVM002, EVM005, and EVM165, or the site directed mutant of EVM154. At 18 hours post transfection cells were lysed and immunoprecipitated with anti-T7. Protein samples were analyzed by western blot with anti-T7 and anti-Flag (Figure 3.13). The data demonstrate that all four of the ECTV encoded ankyrin/F-box proteins interact with Skp1 in an F-box dependent manner (Figure 3.13).

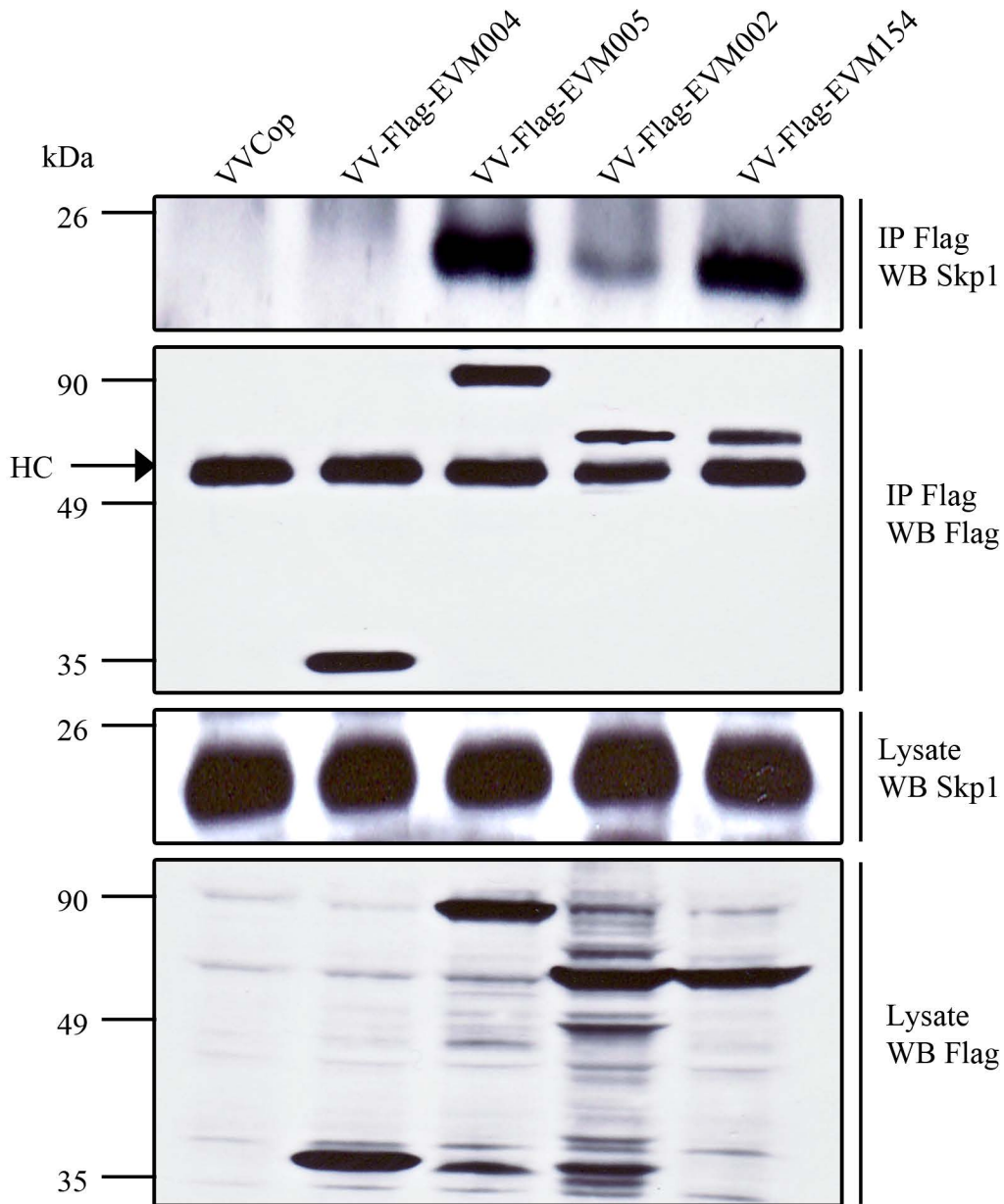


Figure 3.12. EVM002 and EVM154 interact with Skp-1. HEK293T cells were infected with VVCop, VV-Flag-EVM004, VV-Flag-EVM005, VV-Flag-EVM002, or VV-Flag-EVM154. Lysates were immunoprecipitated with anti-Flag and western blotted with anti-Flag to detect the viral proteins or western blotted with anti-Skp1 to detect endogenous Skp1. HC denotes antibody heavy chain.

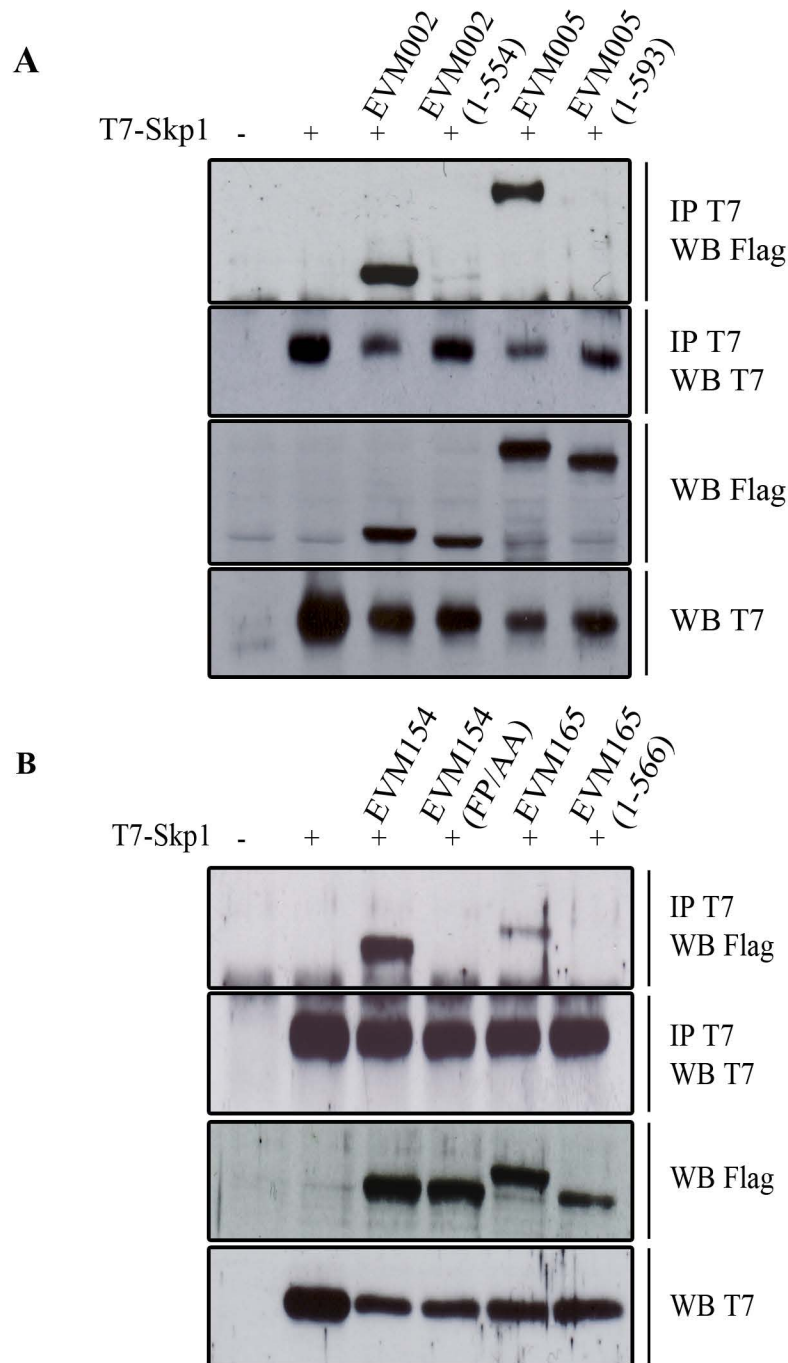


Figure 3.13. The ECTV encoded ankyrin/F-box proteins require an F-box domain to interact with Skp1. HEK293T cells were co-transfected with pcDNA3-T7-Skp1 and (A) pcDNA3-Flag-EVM002, EVM002(1-554), EVM005 or EVM005(1-593) or (B) pcDNA3-Flag-EVM154, EVM154(FP/AA), EVM165 or EVM165(1-566). At 18 hours post transfection cells were lysed in NP40 lysis buffer and subjected to immunoprecipitation with anti-T7. Protein samples were separated by SDS-PAGE and western blotted with anti-T7 and anti-Flag.

Finally, we sought to determine if EVM002 and EVM154 associated with conjugated ubiquitin. To test this, HEK293T cells were mock infected or infected with VVCop, VV-Flag-EVM004, VV-Flag-EVM005, VV-Flag-EVM002 or VV-Flag-EVM154. At 12 hours post infection, cells were lysed and subjected to immunoprecipitation with anti-Flag. Protein samples were subjected to western blot with anti-ubiquitin (FK2) and anti-Flag, to determine if Flag-EVM002 and Flag-EVM154 associate with conjugated ubiquitin, similar to EVM005 (Figure 3.14). Similar to Flag-EVM005, EVM002 and EVM154 displayed strong association with conjugated ubiquitin (Figure 3.14) and co-localized with conjugated ubiquitin (Figure 3.15) during infection. Greater than 95% of cells transfected with pSC66-Flag-EVM002 or pSC66-EVM154 demonstrated co-localization between conjugated ubiquitin and EVM002 or EVM154. These data suggest that the entire family of four ECTV encoded ankyrin/F-box proteins associate with an active SCF ubiquitin ligase and likely all recruit a unique set of substrates for ubiquitylation during ECTV infection.

3.7 Discussion

Previous studies have shown an important role for F-box proteins in substrate recruitment to the SCF complex (5, 14, 28, 38). Multiple cellular proteins containing F-box domains have been identified, many of which function as substrate adaptor molecules for the cellular SCF ubiquitin ligase (5, 14, 28, 38, 41). Using a bioinformatics approach we identified four ECTV genes, EVM002, EVM005, EVM154 and EVM165, which encode N-terminal ankyrin repeats in

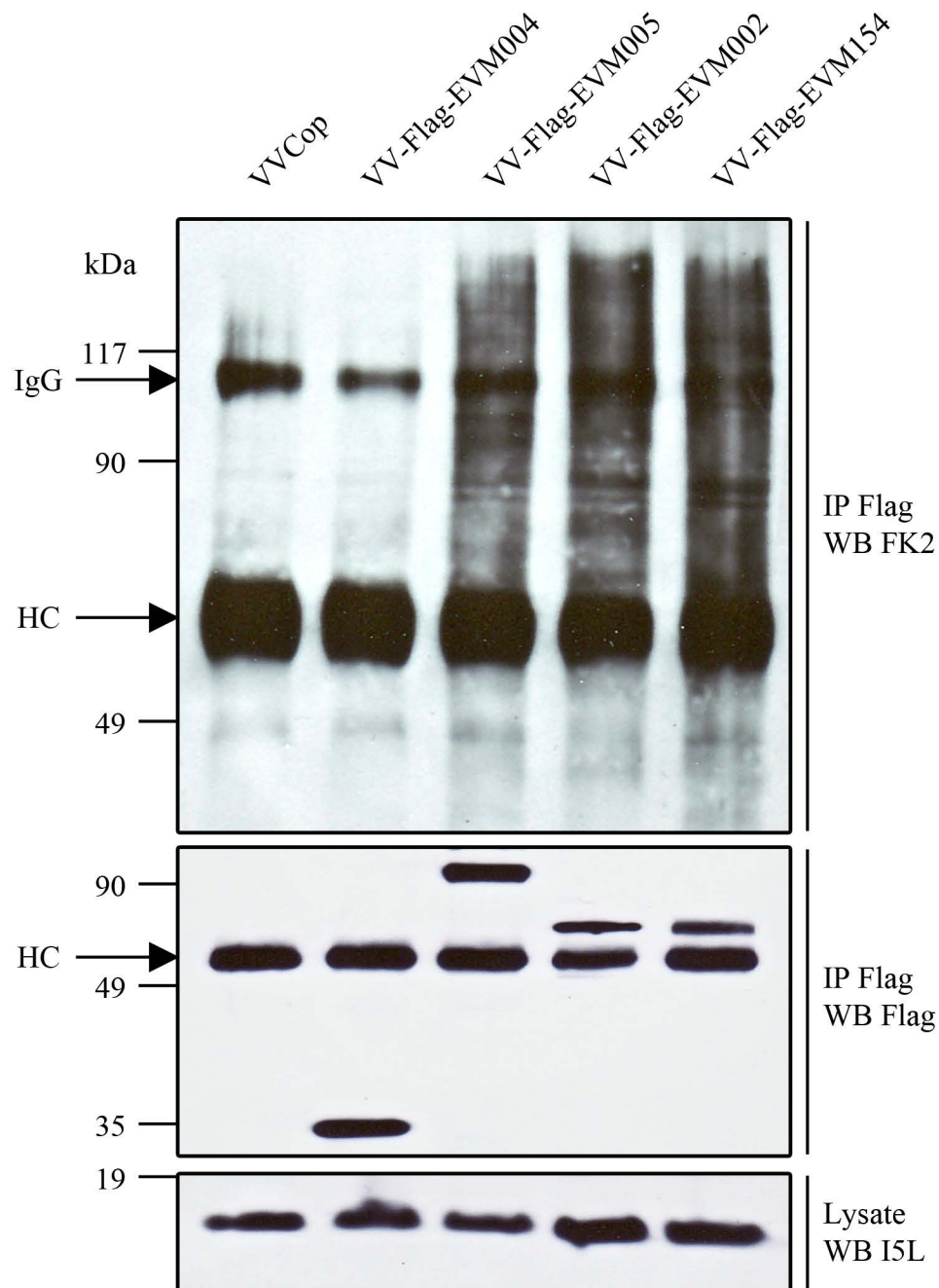


Figure 3.14. EVM002 and EVM154 interact with conjugated ubiquitin. HEK293T cells were mock infected or infected with VVCop, VV-Flag-EVM004, VV-Flag-EVM005, VV-Flag-EVM002, or VV-Flag-EVM154 at a MOI of 5. At 12 hours post infection cells were lysed in NP40 lysis buffer and immunoprecipitated with anti-Flag and western blotted with anti-ubiquitin (clone FK2), to detect conjugated ubiquitin, anti-Flag, to detect Flag-tagged viral proteins, or anti-I5L, to detect the vaccinia virus protein I5L. IgG denotes antibody and HC denotes antibody heavy chain.

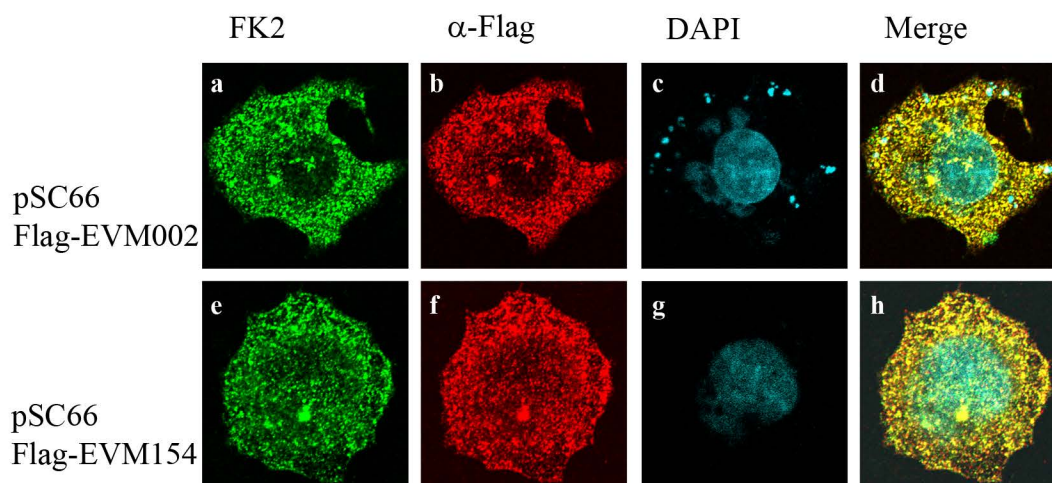


Figure 3.15. EVM002 and EVM154 co-localize with conjugated ubiquitin. HeLa cells were infected with VVCop and transfected with pSC66-Flag-EVM002 or pSC66-Flag-EVM154. Co-localization with conjugated ubiquitin was visualized by confocal microscopy. Twelve hours post infection, coverslips were fixed and co-stained with anti-ubiquitin (FK2), anti-Flag-Cy3, and DAPI, to visualize the nucleus and viral factories. (a-d) VVCop infected and transfected with pSC66-Flag-EVM002. (e-h) Cells infected with VVCop and transfected with pSC66-Flag-EVM154. Greater than 95% of cells transfected with pSC66-Flag-EVM002 or pSC66-EVM154 demonstrated co-localization between conjugated ubiquitin and EVM002 or EVM154.

combination with C-terminal F-box domains (Figure 3.1 and 3.2). Significantly, the combination of ankyrin repeats and F-box domains is unique to poxviruses and not found within cellular F-box proteins (20). The presence of F-box domains, led us to speculate that these four ECTV encoded proteins would play a role in regulating the ubiquitin-proteasome system via interaction with the cellular SCF complex. To perform these studies we used an over-expression strategy in which EVM002, EVM005 and EVM154 were expressed during virus infection and were all shown to associate with the linker protein, Skp1 (Figures 3.7 and 3.12). We also demonstrated that EVM005 interacted with other components of the SCF complex including Skp1, cullin-1, and Roc1 (Figure 3.7). Transient expression of EVM002, EVM005, EVM154 or EVM165 also demonstrated interaction with T7-Skp1 was mediated by the C-terminal F-box domain (Figure 3.13). Together our data indicate that ECTV encodes multiple proteins that interact with components of the SCF complex.

To determine whether the poxvirus ankyrin/F-box proteins were associated with an active ubiquitin ligase or whether they functioned as inhibitors of the SCF complex, we assayed for association with conjugated ubiquitin molecules using the anti-ubiquitin (FK2) antibody. Anti-ubiquitin (FK2) recognizes the isopeptide linkage between the C-terminal glycine of ubiquitin and the lysine residue in the adjoining protein (9). Our data demonstrate that EVM002, EVM005 and EVM154 all associate with conjugated ubiquitin as shown by immunoprecipitation (Figure 3.10 and 3.14) and confocal microscopy (Figure 3.11 and 3.15). This data suggests that each of the ECTV encoded

ankyrin/F-box proteins has the potential to recruit a unique set of substrates to the SCF complex for ubiquitylation during infection. The identification of these substrates remains a major goal of our laboratory.

In contrast to the majority of cellular SCF substrate adaptor proteins, the ECTV F-boxes are located at the C-terminus in combination with a series of N-terminal ankyrin repeats. An alignment of EVM002, EVM005, EVM154, and EVM165 with the F-box from the cellular protein Skp2 demonstrated that key residues were maintained in the ECTV encoded proteins (Figure 3.1)(30, 41). The co-crystal structure of Skp1 and the cellular substrate adaptor protein Skp2 demonstrates that the F-box domain of Skp2 is composed of three α -helices containing residues important for contact with Skp-1 (Figure 3.1)(30, 41). The ECTV F-box domains appear to have conserved key amino acids within helices H1 and H2, but little homology was maintained within the α -helix H3 (Figure 3.1). Recently, a structure prediction program generated F-box structures for each of the ECTV F-box proteins, and the H3 α -helix was either absent or truncated in all cases (34). Interestingly, this study also predicted that EVM005 contained a small amount of β -sheet in place of the H3 α -helix (34). Despite lacking homology to the H3 α -helix, however, we have shown that the ECTV proteins, EVM002, EVM005 EVM154 and EVM165, interact with Skp-1 (Figures 3.7, 3.8, 3.12, and 3.13). Additionally, data from Sperling and colleagues confirm that the VV ortholog of EVM165 also interacts with Skp-1 (36). We were unable, however, to observe an interaction between Skp-1 and a mutant of EVM005, EVM005(381-650), that contains the F-box domain, but lacks the ankyrin repeat

domains, suggesting that the ankyrin domains may also play a role in interaction (Figure 3.7). The cellular substrate adaptor protein, Skp2, contains ten LRRs in conjunction with an N-terminal F-box domain. The first three LRRs in Skp2 serve a structural linker role suggesting that one or more of the ankyrin repeats in EVM005 may provide a similar function (Figure 3.7)(30, 41).

In all cases, the ECTV F-box domains were found in combination with N-terminal ankyrin domains. Ankyrin repeat domains are composed of a 30-34 amino acid repeat important for protein-protein interactions and found in a wide range of proteins (23, 31). Interestingly, the majority of cellular SCF substrate adaptors contain F-box domains in combination with either LRR or WD repeats in order to recruit substrates to the SCF complex (5, 6, 14, 28, 40). Although cellular F-boxes are not found in combination with ankyrin domains, ankyrin/SOCS box proteins, which recruit substrates to cullin-2 ubiquitin ligases are common (27), suggesting that the poxvirus ankyrin/F-box proteins may have evolved through recombination. Given that a large number of cellular F-box proteins function as substrate adaptors for the SCF complex (5, 6, 14, 28, 40), we speculate that the ECTV encoded ankyrin/F-box proteins may also function as substrate adaptors for the SCF complex. The interaction of EVM002, EVM005, EVM154, and EVM165 with components of the SCF complex strongly supports this possibility. Several cellular F-box proteins, however, serve functions other than substrate adaptors (5, 6, 14, 28, 40). The best characterized of these is cyclin F, which contains a cyclin domain and an F-box to regulate levels of itself, ultimately controlling the cell cycle (2). Accordingly, it is possible that the ECTV

encoded ankyrin/F-box proteins may utilize their C-terminal F-box domains to regulate their own levels. Alternatively, the ECTV encoded ankyrin/F-box proteins could simply bind and sequester cullin-1 in order to inhibit the SCF complex. At present, our data do not distinguish between these possibilities; however, the presence of conjugated ubiquitin upon expression of EVM002, EVM005, and EVM154 suggests that active ubiquitination is occurring (Figures 3.10, 3.11, 3.14, 3.15). Undoubtedly, the identification of additional binding partners for the ECTV encoded ankyrin/F-box proteins will lead to further insights regarding their function.

3.8 References

1. **Ardley, H. C., and P. A. Robinson.** 2005. E3 ubiquitin ligases. *Essays Biochem* **41**:15-30.
2. **Bai, C., P. Sen, K. Hofmann, L. Ma, M. Goebel, J. W. Harper, and S. J. Elledge.** 1996. SKP1 connects cell cycle regulators to the ubiquitin proteolysis machinery through a novel motif, the F-box. *Cell* **86**:263-74.
3. **Banadyga, L., J. Gerig, T. Stewart, and M. Barry.** 2007. Fowlpox virus encodes a Bcl-2 homologue that protects cells from apoptotic death through interaction with the proapoptotic protein Bak. *J Virol* **81**:11032-45.
4. **Barry, M., and K. Fruh.** 2006. Viral modulators of cullin RING ubiquitin ligases: culling the host defense. *Sci STKE* **2006**:pe21.
5. **Cardozo, T., and M. Pagano.** 2004. The SCF ubiquitin ligase: insights into a molecular machine. *Nat Rev Mol Cell Biol* **5**:739-51.
6. **Cenciarelli, C., D. S. Chiaur, D. Guardavaccaro, W. Parks, M. Vidal, and M. Pagano.** 1999. Identification of a family of human F-box proteins. *Curr Biol* **9**:1177-9.
7. **Davison, A. J., and B. Moss.** 1990. New vaccinia virus recombination plasmids incorporating a synthetic late promoter for high level expression of foreign proteins. *Nucleic Acids Res* **18**:4285-6.
8. **Esteban, D. J., and R. M. Buller.** 2005. Ectromelia virus: the causative agent of mousepox. *J Gen Virol* **86**:2645-59.
9. **Fujimuro, M., and H. Yokosawa.** 2005. Production of antipolyubiquitin monoclonal antibodies and their use for characterization and isolation of polyubiquitinated proteins. *Methods Enzymol* **399**:75-86.

10. **Furukawa, M., Y. Zhang, J. McCarville, T. Ohta, and Y. Xiong.** 2000. The CUL1 C-terminal sequence and ROC1 are required for efficient nuclear accumulation, NEDD8 modification, and ubiquitin ligase activity of CUL1. *Mol Cell Biol* **20**:8185-97.
11. **Gagne, J. M., B. P. Downes, S. H. Shiu, A. M. Durski, and R. D. Vierstra.** 2002. The F-box subunit of the SCF E3 complex is encoded by a diverse superfamily of genes in Arabidopsis. *Proc Natl Acad Sci U S A* **99**:11519-24.
12. **Hicke, L.** 2001. Protein regulation by monoubiquitin. *Nat Rev Mol Cell Biol* **2**:195-201.
13. **Huang, J., Q. Huang, X. Zhou, M. M. Shen, A. Yen, S. X. Yu, G. Dong, K. Qu, P. Huang, E. M. Anderson, S. Daniel-Issakani, R. M. Buller, D. G. Payan, and H. H. Lu.** 2004. The poxvirus p28 virulence factor is an E3 ubiquitin ligase. *J Biol Chem* **279**:54110-6.
14. **Jin, J., T. Cardozo, R. C. Lovering, S. J. Elledge, M. Pagano, and J. W. Harper.** 2004. Systematic analysis and nomenclature of mammalian F-box proteins. *Genes Dev* **18**:2573-80.
15. **Johnston, J. B., and G. McFadden.** 2003. Poxvirus immunomodulatory strategies: current perspectives. *J Virol* **77**:6093-100.
16. **Johnston, J. B., G. Wang, J. W. Barrett, S. H. Nazarian, K. Colwill, M. Moran, and G. McFadden.** 2005. Myxoma virus M-T5 protects infected cells from the stress of cell cycle arrest through its interaction with host cell cullin-1. *J Virol* **79**:10750-63.
17. **Latres, E., D. S. Chiaur, and M. Pagano.** 1999. The human F box protein beta-Trcp associates with the Cull1/Skp1 complex and regulates the stability of beta-catenin. *Oncogene* **18**:849-54.
18. **Lechner, E., P. Achard, A. Vansiri, T. Potuschak, and P. Genschik.** 2006. F-box proteins everywhere. *Curr Opin Plant Biol* **9**:631-8.
19. **Mackett, M., G. L. Smith, and B. Moss.** 1992. Vaccinia virus: a selectable eukaryotic cloning and expression vector. 1982. *Biotechnology* **24**:495-9.
20. **Mercer, A. A., S. B. Fleming, and N. Ueda.** 2005. F-box-like domains are present in most poxvirus ankyrin repeat proteins. *Virus Genes* **31**:127-33.
21. **Michel, J. J., and Y. Xiong.** 1998. Human CUL-1, but not other cullin family members, selectively interacts with SKP1 to form a complex with SKP2 and cyclin A. *Cell Growth Differ* **9**:435-49.
22. **Minella, A. C., and B. E. Clurman.** 2005. Mechanisms of tumor suppression by the SCF(Fbw7). *Cell Cycle* **4**:1356-9.
23. **Mosavi, L. K., T. J. Cammett, D. C. Desrosiers, and Z. Y. Peng.** 2004. The ankyrin repeat as molecular architecture for protein recognition. *Protein Sci* **13**:1435-48.
24. **Nakayama, K. I., S. Hatakeyama, and K. Nakayama.** 2001. Regulation of the cell cycle at the G1-S transition by proteolysis of cyclin E and p27Kip1. *Biochem Biophys Res Commun* **282**:853-60.

25. **Nakayama, K. I., and K. Nakayama.** 2006. Ubiquitin ligases: cell-cycle control and cancer. *Nat Rev Cancer* **6**:369-81.
26. **Nerenberg, B. T., J. Taylor, E. Bartee, K. Gouveia, M. Barry, and K. Fruh.** 2005. The poxviral RING protein p28 is a ubiquitin ligase that targets ubiquitin to viral replication factories. *J Virol* **79**:597-601.
27. **Nicholson, S. E., and D. J. Hilton.** 1998. The SOCS proteins: a new family of negative regulators of signal transduction. *J Leukoc Biol* **63**:665-8.
28. **Petroski, M. D., and R. J. Deshaies.** 2005. Function and regulation of cullin-RING ubiquitin ligases. *Nat Rev Mol Cell Biol* **6**:9-20.
29. **Pickart, C. M., and D. Fushman.** 2004. Polyubiquitin chains: polymeric protein signals. *Curr Opin Chem Biol* **8**:610-6.
30. **Schulman, B. A., A. C. Carrano, P. D. Jeffrey, Z. Bowen, E. R. Kinnucan, M. S. Finnin, S. J. Elledge, J. W. Harper, M. Pagano, and N. P. Pavletich.** 2000. Insights into SCF ubiquitin ligases from the structure of the Skp1-Skp2 complex. *Nature* **408**:381-6.
31. **Sedgwick, S. G., and S. J. Smerdon.** 1999. The ankyrin repeat: a diversity of interactions on a common structural framework. *Trends Biochem Sci* **24**:311-6.
32. **Seet, B. T., J. B. Johnston, C. R. Brunetti, J. W. Barrett, H. Everett, C. Cameron, J. Sypula, S. H. Nazarian, A. Lucas, and G. McFadden.** 2003. Poxviruses and immune evasion. *Annu Rev Immunol* **21**:377-423.
33. **Skowyra, D., K. L. Craig, M. Tyers, S. J. Elledge, and J. W. Harper.** 1997. F-box proteins are receptors that recruit phosphorylated substrates to the SCF ubiquitin-ligase complex. *Cell* **91**:209-19.
34. **Sonnberg, S., S. B. Fleming, and A. A. Mercer.** 2009. A truncated two-alpha-helix F-box present in poxvirus ankyrin-repeat proteins is sufficient for binding the SCF1 ubiquitin ligase complex. *J Gen Virol* **90**:1224-8.
35. **Sperling, K. M., A. Schwantes, B. S. Schnierle, and G. Sutter.** 2008. The highly conserved orthopoxvirus 68k ankyrin-like protein is part of a cellular SCF ubiquitin ligase complex. *Virology* **374**:234-9.
36. **Sperling, K. M., A. Schwantes, B. S. Schnierle, and G. Sutter.** 2008. The highly conserved orthopoxvirus 68k ankyrin-like protein is part of a cellular SCF ubiquitin ligase complex. *Virology*.
37. **Weissman, A. M.** 2001. Themes and variations on ubiquitylation. *Nat Rev Mol Cell Biol* **2**:169-78.
38. **Willems, A. R., M. Schwab, and M. Tyers.** 2004. A hitchhiker's guide to the cullin ubiquitin ligases: SCF and its kin. *Biochim Biophys Acta* **1695**:133-70.
39. **Wilton, B. A., S. Campbell, N. Van Buuren, R. Garneau, M. Furukawa, Y. Xiong, and M. Barry.** 2008. Ectromelia virus BTB/kelch proteins, EVM150 and EVM167, interact with cullin-3-based ubiquitin ligases. *Virology* **374**:82-99.
40. **Winston, J. T., D. M. Koeppe, C. Zhu, S. J. Elledge, and J. W. Harper.** 1999. A family of mammalian F-box proteins. *Curr Biol* **9**:1180-2.

41. **Zheng, N., B. A. Schulman, L. Song, J. J. Miller, P. D. Jeffrey, P. Wang, C. Chu, D. M. Koepp, S. J. Elledge, M. Pagano, R. C. Conaway, J. W. Conaway, J. W. Harper, and N. P. Pavletich.** 2002. Structure of the Cul1-Rbx1-Skp1-F boxSkp2 SCF ubiquitin ligase complex. *Nature* **416**:703-9.

Chapter 4: Creation of ECTV Recombinant Viruses Using the Selectable and Excisable Marker System

Results contained within this chapter consist of unpublished material.

Construction of ECTV- Δ 002 using SEM has been published in PLOS One:
Rintoul, J., J. Wang, D.B. Gammon, N. van Buuren, K. Garson, K. Jardine, M. Barry, D.H. Evans, and J.C. Bell. 2011. Plos One, 6(9): e24643.

4.1 Introduction

Historically, recombinant poxviruses have been generated by insertion of a gene of interest through homologous recombination into a specific locus on the viral genome. This can be done in order to gain expression of a new gene during infection, or inactivate a viral gene (29). In order to separate recombinant poxviruses from the parental strain, it has been necessary to add a marker to identify recombinants. Many markers have been used including fluorescent genes such as green fluorescent protein (GFP), drug resistance markers such as the *E. coli* guanine phosphoribosyl-transferase (GPT), or genes that can be used in colorimetric assays such as β -galactosidase, or β -glucuronidase (4, 5, 11, 13, 23). Here, we outline the Selectable and Excisable Marker (SEM) system, developed in collaboration with the laboratories of Dr. David Evans and Dr. John Bell (30). The SEM system allows for the insertion of the highly selectable yellow fluorescent protein (YFP)-GPT fusion protein cassette into any non-essential locus in the genome. The *yfp-gpt* cassette is flanked by loxP sites so that the marker can be excised by Cre-mediated recombination following purification of the recombinant poxvirus, leaving behind only a single residual loxP site (1, 30).

The SEM system for creating poxvirus recombinants utilizes the well characterized Cre/loxP system for removing the *yfp-gpt* cassette following purification of recombinant viruses (31, 32). The Cre recombinase is a 38 kDa protein that binds to 34bp loxP sites consisting of two 13bp palindromic sequences flanking an 8bp sequence that determines its directionality (15). Two loxP sites oriented in the same direction, as dictated by the 8bp sequence, will

result in excision of the intervening DNA sequence through recombination, resulting in a circular DNA excision product (1). One component of the SEM system is the vector, pDGloxP-KO, which contains a *yfp-gpt* cassette driven by the synthetic pE/L poxvirus promoter (6), and flanked by two loxP sites oriented in the same direction, and finally, flanked again by multiple cloning sites for insertion of regions of homology corresponding to the destination locus. Additionally, U2OS cells expressing a mutant Cre recombinase leading to a predominantly cytoplasmic localization were created, ideal for recombination of poxvirus genomes containing loxP sites (30).

The YFP-GPT fusion protein represents a highly efficient marker for recovery of recombinant poxviruses. YFP allows for the identification of recombinants through yellow fluorescence of plaques and GPT allows for the selection of recombinants through growth in media containing mycophenolic acid (MPA)(11). The enzymatic function of GPT converts guanine, xanthine and hypoxanthine to their respective purine ribonucleotides, therefore participating in the nucleotide salvage metabolism pathway (11, 27). MPA shuts down *de novo* nucleotide synthesis, rendering only the salvage pathway available for the production of nucleotides. In the presence of MPA, xanthine and hypoxanthine, GPT expressing viruses are capable of producing nucleotides via the salvage pathway, while viruses that lack GPT are not. MPA is extremely selective, and recombinant poxviruses can be purified in as little as three rounds of plaque purification.

We generated pDG-loxP-KO vectors containing two 150bp or 200bp sequences from the ECTV genome flanking the *yfp-gpt* cassette. These regions corresponded to genomic sequence directly up or downstream of the loci encoding one of the four ankyrin/F-box proteins. These vectors were then used to replace gene sequences encoding the ankyrin/F-box proteins with the *yfp-gpt* cassette through homologous recombination. Through subsequent infection of the U20S-Cre cells, the *yfp-gpt* cassette can be removed to create marker-free knockout viruses containing a single residual loxP site. There are several major benefits to marker-free knockout viruses compared to traditional knockout strategies. The first advantage is that experiments performed with marker-containing knockout viruses, require a control virus containing the same marker in a non-essential region of the genome, traditionally an intergenic region. Experiments performed with marker-free knockout viruses can be performed with true wild type viruses as controls. The second benefit is the potential to generate large deletion viruses. Due to the residual loxP site following Cre recombination, the *yfp-gpt* cassette can be subsequently inserted into a nearby locus on the genome, and Cre recombination can excise all intergenic material. Historically, viruses such as VV811, which lacks 55 ORFs, have proven to be invaluable tools during the study of poxvirus-host interactions, but were extremely difficult to generate (28). Finally, many poxviruses are being developed as therapeutics for cancer or as vaccine vectors (2, 3, 10, 14, 19, 21). Licensing of recombinant poxviruses that contain drug resistant markers is a point of contention, and the

SEM system allows companies attempting to license a poxvirus therapeutic the ability to remove all markers following purification.

The SEM system has the potential to create marker-free recombinant poxviruses lacking multiple ORFs, through the sequential insertion and excision of the *yfp-gpt* cassette. We show here that the SEM system is compatible with ECTV through the creation of EVM002 and EVM005 knockout viruses, which both lack markers. Additionally, we test the capability of SEM system in construction of ECTV strains lacking multiple ORFs.

4.2 Deletion of EVM002 and EVM005 from ECTV Strain Moscow Using the Selectable and Excisable Marker System

The SEM system was initially created for the construction of recombinant VVs. The following experiments represent the first attempts to use it with other *Orthopoxviruses*, and suggest that the SEM system may be compatible with a large number of poxviruses. We adopted the SEM system to generate EVM002 and EVM005 deletion viruses; ECTV- Δ 002 and ECTV- Δ 005. The pDGloxP-KO constructs were created containing 150bp regions of homology from up and downstream of the EVM002 and EVM005 loci. The upstream and downstream regions of homology were amplified from ECTV viral genomic DNA using *Taq* polymerase and cloned into pGEMT followed by subcloning into the multiple cloning sites of the pDGloxP-KO vector one at a time to create pDGloxP-EVM002KO and pDGloxP-EVM005KO (Figure 4.1A). To create ECTV- Δ 002 and ECTV- Δ 005 we used the pDGloxP-KO vector to replace the *EVM002* or

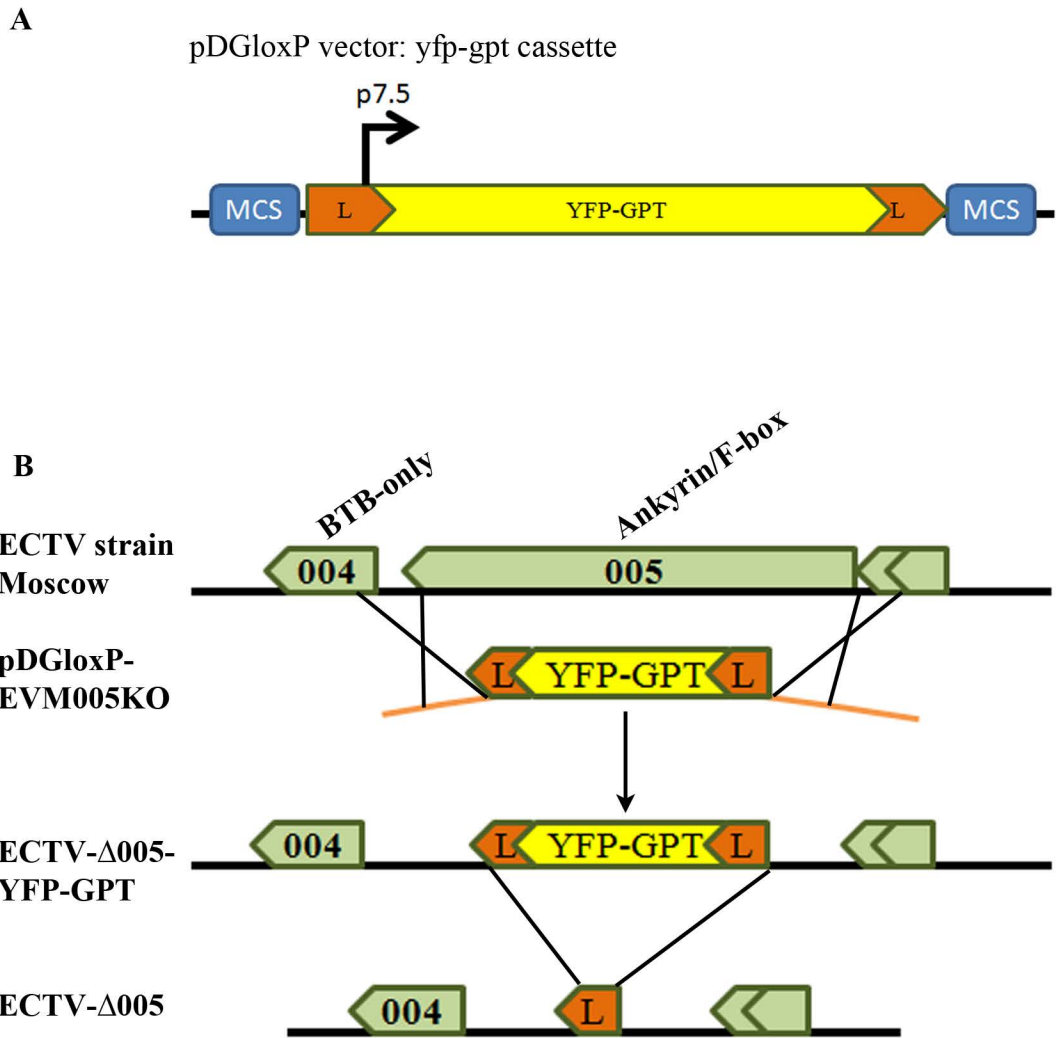


Figure 4.1. Schematic of the Selectable and Excisable Marker System for deletion of EVM005. **A.** The pDGloxP-KO plasmid was designed for the construction of marker-free recombinant poxviruses. The plasmid contains a *yfp-gpt* cassette driven by the synthetic early/late poxvirus promoter p7.5. This cassette is flanked by two loxP sites (L) oriented in the same direction, which are flanked by multiple cloning sites (MCS). Regions of homology are cloned into the multiple cloning sites that correspond to 150bp of DNA up and downstream of the gene of interest. **B.** Transfection of pDGloxP-EVM005KO into ECTV infected cells resulted in recombination of the *yfp-gpt* cassette and generation of ECTV- Δ 005-YFP-GPT. U20S cells expressing a cytoplasmic Cre recombinase are infected in order to excise the *yfp-gpt* cassette, resulting in a marker-free EVM005 deletion virus, ECTV- Δ 005.

EVM005 genes with *yfp-gpt*. BGMK cells were infected with wild type ECTV strain Moscow and transfected with linearized pDGloxP-EVM002KO or pDGloxP-EVM005KO (Figure 4.1B). This recombination reaction created ECTV- Δ 002-YFP-GPT or ECTV- Δ 005-YFP-GPT (Figure 4.1B). We were able to select for these recombinants using media containing MPA, xanthine and hypoxanthine (MPA selection media), as GPT expressing recombinants are resistant to MPA (11, 30). Recombinants were screened for the expression of YFP by picking YFP positive foci identified by immunofluorescence microscopy.

Purified ECTV- Δ 002-YFP-GPT and ECTV- Δ 005-YFP-GPT were then subjected to Cre recombination to remove the *yfp-gpt* cassette, resulting in marker-free deletion constructs (Figure 4.1B). U2OS cells expressing a cytoplasmic mutant of the Cre recombinase (U2OS-Cre) were infected with ECTV- Δ 002-YFP-GPT or ECTV- Δ 005-YFP-GPT and foci lacking YFP fluorescence were purified to create ECTV- Δ 002 and ECTV- Δ 005 (Figure 4.1B).

A revertant virus was successfully generated by transfection with linearized pGEMT-EVM005-rev. We were unable to select for revertant strains of ECTV using the conventional reverse GPT selection commonly used for cloning revertant VVs (17). Therefore, marker-rescue was performed through fluorescence microscopy; white foci were picked and purified to generate ECTV-005-rev.

4.3 Characterization of YFP Fluorescence in ECTV Recombinant Viruses

To show proof of principle, the SEM system was used in assays to detect the presence or absence of YFP fluorescence. Mock infected cells or cells infected with ECTV, ECTV- Δ 002 and ECTV- Δ 005, recombinants that had undergone Cre recombination, did not produce yellow foci, as expected (Figure 4.2 panel a-f, j-l, and p-r). However, foci were clearly observed in cells by DIC, compared to mock infected cells (Figure 4.2 panel a-c, d-f, j-l and p-r). Alternatively, ECTV- Δ 002-YFP-GPT and ECTV- Δ 005-YFP-GPT produced foci with strong yellow fluorescence (Figure 4.2 panel g-i and m-o).

Flow cytometry was used to detect YFP fluorescence in cells infected with ECTV- Δ 002-YFP-GPT. BGMK cells were mock infected or infected at a MOI of 5 for 4 hours with wild type ECTV, ECTV- Δ 002-YFP-GPT or ECTV- Δ 002 (Figure 4.3). Live cells were harvested and analyzed using a BSL-2 FACScan flow cytometer. Our data indicated that strong YFP fluorescence was detected on the FL1 channel in cells infected with ECTV- Δ 002-YFP-GPT (Figure 4.3 panel c). Alternatively, mock infected cells or cells infected with ECTV or ECTV- Δ 002 displayed no fluorescence, as expected (Figure 4.3 panels a, b, and d).

4.4 Characterization of Recombinant ECTV Genomes by PCR Analysis

Insertion and excision of the *yfp-gpt* cassette in the EVM002 and EVM005 loci of the ECTV genome was detected using PCR analysis of viral genomes. BGMK cells were infected with ECTV, ECTV- Δ 002-YFP-GPT, or ECTV- Δ 002 at a MOI of 5 for 24 hours. Viral genomes were analyzed by PCR using primers flanking the EVM002 locus (Figure 4.4A). A similar approach was taken to analyse the

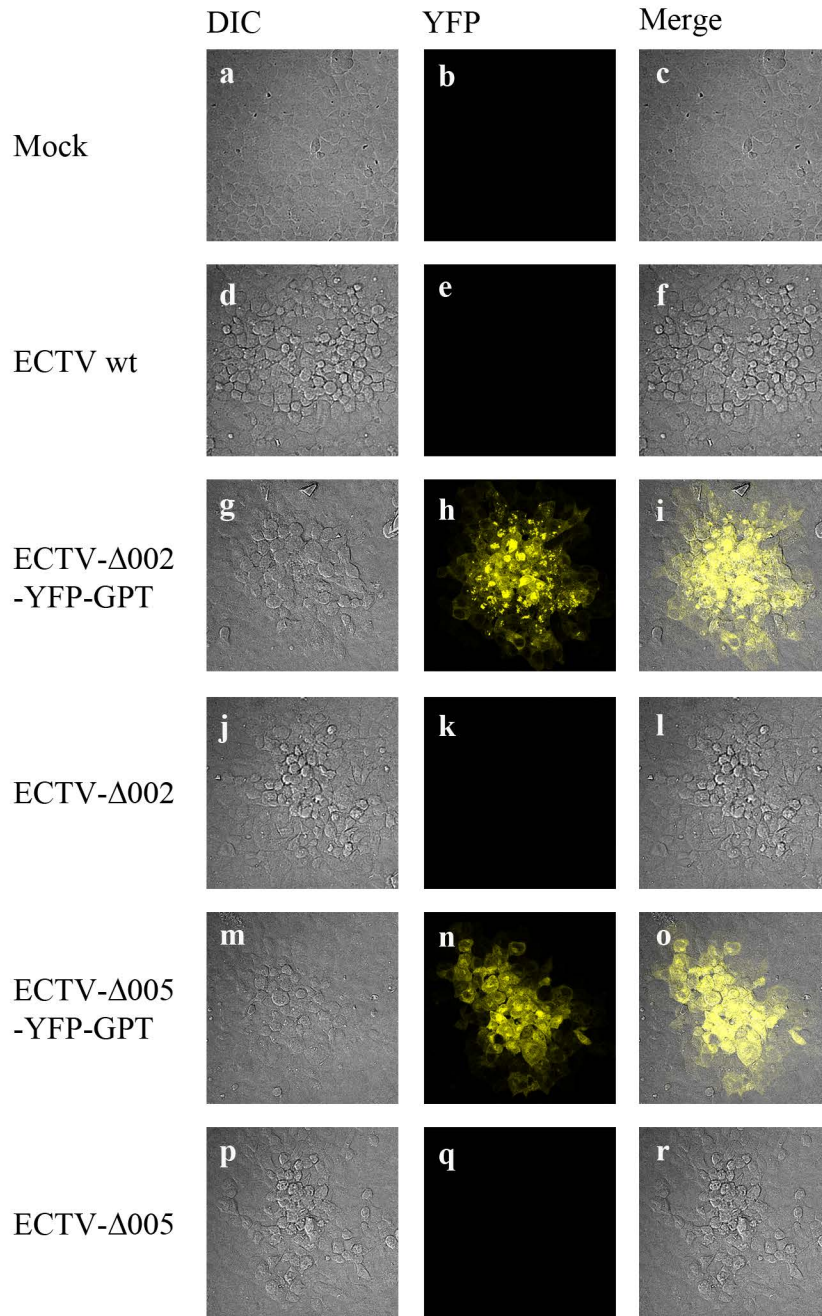


Figure 4.2. Detection of ECTV expressed YFP-GPT fusion proteins by immunofluorescence. BGMK cells were mock infected or infected with ECTV, ECTV-Δ002-YFP-GPT, ECTV-Δ002, ECTV-Δ005-YFP-GT, or ECTV-Δ005 at a MOI of 0.01 for 48 hours to allow formation of foci. Cells were fixed and ECTV foci were visualized by confocal microscopy to detect the presence or absence of YFP fluorescence. The Cre recombinase successfully excised the *yfp-gpt* cassette creating marker-free deletion viruses.

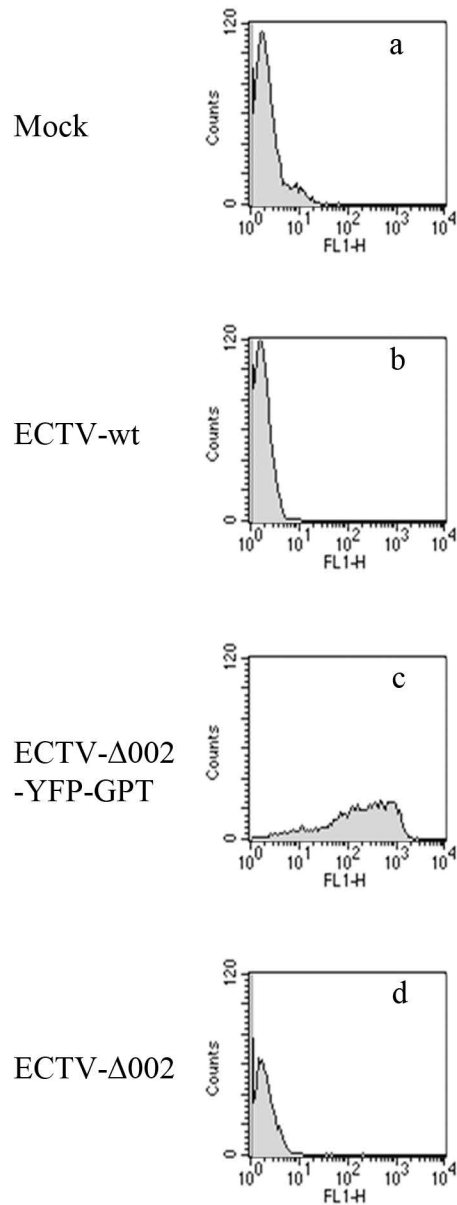
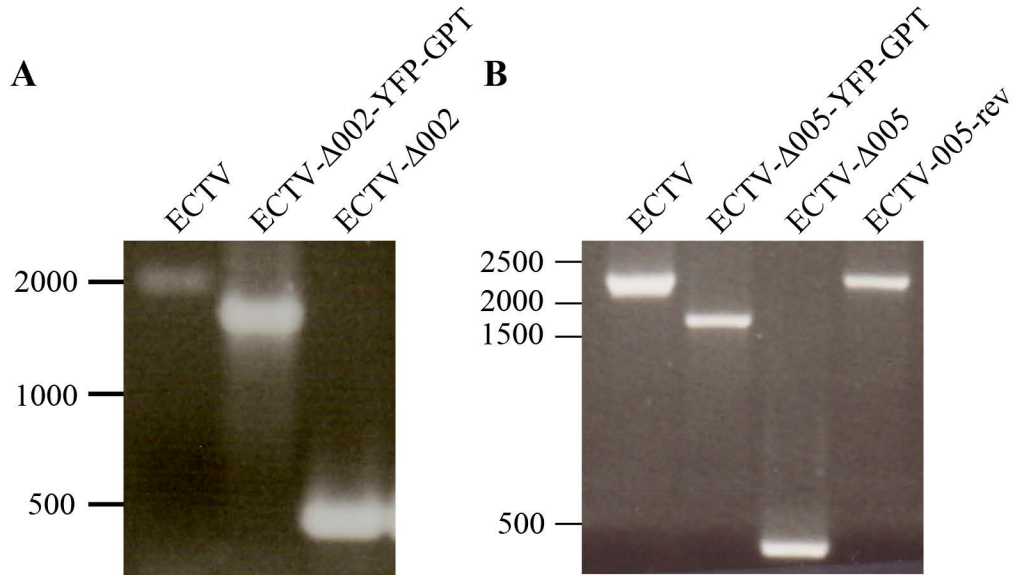


Figure 4.3. Detection of ECTV expressed YFP-GPT fusion proteins by flow cytometry. BGJK cells were uninfected (a) or infected with ECTV (b), ECTV- Δ 002-YFP-GPT (c) or ECTV- Δ 002 (d) at a MOI of 5 for 4 hours. Cells were analyzed by live cell flow cytometry on a FACScan BSL-2 flow cytometer. The YFP-GPT fusion protein was detected on the FL1 channel in viruses containing the *yfp-gpt* cassette (c) and not in viruses in which the cassette had been excised by the Cre recombinase (d).



C

GGATCCGATAACTTCGTATAGCATAACATTATACGAAGTTAT
GTCGACCTGCAGGAAGCTT

Red - Denotes *Bam*HI and *Hind*III restriction sites

Green - Denotes the 34bp *LoxP* site

Black - Denotes remnants from pDGloxP

Figure 4.4. PCR analysis of viral genomes. BGMK cells were infected with ECTV, ECTV-Δ002-YFP-GPT, ECTV-Δ002, ECTV-Δ005-YFP-GPT, ECTV-Δ005 or ECTV-005-rev at a MOI of 5 for 24 hours. Viral genomes were subjected to PCR analysis with primers flanking the EVM002 (**A**) or EVM005 (**B**) locus to detect genetic modifications. PCR products of greater than 2000bp represent amplification of wild type EVM002 and EVM005. PCR products near ~1700bp in length represent insertion of the *yfp-gpt* cassette into the amplified locus. PCR products of ~500bp represent excision of the *yfp-gpt* cassette from the amplified locus. **C.** Sequencing of the EVM002 locus following Cre recombination of ECTV-Δ002-YFP-GPT identified 60bp of DNA between the EVM002 up and downstream regions of homology. These nucleotides consisted of a 34bp *loxP* site, two 6bp restriction sites, and 13bp of DNA from pDGloxP-EVM002KO.

genomes of ECTV- Δ 005-YFP-GPT, ECTV- Δ 005 and ECTV-005-rev (Figure 4.4B). EVM002 and EVM005 are 1754bp and 1953bp in length resulting in PCR products of 2054bp and 2253bp, respectively (Figure 4.4A and B). The *yfp-gpt* cassette is 1436bp in length, resulting in a PCR product of 1736bp in length (Figure 4.4A and B). Upon excision of the *yfp-gpt* cassette, PCR products were generated from the EVM002 and EVM005 loci or roughly 350bp corresponding to the two 150bp regions of homology, a 34bp loxP site and a few remaining nucleotides from the pDGloxP plasmid (Figure 4.4A and B). Finally, the EVM005 locus of ECTV-005-rev was identical to wild type ECTV (Figure 4.4B). These data demonstrate proof of principle, that ECTV supports expression of the *yfp-gpt* cassette upon recombination into the ECTV genome. Additionally, U20S-Cre cells support the formation of ECTV foci and the Cre recombinase excised the *yfp-gpt* cassette from ECTV recombinants.

To characterize this residual sequence left behind following Cre-mediated excision, we sequenced the EVM002 locus of ECTV- Δ 002 to identify the remaining nucleic acid sequence. We amplified the EVM002 locus of ECTV- Δ 002 by PCR with *Taq* polymerase using primers flanking the EVM002 locus to generate a ~350bp PCR product that was subsequently sequenced. Sequencing identified 60bp of DNA between the upstream and downstream regions of homology for EVM002 (Figure 4.4C). The 60bp sequence consisted of a 34bp loxP site flanked on the left by 7bp including a 6bp *Bam*HI cut site and on the right by 19bp including a 6bp *Hind*III cut site (Figure 4.4C). The nucleotides flanking the loxP site represent remnants from the pDGloxP-EVM002KO vector.

These results confirm that following Cre-mediated excision of the *yfp-gpt* cassette, one loxP site remains in the same orientation as its two predecessors.

4.5 Analysis of ECTV- Δ 002 and ECTV- Δ 005 Growth

Growth rates of ECTV- Δ 002, ECTV- Δ 005 and ECTV-005-rev compared to wild type ECTV were measured by multi-step growth curves on BGMK cells. BGMK cells were infected with ECTV, ECTV- Δ 002, ECTV- Δ 005 or ECTV-005-rev and samples were collected up to 72 hours post infection. The data indicated that deletion of EVM002 or EVM005 from the ECTV genome had no effect on virus growth in BGMK cells (Figure 4.5). Typically, the deletion of poxvirus genes that function in virulence, host range, or immune evasion does not result in a reduced growth rate in tissue culture, but does lead to decreased pathogenicity in an animal model or restricted growth in specific cell types (26). Therefore, it will be interesting to test the ECTV deletion constructs for virulence in a mouse model to further characterize the function of the ankyrin/F-box proteins.

4.6 Deletion of Multiple Genes from the Left End of the ECTV Genome

Large deletion viruses constructed on the VV background have proven to be invaluable tools for the study of poxvirus-host interactions, however, these viruses are extremely time-consuming to generate. Modified vaccinia Ankara (MVA) was passaged over 500 times on chicken embryo fibroblast (CEF) cells to create a strain of VV devoid of multiple ORFs (33). The generation of VV811 required complex DNA methodologies and several recombination events to delete 55

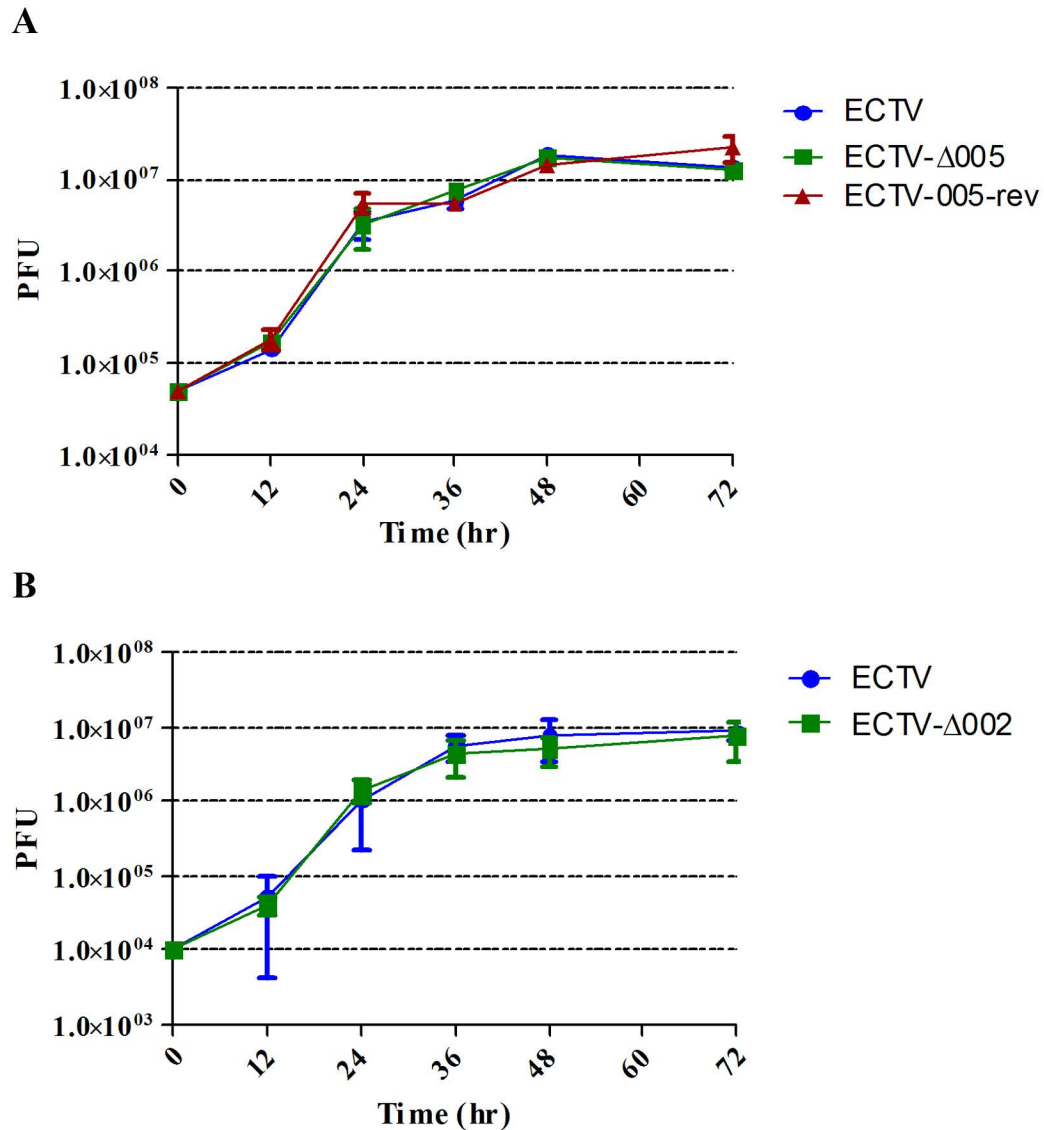


Figure 4.5. Multi-step growth curve analysis of ECTV recombinant viruses. **A.** BGMK cells were infected in triplicate with ECTV, ECTV-Δ005 or ECTV-005-rev at a MOI of 0.05. **B.** BGMK cells were infected in triplicate with ECTV or ECTV-Δ002 at a MOI of 0.01. Samples were collected at 12, 24, 36, 48 and 72 hours post infection and assayed for viral titer using a plaque assay. The average number of pfu at each time point are plotted with standard deviations. No changes in viral growth were detected between wild type ECTV and the analyzed recombinants on BGMK cells.

ORFs from VV, consisting of 38 ORFs at the left-hand end and 17 ORFs at the right-hand end of the VV genome (28). To further explore the potential of the SEM system, we attempted to create large deletion strains of ECTV by sequential insertion and deletion of the *yfp-gpt* cassette into various locations on the ECTV genome; this technique could make generation of large deletion poxvirus strains easily attainable. In addition to the pDGloxP-EVM002KO and pDGloxP-EVM005KO constructs previously constructed, pDGloxP-EVM154KO and pDGloxP-EVM165KO were constructed (K. Burles, M. Edwards and M. Barry, unpublished data). This allowed us to sequentially insert and excise the *yfp-gpt* cassette up to four times from the ECTV genome.

Our first goal was to delete EVM002 and EVM005 from the left-hand end of the genome. To accomplish this goal, we infected BGMK cells with ECTV- Δ 002 and transfected linearized pDGloxP-EVM005KO (Figure 4.6). The resulting recombinants were isolated based on resistance to MPA selection and YFP fluorescence. We obtained a double knockout that lacked EVM002 and EVM005 and contained the *yfp-gpt* cassette in the EVM005 locus (Figure 4.6). Purity of this virus was confirmed by PCR (Figure 4.7) and named ECTV- Δ 002/005-YFP-GPT. Two outcomes were possible following Cre recombination, the first possibility was that the *yfp-gpt* cassette in the EVM005 locus would be excised by Cre resulting in a marker-free double knockout virus. The second possibility was that the loxP site from the EVM002 locus would be in close enough proximity to the new loxP sites inserted into the EVM005 locus resulting in loss of the intergenic EVM003 and EVM004 genes during Cre recombination

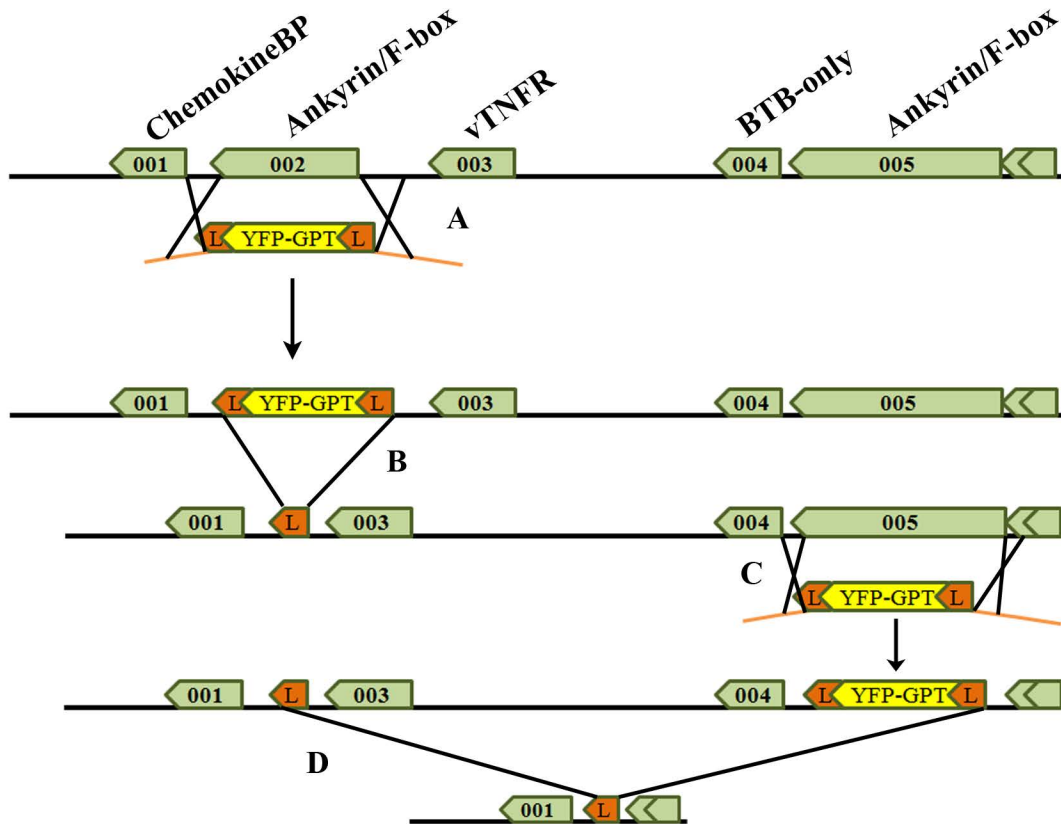


Figure 4.6. Schematic for construction of ECTV-Δ002-005. The Selectable and Excisable Marker System was used to delete four genes, EVM002, EVM003, EVM004, and EVM005 from the left-hand end of the ECTV strain Moscow genome. **A.** BGMK cells were infected with wild type ECTV and transfected with linearized pDGloxP-EVM002KO and YFP-GPT positive viruses were purified. **B.** Excision of the *yfp-gpt* cassette was performed by infecting U20S-Cre cells with ECTV-Δ002-YFP-GPT to create ECTV-Δ002. **C.** The *yfp-gpt* cassette was then inserted into the EVM005 locus by infecting BGMK cells with ECTV-Δ002 and transfected linearized pDGloxP-EVM005KO and YFP-GPT positive viruses were purified. **D.** Finally, we infected U20S-Cre cells with ECTV-Δ002/005-YFP-GPT to remove the *yfp-gpt* cassette. Cre recombination removed all DNA between the loxP site in the EVM002 locus and the loxP site introduced into the EVM005 locus, consisting of EVM002, EVM003, EVM004 and EVM005, to create ECTV-Δ002-005.

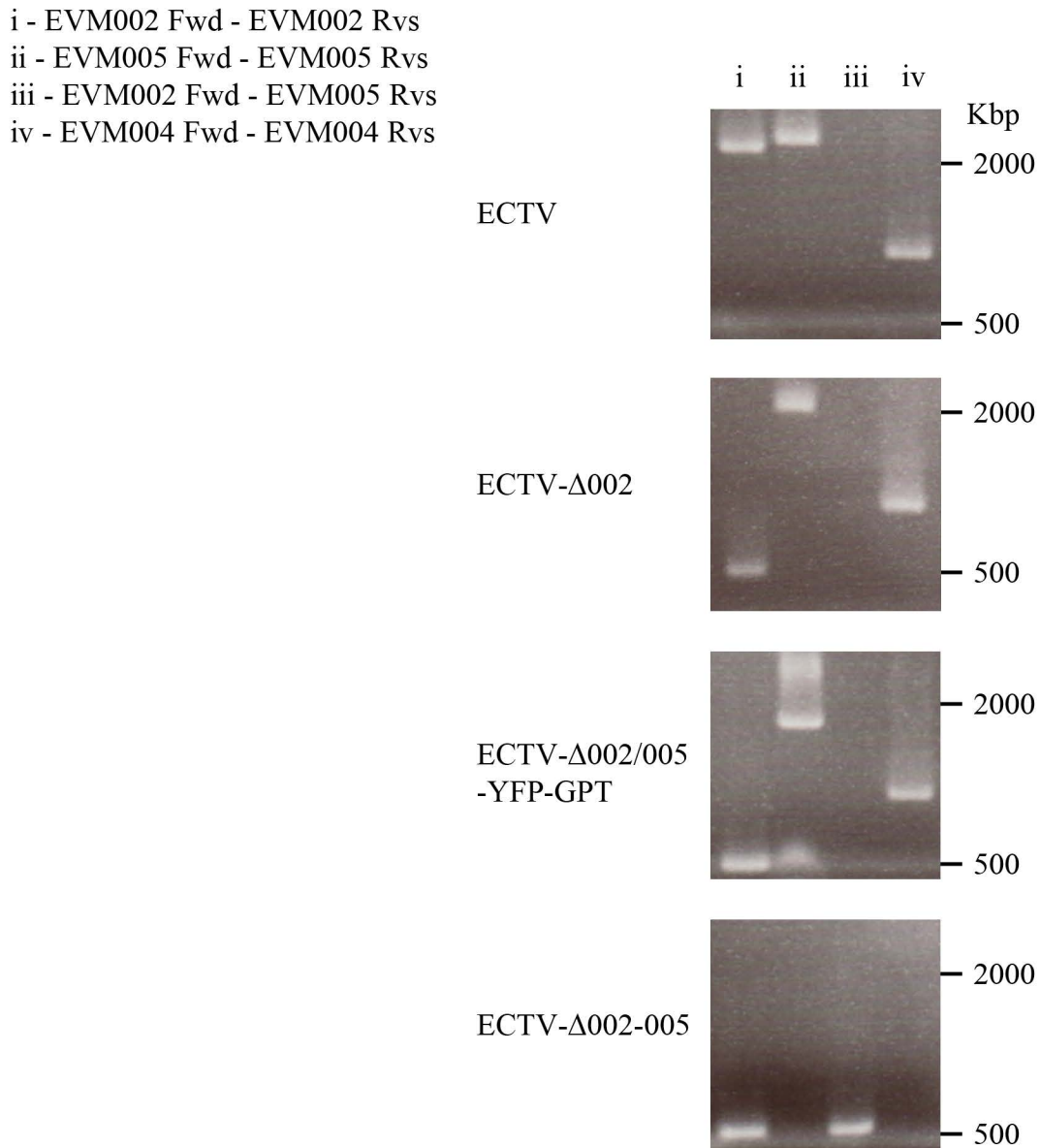


Figure 4.7. PCR analysis of viral genomes to verify construction of ECTV- Δ 002-005. BGMK cells were infected with ECTV, ECTV- Δ 002, ECTV- Δ 002/005-YFP-GPT, and ECTV- Δ 002-005 for 48 hours. Viral genomes were subjected to PCR analysis of the EVM002, EVM004, and EVM005 loci as well as verifying Cre deletion from EVM002 to EVM005. The presence of PCR products near 500bp in length represent excision of the *yfp-gpt* cassette by Cre recombination. Alternatively, PCR products of \sim 1700bp represent an intact *yfp-gpt* cassette, and PCR products larger than 2000bp represent wild type sequences for EVM002 or EVM005. The presence of EVM004 is noted by the presence of a \sim 1000bp PCR product.

(Figure 4.6). Deletion of intergenic DNA is only possible due to the fact that all three loxP sites in ECTV- Δ 002/005-YFP-GPT are oriented in the same direction (Figure 4.6). PCR analysis confirmed that Cre recombination removed EVM003 and EVM004 (Figure 4.7). This is demonstrated as a ~500bp PCR product amplified with the EVM002 locus forward primer and the EVM005 locus reverse primer, as well as the absence of an EVM004 PCR product (Figure 4.7 lane iii and iv). We named the resulting virus ECTV- Δ 002-005. Importantly, even though EVM003, which encodes a vTNFR, is deleted from the left-hand end of the genome, this gene is located in the ITR region of the ECTV genome, and therefore a copy is also present at the right-hand end of the genome (named EVM170). However, EVM004 is not located in the ITR, therefore, EVM004 was deleted along with EVM002 and EVM005 from the genome of ECTV- Δ 002-005 (Figure 4.6 and 4.7).

4.7 Discussion

We demonstrated YFP expression from ECTV genomes by confocal microscopy (Figure 4.2) and flow cytometry (Figure 4.3). Although future experiments were performed with the marker-free strains of the recombinant ECTVs, the expression of YFP-GPT could serve as an indicator of infection during a variety of experiments. Currently, to detect infection by flow cytometry we stain infected cells with an antibody that recognizes the viral early protein I3L. The YFP-GPT expressing versions of these knockout viruses could reduce cost by identifying infected cells by YFP fluorescence instead of using antibodies to detect the

presence of I3L. This could also be useful in experiments using confocal microscopy, as all infected cells would display YFP fluorescence. These experiments would involve the synthesis of an ECTV control virus in which the *yfp-gpt* cassette is inserted into a non-essential locus. Finally, the production of a pDGloxP-KO vector that expresses a mPlum or mCherry fluorescence marker could be beneficial for animal studies utilizing the *In Vivo* Imaging System (IVIS). YFP fluorescence is difficult to detect using the IVIS machine due to interference from animal tissue, but infection of animals with viruses that produce red fluorescence could make detection of virus infection with the IVIS machine possible.

Construction of revertant poxviruses following deletion of specific genes remains a crucial control to ensure that no additional genetic material was affected during cloning. The creation of ECTV-005-rev was completed by reinserting the EVM005 sequence into the ECTV- Δ 005-YFP-GPT genome in order to replace the *yfp-gpt* cassette with EVM005 (Figure 4.4B). Revertant viruses were selected through the lack of YFP fluorescence. This technique proved to be extremely difficult and time consuming, and hence we were unable to create ECTV-002-rev due to time constraints. We screened thousands of foci under a fluorescent microscope to identify the 1 in 1000 recombinants that lacked YFP expression. The selection of VV revertant viruses from GPT-containing knockouts is aided by drug selection that works in an opposite fashion to MPA selection (17). The use of 6-thioguanine (6-TG) shuts down the salvage pathway of nucleotide synthesis as GPT expressing virus will convert 6-TG into toxic nucleotides, while revertant

viruses lacking GPT will not (17). One of the crucial components of 6-TG selection is infection of STO cells that lack expression of the cellular hypoxanthine-guanine phosphoribosyl transferase gene (HPRT) and will therefore not incorporate 6-TG during nucleotide synthesis. Unfortunately, we were unable to observe the growth of ECTV foci on STO cells, suggesting that ECTV produced an abortive infection in this cell line. This was puzzling due to the fact that STO cells are a mouse cell line, but nonetheless, the lack of produced foci created a struggle in the synthesis of ECTV revertant strains.

Through our attempts to generate large ECTV deletion viruses, we noticed that the distance between loxP sites is critical. Intrigued by our successful multigene deletion at the left-hand end of the ECTV genome, we attempted to delete 17 ORFs from the right-hand end of the ECTV genome comprising EVM154 to EVM171 through sequential insertion and excision of the *yfp-gpt* cassette (Appendix A). We demonstrated that deletion of 17 ORFs from the right-hand end of the genome occurred, but this virus existed in a mixed population of viruses, possibly due to the larger distance between loxP sites (Appendix A). This was in contrast to our left-hand end deletion in which EVM002 through EVM005 were deleted through Cre recombination (Figure 4.6 and 4.7). EVM002 and EVM005 are in much closer proximity on the ECTV genome than EVM154 and EVM171. This raises the question as to how close loxP sites need to be on poxvirus genomes in order to participate in Cre recombination. Future construction of poxviruses lacking multiple ORFs using the SEM system will determine the optimal distance for sequential insertion and excision of the *yfp-gpt*

cassette for the generation of large deletion viruses. Deletions spanning larger regions of the genome may require an additional insertion and excision recombination event.

The orientation of loxP sites and the *yfp-gpt* cassette is important for the successful generation of large deletion poxviruses using the SEM system. If the two loxP sites are oriented in the same direction, as they are within the pDGloxP-KO vector (Figure 4.1A), the Cre recombinase will excise the intervening DNA and one loxP site will remain (Figure 4.4C). The residual loxP site will be present in the same orientation as the two before it. Alternatively, if the two loxP sites are oriented in opposite directions, the Cre recombinase will invert the intervening DNA sequence (1). This has potential consequences on the construction of large deletion viruses. Perhaps if we had constructed a pDGloxP-EVM005KO vector that inserted the *yfp-gpt* cassette into the EVM005 locus in the opposite orientation, we could have removed only EVM005 and EVM002 as the intergenic region would not be subjected to Cre excision due to oppositely oriented loxP sites. If future endeavours to produce large deletion poxvirus strains are to be undertaken, the orientation of loxP sites during insertion of the *yfp-gpt* cassette will be of the utmost importance for the obtaining the desired outcome.

Construction of an ABSL-3 facility at the University of Alberta will allow animal studies involving strains of ECTV. The SEM system will provide a fast, cost effective method for the creating recombinant ECTVs for use in animal studies. Importantly, when studying recombinant poxviruses in animals, the use of appropriate controls is mandatory. Excision of the *yfp-gpt* cassette through the

SEM system will allow us to investigate marker-free recombinant ECTV strains in animals. This is important as experiments with recombinants that contain markers require a control strain containing the same marker. Historically, ECTV knockout viruses have been constructed by insertion of GFP or β -galactosidase markers, making the construction of a control ECTV containing the same marker mandatory. However, even though there exist areas on the ECTV genome that are non-essential and insertion has no effect on virulence in mice, a pure wild type strain will serve as a superior control. Additionally, with the development of the C57BL/6 mouse model for ECTV infection, and the subsequent ability to infect a variety of transgenics and knockout mice, these recombinant controls could have unknown phenotypes in various mouse strains.

Finally, since the eradication of variola virus in 1977, smallpox vaccination campaigns have ended leaving the majority of the population with no immunity against poxviruses (7, 12). Recently, researchers have used a variety of recombinant poxviruses as vaccine vectors for potential treatment of HIV (18), malaria (2) and tuberculosis (16). Additionally, attempts have been made to make poxvirus-based cancer vaccines (9, 14, 19, 24), gene delivery vectors (2, 3, 8, 14), and oncolytic viruses (10, 20, 22, 25). The lack of existing immunity in many patients provides an environment in which the recombinant poxviruses survive long enough to have strong therapeutic effects. The SEM system provides researchers the opportunity to synthesize poxvirus therapeutics that lack markers, a feature that could prove vital during FDA approval.

4.8 References

1. **Abremski, K., and R. Hoess.** 1984. Bacteriophage P1 site-specific recombination. Purification and properties of the Cre recombinase protein. *J Biol Chem* **259**:1509-14.
2. **Bejon, P., E. Ogada, T. Mwangi, P. Milligan, T. Lang, G. Fegan, S. C. Gilbert, N. Peshu, K. Marsh, and A. V. Hill.** 2007. Extended follow-up following a phase 2b randomized trial of the candidate malaria vaccines FP9 ME-TRAP and MVA ME-TRAP among children in Kenya. *PLoS One* **2**:e707.
3. **Cadoz, M., A. Strady, B. Meignier, J. Taylor, J. Tartaglia, E. Paoletti, and S. Plotkin.** 1992. Immunisation with canarypox virus expressing rabies glycoprotein. *Lancet* **339**:1429-32.
4. **Carroll, M. W., and B. Moss.** 1995. E. coli beta-glucuronidase (GUS) as a marker for recombinant vaccinia viruses. *Biotechniques* **19**:352-4, 356.
5. **Chakrabarti, S., K. Brechling, and B. Moss.** 1985. Vaccinia virus expression vector: coexpression of beta-galactosidase provides visual screening of recombinant virus plaques. *Mol Cell Biol* **5**:3403-9.
6. **Chakrabarti, S., J. R. Sisler, and B. Moss.** 1997. Compact, synthetic, vaccinia virus early/late promoter for protein expression. *Biotechniques* **23**:1094-7.
7. **Damon, I. K.** 2007. Poxviruses. *In* D. a. P. H. Knipe (ed.), *Field's Virology*, 5 ed. Lippincott Williams & Wilkins.
8. **Dasgupta, S., M. Bhattacharya-Chatterjee, B. W. O'Malley, Jr., and S. K. Chatterjee.** 2006. Recombinant vaccinia virus expressing interleukin-2 invokes anti-tumor cellular immunity in an orthotopic murine model of head and neck squamous cell carcinoma. *Mol Ther* **13**:183-93.
9. **Erbs, P., A. Findeli, J. Kintz, P. Cordier, C. Hoffmann, M. Geist, and J. M. Balloul.** 2008. Modified vaccinia virus Ankara as a vector for suicide gene therapy. *Cancer Gene Ther* **15**:18-28.
10. **Evgin, L., M. Vaha-Koskela, J. Rintoul, T. Falls, F. Le Boeuf, J. W. Barrett, J. C. Bell, and M. M. Stanford.** 2010. Potent oncolytic activity of raccoonpox virus in the absence of natural pathogenicity. *Mol Ther* **18**:896-902.
11. **Falkner, F. G., and B. Moss.** 1988. Escherichia coli gpt gene provides dominant selection for vaccinia virus open reading frame expression vectors. *J Virol* **62**:1849-54.
12. **Fenner, F., DA Henderson, I Arita, Z Jezek, and ID Ladnyi.** 1988. Smallpox and its Eradication. World Health Organization.
13. **Franke, C. A., C. M. Rice, J. H. Strauss, and D. E. Hruby.** 1985. Neomycin resistance as a dominant selectable marker for selection and isolation of vaccinia virus recombinants. *Mol Cell Biol* **5**:1918-24.
14. **Harrop, R., N. Drury, W. Shingler, P. Chikoti, I. Redchenko, M. W. Carroll, S. M. Kingsman, S. Naylor, A. Melcher, J. Nicholls, H. Wassan, N. Habib, and A. Anthoney.** 2007. Vaccination of colorectal

- cancer patients with modified vaccinia ankara encoding the tumor antigen 5T4 (TroVax) given alongside chemotherapy induces potent immune responses. *Clin Cancer Res* **13**:4487-94.
15. **Hoess, R. H., and K. Abremski.** 1984. Interaction of the bacteriophage P1 recombinase Cre with the recombining site loxP. *Proc Natl Acad Sci U S A* **81**:1026-9.
 16. **Huygen, K., J. Content, O. Denis, D. L. Montgomery, A. M. Yawman, R. R. Deck, C. M. DeWitt, I. M. Orme, S. Baldwin, C. D'Souza, A. Drowart, E. Lozes, P. Vandenbussche, J. P. Van Vooren, M. A. Liu, and J. B. Ulmer.** 1996. Immunogenicity and protective efficacy of a tuberculosis DNA vaccine. *Nat Med* **2**:893-8.
 17. **Isaacs, S. N., G. J. Kotwal, and B. Moss.** 1990. Reverse guanine phosphoribosyltransferase selection of recombinant vaccinia viruses. *Virology* **178**:626-30.
 18. **Kanasa-thasan, N., J. J. Smucny, C. H. Hoke, D. H. Marks, E. Konishi, I. Kurane, D. B. Tang, D. W. Vaughn, P. W. Mason, and R. E. Shope.** 2000. Safety and immunogenicity of NYVAC-JEV and ALVAC-JEV attenuated recombinant Japanese encephalitis virus--poxvirus vaccines in vaccinia-nonimmune and vaccinia-immune humans. *Vaccine* **19**:483-91.
 19. **Kantoff, P. W., T. J. Schuetz, B. A. Blumenstein, L. M. Glode, D. L. Bilhartz, M. Wyand, K. Manson, D. L. Panicali, R. Laus, J. Schlom, W. L. Dahut, P. M. Arlen, J. L. Gulley, and W. R. Godfrey.** 2010. Overall survival analysis of a phase II randomized controlled trial of a Poxviral-based PSA-targeted immunotherapy in metastatic castration-resistant prostate cancer. *J Clin Oncol* **28**:1099-105.
 20. **Kim, J. H., J. Y. Oh, B. H. Park, D. E. Lee, J. S. Kim, H. E. Park, M. S. Roh, J. E. Je, J. H. Yoon, S. H. Thorne, D. Kirn, and T. H. Hwang.** 2006. Systemic armed oncolytic and immunologic therapy for cancer with JX-594, a targeted poxvirus expressing GM-CSF. *Mol Ther* **14**:361-70.
 21. **Lorenz, M. G., J. A. Kantor, J. Schlom, and J. W. Hodge.** 1999. Anti-tumor immunity elicited by a recombinant vaccinia virus expressing CD70 (CD27L). *Hum Gene Ther* **10**:1095-103.
 22. **Lun, X., T. Alain, F. J. Zemp, H. Zhou, M. M. Rahman, M. G. Hamilton, G. McFadden, J. Bell, D. L. Senger, and P. A. Forsyth.** 2010. Myxoma virus virotherapy for glioma in immunocompetent animal models: optimizing administration routes and synergy with rapamycin. *Cancer Res* **70**:598-608.
 23. **Mackett, M., G. L. Smith, and B. Moss.** 1984. General method for production and selection of infectious vaccinia virus recombinants expressing foreign genes. *J Virol* **49**:857-64.
 24. **Mastrangelo, M. J., H. C. Maguire, Jr., L. C. Eisenlohr, C. E. Laughlin, C. E. Monken, P. A. McCue, A. J. Kovatich, and E. C. Lattime.** 1999. Intratumoral recombinant GM-CSF-encoding virus as gene therapy in patients with cutaneous melanoma. *Cancer Gene Ther* **6**:409-22.

25. **McCart, J. A., J. M. Ward, J. Lee, Y. Hu, H. R. Alexander, S. K. Libutti, B. Moss, and D. L. Bartlett.** 2001. Systemic cancer therapy with a tumor-selective vaccinia virus mutant lacking thymidine kinase and vaccinia growth factor genes. *Cancer Res* **61**:8751-7.
26. **Moss, B.** 2007. Poxviridae: The Viruses and Their Replication. *In* D. a. P. H. Knipe (ed.), *Fields Virology*, 5 ed. Lippincott Williams & Wilkins.
27. **Mulligan, R. C., and P. Berg.** 1981. Selection for animal cells that express the *Escherichia coli* gene coding for xanthine-guanine phosphoribosyltransferase. *Proc Natl Acad Sci U S A* **78**:2072-6.
28. **Perkus, M. E., S. J. Goebel, S. W. Davis, G. P. Johnson, E. K. Norton, and E. Paoletti.** 1991. Deletion of 55 open reading frames from the termini of vaccinia virus. *Virology* **180**:406-10.
29. **Piccini, A., M. E. Perkus, and E. Paoletti.** 1987. Vaccinia virus as an expression vector. *Methods Enzymol* **153**:545-63.
30. **Rintoul, J. L., J. Wang, D. B. Gammon, N. J. van Buuren, K. Garson, K. Jardine, M. Barry, D. H. Evans, and J. C. Bell.** 2011. A selectable and excisable marker system for the rapid creation of recombinant poxviruses. *PLoS One* **6**:e24643.
31. **Sauer, B., and N. Henderson.** 1988. Site-specific DNA recombination in mammalian cells by the Cre recombinase of bacteriophage P1. *Proc Natl Acad Sci U S A* **85**:5166-70.
32. **Sternberg, N., and D. Hamilton.** 1981. Bacteriophage P1 site-specific recombination. I. Recombination between loxP sites. *J Mol Biol* **150**:467-86.
33. **Wyatt, L. S., P. L. Earl, L. A. Eller, and B. Moss.** 2004. Highly attenuated smallpox vaccine protects mice with and without immune deficiencies against pathogenic vaccinia virus challenge. *Proc Natl Acad Sci U S A* **101**:4590-5.

Chapter 5: Ectromelia Virus Encoded EVM005 Inhibits NF- κ B Signalling Through Manipulation of the SCF Ubiquitin Ligase Complex

The results contained within this chapter consist of unpublished material. The majority of the experiments included within this chapter were performed by N. van Buuren. Figure 5.9 was provided by Kristin Burles, and Figures 5.15 and 5.16 were provided by Dr. Mark Buller and Jill Schriewer at St. Louis University. The original manuscript was written by N. van Buren with a major editorial contribution by Dr. M. Barry.

5.1 Introduction

The NF- κ B signalling cascade is an important mediator of innate immunity and inflammation, and is tightly regulated by ubiquitylation at several key points. The NF- κ B family of transcription factors consists of five members, p50, p52, p65(RelA), RelB, and c-Rel, that function as homo- or heterodimers to activate specific genes. The best characterized NF- κ B dimer is the p50/p65 heterodimer, which is held inactive in the cytoplasm by the inhibitor of κ B (I κ B α)(11, 28). Signalling cascades initiated by both tumour necrosis factor (TNF α) and interleukin 1 β (IL-1 β) trigger the activation of a set of kinases known as the I κ B kinase (IKK) complex, which is composed of IKK α , IKK β and IKK γ (NEMO)(28). Upon activation of the IKK complex, IKK β phosphorylates I κ B α on serines 32 and 36, which targets I κ B α for polyubiquitination and degradation by the 26S proteasome (11, 28). The SCF (Skp1/Cul1/F-box) ubiquitin ligase complex recruits phospho-I κ B α through the adaptor molecule, β -TRCP, a cellular F-box protein, resulting in the degradation of I κ B α , and translocation of the p50/p65 heterodimer into the nucleus activating transcription of immune regulatory and pro-survival genes (11, 28).

We show here that upon stimulation with TNF α or IL-1 β , *Orthopoxvirus*-infected cells accumulate phospho-I κ B α suggesting inhibition of I κ B α degradation by poxvirus encoded proteins. We previously identified a family of four ECTV encoded genes (EVM002, EVM005, EVM154 and EVM165) that contain N-terminal ankyrin repeats and C-terminal F-box domains that interact with the cellular SCF ubiquitin ligase complex (29). Degradation of I κ B α is

catalyzed by the SCF ^{β -TRCP} ubiquitin ligase, therefore, we investigated the role of the ECTV encoded ankyrin/F-box protein, EVM005, in the regulation of NF- κ B during ECTV infection. Expression of Flag-EVM005 inhibited both I κ B α degradation and p65 nuclear translocation in response to TNF α or IL-1 β . Regulation of the NF- κ B pathway by EVM005 was dependent on the F-box domain, and interaction with the SCF complex. Additionally, an EVM005 deletion virus was shown to inhibit NF- κ B activation despite lacking the EVM005 open reading frame. However, ECTV- Δ 005 was attenuated in resistant C57BL/6 and susceptible A/NCR mice suggesting an additional NF- κ B-independent mechanism for EVM005.

5.2 ECTV Infection Leads to an Accumulation of Phospho-I κ B α and Inhibition of NF- κ B Activation

The NF- κ B signalling cascade activates a family of transcription factors that initiate the pro-inflammatory response and antiviral innate immunity (11, 28). Recent evidence indicates that many poxviruses encode proteins that tightly regulate the activation of NF- κ B through the expression of secreted and intracellular factors (14, 18). However, the regulation of NF- κ B during ECTV infection has not been explored. Unlike strains of VV, ECTV lacks M2, B14, K7 and A52, all important inhibitors of NF- κ B activation (3, 9, 12, 21). Therefore, we sought to determine if ECTV inhibited NF- κ B activation. Given that the degradation of I κ B α plays a central role in activation of the NF- κ B pathway, we

examined the kinetics of I κ B α degradation during infection. HeLa cells were mock-infected, infected with ECTV, vaccinia virus strain Copenhagen (VVCop), or cowpox virus strain Brighton Red (CPXV) and then treated with TNF α up to 120 minutes. Mock-infected cells treated with TNF α showed a typical pattern of I κ B α degradation kinetics (Figure 5.1A). As early as 10 minutes post-TNF α treatment, mock-infected cells showed phosphorylated I κ B α that was subsequently degraded (Figure 5.1A and B)(16, 27). ECTV, VVCop and CPXV infected cells treated with TNF α also showed obvious phosphorylation of I κ B α (Figure 5.1A and B), however, the levels of both I κ B α and phospho-I κ B α were sustained compared to mock-infected cells (Figure 5.1A and B). Western blotting for I5L, a late poxvirus protein, and cellular β -tubulin were used as loading controls (Figure 5.1C and D). We obtained similar results following treatment with IL-1 β (Figure 5.1 E-H), indicating that members of *Orthopoxvirus* genera, including ECTV, sustained levels of phospho-I κ B α and inhibited the degradation of I κ B α .

I κ B α appeared to be phosphorylated, but not rapidly degraded upon infection with ECTV, VVCop or CPXV. Therefore, we sought to determine if the NF- κ B transcription factor, p65, was retained within the cytoplasm during infection. HeLa cells were mock-infected or infected with ECTV, VVCop or CPXV, and p65 nuclear accumulation was assayed by immunofluorescence (Figure 5.2 and 5.3). Mock-infected cells lacking TNF α or IL-1 β stimulation showed little p65 translocation into the nucleus, as expected (Figures 5.2 and 5.3 panels a-c). In contrast, mock-infected cells stimulated with TNF α or IL-1 β

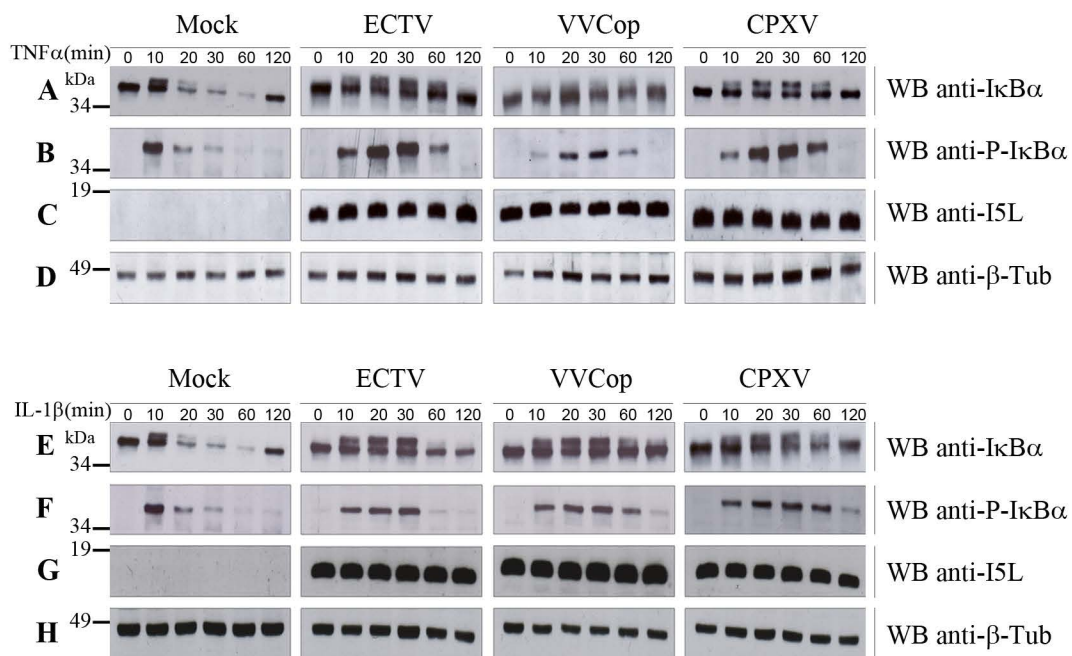


Figure 5.1. ECTV infection inhibits I κ B α degradation. HeLa cells were mock infected or infected with ECTV, VVCop, or CPXV at a MOI of 5 for 12 hours and stimulated with 10ng/ml TNF α or 10ng/ml IL-1 β . Protein samples were collected at 0, 10, 20, 30, 60 and 120 minutes post treatment. Cellular lysates were western blotted with (A and E) anti-I κ B α , (B and F) anti-phospho-I κ B α , (C and G) anti-I5L, and (D and H) anti- β -tubulin.

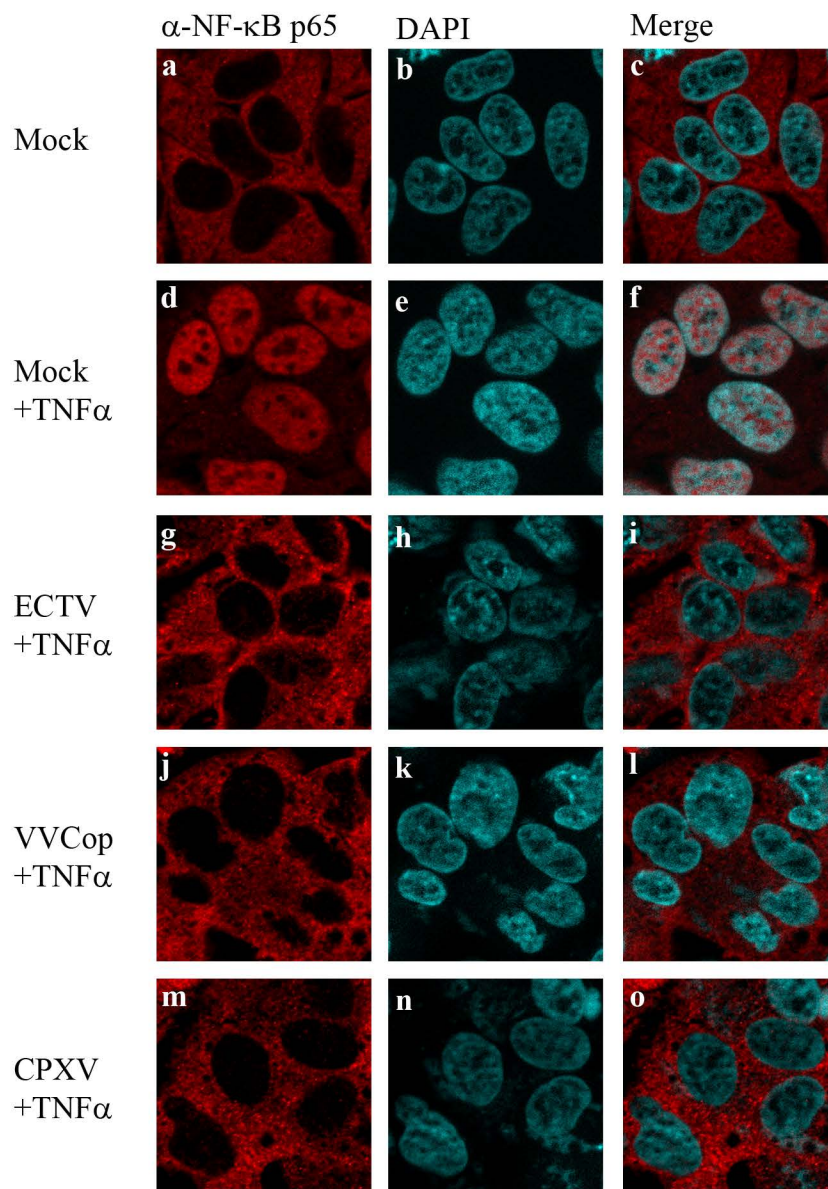


Figure 5.2. ECTV infection inhibits TNF α induced nuclear accumulation of p65. HeLa cells were mock infected (a-f) or infected with ECTV (g-i), VVCop (j-l), or CPXV (m-o) at a MOI of 5 for 12 hours followed by stimulation with 10ng/ml TNF α for 20 minutes. Cells were stained with anti-p65 and DAPI to visualize nuclei and viral factories. HeLa cells infected with ECTV, VVCop or CPXV inhibit p65 nuclear translocation during infection.

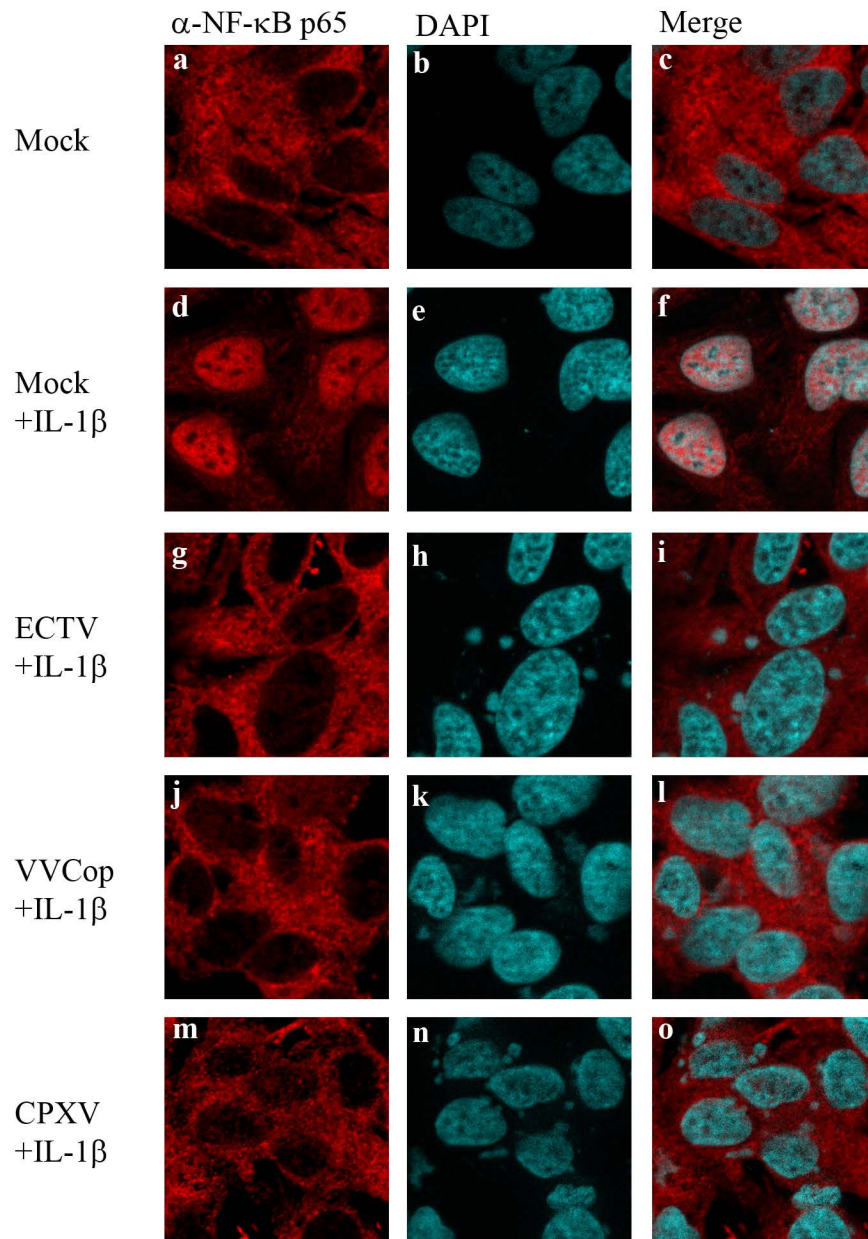


Figure 5.3. ECTV infection inhibits IL-1 β induced nuclear accumulation of p65. HeLa cells were mock infected (a-f) or infected with ECTV (g-i), VVCop (j-l), or CPXV (m-o) at a MOI of 5 for 12 hours followed by stimulation with 10ng/ml IL-1 β for 20 minutes. Cells were stained with anti-p65 and DAPI to visualize nuclei and viral factories. HeLa cells infected with ECTV, VVCop or CPXV inhibit p65 nuclear translocation during infection.

showed nuclear accumulation of p65 (Figures 5.2 and 5.3 panels d-f). Upon infection with ECTV, VVCop, or CPXV and subsequent treatment with TNF α or IL-1 β , p65 was retained in the cytoplasm indicating that despite the lack of M2, K7, B14 and A52 orthologs in ECTV, p65 nuclear translocation was inhibited (Figures 5.2 and 5.3 panels g-o). These data were confirmed by western blotting cytoplasmic and nuclear extracts from infected HeLa cells with an antibody specific for p65 (Figure 5.4A and 5.5A). As expected, p65 was absent from the nuclear extract of mock-infected cells. In contrast, mock-infected cells treated with TNF α or IL-1 β showed nuclear p65 (Figure 5.4A and 5.5A). Cells infected with ECTV, VVCop or CPXV and treated with TNF α or IL-1 β resulted in little p65 accumulation in the nuclear extract (Figure 5.4A and 5.5A). These results were also confirmed in mouse embryonic fibroblasts (MEF)(Figure 5.4B and 5.5B). Together, these data indicate that NF- κ B signalling is inhibited upon infection with members of the *Orthopoxvirus* genus. Importantly, ECTV infection inhibited p65 translocation to the nucleus despite the lack of M2, K7, B14 and A52.

5.3 Flag-EVM005 Inhibits Nuclear Accumulation of p65 in an F-box Dependent Manner

We recently identified a family of four ankyrin/F-box proteins in ECTV; EVM002, EVM005, EVM154 and EVM165, which interact with the cellular SCF ubiquitin ligase (Figures 3.1 and 3.2)(29). The poxvirus family of ankyrin/F-box proteins differs substantially from the cellular F-box proteins. In contrast to the

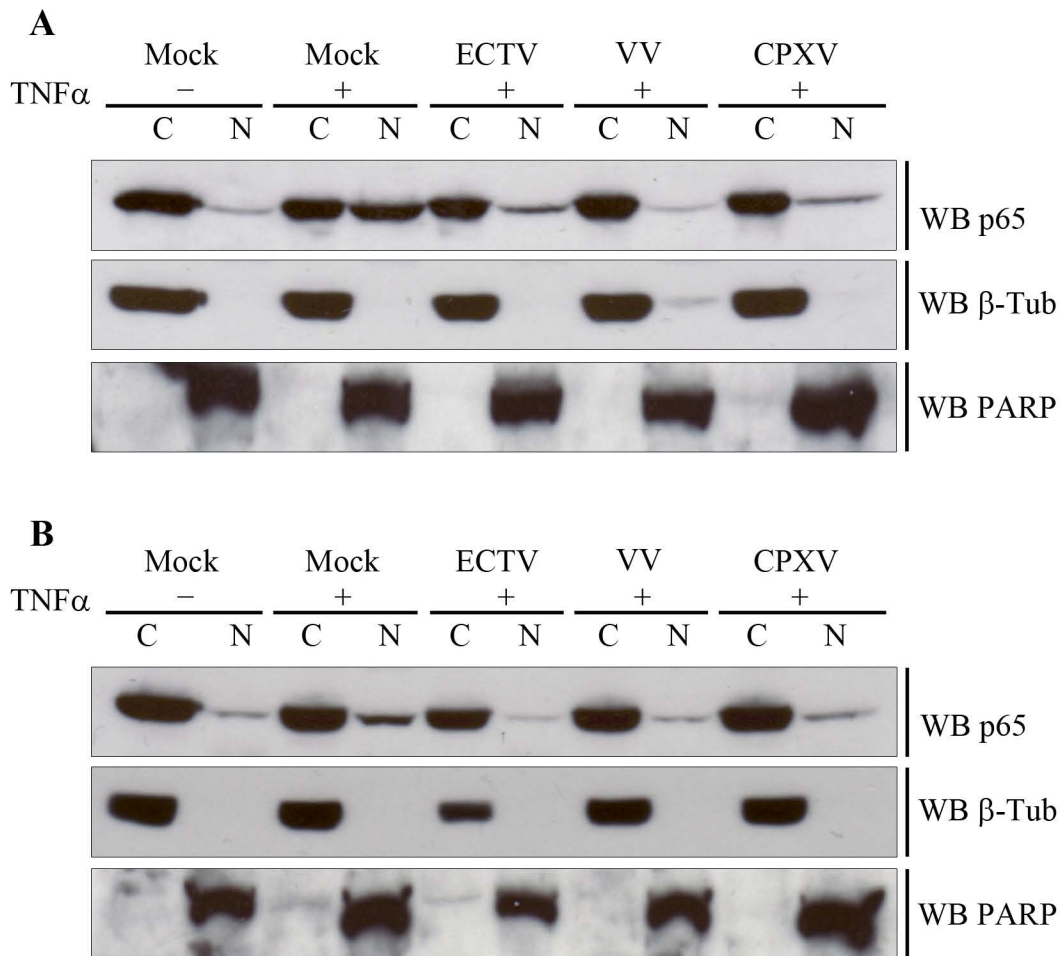


Figure 5.4. ECTV infection prevents TNF α induced p65 nuclear translocation in HeLa and MEF cells. **A.** HeLa cells were mock infected or infected with ECTV, VV or CPXV for 12 hours followed by stimulation with 10ng/ml TNF α for 20 minutes. Nuclear and cytoplasmic extracts were collected and western blotted with anti-p65, anti- β -tubulin, or anti-PARP. **B.** MEF cells were mock infected or infected with ECTV, VVCop or CPXV for 12 hours followed by stimulation with 10ng/ml TNF α for 20 minutes. Nuclear and cytoplasmic extracts were collected and western blotted with anti-p65, anti- β -tubulin, or anti-PARP. p65 nuclear accumulation is inhibited by ECTV infection.

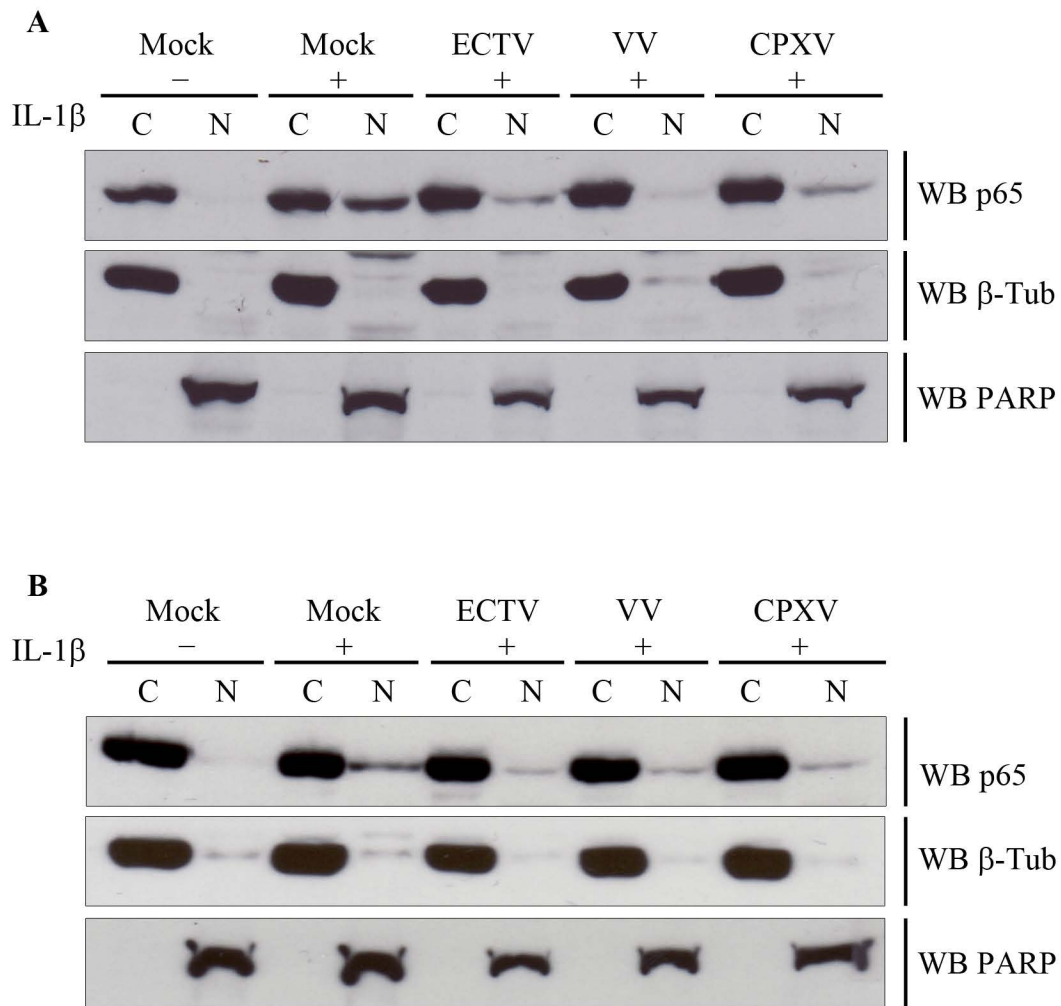


Figure 5.5. ECTV infection prevents IL-1 β induced p65 nuclear translocation in HeLa and MEF cells. **A.** HeLa cells were mock infected or infected with ECTV, VV or CPXV for 12 hours followed by stimulation with 10ng/ml IL-1 β for 20 minutes. Nuclear and cytoplasmic extracts were collected and western blotted with anti-p65, anti- β -tubulin, or anti-PARP. **B.** MEF cells were mock infected or infected with ECTV, VVCop or CPXV for 12 hours followed by stimulation with 10ng/ml IL-1 β for 20 minutes. Nuclear and cytoplasmic extracts were collected and western blotted with anti-p65, anti- β -tubulin, or anti-PARP. p65 nuclear accumulation is inhibited by ECTV infection.

cellular F-box proteins, the poxviral F-box domains are found at the C-terminus in combination with N-terminal ankyrin repeats (5, 15, 17, 19, 22, 23, 25, 29). With the exception of EVM005, which has only one ortholog in CPXV strain Brighton Red, CPXVBR011, multiple orthologs exist for EVM002, EVM154 and EVM165. Since the SCF ^{β -TRCP} ubiquitin ligase is a multi-subunit complex that plays an essential role in activation of NF- κ B via the degradation of phospho-I κ B α we sought to determine the role of EVM005 in the regulation of NF- κ B activation and I κ B α degradation during ECTV infection (16, 27).

We first tested the ability of EVM005 to inhibit the nuclear accumulation of the NF- κ B transcription factor, p65. HeLa cells were mock-transfected or transfected with full length Flag-EVM005. At 12 hours post-transfection cells were stimulated with TNF α or IL-1 β for 20 minutes and nuclear accumulation of p65 was detected by immunofluorescence (Figure 5.6, 5.7 and 5.8). As expected, unstimulated HeLa cells demonstrated cytoplasmic staining of p65 (Figures 5.6 and 5.7 panels a-c), and strong nuclear accumulation of p65 was seen following TNF α and IL-1 β stimulation (Figures 5.6 and 5.7 panels d-f). In contrast, cells expressing Flag-EVM005 and stimulated with TNF α or IL-1 β strongly inhibited p65 nuclear accumulation (Figures 5.6 and 5.7 panels g-i). To determine the role of the EVM005 F-box domain in p65 nuclear accumulation, we utilized an EVM005 mutant, Flag-EVM005(1-593), which lacks the C-terminal F-box domain and fails to interact with the SCF complex (Figure 3.2)(29). Interestingly, cells expressing Flag-EVM005(1-593) displayed strong nuclear staining of p65 following TNF α or IL-1 β stimulation (Figures 5.6 and 5.7 panels

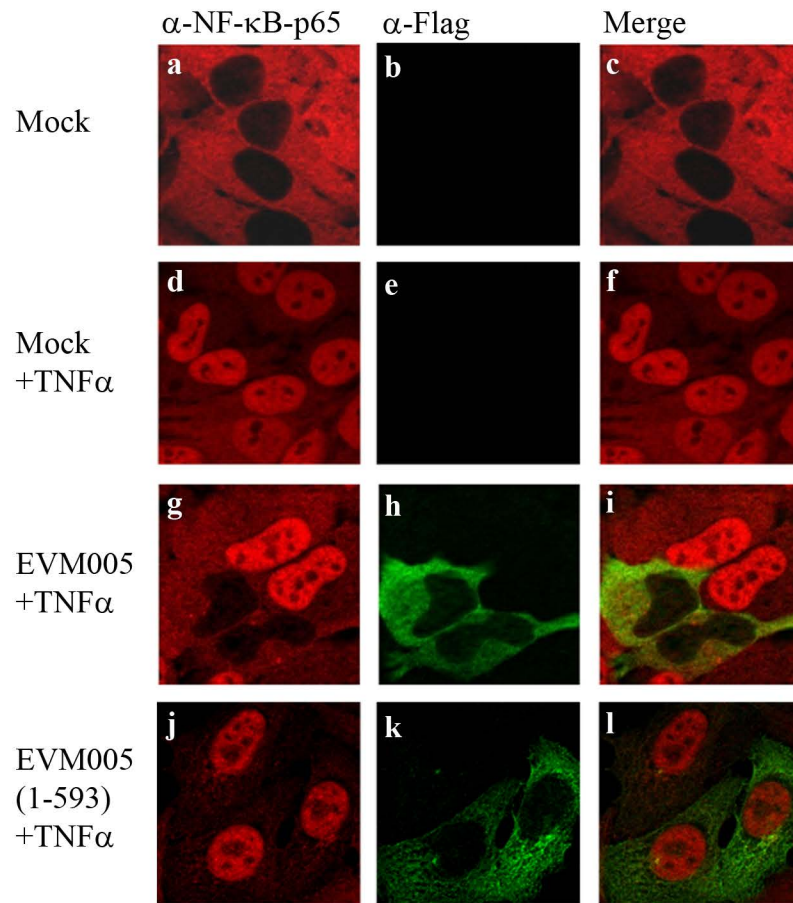


Figure 5.6. Flag-EVM005 inhibits TNF α induced p65 nuclear accumulation in an F-box dependent manner. HeLa cells were mock transfected or transfected with pcDNA-Flag-EVM005 or pcDNA-Flag-EVM005(1-593). At 12 hours post transfection cells were treated with 10ng/ml TNF α for 20 minutes. Cells were fixed and stained with anti-Flag to detect EVM005 and anti-p65 and visualized by immunofluorescence. Full-length EVM005 inhibits p65 nuclear accumulation while the F-box deletion mutant is unable to inhibit.

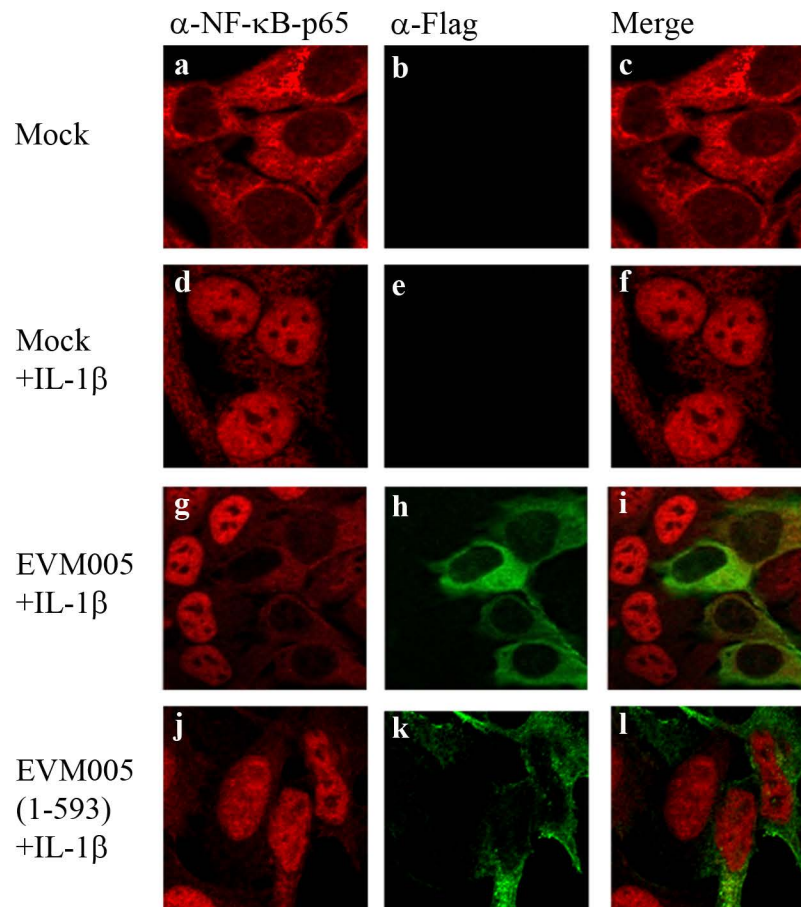


Figure 5.7. Flag-EVM005 inhibits IL-1 β induced p65 nuclear accumulation in an F-box dependent manner. HeLa cells were mock transfected or transfected with pcDNA-Flag-EVM005 or pcDNA-Flag-EVM005(1-593). At 12 hours post transfection cells were treated with 10ng/ml IL-1 β for 20 minutes. Cells were fixed and stained with anti-Flag to detect EVM005 and anti-p65 and visualized by immunofluorescence. Full-length EVM005 inhibits p65 nuclear accumulation while the F-box deletion mutant is unable to inhibit.

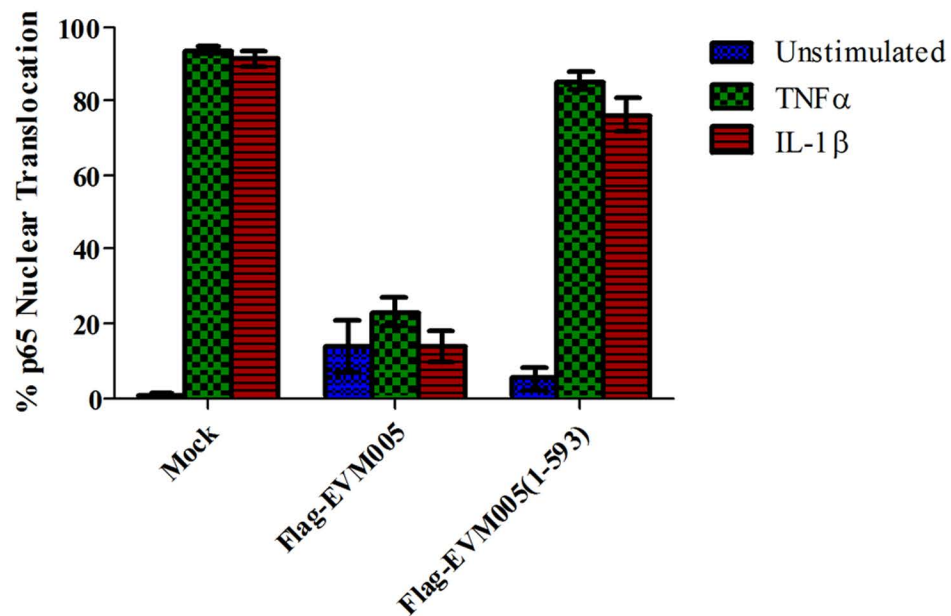
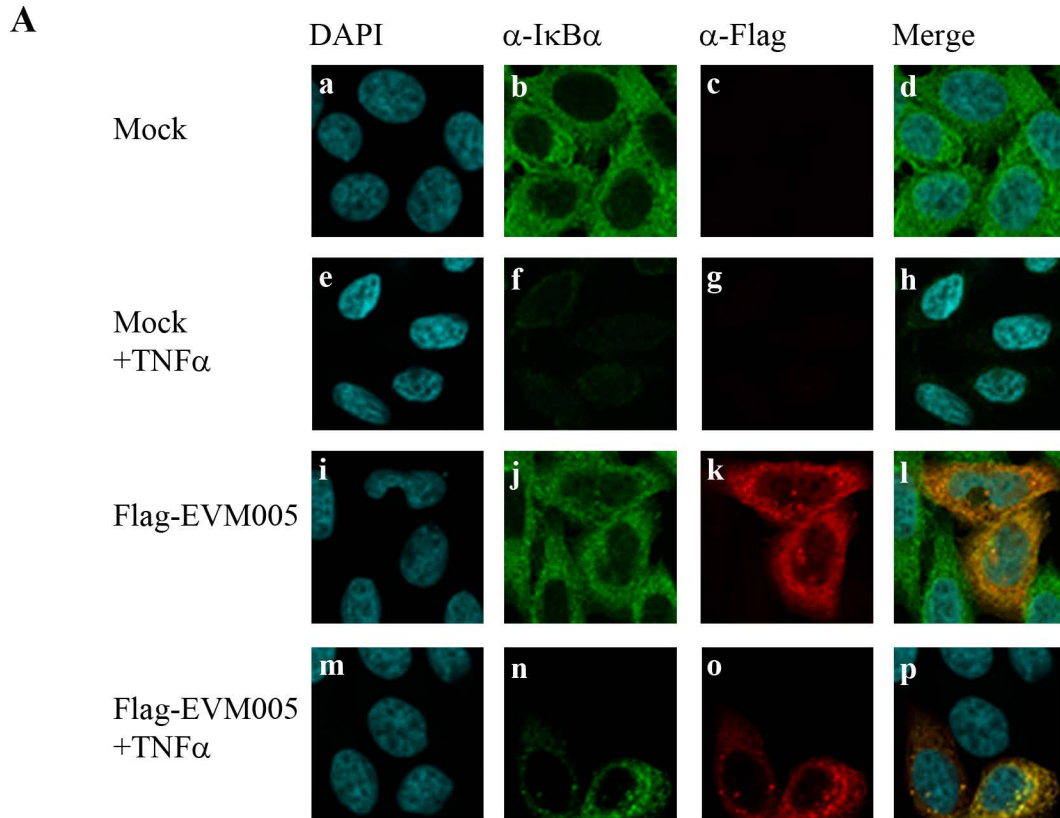


Figure 5.8. Quantification of p65 nuclear accumulation in cells transfected with Flag-EVM005 and Flag-EVM005(1-593). At least 50 cells were counted in three independent experiments to obtain the mean percentage of cells displaying nuclear accumulation of p65. Unstimulated cells are represented in blue, TNF α stimulated cells are represented in green, and IL-1 β stimulated cells are represented in red. These data indicate that EVM005 requires its C-terminal F-box domain to inhibit TNF α and IL-1 β induced p65 nuclear accumulation.

j-l). Nuclear translocation of p65 was quantified by counting cells from three independent experiments (Figure 5.8). These data indicate that Flag-EVM005 expression inhibited both TNF α and IL-1 β induced nuclear accumulation of p65, and inhibition of p65 nuclear accumulation required a functional F-box domain.

5.4 EVM005 Inhibits TNF α - and IL-1 β -Induced I κ B α Degradation.

Transient expression of EVM005 inhibited p65 translocation (Figures 5.6, 5.7 and 5.8), therefore, we sought to determine if EVM005 stabilized I κ B α . HeLa cells were transfected with Flag-EVM005 and I κ B α was visualized by immunofluorescence. As expected, in unstimulated cells significant amounts of I κ B α were present within the cytoplasm (Figure 5.9A panel b). Following 20 minutes of treatment with TNF α , the level of I κ B α within the cytoplasm was dramatically decreased due to ubiquitination and the subsequent degradation of I κ B α (Figure 5.9A panel f)(16, 27). In the absence of TNF α stimulation, expression of Flag-EVM005 did not affect the levels of I κ B α (Figure 5.9A panel j). In contrast, HeLa cells expressing Flag-EVM005 and stimulated with TNF α demonstrated that ectopic expression of EVM005 stabilized I κ B α compared to the surrounding cells (Figure 5.9A panel n). To further test this data, HeLa cells were mock-transfected or transfected with Flag-EVM005 in the absence or presence of TNF α and analysed by western blot for I κ B α , Flag to detect EVM005, and β -tubulin. Cells treated with TNF α showed a substantial decrease in I κ B α (Figure 5.9B). However, upon expression of EVM005, I κ B α was substantially stabilized (Figure 5.9B). We next determined if the inhibition of



B

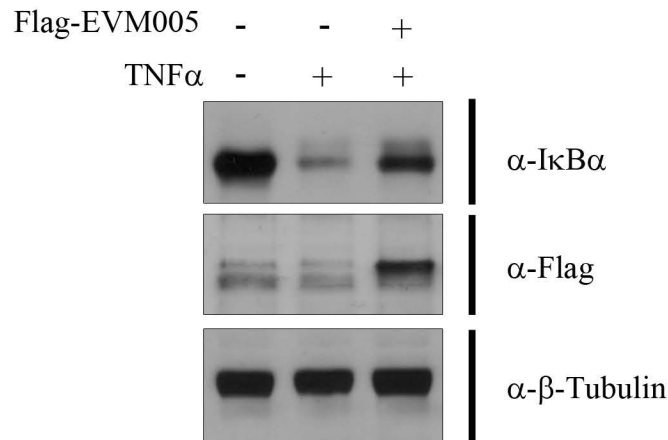
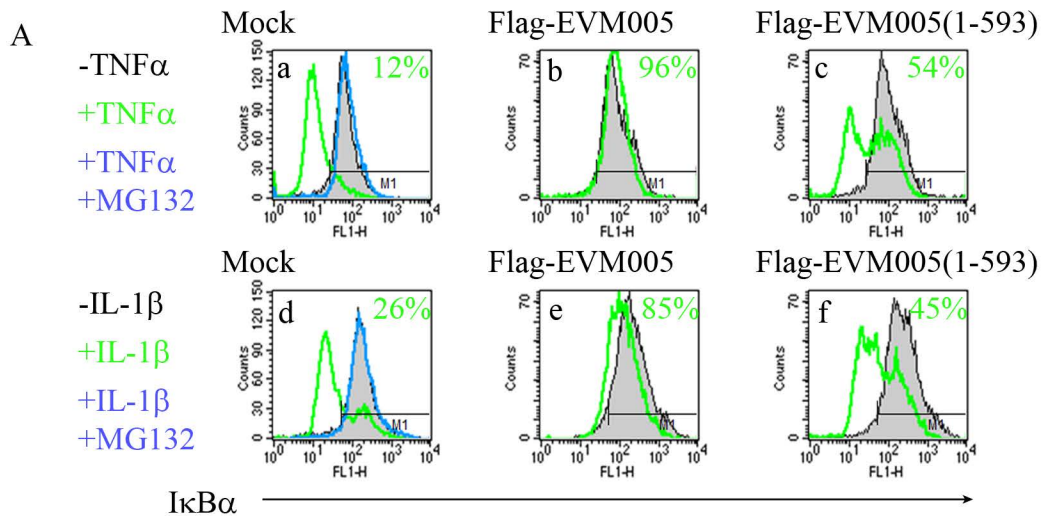


Figure 5.9. Flag-EVM005 inhibits TNF α induced I κ B α degradation. **A.** HeLa cells were mock-transfected (a-h) or transfected with pcDNA-Flag-EVM005 (i-p). At 12 hours post-transfection, cells were untreated or treated with 10ng/ml TNF α for 20 minutes. Cells were fixed and stained with DAPI, anti-I κ B α , and anti-Flag, and visualized by confocal microscopy. **B.** HeLa cells were mock-transfected or transfected with pcDNA-Flag-EVM005. At 12 hours post-transfection, cells were left unstimulated or stimulated with 10ng/ml TNF α for 20 minutes. Protein samples were separated by SDS-PAGE, and western blotted with anti-Flag, anti-I κ B α and anti- β -tubulin.

I κ B α degradation by EVM005 was dependent on the C-terminal F-box domain. To test this, I κ B α degradation was assessed by flow cytometry. Unstimulated cells demonstrated physiological levels of I κ B α that were significantly decreased following TNF α or IL-1 β stimulation as indicated by a leftward shift shown in green on the histogram (Figure 5.10A panels a and d). Pre-treatment of HeLa cells with the proteasome inhibitor MG132, and subsequent TNF α or IL-1 β treatment, inhibited the degradation of I κ B α as expected (Figure 5.10A panels a and d)(16). To determine the role of EVM005 in I κ B α degradation, HeLa cells were transfected with Flag-EVM005 or Flag-EVM005(1-593), devoid of the F-box domain (29). At 24 hours post-transfection, cells were stimulated with TNF α or IL-1 β , fixed and stained with anti-Flag and anti-I κ B α to detect EVM005 and I κ B α , respectively, and Flag-positive cells were gated for analysis (Figure 5.10A panels b and e). HeLa cells expressing Flag-EVM005 and stimulated with TNF α or IL-1 β inhibited I κ B α degradation (Figure 5.10A panels b and e). However, expression of Flag-EVM005(1-593), which lacks the F-box domain, was unable to stabilize I κ B α resulting in significant degradation of I κ B α (Figure 5.10A panels c and f). This data was quantified by measuring the mean fluorescence intensities of three independent experiments to obtain standard errors (Figure 5.10B). These data indicate that Flag-EVM005 strongly inhibits TNF α and IL-1 β induced I κ B α degradation, whereas the F-box deletion mutant failed to inhibit I κ B α degradation (Figures 5.9 and 5.10). Together, these data indicated that EVM005 expression blocked I κ B α degradation and subsequent nuclear



B

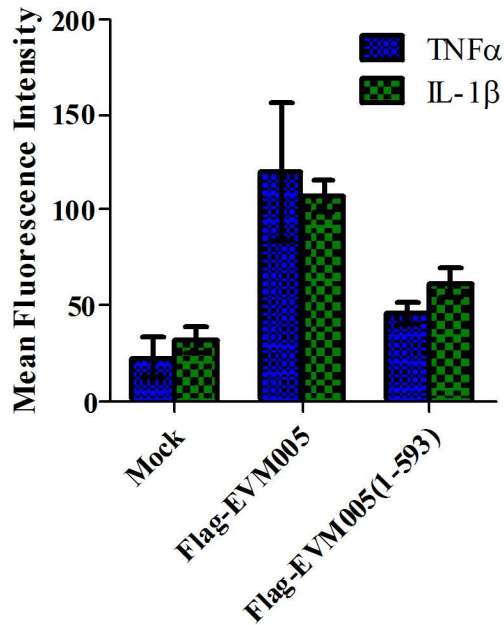


Figure 5.10. EVM005 requires the C-terminal F-box domain in order to inhibit TNF α and IL-1 β induced I κ B α degradation. **A.** HeLa cells were mock transfected or transfected with pcDNA-Flag-EVM005 or pcDNA-Flag-EVM005(1-593). Mock cells were untreated or pre-treated with 10 μ M MG132 for one hour as a positive control for inhibition of I κ B α degradation. At 18 hours post transfection, cells were stimulated with 10ng/ml TNF α (panels a-c) or 10ng/ml IL-1 β (panels d-f) for 20 minutes. Cells were harvested, fixed and co-stained with anti-Flag and anti-I κ B α . Cells were analyzed by flow cytometry, Flag-positive populations were gated for analysis and I κ B α fluorescence was measured on the x-axis. **B.** I κ B α fluorescence was quantified by calculating the mean fluorescence intensity from three independent experiments and plotted with standard errors.

accumulation of p65 in an F-box-dependent manner.

5.5 ECTV- Δ 005 Inhibits p65 Nuclear Accumulation and Synthesis of NF- κ B Regulated Transcripts

To further examine the role of EVM005 in NF- κ B activation during infection we generated an EVM005 deletion virus. In the past, deletion of open reading frames from poxvirus genomes has been performed by insertion of drug selection or fluorescent markers into the genome to disrupt the gene of interest. Instead, we used the novel Selectable and Excisable Marker (SEM) system that utilizes the Cre/LoxP recombinase to delete the EVM005 open reading frame (Chapter 2 and 4)(8, 20). As described in the previous chapter, the SEM cloning technique provided us with a marker-free EVM005 deletion virus that displayed no growth defects on BGMK cells.

To determine if ECTV lacking EVM005 affected the nuclear accumulation of p65 following TNF α stimulation, HeLa cells were mock-infected, infected with ECTV or ECTV- Δ 005. Similar to ECTV, infection with ECTV- Δ 005 also inhibited the nuclear accumulation of p65 by immunofluorescence (Figure 5.11 panel g-i). This was further supported by nuclear and cytoplasmic extracts in both HeLa (Figure 5.12A) and MEF cells (Figure 5.12B). We also examined the effect of ECTV or ECTV- Δ 005 infection on the production of NF- κ B regulated transcripts. HeLa cells were mock-infected or infected with ECTV or ECTV- Δ 005 at a MOI of 5. At 12 hours post-infection cells were stimulated with TNF α , and RNA samples were collected at 0, 2, 4, and

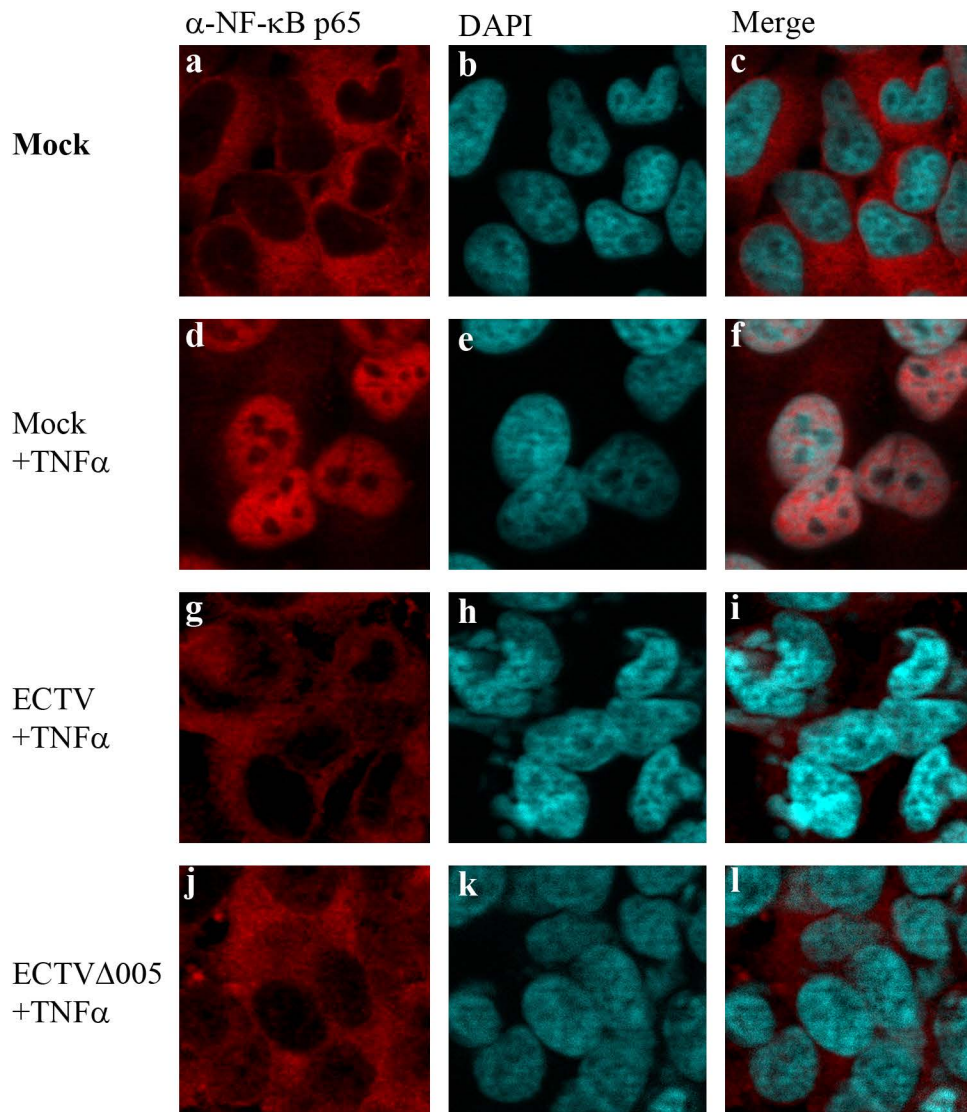


Figure 5.11. ECTV- Δ 005 inhibits TNF α induced p65 nuclear accumulation. HeLa cells were mock infected (a-f) or infected with ECTV (g-i) or ECTV- Δ 005 (j-l) at a MOI of 5. At 12 hours post infection, cells were stimulated with 10ng/ml TNF α for 20 minutes, fixed and stained with anti-p65 and DAPI and cells were visualized by immunofluorescence. ECTV- Δ 005 still inhibits p65 nuclear accumulation.

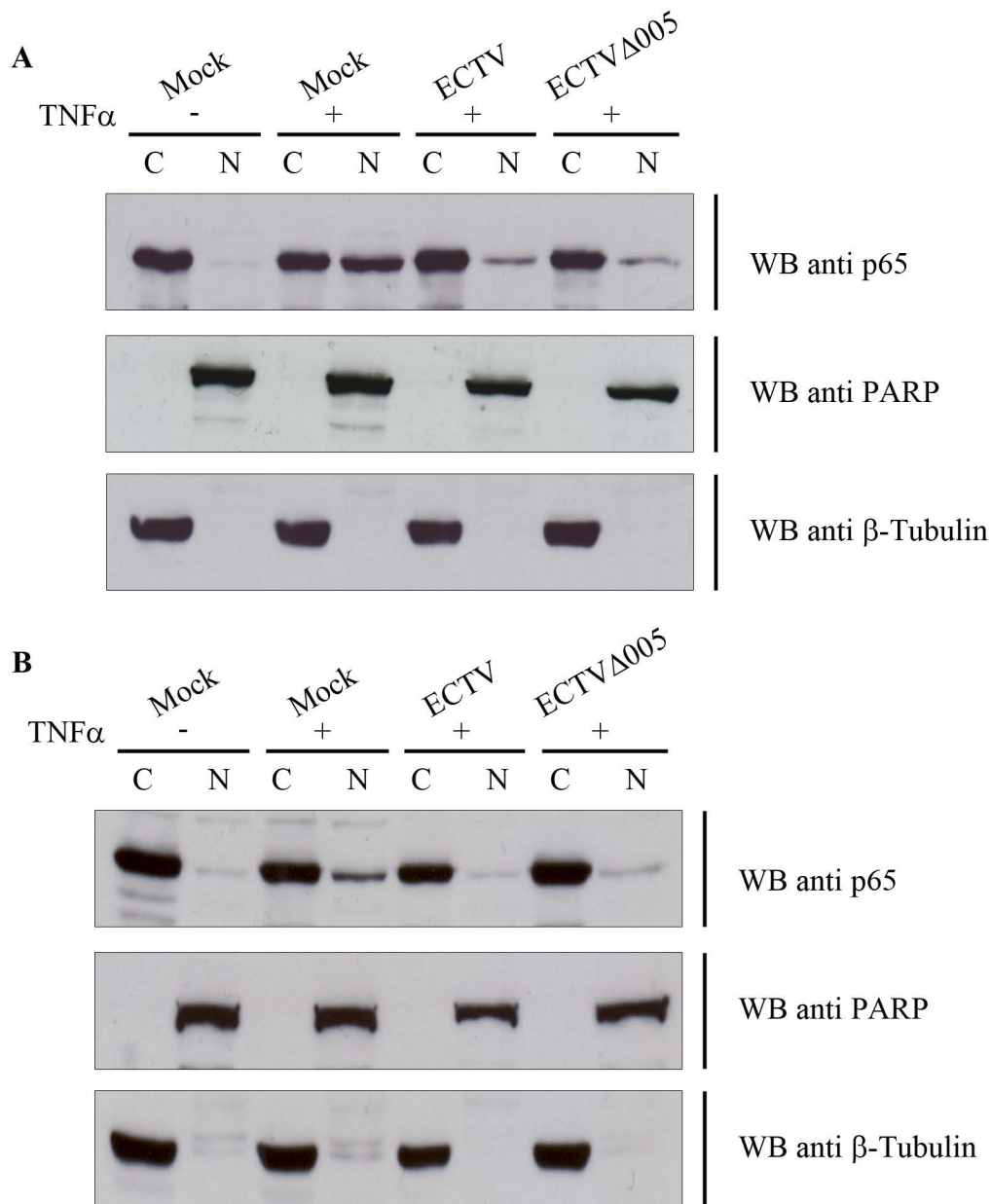


Figure 5.12. ECTV- Δ 005 inhibits TNF α induced p65 nuclear accumulation.
A. HeLa cells or **B.** MEF cells were mock infected or infected with ECTV or ECTV- Δ 005 at a MOI of 5. At 12 hours post infection, cells were stimulated with 10ng/ml TNF α for 20 minutes and nuclear and cytoplasmic extracts were collected. Protein samples were separated by SDS-PAGE and western blotted with anti-p65, anti-PARP, and anti- β -tubulin. The EVM005 deletion virus is still capable of inhibiting p65 nuclear translocation.

6 hours post-TNF α treatment. We screened these samples for the relative levels of RNA transcripts corresponding to TNF α , IL-1 β and IL-6, all genes known to be upregulated by NF- κ B (10). Mock-infected cells displayed an increase the transcript levels corresponding to TNF α , IL-1 β and IL-6, at 2 hours post-TNF α stimulation, as expected (Figure 5.13). Transcript levels decreased at 4 and 6 hours post stimulation due to the up-regulation of NF- κ B inhibitors such as I κ B α (Figure 5.1A)(13). HeLa cells infected with ECTV or ECTV- Δ 005 inhibited transcription of TNF α , IL-1 β and IL-6. This data correlated well with our previous data indicating that infection with ECTV or ECTV- Δ 005 inhibited the nuclear accumulation of the NF- κ B transcription factor, p65 (Figure 5.11 and 5.12).

5.6 ECTV- Δ 005 Inhibits I κ B α Degradation

Finally, we looked upstream directly at I κ B α levels in cells infected with ECTV, ECTV- Δ 005, or ECTV-005-rev. At 12 hours post infection HeLa cells were stimulated with TNF α , fixed and stained with anti-I κ B α or anti-I3L, an early poxvirus protein, and analyzed by flow cytometry. Unstimulated cells (shown in black) demonstrated physiological levels of I κ B α that decreased following TNF α stimulation (shown in green)(Figure 5.14A panel a). HeLa cells pre-treated with MG132 and further stimulated with TNF α maintained the physiological level of I κ B α , as expected (shown in blue)(Figure 5.14A panel a). ECTV infected cells stimulated with TNF α indicated no change in the level of I κ B α , further

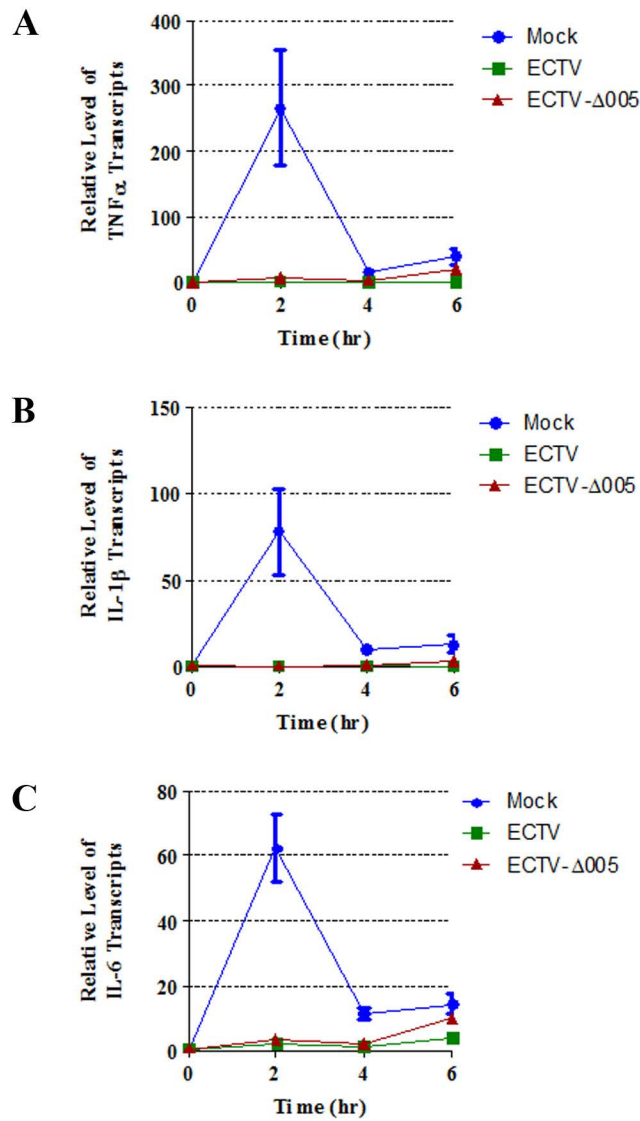


Figure 5.13. ECTV- Δ 005 inhibits the production of NF- κ B regulated transcripts. HeLa cells were mock infected or infected with ECTV or ECTV- Δ 005 at a MOI of 5. At 12 hours post infection cells were stimulated with TNF α . RNA samples were collected at 0, 2, 4 and 6 hours post TNF α treatment. Samples were reverse transcribed, followed by real time PCR analysis for relative levels of (A) TNF α , (B) IL-1 β , and (C) IL-6 transcripts, as compared to GAPDH. Time courses were performed in triplicate and plotted as the mean with standard error.

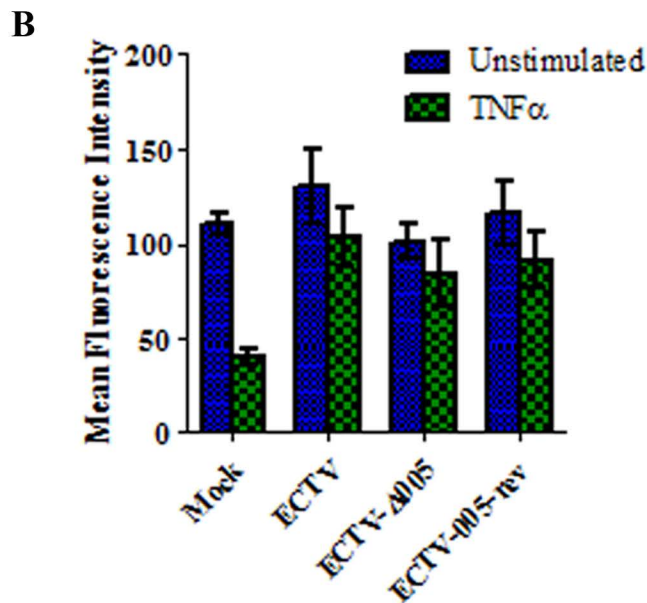
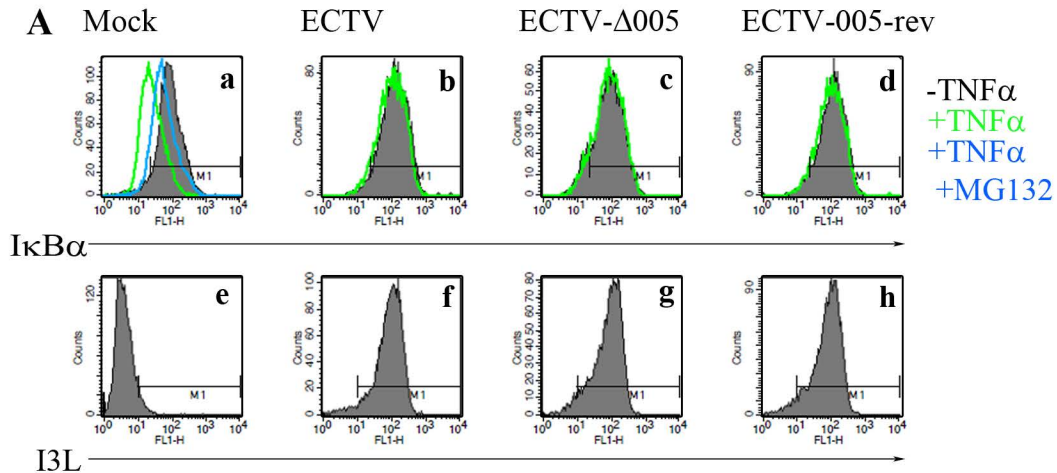


Figure 5.14. ECTV-Δ005 inhibits TNF α induced $I\kappa B\alpha$ degradation. **A.** HeLa cells were mock infected or infected with ECTV, ECTV-Δ005 or ECTV-005-rev at a MOI of 5. At 12 hours post infection, cells were stimulated with 10 μ M MG132 for 1 hour and/or 10ng/ml TNF α for 20 minutes. Cells were harvested, fixed and permeabilized, and stained with anti- $I\kappa B\alpha$ and anti-I3L. Samples were subjected to flow cytometry to measure $I\kappa B\alpha$ (a-d) or I3L (e-h). **B.** The mean fluorescence intensities were measured and plotted as the average of three independent experiments with standard error.

supporting the fact that I κ B α is not degraded in ECTV infected cells (Figure 5.14A panel b). Additionally, HeLa cells infected with ECTV- Δ 005 or ECTV-005-rev and stimulated with TNF α inhibited I κ B α degradation (Figure 5.14A panels c and d). Cells were also analyzed for I3L expression to demonstrate virus infection (Figure 5.14A panels e-h). This data was quantified by measuring the mean fluorescence intensities of three independent experiments to obtain standard errors (Figure 5.14B). Overall, this data demonstrates that upon ECTV- Δ 005 infection, I κ B α degradation is inhibited.

5.7 EVM005 is Required for Virulence

To determine if EVM005 was required for virulence, we infected mice at Saint Louis University in collaboration with Dr. Mark Buller. All experiments were approved by the Canadian Council for Animal Care. Two separate preliminary experiments were performed to determine if deletion of the EVM005 open reading frame from ECTV strain Moscow had an effect on virulence in A/NCR or C57BL/6 mouse strains (4, 6, 7). Initially, five female C57BL/6 mice were mock infected or infected with 10-fold escalating doses of ECTV, ECTV- Δ 005 or ECTV-005-rev via the intranasal route with doses ranging between 10^2 and 10^6 pfu (Figure 5.15A). Following infection, body weight, day of death and mortality was monitored daily. Mice were euthanized if body weight fell below 70% of their initial mass, or if severe morbidity was observed. C57BL/6 mice infected with ECTV- Δ 005 showed a decrease in virulence, whereas mice infected with ECTV or ECTV-005-rev succumbed to infection by day 7 (Figure 5.15A). Mice

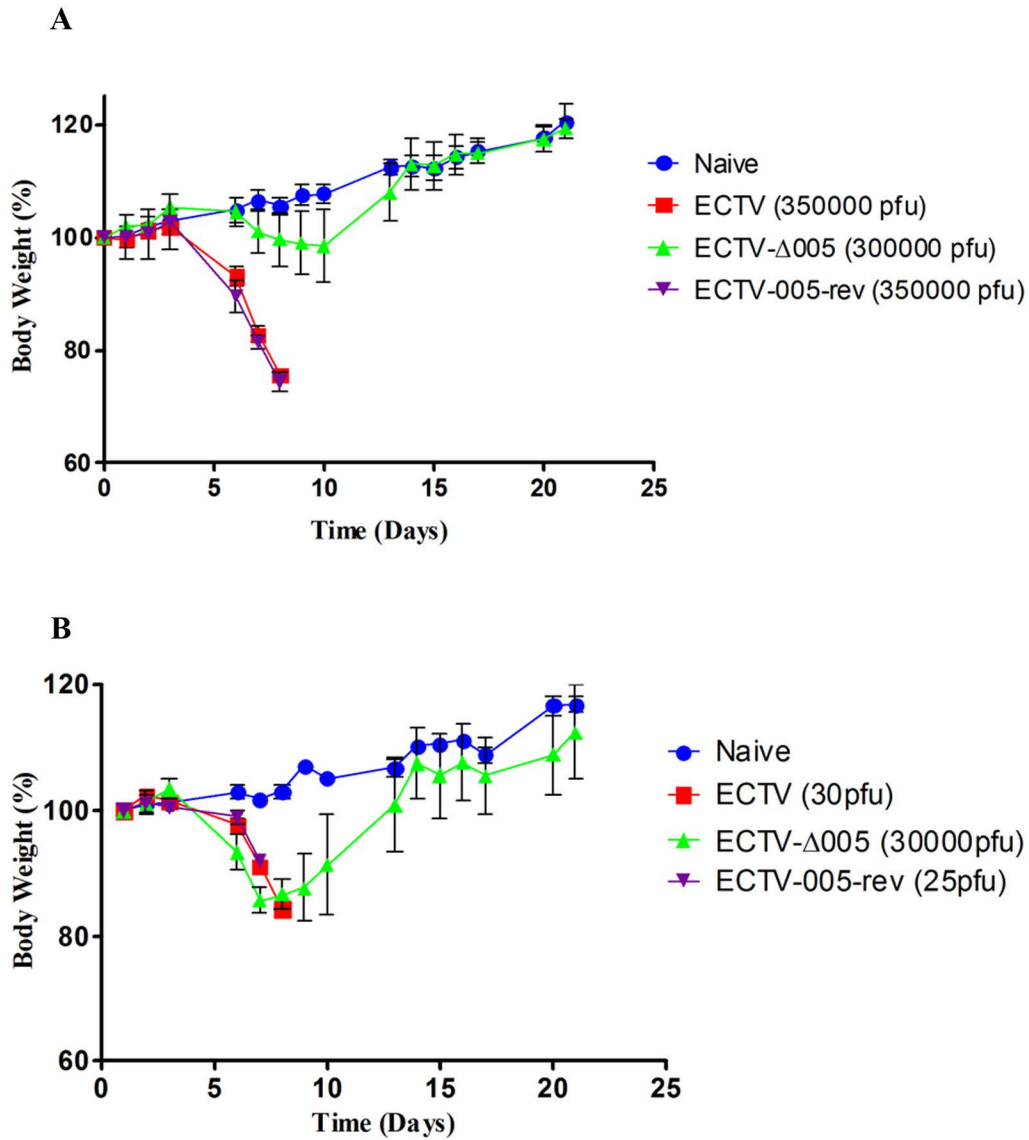


Figure 5.15. ECTV-Δ005 is attenuated in C57BL/6 and A/NCR mice. **A.** Female C57BL/6 mice were mock infected or infected with ECTV, ECTV-Δ005, or ECTV-005-rev via intranasal inoculation with the indicated doses. Body weights were measured over 21 days and plotted over time. Mice were euthanized if individual weights dropped below 70% of their initial mass or if severe morbidity was observed. **B.** Alternatively, susceptible female A/NCR mice were mock infected or infected with ECTV, ECTV-Δ005, or ECTV-005-rev at the indicated dose via footpad injection. Body weights were measured over 21 days. Mice were euthanized if their individual weights dropped below 70% of their initial mass or if severe morbidity was observed.

infected with ECTV- Δ 005 survived through day 21, with initial weight loss through day 10, followed by weight gain similar to naive mice by day 21 (Figure 5.15A).

We next determined if EVM005 also contributed to virulence in the susceptible A/NCR mouse strain (7). In this experiment, 5 to 10 week old female A/NCR mice were mock infected or infected with ECTV, ECTV- Δ 005 or ECTV-005-rev via footpad injections (Figure 5.15B)(7). We infected four sets of five mice with escalating 10-fold doses between 10^1 and 10^5 pfu per mouse and monitored changes in body weight, day of death and mortality daily. Mice were euthanized if body weight dropped below 70% of the initial mass or if we observed severe morbidity. Similar to the data observed in C57BL/6 mice (Figure 5.15A), ECTV- Δ 005 was attenuated compared to wild type ECTV and ECTV-005-rev in A/NCR mice (Figure 5.15B). The data demonstrated that ECTV and ECTV-005-rev infected mice succumb to infection between day 7 and 8 post infection, even at low doses (Figure 5.15B). Alternatively, mice infected with ECTV- Δ 005 survived through day 21 with minimal weight loss, even in mice receiving high doses (Figure 5.15B). Together, our preliminary results suggest that EVM005 is a critical virulence factor for infection of both resistant C57BL/6 and susceptible A/NCR mouse strains. As ECTV- Δ 005 was still capable of inhibiting I κ B α degradation, p65 nuclear accumulation and the synthesis of NF- κ B regulated transcripts, the data suggested that the mechanism by which EVM005 contributes to virulence observed in mice is independent of NF- κ B inhibition.

5.8 Discussion

We have previously identified four ankyrin/F-box proteins encoded by ECTV that interact with the SCF ubiquitin ligase complex via C-terminal F-box domains (Chapter 3)(29). We hypothesize that each of these proteins recruits a unique set of target proteins to the complex during infection, via their ankyrin domains, to promote ubiquitylation and degradation of these targets through the 26S proteasome. The presence of four ankyrin/F-box proteins encoded by ECTV suggests that the SCF complex is an important target during ECTV infection. Additionally, the host NF- κ B signalling pathway is dependent on the SCF complex for the ubiquitylation and degradation of the inhibitory protein, I κ B α (24, 30). Here we demonstrate that I κ B α is phosphorylated but not degraded during ECTV infection, suggesting that signalling is inhibited at the point of I κ B α ubiquitylation, an event mediated by the SCF complex (Figure 5.1). Additionally, we demonstrate that the ECTV encoded ankyrin/F-box protein, EVM005, inhibits p65 nuclear accumulation and I κ B α degradation in a process that requires its C-terminal F-box domain (Figure 5.6, 5.7, 5.8, 5.9 and 5.10). Therefore, EVM005 is an inhibitor of NF- κ B signalling through manipulation of the SCF complex. An ECTV recombinant lacking the EVM005 open reading frame, ECTV- Δ 005, was created and tested for its ability to inhibit NF- κ B activation. Even though EVM005 was deleted, ECTV- Δ 005 still inhibited I κ B α degradation, p65 nuclear accumulation and the production of NF- κ B regulated transcripts (Figure 5.11, 5.12, 5.13 and 5.14). EVM005 is one of many open

reading frames encoded by ECTV that inhibits NF- κ B activation (18), and deletion of multiple open reading frames is likely required to render ECTV susceptible to NF- κ B activation.

Viral manipulation of the cellular SCF ubiquitin ligase by poxvirus encoded ankyrin/F-box proteins is likely a key contributor to the accumulation of phospho-I κ B α seen during poxvirus infection (Figure 5.1). The cellular F-box protein, β -TRCP, recognizes phospho-I κ B α in uninfected cells and mediates its ubiquitination and subsequent degradation via the 26S proteasome (30). However, ECTV encodes four ankyrin/F-box proteins that hijack the SCF complex during infection (29). Therefore, we tested the ability of EVM005, an ECTV encoded ankyrin/F-box protein that is unique to ECTV and CPXV, to inhibit NF- κ B signalling. Our data demonstrated that EVM005 inhibited I κ B α degradation, perhaps through competition with β -TRCP for available Skp1 binding sites at the SCF complex (Figure 5.10). This competition would disrupt the association between Skp1 and β -TRCP, an interaction that is required for I κ B α ubiquitylation and degradation (26, 30). This hypothesis is consistent with our data demonstrating the requirement of the C-terminal F-box domain for the inhibition of I κ B α degradation by EVM005. This is similar to the mechanism of the HIV protein, Vpu (1, 2). Vpu binds to β -TRCP and disrupts the association between the cellular F-box protein and Skp1, therefore inhibiting the ubiquitylation and degradation of I κ B α in addition to other SCF ^{β -TRCP} substrates (1). However, our data do not rule out the possibility that EVM005 recruits substrates for degradation that are involved in NF- κ B activation.

However, we were unable to detect degradation of I κ B α , NF- κ B1 p50/105, or p65 in ECTV infected cells.

Finally, we determined that EVM005 was a required virulence factor for ECTV during infection of resistant C57BL/6 and susceptible A/NCR mouse strains. Interestingly, we have observed late gene synthesis and/or virus spread during ECTV- Δ 005 infection in several tissue culture cell lines including HeLa, HEK293T, U20S, MEF, CV-1, and BGMK, suggesting that EVM005 is not required for growth, but likely functions in regulation of the host immune response. However, ECTV- Δ 005 was capable of inhibiting I κ B α degradation, p65 nuclear accumulation and the synthesis of NF- κ B regulated transcripts. These data suggest that an EVM005 function independent of NF- κ B inhibition may be responsible for mediating virulence of ECTV. If proteins targeted for ubiquitylation by the SCF^{EVM005} ubiquitin ligase exist, their identification could provide insight into the contribution of EVM005 to virulence.

In conclusion, our data show that ECTV encodes a unique inhibitor of NF- κ B activation. EVM005 requires its C-terminal F-box domain to manipulate the cellular SCF complex and inhibit I κ B α degradation (Figure 5.6, 5.7, 5.8, 5.9 and 5.10). Although ECTV- Δ 005 still inhibits NF- κ B activation (Figure 5.11, 5.12, 5.13 and 5.14), this virus demonstrated decreased virulence in both A/NCR and C57BL/6 mice (Figure 5.15), implying that EVM005 has an additional role, independent of NF- κ B inhibition. The identification of protein targets for ubiquitylation remains a major goal of our laboratory and has the potential to provide insight into the additional role(s) for EVM005 *in vivo*.

5.9 References

1. **Besnard-Guerin, C., N. Belaidouni, I. Lassot, E. Segeal, A. Jobart, C. Marchal, and R. Benarous.** 2004. HIV-1 Vpu sequesters beta-transducin repeat-containing protein (betaTrCP) in the cytoplasm and provokes the accumulation of beta-catenin and other SCFbetaTrCP substrates. *J Biol Chem* **279**:788-95.
2. **Bour, S., C. Perrin, H. Akari, and K. Strebel.** 2001. The human immunodeficiency virus type 1 Vpu protein inhibits NF-kappa B activation by interfering with beta TrCP-mediated degradation of Ikappa B. *J Biol Chem* **276**:15920-8.
3. **Bowie, A., E. Kiss-Toth, J. A. Symons, G. L. Smith, S. K. Dower, and L. A. O'Neill.** 2000. A46R and A52R from vaccinia virus are antagonists of host IL-1 and toll-like receptor signaling. *Proc Natl Acad Sci U S A* **97**:10162-7.
4. **Buller, R. M., M. Potter, and G. D. Wallace.** 1986. Variable resistance to ectromelia (mousepox) virus among genera of Mus. *Curr Top Microbiol Immunol* **127**:319-22.
5. **Chang, S. J., J. C. Hsiao, S. Sonnberg, C. T. Chiang, M. H. Yang, D. L. Tzou, A. A. Mercer, and W. Chang.** 2009. Poxvirus host range protein CP77 contains an F-box-like domain that is necessary to suppress NF-kappaB activation by tumor necrosis factor alpha but is independent of its host range function. *J Virol* **83**:4140-52.
6. **Chaudhri, G., V. Panchanathan, R. M. Buller, A. J. van den Eertwegh, E. Claassen, J. Zhou, R. de Chazal, J. D. Laman, and G. Karupiah.** 2004. Polarized type 1 cytokine response and cell-mediated immunity determine genetic resistance to mousepox. *Proc Natl Acad Sci U S A* **101**:9057-62.
7. **Esteban, D. J., and R. M. Buller.** 2005. Ectromelia virus: the causative agent of mousepox. *J Gen Virol* **86**:2645-59.
8. **Gammon, D. B., B. Gowrishankar, S. Duraffour, G. Andrei, C. Upton, and D. H. Evans.** 2010. Vaccinia virus-encoded ribonucleotide reductase subunits are differentially required for replication and pathogenesis. *PLoS Pathog* **6**:e1000984.
9. **Gedey, R., X. L. Jin, O. Hinthong, and J. L. Shisler.** 2006. Poxviral regulation of the host NF-kappaB response: the vaccinia virus M2L protein inhibits induction of NF-kappaB activation via an ERK2 pathway in virus-infected human embryonic kidney cells. *J Virol* **80**:8676-85.
10. **Ghosh, S., M. J. May, and E. B. Kopp.** 1998. NF-kappa B and Rel proteins: evolutionarily conserved mediators of immune responses. *Annu Rev Immunol* **16**:225-60.
11. **Hayden, M. S., and S. Ghosh.** 2008. Shared principles in NF-kappaB signaling. *Cell* **132**:344-62.

12. **Hinthong, O., X. L. Jin, and J. L. Shisler.** 2008. Characterization of wild-type and mutant vaccinia virus M2L proteins' abilities to localize to the endoplasmic reticulum and to inhibit NF-kappaB activation during infection. *Virology* **373**:248-62.
13. **Hoffmann, A., G. Natoli, and G. Ghosh.** 2006. Transcriptional regulation via the NF-kappaB signaling module. *Oncogene* **25**:6706-16.
14. **Johnston, J. B., and G. McFadden.** 2003. Poxvirus immunomodulatory strategies: current perspectives. *J Virol* **77**:6093-100.
15. **Johnston, J. B., G. Wang, J. W. Barrett, S. H. Nazarian, K. Colwill, M. Moran, and G. McFadden.** 2005. Myxoma virus M-T5 protects infected cells from the stress of cell cycle arrest through its interaction with host cell cullin-1. *J Virol* **79**:10750-63.
16. **Karin, M., and Y. Ben-Neriah.** 2000. Phosphorylation meets ubiquitination: the control of NF-[kappa]B activity. *Annu Rev Immunol* **18**:621-63.
17. **Mercer, A. A., S. B. Fleming, and N. Ueda.** 2005. F-box-like domains are present in most poxvirus ankyrin repeat proteins. *Virus Genes* **31**:127-33.
18. **Mohamed, M. R., and G. McFadden.** 2009. NFkB inhibitors: strategies from poxviruses. *Cell Cycle* **8**:3125-32.
19. **Mohamed, M. R., M. M. Rahman, J. S. Lanchbury, D. Shattuck, C. Neff, M. Dufford, N. van Buuren, K. Fagan, M. Barry, S. Smith, I. Damon, and G. McFadden.** 2009. Proteomic screening of variola virus reveals a unique NF-kappaB inhibitor that is highly conserved among pathogenic orthopoxviruses. *Proc Natl Acad Sci U S A* **106**:9045-50.
20. **Rintoul, J. L., J. Wang, D. B. Gammon, N. J. van Buuren, K. Garson, K. Jardine, M. Barry, D. H. Evans, and J. C. Bell.** 2011. A selectable and excisable marker system for the rapid creation of recombinant poxviruses. *PLoS One* **6**:e24643.
21. **Schroder, M., M. Baran, and A. G. Bowie.** 2008. Viral targeting of DEAD box protein 3 reveals its role in TBK1/IKKepsilon-mediated IRF activation. *EMBO J* **27**:2147-57.
22. **Sonnberg, S., S. B. Fleming, and A. A. Mercer.** 2009. A truncated two-alpha-helix F-box present in poxvirus ankyrin-repeat proteins is sufficient for binding the SCF1 ubiquitin ligase complex. *J Gen Virol* **90**:1224-8.
23. **Sonnberg, S., B. T. Seet, T. Pawson, S. B. Fleming, and A. A. Mercer.** 2008. Poxvirus ankyrin repeat proteins are a unique class of F-box proteins that associate with cellular SCF1 ubiquitin ligase complexes. *Proc Natl Acad Sci U S A* **105**:10955-60.
24. **Spencer, E., J. Jiang, and Z. J. Chen.** 1999. Signal-induced ubiquitination of IkappaBalpha by the F-box protein Slimb/beta-TrCP. *Genes Dev* **13**:284-94.
25. **Sperling, K. M., A. Schwantes, B. S. Schnierle, and G. Sutter.** 2008. The highly conserved orthopoxvirus 68k ankyrin-like protein is part of a cellular SCF ubiquitin ligase complex. *Virology* **374**:234-9.

26. **Suzuki, H., T. Chiba, M. Kobayashi, M. Takeuchi, T. Suzuki, A. Ichiyama, T. Ikenoue, M. Omata, K. Furuichi, and K. Tanaka.** 1999. IkappaBalpha ubiquitination is catalyzed by an SCF-like complex containing Skp1, cullin-1, and two F-box/WD40-repeat proteins, betaTrCP1 and betaTrCP2. *Biochem Biophys Res Commun* **256**:127-32.
27. **Tanaka, K., T. Kawakami, K. Tateishi, H. Yashiroda, and T. Chiba.** 2001. Control of IkappaBalpha proteolysis by the ubiquitin-proteasome pathway. *Biochimie* **83**:351-6.
28. **Vallabhapurapu, S., and M. Karin.** 2009. Regulation and function of NF-kappaB transcription factors in the immune system. *Annu Rev Immunol* **27**:693-733.
29. **van Buuren, N., B. Couturier, Y. Xiong, and M. Barry.** 2008. Ectromelia virus encodes a novel family of F-box proteins that interact with the SCF complex. *J Virol* **82**:9917-27.
30. **Winston, J. T., P. Strack, P. Beer-Romero, C. Y. Chu, S. J. Elledge, and J. W. Harper.** 1999. The SCFbeta-TRCP-ubiquitin ligase complex associates specifically with phosphorylated destruction motifs in IkappaBalpha and beta-catenin and stimulates IkappaBalpha ubiquitination in vitro. *Genes Dev* **13**:270-83.

Chapter 6: EVM002, EVM154 and EVM165 Encoded Ankyrin/F-box Proteins That Inhibit NF- κ B Activation

The results contained within this chapter consist of unpublished material. Experiments included in this chapter were performed by N. van Buuren. The original manuscript was written by N. van Buuren with an editorial contribution by M. Barry.

Significant contributions to experimentation presented in Figures 6.1 to 6.6 were made by Kristin Burles and Megan Edwards. The final figures were constructed by N. van Buuren.

Inhibition of p65 nuclear accumulation by EVM002 has been published in 2009: Mohamed, M.R., M.M. Rahman, J.S. Lanchbury, D. Shattuck, C. Neff, M. Dufford, **N. van Buuren**, K. Fagan, M. Barry, S. Smith, I. Damon and G. McFadden. 2009. PNAS, **106**: 9045-50.

6.1 Introduction

Previously, we demonstrated that EVM005, an ECTV encoded ankyrin/F-box protein, was a potent inhibitor of NF- κ B activation. EVM005 inhibits TNF α and IL-1 β induced I κ B α degradation (Figure 5.9 and 5.10) and p65 nuclear accumulation (Figure 5.6, 5.7 and 5.8). Additionally, EVM005 requires a functional C-terminal F-box domain in order to bind the SCF complex, as well as, disrupt NF- κ B activation (Figure 5.6, 5.7, 5.8 and 5.10). These data suggest two mechanisms, one, that EVM005 is binding the SCF complex and preventing the degradation of cellular F-box targets, such as phospho-I κ B α , or two, that EVM005 has its own targets within the NF- κ B signalling cascade. If EVM005 is inhibiting the degradation of cellular F-box protein targets through manipulation of the SCF complex, EVM002, EVM154 and EVM165, also ECTV encoded ankyrin/F-box proteins, may also be capable of inhibiting NF- κ B activation.

Previously, we demonstrated that EVM002, EVM154 and EVM165 required a functional F-box domain to mediate interaction with Skp1, and the SCF complex (Figure 3.13). The F-box domain at the C-terminus of EVM002, EVM154 and EVM165 suggests that these ECTV encoded proteins may also inhibit NF- κ B activation through manipulation of the cellular SCF complex. EVM165 is the ortholog of a previously characterized MVA protein named 68k-Ank (1). 68k-Ank interacts with Skp1 and cullin-1 through its F-box domain (13). Additionally, 68k-Ank is a host range factor that mediates MVA infection of non-permissive human and murine cells through promoting late gene transcription (14). EVM154 is the ortholog of VV encoded B4R, an

uncharacterized protein. We recently listed B4R as a potential NF- κ B inhibitor encoded by VV811 (3). Although the large deletion virus, VV811, is missing all known inhibitors of TNF α induced NF- κ B activation, including M2L, K7R, K1L, B14R, and N1L, this virus still inhibits TNF α induced NF- κ B activation, suggesting the presence of additional NF- κ B inhibitors (3). We compiled a list of potential NF- κ B inhibitors that included B4R, through comparison of VV811 to MVA, a virus that induces NF- κ B activation (3, 10, 19).

Regulation of NF- κ B activation by G1R and CPXV006, orthologs of EVM002 encoded by VARV and CPXV, respectively, has been characterized. It was initially observed that G1R interacted with both Skp1 and NF- κ B1/p105 in a yeast two-hybrid screen (8). These data demonstrated that G1R and its orthologs, EVM002, MPXV003 and CPXV006, inhibit the nuclear translocation of p65 and the TNF α induced proteasomal degradation of NF- κ B1/p105 (6, 8). A subsequent paper, published by the same group, characterized the mechanism with which CPXV006 regulates the NF- κ B pathway (9). Cells infected with CPXV- Δ 006, a virus devoid of CPXV006, displayed increased synthesis of pro-inflammatory cytokines, and were unable to prevent the degradation of I κ B α or NF- κ B1/p105 (9). Finally, CPXV006 is a critical virulence factor during infection of C57BL/6 mice (9). These data indicate that the EVM002 ortholog, CPXV006, is a critical regulator of NF- κ B signalling in CPXV, as its deletion renders CPXV susceptible to NF- κ B activation in activated THP1 cells.

However, regulation of NF- κ B activation by CPXV006 has not been linked to its C-terminal F-box domain (9).

We hypothesize that EVM002, EVM154 and EVM165 inhibit NF- κ B activation through manipulation of the cellular SCF ubiquitin ligase, a mechanism dependent on the F-box domain. Here we test the ability of EVM002, EVM154 and EVM165 to inhibit the nuclear accumulation of p65, and compare this with mutant proteins lacking a functional F-box domain. We further explore the mechanisms whereby EVM002 regulates NF- κ B activation.

6.2 ECTV Ankyrin/F-box Proteins Inhibit TNF α and IL-1 β Induced p65 Nuclear Accumulation in an F-box Dependent Manner

We first examined the ability of Flag-EVM002, Flag-EVM154 and Flag-EVM165 to inhibit NF- κ B activation through immunofluorescence analysis of p65 nuclear accumulation. HeLa cells were mock transfected or transfected with pcDNA3-Flag-EVM002, pcDNA3-Flag-EVM005, pcDNA3-Flag-EVM154, and pcDNA3-Flag-EVM165. Cells were untreated or treated with 10ng/ml TNF α for 20 minutes and co-stained with anti-Flag and anti-NF- κ B p65 to visualize the ankyrin/F-box proteins and nuclear accumulation of p65. Unstimulated cells displayed a cytoplasmic staining pattern for p65, following stimulation with TNF α , p65 translocated to the nucleus as expected (Figure 6.1 panels a-f). As shown previously, Flag-EVM005 inhibits TNF α induced p65 nuclear accumulation (Figure 6.1 panels j-l). Additionally, Flag-EVM002, Flag-EVM154

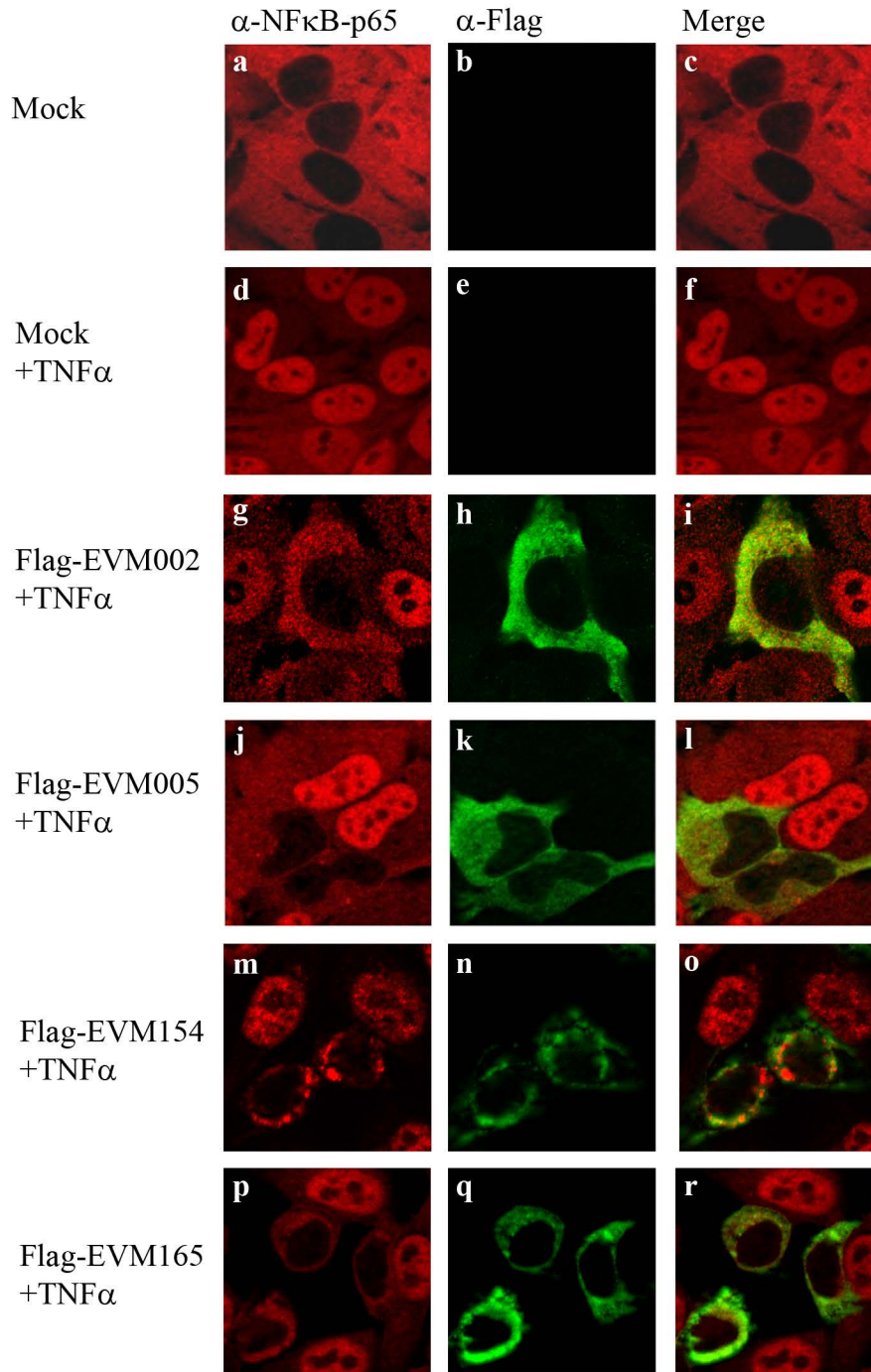


Figure 6.1. All ECTV encoded ankyrin/F-box proteins inhibit TNF α induced p65 nuclear accumulation. HeLa cells were mock transfected or transfected with pcDNA-Flag-EVM002, pcDNA-Flag-EVM005, pcDNA3-Flag-EVM154 or pcDNA3-Flag-EVM165. At 12 hours post transfection cells were treated with 10ng/ml TNF α for 20 minutes. Cells were fixed and stained with anti-Flag to detect the ECTV encoded ankyrin/F-box proteins and anti-NF- κ B-p65. All four ECTV encoded ankyrin/F-box proteins inhibited TNF α induced p65 nuclear accumulation.

and Flag-EVM165, also potently inhibited TNF α induced p65 nuclear accumulation (Figure 6.1 panels g-i and m-r).

We next tested the ability of Flag-EVM002, Flag-EVM154 and Flag-EVM165 to inhibit IL-1 β induced p65 nuclear accumulation. Similar to results from Figure 6.1, expression of EVM002, EVM154 and EVM165 inhibited IL-1 β induced p65 nuclear accumulation (Figure 6.2). Nuclear accumulation of p65 was quantified by counting cells with nuclear p65 from three independent experiments (Figure 6.3). Together, these data suggest that EVM002, EVM154 and EVM165 all inhibit NF- κ B signalling downstream of the IKK complex. IKK activation is the point of conversion of the TNF α and IL-1 β signalling pathways (4). Importantly, degradation of phospho-I κ B α by the SCF ubiquitin ligase falls downstream of IKK activation (4, 16, 18). Therefore, our data support the hypothesis that the ECTV encoded ankyrin/F-box proteins regulate NF- κ B activation through manipulation of the SCF complex.

To test whether or not the C-terminal F-box domain was essential for the inhibition of NF- κ B activation, we constructed F-box deletion mutants for EVM002, EVM154 and EVM165 (Figure 3.2). HeLa cells were transfected with pcDNA3-Flag-EVM002(1-554), pcDNA3-Flag-EVM005(1-593), pcDNA3-Flag-EVM154(F534A/P535A), or pcDNA3-Flag-EVM165(1-566). At 12 hours post transfection, cells were stimulated with TNF α (Figure 6.4) or IL-1 β (Figure 6.5) for 20 minutes. As shown previously, the Flag-EVM005(1-593) mutant failed to inhibit both TNF α and IL-1 β induced p65 nuclear accumulation, demonstrating a dependence on the C-terminal F-box domain and interaction with the SCF

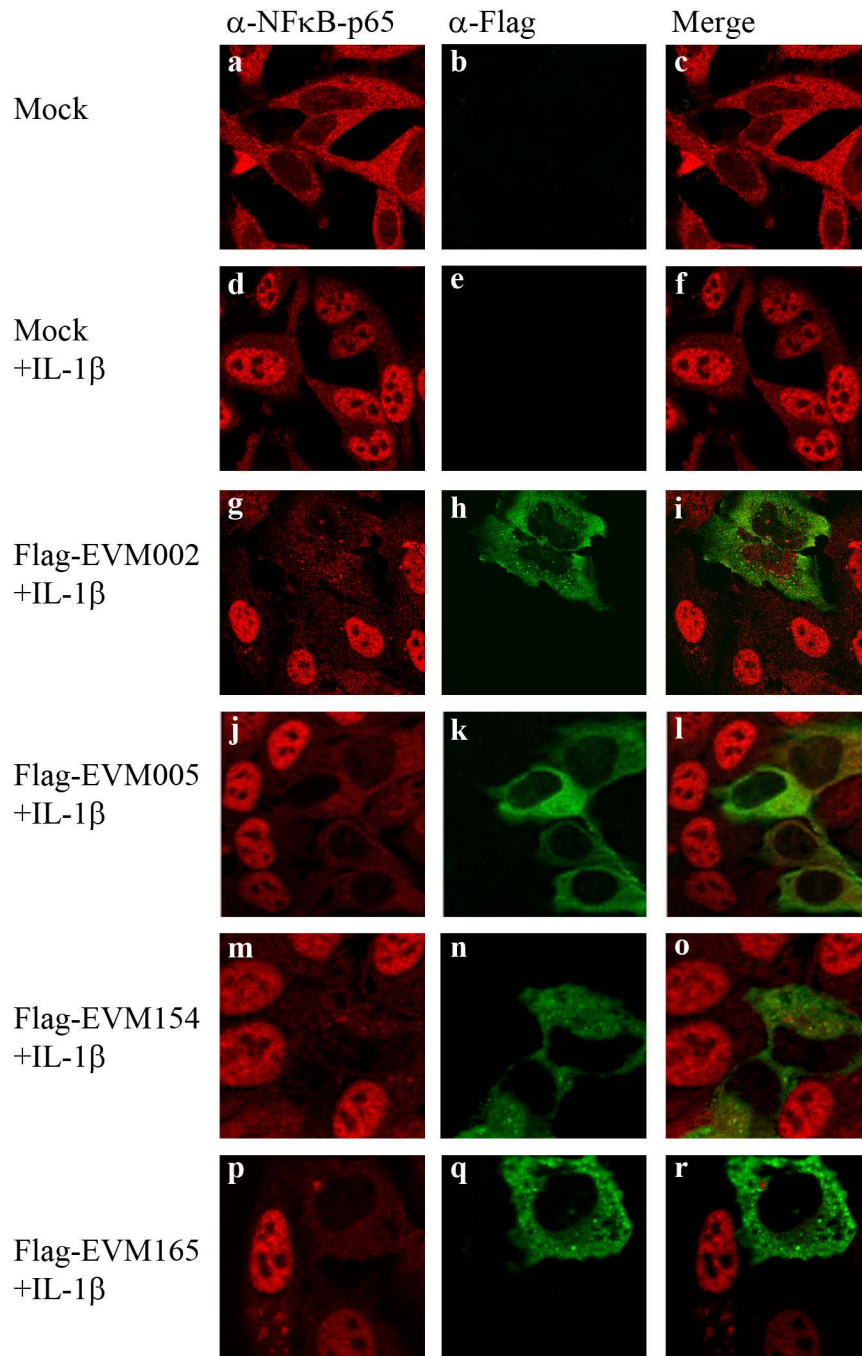


Figure 6.2. All ECTV encoded ankyrin/F-box proteins inhibit IL-1 β induced p65 nuclear accumulation. HeLa cells were mock transfected or transfected with pcDNA-Flag-EVM002, pcDNA-Flag-EVM005, pcDNA3-Flag-EVM154 or pcDNA3-Flag-EVM165. At 12 hours post transfection cells were treated with 10ng/ml IL-1 β for 20 minutes. Cells were fixed and stained with anti-Flag to detect the ECTV encoded ankyrin/F-box proteins and anti-NF- κ B-p65. All four ECTV encoded ankyrin/F-box proteins inhibited IL-1 β induced p65 nuclear accumulation.

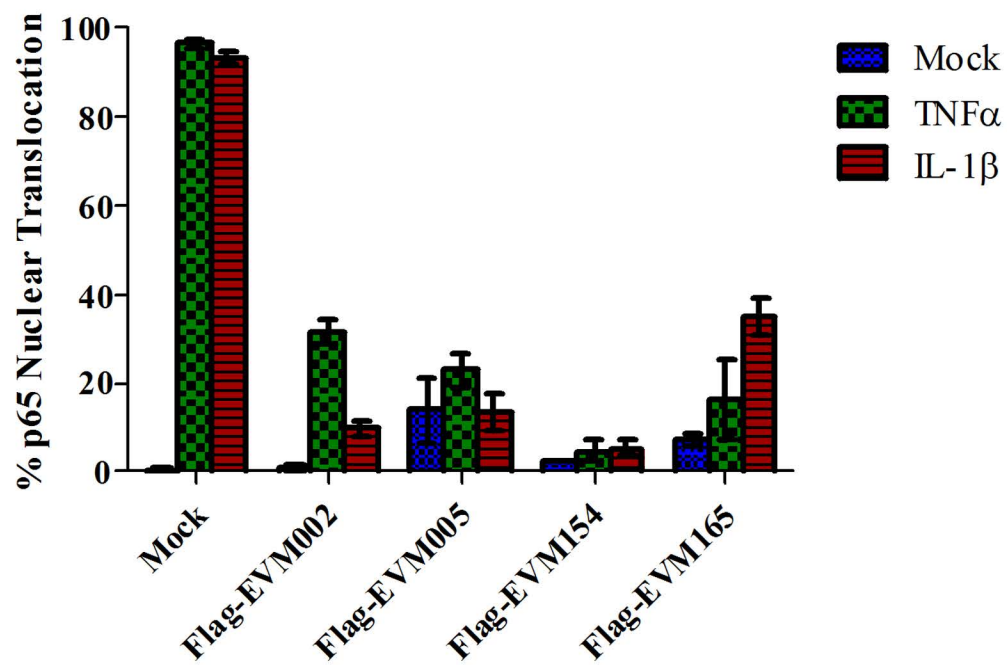


Figure 6.3. Nuclear translocation of p65 in cells expressing the ECTV encoded ankyrin/F-box proteins. The data presented in Figures 6.1 and 6.2 were repeated in triplicate in three independent experiments. The mean number of cells displaying a nuclear staining pattern for p65 was calculated and presented with standard errors. All four of the ECTV encoded ankyrin/F-box proteins inhibit TNF α and IL-1 β induced p65 nuclear accumulation.

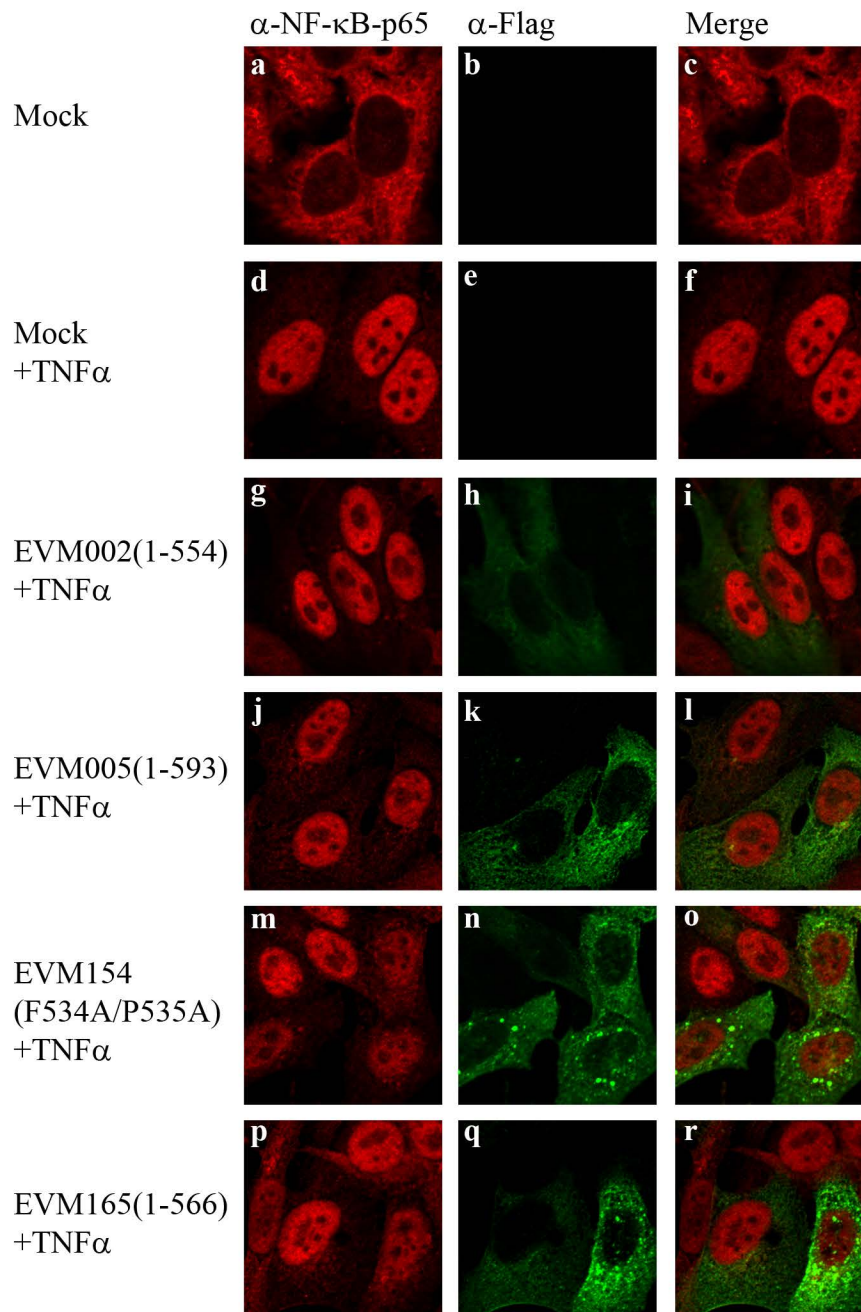


Figure 6.4. All ECTV encoded ankyrin/F-box proteins require an F-box domain to inhibit TNF α induced p65 nuclear accumulation. HeLa cells were mock transfected or transfected with pcDNA-Flag-EVM002(1-554), pcDNA-Flag-EVM005(1-593), pcDNA3-Flag-EVM154(F534A/P535A) or pcDNA3-Flag-EVM165(1-566). At 12 hours post transfection cells were treated with 10ng/ml TNF α for 20 minutes. Cells were fixed and stained with anti-Flag, to detect the ankyrin/F-box proteins, and anti-NF- κ B-p65, to detect p65. All four ECTV encoded ankyrin/F-box mutants failed to inhibit TNF α induced p65 nuclear accumulation.

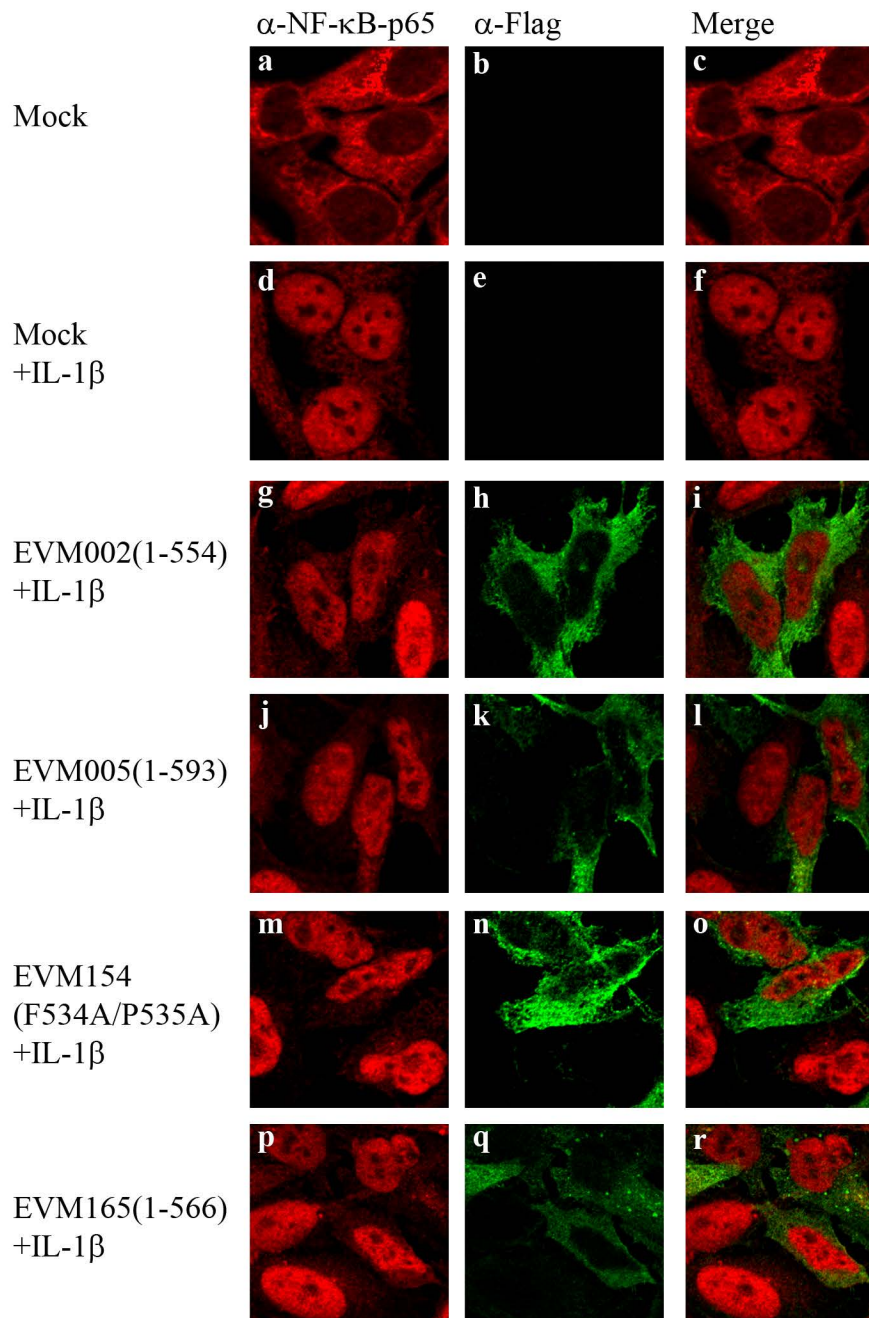


Figure 6.5. All ECTV encoded ankyrin/F-box proteins require an F-box domain to inhibit IL-1 β induced p65 nuclear accumulation. HeLa cells were mock transfected or transfected with pcDNA-Flag-EVM002(1-554), pcDNA-Flag-EVM005(1-593), pcDNA3-Flag-EVM154(F534A/P535A) or pcDNA3-Flag-EVM165(1-566). At 12 hours post transfection cells were treated with 10ng/ml IL-1 β for 20 minutes. Cells were fixed and stained with anti-Flag, to detect the ankyrin/F-box proteins, and anti-NF- κ B-p65, to detect p65. All four ECTV encoded ankyrin/F-box mutants failed to inhibit IL-1 β induced p65 nuclear accumulation.

complex in order to inhibit p65 nuclear translocation (Figures 6.4 panel j-l and 6.5 panel j-l). Likewise, Flag-EVM002(1-554), Flag-EVM154 (F534A/P535A) and Flag-EVM165(1-566) all failed to inhibit TNF α and IL-1 β induced p65 nuclear accumulation (Figures 6.4 panel g-l and m-r and 6.5 panel g-i and m-r). Nuclear accumulation of p65 was quantified by counting cells with nuclear p65 from three independent experiments (Figure 6.6). These data were consistent with the hypothesis that the ECTV encoded ankyrin/F-box proteins inhibited NF- κ B activation through manipulation of the cellular SCF complex. However, we cannot rule out the possibility that each of these proteins is targeting a unique signalling molecule for ubiquitin mediated degradation that lies upstream of p65 nuclear accumulation and downstream of activation of the IKK complex.

6.3 Flag-EVM002 Inhibits I κ B α Degradation in an F-box Dependent Manner

We chose to further characterize the mechanism of EVM002 NF- κ B regulation by investigating the inhibition of I κ B α degradation. To test whether EVM002 inhibited I κ B α degradation, HeLa cells were mock transfected or transfected with pcDNA3-Flag-EVM002 or pcDNA3-Flag-EVM002(1-554), a mutant lacking the F-box domain, and assayed I κ B α degradation by flow cytometry. Unstimulated cells demonstrated physiological levels of I κ B α that were significantly decreased following TNF α or IL-1 β stimulation (Figure 6.7 a and d). Pre-treatment of HeLa cells with the proteasome inhibitor MG132, and subsequent TNF α or IL-1 β treatment, inhibited the degradation of I κ B α as expected (Figure 6.7 a and d). At 24 hours post-transfection, cells were stimulated with TNF α or IL-1 β , fixed and

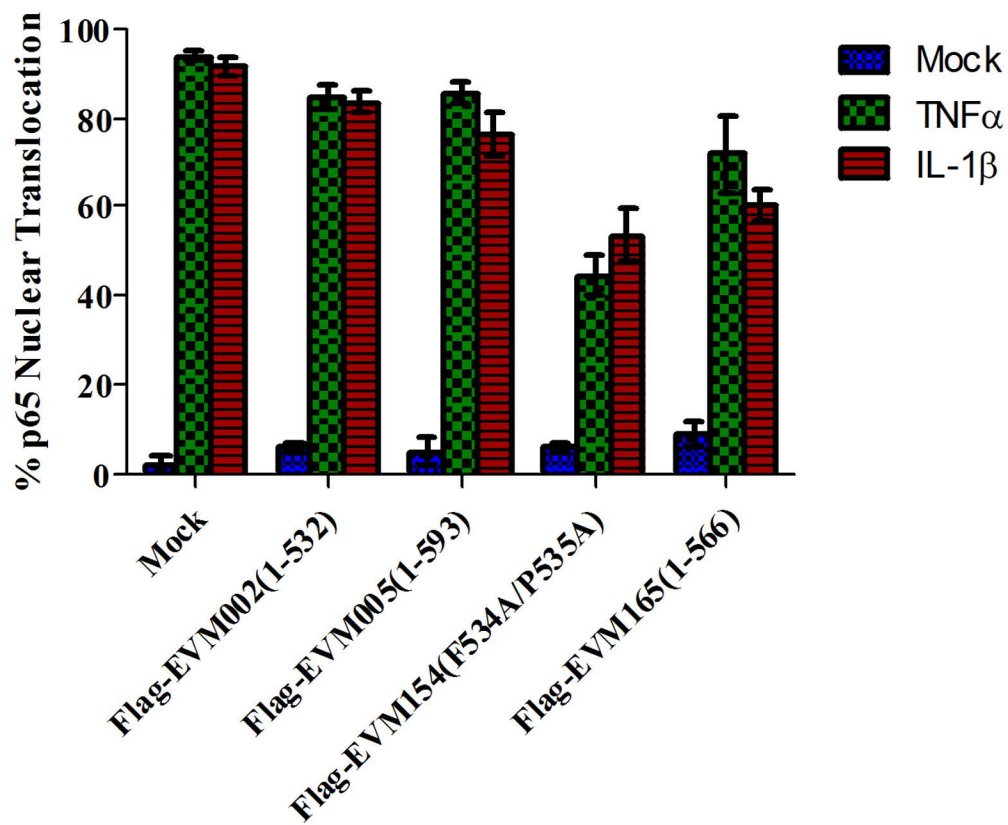


Figure 6.6. Nuclear translocation of p65 in cells expressing the ECTV encoded ankyrin/F-box proteins with truncated or mutated F-box domains. The data presented in Figures 6.4 and 6.5 were repeated in triplicate in three independent experiments. The mean number of cells displaying a nuclear staining pattern for p65 was calculated and presented with standard errors. All four of the ECTV encoded ankyrin/F-box proteins required a function F-box domain in order to inhibit TNF α and IL-1 β induced p65 nuclear accumulation.

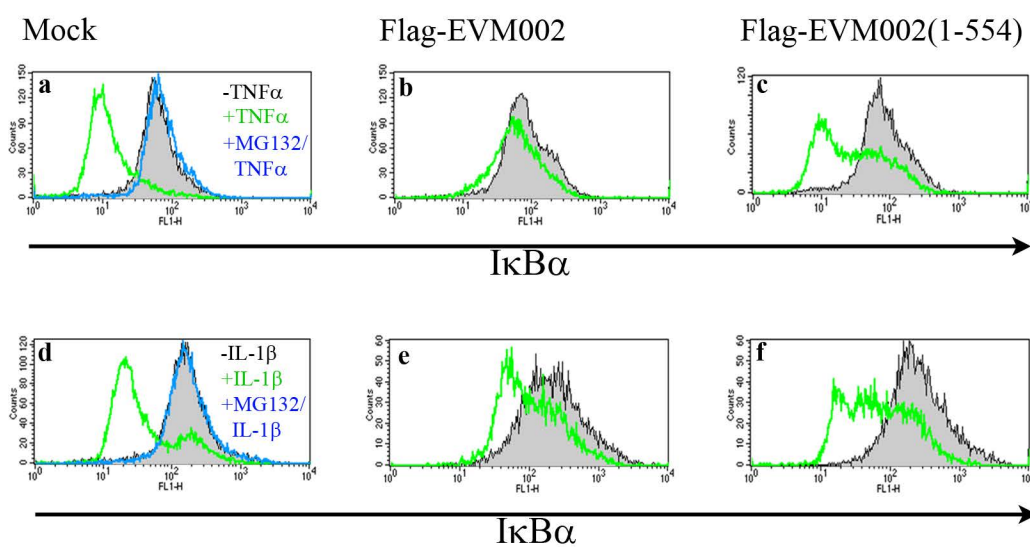


Figure 6.7. Flag-EVM002 inhibits the degradation of $\text{I}\kappa\text{B}\alpha$ in an F-box dependent manner. HeLa cells were mock transfected or transfected with pcDNA-Flag-EVM002 or pcDNA-Flag-EVM002(1-554) lacking the F-box. Mock cells were untreated or pre-treated with $10\mu\text{M}$ MG132 for one hour as a positive control for inhibition of $\text{I}\kappa\text{B}\alpha$ degradation. At 18 hours post transfection, cells were stimulated with 10ng/ml $\text{TNF}\alpha$ (panels a-c) or 10ng/ml $\text{IL-1}\beta$ (panels d-f) for 20 minutes. Cells were co-stained with anti-Flag and anti- $\text{I}\kappa\text{B}\alpha$, and analyzed by flow cytometry. Flag-positive populations were gated for analysis and $\text{I}\kappa\text{B}\alpha$ fluorescence was measured on the x-axis.

stained with anti-Flag and anti-I κ B α to detect EVM002 and I κ B α , respectively, and Flag-positive cells were gated for analysis. Expression of Flag-EVM002(1-554), which lacks the F-box domain, was unable to stabilize I κ B α resulting in significant degradation of I κ B α (Figure 6.7 c and f). Data demonstrated that cells expressing full length Flag-EVM002 inhibited both TNF α and IL-1 β induced I κ B α degradation (Figure 6.7 panels b and e). Alternatively, cells expressing Flag-EVM002(1-554) were unable to inhibit the proteasomal degradation of I κ B α (Figure 6.7 panels c and f). These data were consistent with our previous results, and suggested that EVM002 required the C-terminal F-box domain in order to inhibit TNF α and IL-1 β induced p65 nuclear accumulation and I κ B α degradation.

6.4 ECTV- Δ 002 Inhibits NF- κ B Activation

We next used the ECTV- Δ 002 virus to investigate the contribution of EVM002 to the overall inhibition of NF- κ B activation during ECTV infection. ECTV- Δ 002 is a marker-free knockout virus constructed using the SEM cloning system (Chapter 4)(11). HeLa cells were mock infected or infected with ECTV or ECTV- Δ 002 at a MOI of 5. At 12 hours post infection cells were treated with 10ng/ml TNF α and nuclear and cytoplasmic extracts were analyzed by western blot for p65 nuclear accumulation. Unstimulated HeLa cells displayed little p65 in the nuclear fraction, as expected (Figure 6.8A). Mock infected cells treated with TNF α displayed an increase in the level of p65 in nuclear fraction as expected (Figure 6.8A). In contrast, cells infected with both ECTV and ECTV- Δ 002 inhibited p65 nuclear accumulation following TNF α stimulation (Figure 6.9A). These

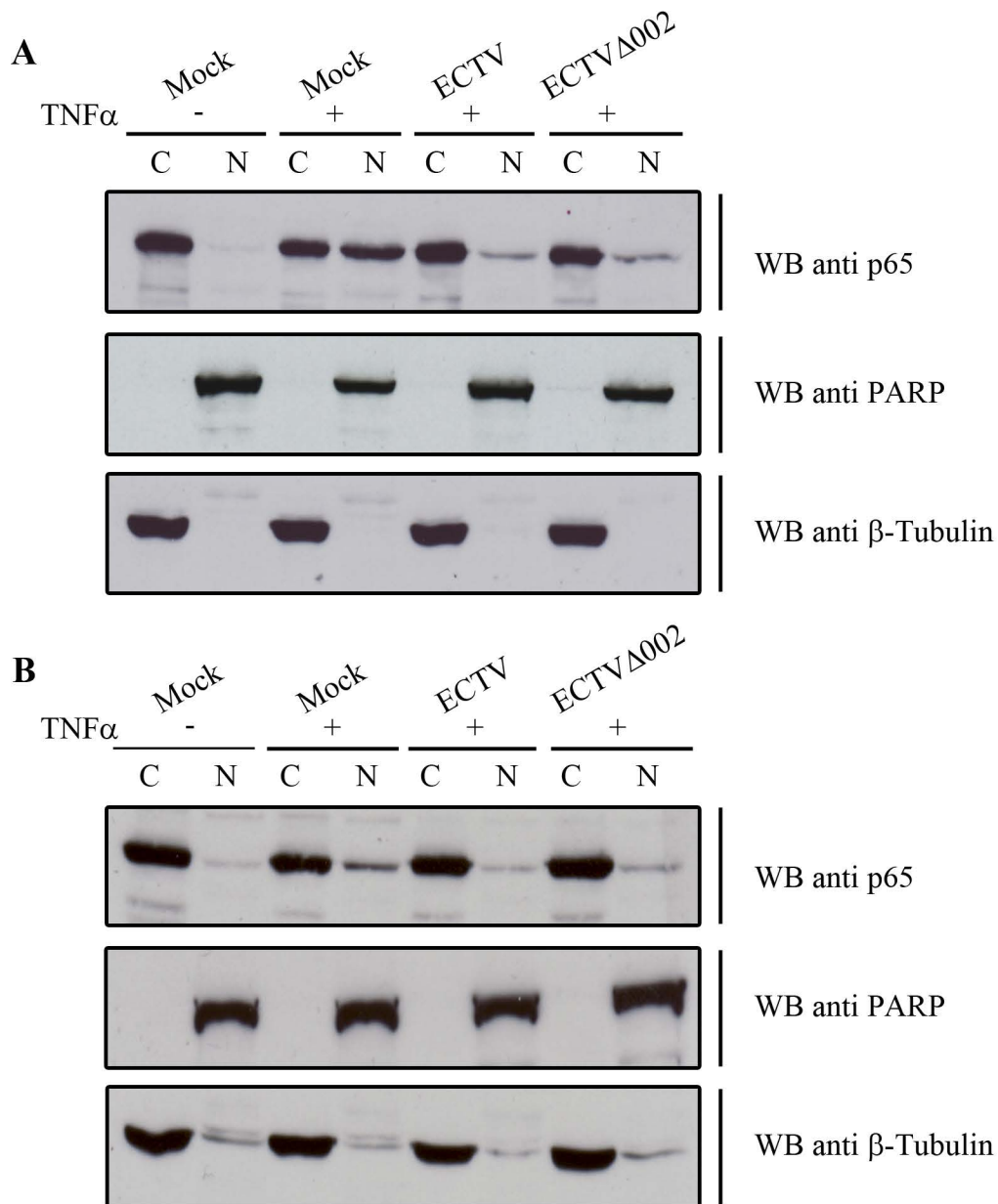


Figure 6.8. ECTV- Δ 002 inhibits p65 nuclear accumulation. **A.** HeLa cells were mock infected or infected with ECTV or ECTV- Δ 002 at a MOI of 5. At 12 hours post infection, cells were stimulated with 10ng/ml TNF α for 20 minutes, and nuclear and cytoplasmic extracts were generated. **B.** MEF cells were mock infected or infected with ECTV or ECTV- Δ 002 at a MOI of 5. At 12 hours post infection, cells were stimulated with 10ng/ml TNF α for 20 minutes, and nuclear and cytoplasmic extracts were generated. Protein samples were separated by SDS-PAGE and western blotted with anti-p65, anti- β -tubulin, and anti-PARP.

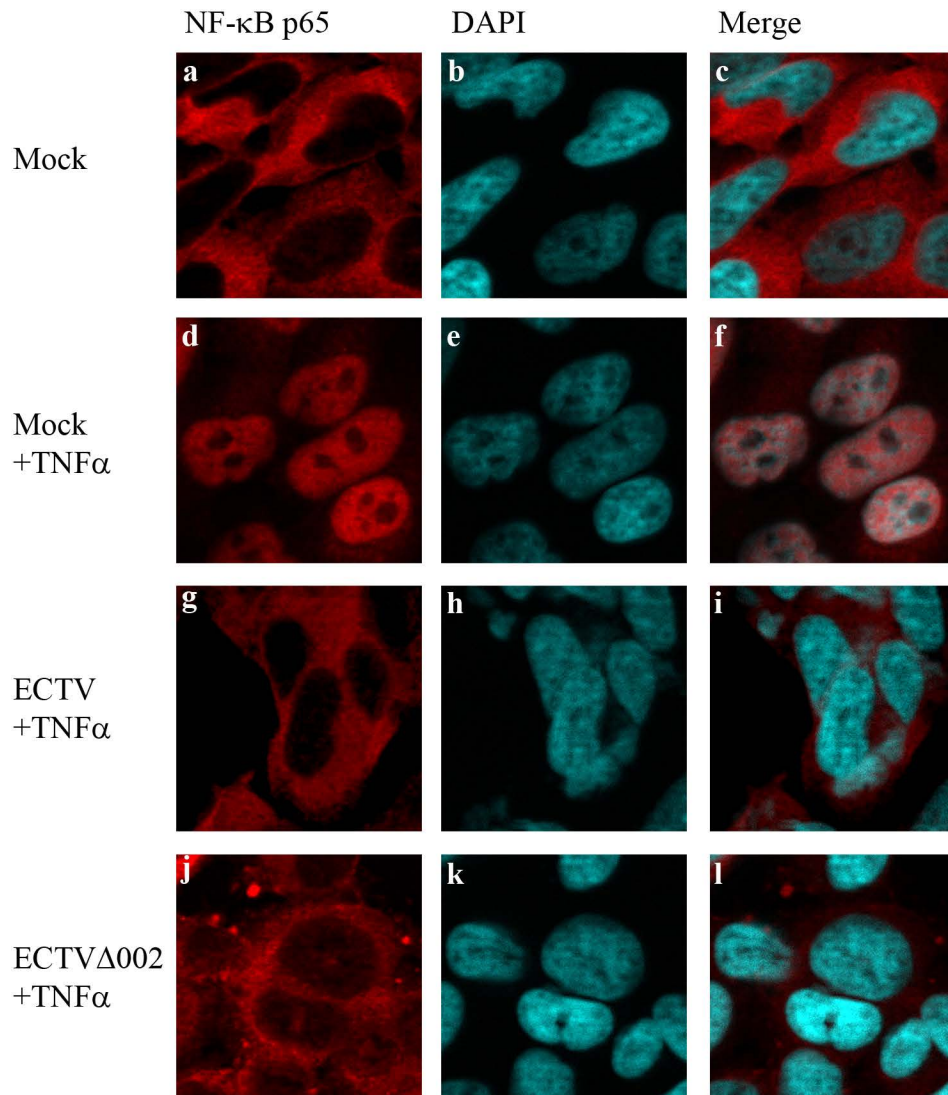


Figure 6.9. ECTV- Δ 002 inhibits p65 nuclear accumulation following TNF α stimulation. HeLa cells were mock infected or infected with ECTV or ECTV- Δ 002 at a MOI of 5. At 12 hours post infection, cells were stimulated with 10ng/ml TNF α for 20 minutes, fixed and stained with anti-p65 and DAPI and cells were visualized by immunofluorescence. ECTV- Δ 002 is still capable of inhibiting the nuclear accumulation of p65.

experiments were repeated in MEF cells to test whether these mouse specific viruses also inhibited p65 nuclear accumulation in mouse cells (Figure 6.8B).

Nuclear translocation of p65 during ECTV infection was also investigated by immunofluorescence. HeLa cells were mock infected or infected with ECTV or ECTV- Δ 002. Unstimulated HeLa cells demonstrated cytoplasmic staining for p65 that became nuclear following TNF α stimulation (Figure 6.9 panels a-f). Cells infected with either ECTV or ECTV- Δ 002 inhibited p65 nuclear accumulation following TNF α stimulation (Figure 6.9 panels g-l). These data are similar to ECTV- Δ 005 data in Chapter 5, suggesting that deletion of more than one of the ankyrin/F-box proteins may be necessary to render ECTV susceptible to TNF α mediated NF- κ B activation.

Next, we assessed the downstream synthesis of NF- κ B regulated transcripts following TNF α stimulation in cells infected with ECTV or ECTV- Δ 002. HeLa cells were mock infected or infected with ECTV or ECTV- Δ 002 at a MOI of 5. At 12 hours post infection, cells were stimulated with 10ng/ml TNF α and total cellular and viral RNA samples were collected at 2, 4 and 6 hours post TNF α treatment. RNA was reverse transcribed into cDNA and real time PCR (RT-PCR) was performed to analyze the levels of TNF α , IL-1 β and IL-6 transcripts relative to glyceraldehyde 3-phosphate dehydrogenase (GAPDH) (Figure 6.10 A-C). Mock infected cells stimulated with TNF α produce a spike in transcript levels for TNF α , IL-1 β and IL-6 (Figure 6.10 A-C). In contrast, cells infected with ECTV or ECTV- Δ 002 inhibited the synthesis of TNF α , IL-1 β and

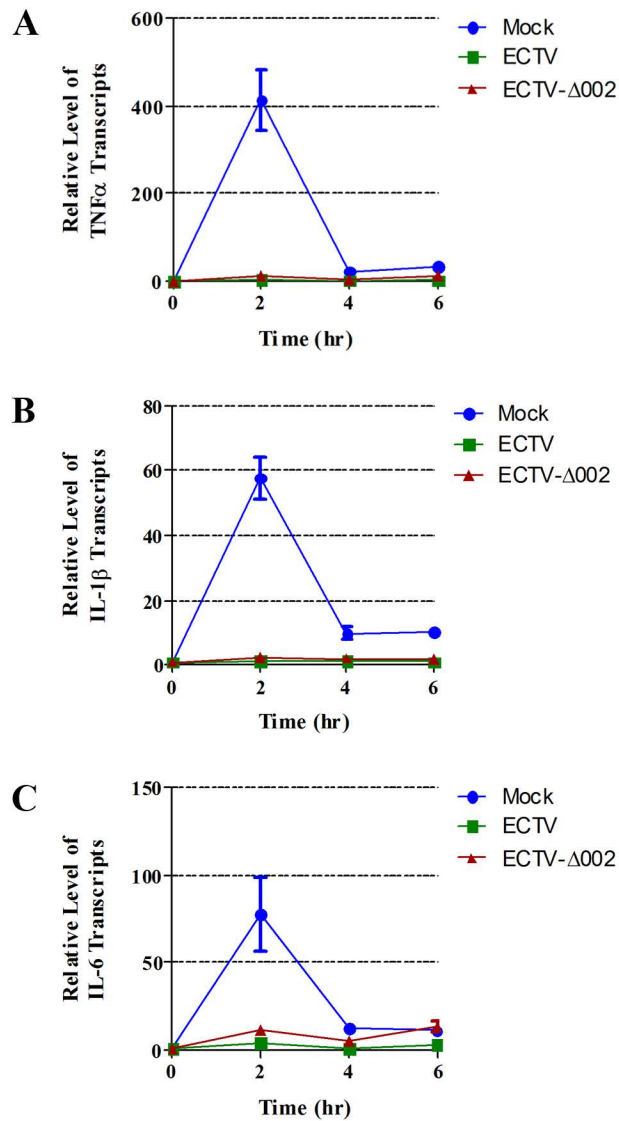


Figure 6.10. ECTV and ECTV-Δ002 inhibit the production of NF-κB regulated transcripts. HeLa cells were mock infected or infected with ECTV or ECTV-Δ002 at a MOI of 5. At 12 hours post infection cells were stimulated with TNFα. RNA samples were collected at 0, 2, 4 and 6 hours post TNFα treatment. Samples were reverse transcribed, followed by real time PCR analysis for relative levels of (A) TNFα, (B) IL-1β, and (C) IL-6 transcripts, as compared to GAPDH. Time courses were performed in triplicate and plotted as the average with standard error.

IL-6 transcripts (Figure 6.10 A-C). These data support our previous findings that cells infected with ECTV and ECTV- Δ 002 inhibited p65 nuclear accumulation.

Finally, we investigated the components associated with I κ B α during infection with ECTV and ECTV- Δ 002. p65 did not translocate to the nucleus following TNF α stimulation in cells infected with ECTV- Δ 002. Therefore, we determined if both p65 and p50 remained associated with the regulatory molecule I κ B α in infected cells. To test this, HeLa cells were mock infected or infected with ECTV or ECTV- Δ 002 at a MOI of 5. At 12 hours post infection, cells were stimulated with TNF α for 20 minutes. Cells were lysed and subjected to immunoprecipitation with anti-I κ B α to determine if I κ B α maintained an interaction with p50 or p65 by western blotting. Mock infected cells immunoprecipitated I κ B α in association with the NF- κ B transcription factors p65 and p50 (Figure 6.11). In contrast, mock infected cells stimulated with TNF α demonstrated loss of I κ B α in both the lysates and the IPs, correlating with loss of p65 and p50 (Figure 6.11). HeLa cells infected with ECTV or ECTV- Δ 002 protected I κ B α from degradation, and therefore I κ B α remained in the lysates and immunoprecipitates, along with p65 and p50 (Figure 6.11). This data supports our earlier data demonstrating that p65 remains in the cytoplasm of ECTV and ECTV- Δ 002 infected cells following TNF α stimulation.

6.5 ECTV- Δ 002-005 Inhibits I κ B α Degradation

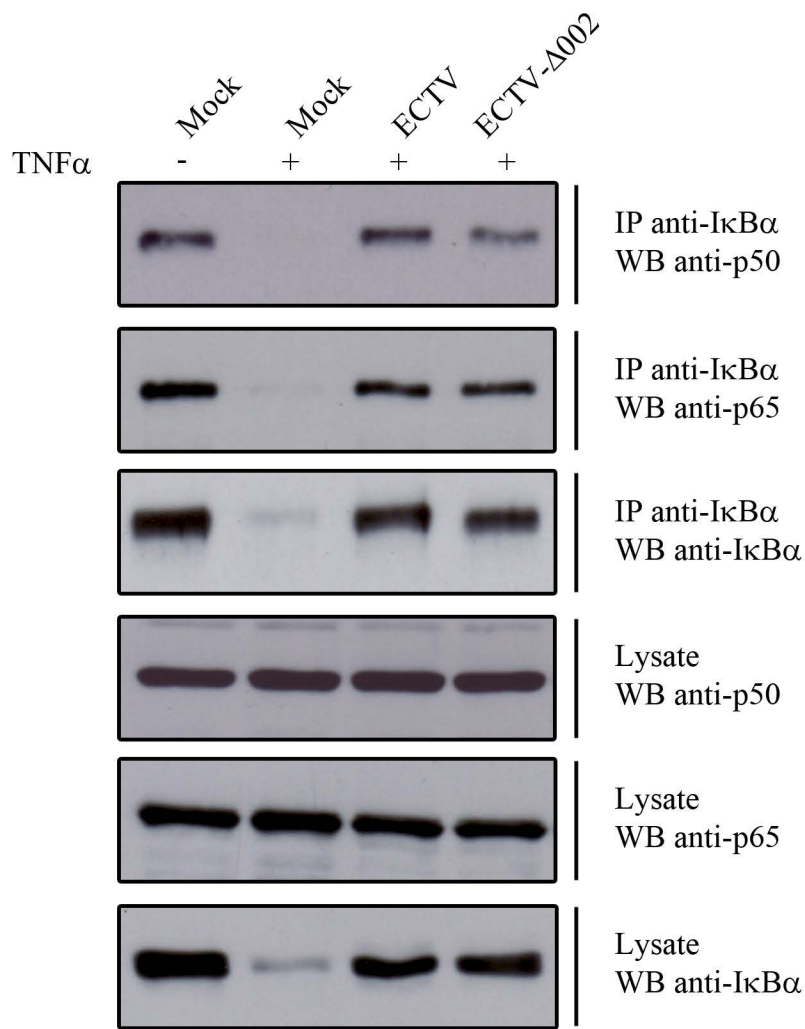


Figure 6.11. ECTV and ECTV-Δ002 infection prevents IκBα-p65/p50 dissociation. HeLa cells were mock infected or infected with ECTV or ECTV-Δ002 for at a MOI of 5. At 12 hours post infection cells were left untreated or treated with 10ng/ml TNFα for 20 minutes. Cells were lysed with 1% NP40 lysis buffer and subjected to immunoprecipitation with anti-IκBα. Immunoprecipitates and lysates were separated by SDS-PAGE and analyzed by western blot analysis with anti-IκBα, anti-NF-κB-p50 and anti-NF-κB-p65.

Both ECTV- Δ 005 and ECTV- Δ 002 inhibited NF- κ B activation, we therefore generated a recombinant virus that lacked EVM002, EVM003, EVM004 and EVM005 using the novel SEM cloning system. We named this virus ECTV- Δ 002-005 (Figure 4.6 and 4.7)(11). The first step was to create a recombinant ECTV lacking EVM002 using the SEM cloning system (11). We inserted the *yfp-gpt* cassette into the EVM002 locus, followed by Cre-mediated excision, to create a marker-free EVM002 knockout virus named ECTV- Δ 002. Next, we inserted the *yfp-gpt* cassette into the EVM005 locus of ECTV- Δ 002 to produce a YFP-GPT expressing double knockout. Infection of U20S-Cre cells resulted in excision of EVM002 and EVM005, as well as the intergenic sequence including the vTNFR, EVM003, and the BTB-only protein, EVM004 (Figure 4.6 and 4.7). EVM003 is located in the ITR region of the ECTV genome and is expressed from the right-hand end of the genome. However, this virus lacks EVM004, and hence, any phenotype that presents during infection with ECTV- Δ 002-005 could potentially be due to the absence of EVM002, EVM004 or EVM005, but not EVM003.

We investigated the proteasomal degradation of I κ B α in cells infected with ECTV, ECTV- Δ 002, ECTV- Δ 005 or ECTV- Δ 002-005, to determine if a virus lacking two ankyrin/F-box proteins was rendered susceptible to NF- κ B activation. HeLa cells were mock infected or infected with ECTV, ECTV- Δ 002, ECTV- Δ 005 or ECTV- Δ 002-005 at a MOI of 5. Mock infected cells demonstrated proteasomal degradation of I κ B α following TNF α stimulation, as shown by a leftward shift on the histogram, that was inhibited by pretreatment

with the proteasome inhibitor MG132 (Figure 6.12A panel a). HeLa cells infected with ECTV, ECTV- Δ 002 or ECTV- Δ 005 inhibited TNF α induced I κ B α degradation (Figure 6.12A panels b-d). These data support earlier data suggesting that ECTV- Δ 002 inhibits TNF α induced p65 nuclear accumulation and NF- κ B transcript synthesis. Additionally, cells infected with ECTV- Δ 002-005, a virus lacking EVM002 and EVM005, two inhibitors of NF- κ B activation, were still capable of inhibiting TNF α induced I κ B α degradation (Figure 12A panel e). To test for infection in each of our samples, infected HeLa cells were harvested and stained for the early protein I3L (Figure 12A panels f-j). The mean fluorescent intensity for three independent experiments was calculated to quantify I κ B α degradation (Figure 12B). In order to render ECTV susceptible to NF- κ B activation, these data suggest that it will be necessary to delete additional NF- κ B inhibitors, likely including the other ankyrin/F-box proteins, EVM154 and EVM165.

6.6 Discussion

The list of known NF- κ B inhibitors encoded by ECTV continues to grow with the addition of four encoded ankyrin/F-box proteins (7). EVM002, EVM005, EVM154 and EVM165 all contain N-terminal ankyrin repeats and C-terminal F-box domains that mediate binding to Skp1, the linker protein of the cellular SCF ubiquitin ligase (Figure 3.13)(12, 17). We demonstrate that each of the four ankyrin/F-box proteins require the C-terminal F-box domain to bind the SCF complex and inhibit NF- κ B activation (Figure 6.1 to 6.6). The data support a

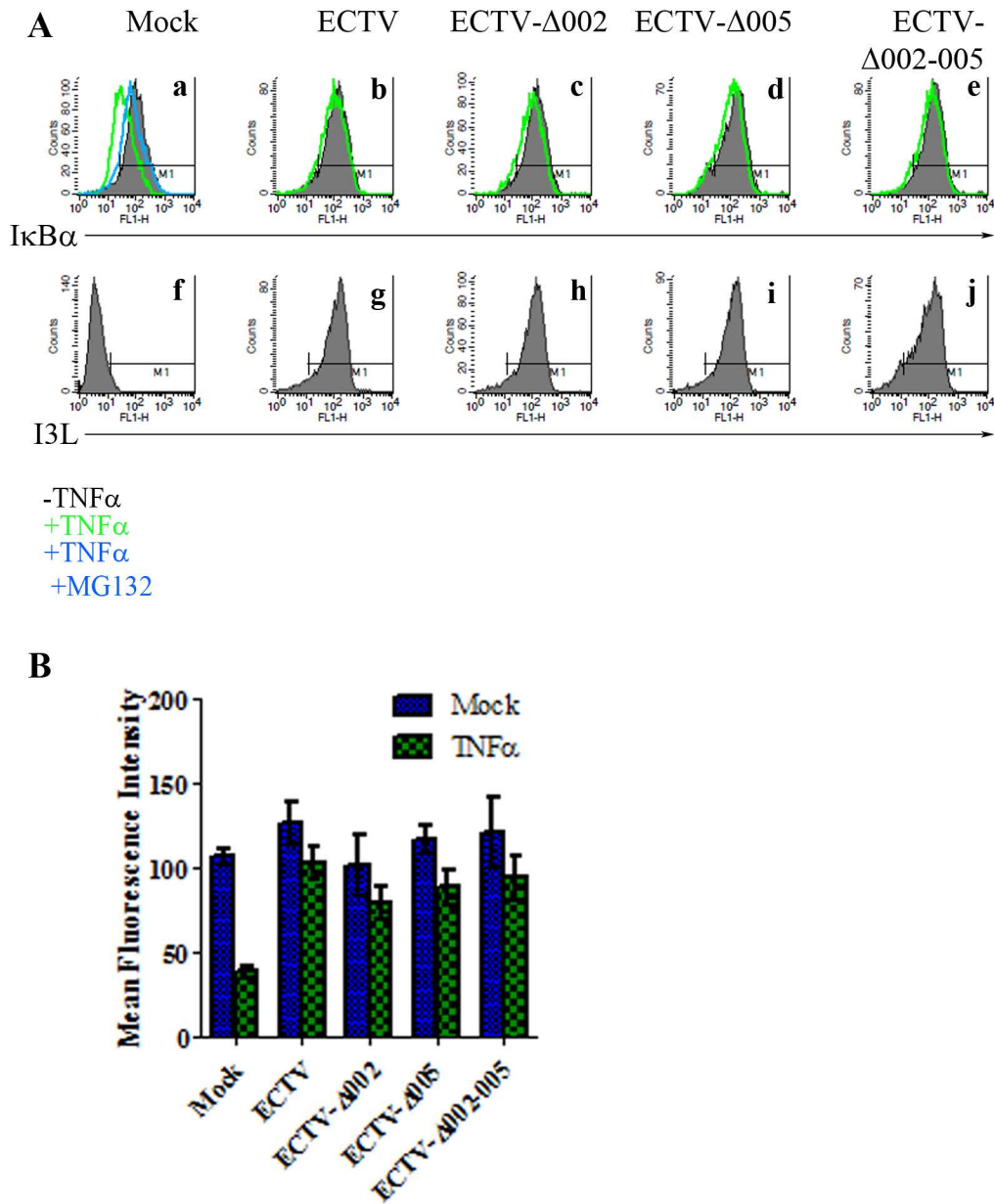


Figure 6.12. ECTV- Δ 002 and ECTV- Δ 002-005 inhibit TNF α induced I κ B α degradation. **A.** HeLa cells were mock infected or infected with ECTV, ECTV- Δ 002, ECTV- Δ 005, or ECTV- Δ 002-005 at a MOI of 5. At 12 hours post infection, mock infected cells were stimulated with 10 μ M MG132 for 1 hour as a control. Samples were then stimulated with 10ng/ml TNF α for 20 minutes. Cells were harvested, fixed and stained with anti-I κ B α or anti-I3L and analyzed by flow cytometry using a FACScalibur flow cytometer. **B.** The mean fluorescence intensities from three independent experiments have been plotted with standard error measurements.

model in which the ankyrin/F-box proteins are hijacking the SCF complex during infection, preventing ubiquitylation and degradation of its normal targets, including phospho-I κ B α (5, 15, 18). This mechanism is similar to that of HIV encoded Vpu, which binds β -TRCP to inhibit I κ B α degradation (2). We hypothesized that the ankyrin/F-box proteins function as substrate adaptors for the SCF complex during infection, each recruiting a unique set of substrates for ubiquitylation. To determine whether NF- κ B inhibition is simply a beneficial side effect of viral manipulation of the SCF complex, or whether the ankyrin/F-box proteins specifically target the NF- κ B pathway will depend on identification of their individual target substrates.

Further characterization of EVM002 determined that EVM002 inhibited I κ B α degradation in an F-box-dependent manner following TNF α and IL-1 β stimulation. Interestingly, EVM002 did not protect cells against IL-1 β stimulated I κ B α degradation as efficiently as EVM005, suggesting that some differences exist between the four ankyrin/F-box proteins (Figure 6.7). We also determined that ECTV- Δ 002 inhibited I κ B α degradation, p65 nuclear accumulation and the synthesis of NF- κ B regulated transcripts (Figure 6.8, 6.9 and 6.10). This data was not surprising in that ECTV- Δ 002 encodes multiple inhibitors of NF- κ B activation, including EVM005. However, these data contrast with published results demonstrating that CPXV- Δ 006, a CPXV strain devoid of the EVM002 ortholog, was rendered susceptible to NF- κ B activation and I κ B α degradation. It is still unclear why CPXV- Δ 006 is incapable of NF- κ B inhibition. This virus encodes a large array of NF- κ B inhibitors, including CPXV011, the EVM005

ortholog. Even though we show that ECTV- Δ 002 is not susceptible to NF- κ B activation in tissue culture, it may have increased susceptibility to NF- κ B activation in a mouse model or in an alternative cell line. Future analysis of ECTV- Δ 002 *in vivo* could aid in the understanding the differences observed between ECTV- Δ 002 and CPXV- Δ 006. Additionally, ECTV- Δ 002-005, which lacks two ankyrin/F-box proteins inhibit NF- κ B activation, was still protective against TNF α induced I κ B α degradation in HeLa cells (Figure 6.12). These data suggest that deletion of multiple genes in addition to EVM002 and EVM005 will be necessary to render ECTV susceptible to NF- κ B activation.

Although previous data indicates mechanisms whereby EVM002 binds NF- κ B1/p105 and inhibits NF- κ B activation through non-canonical pathways (8, 9), all data presented in this chapter investigates canonical NF- κ B activation cascade. We have attempted to investigate the role of EVM002 in regulation of p105 processing but were unsuccessful in repeating these experiments, and therefore could not perform further investigations into mechanism. Upon transfection of HEK293 cells with pcDNA3-Flag-EVM002 and stimulation with TNF α , we were unable to observe protection against proteasomal degradation of p105. This could perhaps be due to differences in transfection efficiency. We have observed roughly 20% transfection efficiency with our Flag-EVM002 construct, leaving 80% of cells in each sample susceptible to TNF α induced p105 degradation. This transfection efficiency may not be high enough to observe the protective effects demonstrated by the McFadden laboratory (8). Additionally,

this is the first demonstration that a member of the EVM002 family of orthologs requires a functional F-box domain to regulate the NF- κ B pathway.

Finally, we have noticed that β -TRCP is degraded during ECTV infection, however the viral protein responsible for this degradation is not known (data not shown). The degradation of β -TRCP during ECTV infection could make a major contribution to the inhibition of NF- κ B activation, as I κ B α appears to be phosphorylated but not degraded in ECTV infected cells. These data are preliminary, but β -TRCP degradation appears to occur during ECTV and CPXV infection, but not VV infection, suggesting that an ORF encoded by ECTV and CPXV but absent from VV is responsible. EVM002 and EVM005 fit these criteria, but preliminary investigations suggest that neither of these proteins contribute to β -TRCP degradation. Other signalling proteins including p50/105, p65, and I κ B α are not degraded during ECTV infection.

6.7 References

1. **Barry, M., N. van Buuren, K. Burles, K. Mottet, Q. Wang, and A. Teale.** 2010. Poxvirus exploitation of the ubiquitin-proteasome system. *Viruses* **2**:2356-80.
2. **Besnard-Guerin, C., N. Belaidouni, I. Lassot, E. Segeral, A. Jobart, C. Marchal, and R. Benarous.** 2004. HIV-1 Vpu sequesters beta-transducin repeat-containing protein (betaTrCP) in the cytoplasm and provokes the accumulation of beta-catenin and other SCFbetaTrCP substrates. *J Biol Chem* **279**:788-95.
3. **Fagan-Garcia, K., and M. Barry.** 2011. A vaccinia virus deletion mutant reveals the presence of additional inhibitors of NF-kappaB. *J Virol* **85**:883-94.
4. **Hayden, M. S., and S. Ghosh.** 2008. Shared principles in NF-kappaB signaling. *Cell* **132**:344-62.

5. **Karin, M., and Y. Ben-Neriah.** 2000. Phosphorylation meets ubiquitination: the control of NF-[kappa]B activity. *Annu Rev Immunol* **18**:621-63.
6. **Lang, V., J. Janzen, G. Z. Fischer, Y. Soneji, S. Beinke, A. Salmeron, H. Allen, R. T. Hay, Y. Ben-Neriah, and S. C. Ley.** 2003. betaTrCP-mediated proteolysis of NF-kappaB1 p105 requires phosphorylation of p105 serines 927 and 932. *Mol Cell Biol* **23**:402-13.
7. **Mohamed, M. R., and G. McFadden.** 2009. NFkB inhibitors: strategies from poxviruses. *Cell Cycle* **8**:3125-32.
8. **Mohamed, M. R., M. M. Rahman, J. S. Lanchbury, D. Shattuck, C. Neff, M. Dufford, N. van Buuren, K. Fagan, M. Barry, S. Smith, I. Damon, and G. McFadden.** 2009. Proteomic screening of variola virus reveals a unique NF-kappaB inhibitor that is highly conserved among pathogenic orthopoxviruses. *Proc Natl Acad Sci U S A* **106**:9045-50.
9. **Mohamed, M. R., M. M. Rahman, A. Rice, R. W. Moyer, S. J. Werden, and G. McFadden.** 2009. Cowpox virus expresses a novel ankyrin repeat NF-kappaB inhibitor that controls inflammatory cell influx into virus-infected tissues and is critical for virus pathogenesis. *J Virol* **83**:9223-36.
10. **Oie, K. L., and D. J. Pickup.** 2001. Cowpox virus and other members of the orthopoxvirus genus interfere with the regulation of NF-kappaB activation. *Virology* **288**:175-87.
11. **Rintoul, J. L., J. Wang, D. B. Gammon, N. J. van Buuren, K. Garson, K. Jardine, M. Barry, D. H. Evans, and J. C. Bell.** 2011. A selectable and excisable marker system for the rapid creation of recombinant poxviruses. *PLoS One* **6**:e24643.
12. **Schulman, B. A., A. C. Carrano, P. D. Jeffrey, Z. Bowen, E. R. Kinnucan, M. S. Finnin, S. J. Elledge, J. W. Harper, M. Pagano, and N. P. Pavletich.** 2000. Insights into SCF ubiquitin ligases from the structure of the Skp1-Skp2 complex. *Nature* **408**:381-6.
13. **Sperling, K. M., A. Schwantes, B. S. Schnierle, and G. Sutter.** 2008. The highly conserved orthopoxvirus 68k ankyrin-like protein is part of a cellular SCF ubiquitin ligase complex. *Virology* **374**:234-9.
14. **Sperling, K. M., A. Schwantes, C. Staib, B. S. Schnierle, and G. Sutter.** 2009. The orthopoxvirus 68-kilodalton ankyrin-like protein is essential for DNA replication and complete gene expression of modified vaccinia virus Ankara in nonpermissive human and murine cells. *J Virol* **83**:6029-38.
15. **Suzuki, H., T. Chiba, M. Kobayashi, M. Takeuchi, T. Suzuki, A. Ichiyama, T. Ikenoue, M. Omata, K. Furuichi, and K. Tanaka.** 1999. I kappa B alpha ubiquitination is catalyzed by an SCF-like complex containing Skp1, cullin-1, and two F-box/WD40-repeat proteins, betaTrCP1 and betaTrCP2. *Biochem Biophys Res Commun* **256**:127-32.
16. **Traenckner, E. B., H. L. Pahl, T. Henkel, K. N. Schmidt, S. Wilk, and P. A. Baeuerle.** 1995. Phosphorylation of human I kappa B-alpha on

- serines 32 and 36 controls I kappa B-alpha proteolysis and NF-kappa B activation in response to diverse stimuli. *EMBO J* **14**:2876-83.
17. **van Buuren, N., B. Couturier, Y. Xiong, and M. Barry.** 2008. Ectromelia virus encodes a novel family of F-box proteins that interact with the SCF complex. *J Virol* **82**:9917-27.
 18. **Winston, J. T., P. Strack, P. Beer-Romero, C. Y. Chu, S. J. Elledge, and J. W. Harper.** 1999. The SCFbeta-TRCP-ubiquitin ligase complex associates specifically with phosphorylated destruction motifs in IkappaBalpha and beta-catenin and stimulates IkappaBalpha ubiquitination in vitro. *Genes Dev* **13**:270-83.
 19. **Wyatt, L. S., P. L. Earl, L. A. Eller, and B. Moss.** 2004. Highly attenuated smallpox vaccine protects mice with and without immune deficiencies against pathogenic vaccinia virus challenge. *Proc Natl Acad Sci U S A* **101**:4590-5.

Chapter 7: Discussion

7.1 Poxviral Ankyrin/F-box Proteins

Poxvirus encoded ankyrin repeat proteins represent one of the largest families of proteins encoded by poxviruses. The ankyrin repeat consists of a 33 amino acid helix-loop-helix motif with a highly conserved amino acid sequence (52). Ankyrin repeats were first identified in a cellular protein called ankyrin, which contains 24 of these repeats and functions in the cytoskeleton (33). Specifically, ankyrin is required for the maturity of red blood cells during erythropoiesis through formation of membranes structures (2, 28). Since its discovery, the ankyrin repeat has been characterized in a wide variety of cellular proteins, and typically mediates unique protein-protein interactions. All but one family of poxviruses, the molluscipox viruses, encode a large repertoire of ankyrin repeat proteins; the largest family is comprised of 51 ankyrin repeat proteins encoded by canarypox virus, representing 21% of its genome (3, 37, 63). Poxviral ankyrin repeat proteins are large proteins, ranging from 400-650 amino acids in length, containing between 5-10 ankyrin repeats located at their N-termini. Although the poxviral ankyrin repeat proteins contain no obvious structural domains at their C-termini, many of the proteins display a conserved sequence, which, upon closer inspection was shown to resemble the F-box domain (37). This poxviral F-box-like domain was later named PRANC (pox protein repeat of ankyrin C-terminus – referred to as F-box). Here, we highlighted the initial identification and characterization of four ankyrin/F-box proteins encoded by ECTV: EVM002, EVM005, EVM154 and EVM165.

The family of ankyrin/F-box proteins that we identified in ECTV are common in many viruses within the *Orthopoxvirus* genus. The least conserved is EVM005, which contains only one ortholog encoded by CPXV011. EVM002 orthologs exist in a wide variety of *Orthopoxviruses*, including taterapox virus (TATV)006, horsepox virus (HSPV)004, camelpox virus (CMLV)003, CPXV006, MPXV003 and VARV G1R. All of these EVM002 orthologs except for G1R are located in the ITR region at the terminus of their corresponding genomes, and therefore contain two copies. G1R is unique amongst this group as it is located only at the right-hand end of the VARV genome. Only two genes separate G1R from the terminus of the genome, but this gene is not copied in the VARV ITR. EVM154 has the following orthologs: VVCop B4R, CPXV204, TATV187, rabbitpox virus (RPXV)168, MPXV172, VARV176, HSPV206 and CMLV182. EVM165 has the following orthologs: VVCop B18R, RPXV180, VARV197, CPXV217 and HSPV220. The characterization of EVM154 and EVM165 and their orthologs is currently being investigated by Kristin Burles in our laboratory.

Cellular F-box proteins typically function in substrate recruitment to a multi-component SCF (Skp1/Cul1/F-box) ubiquitin ligase complex, through an interaction between the F-box domain and Skp1 (55, 71). Recently, several of the poxviral ankyrin/F-box proteins have been shown to regulate the SCF ubiquitin ligase complex during infection. These proteins are thought to function to recruit cellular or viral substrates for SCF mediated ubiquitylation. However, substrate identification remains a major hurdle within this field. Until the recent

identification of ankyrin/F-box proteins in the parasitoid wasp, *Nasonia*, these proteins were thought to be unique to poxviruses (67). The ankyrin/F-box proteins differ from cellular F-box proteins in two aspects. First, the poxvirus encoded F-box domains are located at the C-terminus. Second, the ankyrin/F-box proteins have truncated F-boxes, consisting of α -helices 1 and 2, but the majority lack α -helix 3 (37, 57, 65). The cowpox virus encoded ankyrin/F-box protein CP77 contains an F-box domain that is only 13 amino acids in length and may represent the minimum requirement for interaction with Skp1 (9). A related family of cellular proteins, the suppressor of cytokine signalling (SOCS)-box family, do appear in conjunction with ankyrin repeats. SOCS-box proteins interact with elonginB/C, the linker proteins of the cullin-2/5 complexes, and function to recruit substrates for ubiquitylation (Figure 1.7C). The SOCS-box and the F-box share sequence similarity, and it has therefore been proposed that the poxviral ankyrin/F-box proteins were acquired as SOCS-box proteins in an ancestral poxvirus and have evolved to regulate the cullin-1 based ligase (37, 58). However, there is no evidence of poxviral proteins regulating cullin-2/5 based ubiquitin ligases. Upwards of 80% of all poxviral ankyrin repeat proteins contain the C-terminal F-box domain. However, several ankyrin-only proteins have been characterized as functional. The ankyrin-only proteins are generally shorter (100-200 amino acids) than the ankyrin/F-box proteins. These shorter ankyrin-only proteins do not contain F-box domains, and have been proposed to have arisen from full length ankyrin/F-box proteins (37). Additionally, an F-box only protein has been identified in fowlpox virus (63). This F-box-only protein is

downstream of a truncated ankyrin-only protein, and likely represents two truncated halves of a formerly full ankyrin/F-box protein (37).

Ankyrin/F-box proteins have been characterized in myxoma virus (MYXV), a poxvirus infecting rabbits, Orf virus, a poxvirus infecting sheep and goats, cowpox virus (CPXV), variola virus, the causative agent of smallpox, vaccinia virus (VV), the virus used as the smallpox vaccine, as well as the four we identified in ECTV. The first characterized interaction between a poxviral ankyrin/F-box protein and the SCF complex was between the MYXV protein, MT-5, and cullin-1 (24). MT-5, one of four ankyrin/F-box proteins in MYXV, interacts and co-localizes with cullin-1 in the nucleus and regulates the cell cycle, potentially through an interaction with the kinase Akt (66). Each of the five Orf virus encoded ankyrin repeat proteins contain the C-terminal F-box domain and have been shown to associate with a functional SCF ubiquitin ligase complex, as demonstrated through *in vitro* ubiquitylation assays (58). In the case of the Orf virus proteins, the F-box domain was both necessary and sufficient to mediate the interaction with Skp1 and cullin-1. The CPXV proteins CP77 and CPV006 have both been shown to interact with Skp1 and inhibit NF- κ B signalling (9, 41). CPV006, and its variola virus ortholog, G1R, interact with the NF- κ B regulatory protein p105 and inhibit its degradation following TNF α stimulation (40, 41). CP77 functions as a host range protein for infection of RK13 cells, and, additionally, interacts with the NF- κ B transcription factor, p65, to inhibit the transcription of inflammatory cytokines (9, 22). CP77 also interacts with the cellular protein HMG20A and co-localizes with this protein in viral factories (22).

The modified vaccinia virus Ankara (MVA) encoded ankyrin/F-box protein termed 68K-ank, also interacts with the SCF complex in an F-box-dependent manner (59). 68K-ank functions as a host range factor for replication of MVA in non-permissive human and murine cell lines (60). Finally, we found that four of seven ankyrin repeat proteins encoded by ECTV contained the C-terminal F-box domain during our bioinformatics screen of the ECTV strain Moscow genome. Each of these proteins, EVM002, EVM005, EVM154 and EVM165, have now been shown to interact with Skp1 and cullin-1 in an F-box-dependent manner (Chapter 3)(65). Contrary to the Orf encoded ankyrin/F-box proteins, the F-box-only mutant of EVM005 was not sufficient to mediate interaction with Skp1 (Figure 3.7). Additionally, the ECTV proteins associate with conjugated ubiquitin suggesting that they form part of a functional SCF complex (Figure 3.10, 3.11, 3.14 and 3.15). Currently, all characterized poxviral ankyrin/F-box proteins interact with Skp1 and cullin-1, but identification of target substrates has eluded the field. Alternatively, the poxvirus encoded ankyrin/F-box proteins could function to inhibit the cellular SCF complex to inhibit degradation of its normal targets such as the NF- κ B regulatory protein, I κ B α .

Although cellular binding partners have been identified for several of the poxviral ankyrin/F-box proteins, none of these interacting partners have been shown to be directly ubiquitylated by a poxviral ankyrin/F-box protein. One hypothesis is that these proteins function to inhibit the SCF complex instead of recruiting substrates, a hypothesis supported by our data demonstrating inhibition of I κ B α degradation by the ECTV encoded ankyrin/F-box proteins. However, the

ECTV and Orf virus ankyrin/F-box proteins have both been shown to associate with conjugated ubiquitin suggesting functionality of SCF ligase while in complex with poxviral ankyrin/F-box proteins. Additionally, although the ankyrin repeat domains share structural homology, each protein sequence is unique and likely mediates interactions with a specific set of proteins. Finally, if the ankyrin/F-box proteins function strictly to inhibit the SCF complex, this implies redundancy with viral genomes, a characteristic not typically seen. However, the hypothesis that these proteins function as substrate adaptors and recruit target substrates for ubiquitylation relies on the identification of bona fide substrates (Figure 7.1). The tools needed for substrate identification are becoming more readily available due to the expansion on the field of proteomics and the identification of inhibitors of the ubiquitin-proteasome system such as Velcade.

In addition to the poxvirus encoded ankyrin/F-box proteins, one of the ankyrin-only proteins has been characterized. VV encoded K1L is 284 amino acids in length and consists of nine ankyrin-repeats; the length of K1L suggests that this protein potentially arose from a larger ancestral ankyrin/F-box protein (30). K1L is an ankyrin-only protein that mediates host range function, and has more recently been shown to inhibit NF- κ B activation (7, 54). Additionally, we identified three ECTV encoded ankyrin only proteins EVM010, EVM021, and EVM022, which do not contain putative C-terminal F-box domains, are likely to serve functions during ECTV infection. EVM022 is an ortholog to the VV encoded K1L that confers host range function to VV, allowing productive

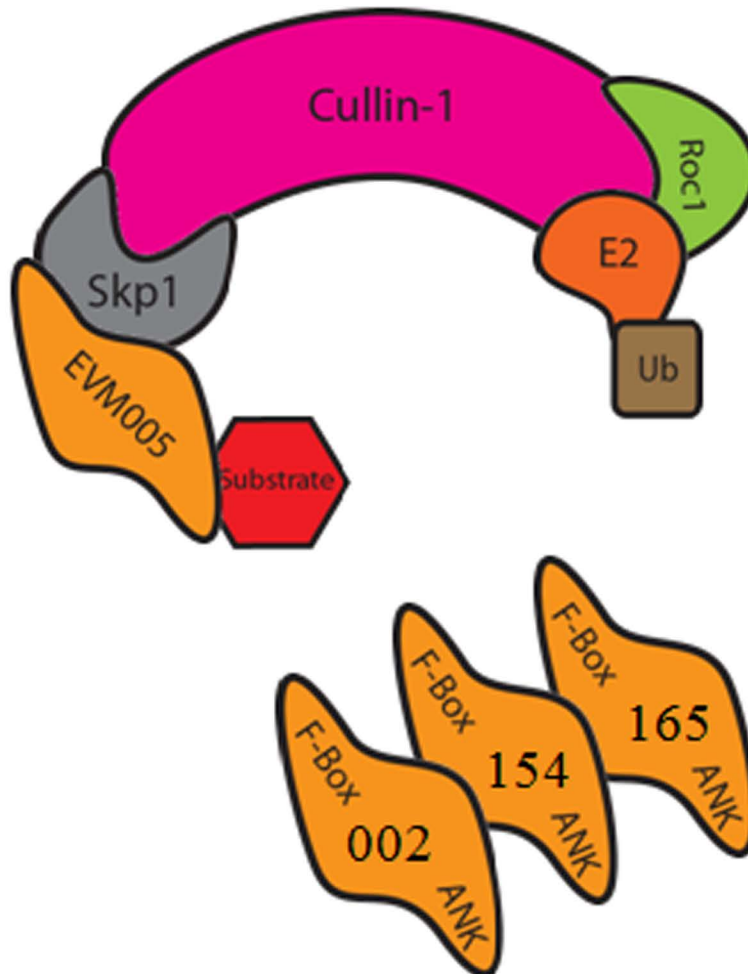


Figure 7.1. The ECTV encoded ankyrin/F-box proteins function as substrate adaptors for the cellular SCF complex. We have shown that EVM005 associates with both endogenous and over-expressed components of the SCF ubiquitin ligase complex. This interaction is mediated by the C-terminal F-box domain of EVM005 and the linker protein Skp1. Notably, EVM005 also associated with the E3 ligase component, Roc1, and conjugated ubiquitin, suggesting that EVM005 was associated with an active SCF complex. Additionally, EVM002, EVM154, and EVM165 all associate with the SCF complex in an F-box dependent manner. These four proteins are likely each recruiting a unique set of protein substrates for ubiquitylation during virus infection.

infection of RK-13 cells. ECTV and ECTV devoid of EVM022 (ECTV- Δ 022) fail to replicate in RK-13 cells (11). This is possibly due to lower EVM022 expression as EVM022 is expressed to 20-fold lower levels in comparison to VV K1L (11). Additionally, ECTV- Δ 022 did not demonstrate decreased virulence in either the susceptible A/NCR or resistant C57BL/6 mouse strains (11). It would be interesting to determine if EVM022 can also inhibit I κ B α degradation and NF- κ B activation like K1L.

In addition to encoding ankyrin/F-box proteins, poxviruses encode multiple proteins to exploit the ubiquitin-proteasome system. The avipoxviruses encode an extended family of RING finger proteins that are predicted to function as ubiquitin ligases (63, 69). Additionally, canarypox virus and two of the *Entomopoxviruses* encode their own molecule of ubiquitin (63). Orf and crocodilepox viruses encode a homolog to APC11, a member of the anaphase-promoting complex/cyclosome (APC/C) ubiquitin ligase (1, 38). Myxoma virus regulates the cell surface expression of MHC class I and CD4 molecules via expression of the ubiquitin ligase M153R (19, 35). Moreover, members of the *Orthopoxvirus* and *Leporipoxvirus* genus encode unique ubiquitin ligases called p28 that localize to the virus factories (23, 42). Several members of the poxvirus family encode multiple BTB/kelch proteins, two of which we have shown to interact with cullin-3 ubiquitin ligases (69). Thus, it is clear that poxviruses have evolved a wide variety of strategies to exploit the ubiquitin-proteasome system, and the presence of multiple ankyrin/F-box proteins suggests that poxviruses have also evolved a unique mechanism to exploit the cellular SCF complex. With the

potential threat of poxviruses being used as bioterror agents, and the expanding number of poxviruses that cause zoonotic infection of humans, including MPXV and CPXV, it will be important to determine if proteasome inhibitors, such as the previously licensed Velcade, can inhibit poxvirus replication *in vivo*.

7.2 Poxviruses Require A Functional Ubiquitin-Proteasome System For Replication

The identification of four ankyrin/F-box proteins encoded by ECTV adds to a list of unique proteins encoded by ECTV that manipulate the ubiquitin-proteasome system that already includes four BTB-Kelch proteins and the RING finger protein p28 (42, 69). The large numbers of ECTV encoded proteins that regulate ubiquitylation during infection, and the large numbers of orthologs of these proteins encoded by other members of the *Orthopoxvirus* genus, lead us to investigate the effect of inhibition of the ubiquitin-proteasome system on *Orthopoxvirus* infection. We hypothesized that due to the apparently high dependence on the ubiquitin-proteasome system, that inhibition of either proteasomal degradation, via proteasome inhibitors, or ubiquitylation, via an E1 inhibitor, would drastically effect the poxvirus life cycle (Appendix B.1)(62).

We determined that inhibition of the proteasome with MG132, MG115, lactacystin or Velcade, or alternatively inhibition of ubiquitylation with the E1 inhibitor, PYR41, inhibited replication of VV, CPXV and ECTV (Appendix B.1)(62). We demonstrate that HeLa cells that were pre-treated with inhibitors for one hour pre-infection, inhibited the synthesis of the late protein I5L, while

the synthesis of the early protein, I3L was unaffected in cells infected with VV, CPXV or ECTV. We went one step further, to demonstrate that these inhibitors also inhibit poxviral DNA replication and the formation of cytoplasmic viral factories. Therefore, it appears that the ubiquitin-proteasome system is not required for poxvirus entry, or the synthesis of early proteins, but becomes essential during the transition into the DNA replication phase.

The ubiquitin-proteasome system could be essential for the uncoating step during poxvirus infection, which is an essential pre-requisite for DNA replication (Figure 1.4). Mass spectrometry has identified up to 70 unique components of the VV core, which is composed of up to 3% ubiquitin, suggesting that components of the VV core can be ubiquitylated (12, 45). Of these constituents, it has been hypothesized that A3L, A4L and A10L may be surface exposed and therefore potential candidates for ubiquitylation (45). The inhibition of poxvirus replication by Velcade is intriguing as this drug has already been FDA approved for the treatment of multiple myeloma (25, 50). If our preliminary results hold true *in vivo*, Velcade could serve as an improvement over the current poxvirus therapeutics Cidofovir or ST-246 in the treatment of poxvirus infections in humans (43, 47).

7.3 Creation of Marker-Free Recombinant Poxviruses Using SEM

The generation of the Selectable and Excisable Marker system for the generation of recombinant poxviruses will have a dramatic effect on research performed not only in our laboratory but in a large number of poxvirology laboratories all over

the world. The SEM system utilizes the Cre/loxP system for the removal of inserted markers following the purification of recombinant poxviruses (Chapter 4)(49). These marker-free recombinants serve as improved vectors for a variety of applications. The generation of marker-free poxvirus therapeutics was the driving force behind the creation of this system. Poxviruses are currently being constructed for the use as vaccine vectors for a variety of diseases, gene therapy vectors, and cancer therapy oncolytic viruses (5, 8, 13, 20, 26, 32, 36). Licensing of recombinant poxviruses that contain fluorescent and/or drug resistance markers is a point of contention amongst several organizations responsible for approval of these poxviral therapies. Groups interested in licensing of a poxvirus-based therapeutic will likely utilize this system to remove markers that do not contribute to the intended therapy. Additionally, academic laboratories will likely adopt this system due to its ease of use. The SEM system also allows comparison of recombinant viruses to true wild type control viruses. Traditionally, control poxviruses have been constructed for the comparison to recombinants by inserting an identical marker into a non-essential region of the genome. For VV, this is typically done by inserting a marker such as *LacZ* or *gfp* into the TK locus, which has been shown to be non-essential for growth in tissue culture. However, insertion into the TK region of ECTV results in a virus with decreased virulence *in vivo*. The generation of marker-free recombinants will allow for the use of wild-type strains of poxviruses as controls, which is an improvement over genetically modified controls. Finally, the ability to insert and remove the *yfp-gpt* cassette leads to the potential for subsequent insertion and excision reactions to

create poxviruses devoid of multiple open reading frames. Large deletion viruses such as MVA or VV811 have proven to be valuable tools for the study of poxvirus-host interactions (46, 70).

One of the key features of the SEM system was the construction of U20S cells that stably express a cytoplasmic mutant of the Cre recombinase. We did not know whether or not ECTV would be able to infect these cells. Poxviruses are notorious for the specificity of their host range and U20S cells are human. ECTV was able to sustain productive infection of the U20S cells and produced foci with similar morphology to those seen during infection of BGMK cells, the cell line typically used for ECTV growth experiments. Marker excision through infection of the U20S-Cre cells was extremely efficient, as we were able to purify marker-free constructs in as little as three rounds of focus purifications. Interestingly, we observed that marker excision occurred in VV during infection of U20S cells expressing wild type Cre recombinase (49). Although the cytoplasmic mutant of the Cre recombinase demonstrated increased efficiency in terms of marker excision, the observation that the nuclear Cre recombinase was able to excise markers at all is interesting. Traditionally, it has been thought that poxviruses can replicate in the cytoplasm of infected cells due to the fact that they encode “everything” required for viral replication. Evidence continues to accumulate supporting translocation of nuclear proteins into the cytoplasm during poxvirus infection. The fact that the over-expressed Cre recombinase is present, at least partially, in the cytoplasm is not a surprise, but does strike ones curiosity

in terms of what nuclear factors are actively translocated into the cytoplasm to support poxvirus replication and potentially host range.

Through the construction of large deletion strains of ECTV using the SEM system, we noticed the loss of intergenic regions of DNA during Cre recombination when inserting the *yfp-gpt* cassette into multiple locations on the ECTV genome. We were able to successfully insert and excise the *yfp-gpt* cassette from individual sites on the genome in the construction of ECTV strains devoid of EVM002, EVM005, EVM154 and EVM165. Additionally, upon removal of the *yfp-gpt* cassette through Cre recombination, a single residual loxP site remains on the genome at the site where the cassette was originally inserted (Figure 4.4C). We took advantage of these residual loxP sites to delete large sections of the genome from the left-hand end (Figure 4.6 and 4.7) and the right-hand end of the ECTV genome (Appendix A). When constructing future large deletion poxvirus strains it will be crucial to monitor the distance between loxP sites, as we struggled to get efficient excision of EVM154 to EVM171 at the right-hand end of the ECTV genome (Appendix A).

7.4 Regulation of NF- κ B by Poxvirus Encoded Ankyrin/F-box Proteins

Regulation of the NF- κ B pathway by poxviruses has been investigated for many years, and a variety of unique NF- κ B inhibitors have been found in all poxviruses (39, 48). These inhibitors include secreted proteins such as the soluble vTNFR and vIL-1R encoded by many poxviruses (53, 56, 64). Additionally, there have been seven VV encoded proteins shown to inhibit NF- κ B activation by disrupting

intracellular signalling: M2, K1, B14, N1, A46, K7, and A52 (6, 10, 14, 17, 51, 54, 61). Although many inhibitors of NF- κ B activation have been characterized in vaccinia virus (VV), our data show that there is at least some signalling during infection as we noticed an accumulation of phospho-I κ B α in cells infected with VV, ECTV or CPXV that were stimulated with TNF α or IL-1 β (Figure 5.1A and E). Of the known intracellular inhibitors of TNF α induced NF- κ B activation encoded by VV (M2, K1, B14, and N1), only K1 and N1 contain orthologs in ECTV (10, 14, 17, 54). This perhaps contributes to the variation we observed in phospho-I κ B α accumulation between ECTV and VV infected HeLa cells stimulated with TNF α (Figure 5.1A). VV infected HeLa cells showed lower levels of phospho-I κ B α accumulation that was also delayed compared to ECTV infected cells (Figure 5.1B). Additionally, of the three previously characterized VV encoded inhibitors of IL-1 β induced NF- κ B activation (A46, A52 and K7), only A46 has an ortholog encoded in ECTV (6, 51, 61). The lack of an encoded K7 or A52 ortholog does not appear to have an effect on the accumulation of phospho-I κ B α in ECTV infected HeLa cells, as both ECTV and VV display similar I κ B α kinetics following IL-1 β stimulation (Figure 5.1E).

Regulation of NF- κ B activation by poxviral ankyrin/F-box proteins has previously been investigated for the cowpox protein, CP77, and the variola protein, G1R, and its CPXV encoded ortholog, CPXV006 (9, 40, 41). Similar to ECTV encoded ankyrin/F-box proteins, these proteins contain N-terminal ankyrin repeats in conjunction with a C-terminal F-box domain and interact with the cellular SCF ubiquitin ligase (9, 40). CP77 contains a very short, 13 amino acid

F-box domain, and has been shown to interact with p65 through its ankyrin repeat domains, however, the F-box domain is also required for CP77 to inhibit NF- κ B activation (9). The model for CP77 suggests that it replaces the regulatory protein I κ B α , following its degradation, holding the NF- κ B transcription factor p65 inactive in the cytoplasm. Conversely, G1R encoded by variola mediates NF- κ B activation through an interaction with NF- κ B1/p105, a regulatory protein similar to I κ B α (4, 40). Degradation of p105 is mediated by the SCF ^{β -TRCP} ubiquitin ligase following a TNF α stimulation, similar to I κ B α (27). Interestingly, EVM002, the ECTV ortholog for G1R, has also been shown to interact with p105 to inhibit its degradation (40, 41).

Characterization of the CPXV encoded ortholog of G1R (VARV) and EVM002 has led to some discrepancies between the roles of EVM002 versus CPXV006 in NF- κ B activation (41). The current model for CPXV006 suggests that this ankyrin/F-box protein interacts with the C-terminus of p105 and blocks its phosphorylation by IKK β . The phosphorylated form of p105 is targeted for proteasomal degradation through SCF ^{β -TRCP} mediated ubiquitylation. Therefore, CPXV006 inhibits the degradation of the I κ B family member p105 by binding to its C-terminus and inhibiting its phosphorylation and subsequent proteasomal degradation. The authors of the paper suggest that expression of CPXV006 has no effect of I κ B α degradation, but can inhibit p65 nuclear translocation through regulating p105 degradation. Here, we present data suggesting that EVM002 can inhibit I κ B α degradation by a mechanism dependent on the C-terminal F-box domain and its association with the SCF ubiquitin ligase complex. Notably, the

SCF complex is also required for the ubiquitylation of phospho-p105. The authors of the CPXV006 manuscript did not comment on the potential role of SCF manipulation by CPXV006 as a mechanism for p105 stabilization. Additionally, deletion of CPXV006 from the CPXV genome led to the activation of NF- κ B during virus infection of activated THP-1 cells. Infection of HeLa cells with ECTV- Δ 002 did not lead to NF- κ B activation. In stark contrast, HeLa cells infected with ECTV- Δ 002 and stimulated with TNF α or IL-1 β still inhibited I κ B α degradation, p65 nuclear accumulation and the synthesis of NF- κ B regulated transcripts including IL-6, TNF α and IL-1 β (Figure 6.8, 6.9 and 6.10). Additionally, we were unable to activate NF- κ B in THP-1 cells by infection with ECTV- Δ 002. It is surprising that deletion of a single open reading frame from CPXV created a virus rendered susceptible to NF- κ B activation, as CPXV- Δ 006, still encodes a large number of NF- κ B inhibitors including CPXV011, the EVM005 ortholog. The only other poxvirus known to activate NF- κ B is modified vaccinia Ankara (MVA), a strain of vaccinia virus containing a large number of gene deletions, truncations and mutations (44). We attempted to render ECTV susceptible to TNF α induced NF- κ B activation by deletion of both EVM002 and EVM005, two proteins that we have characterized as NF- κ B inhibitors. This virus still inhibited NF- κ B activation, which was no surprise as ECTV still encodes a number of additional NF- κ B inhibitors. Additionally, THP-1 cells infected with CPXV- Δ 006 led to increased phosphorylation of IKK α/β compared to wild type CPXV (41). This is inconsistent with the proposed model which

suggests that CPXV006 functions downstream of IKK activation at the point of p105 degradation.

Due to the large number of poxvirus encoded inhibitors of the NF- κ B pathway, it is fascinating that MVA actually activates NF- κ B (44). MVA is a strain of vaccinia virus that has been passaged over 500 times on chicken embryo fibroblast (CEF) cells, and has acquired a large number of mutations and truncations to the existing set of genes (70). In contrast to all studied *Orthopoxviruses*, MVA stimulates I κ B α degradation and p65/p50 nuclear translocation (44). This virus could serve as a valuable tool for the study of poxvirus induced NF- κ B activation, as the actual viral triggers are still incompletely understood, although recent evidence suggests that viral dsRNA and the PKR response may be involved (34). Another large deletion strain of VV, called VV811, was characterized in our lab as a virus that inhibits NF- κ B activation induced by TNF α and IL-1 β (15). Interestingly, although VV811 still encodes A46R and A52R, the TIR containing proteins that inhibit IL-1 β induced NF- κ B activation, the virus lacks all known inhibitors of TNF α induced NF- κ B activation including K1L, K7R, N1L, B14R and M2L (15). These data suggest that VV encodes at least one additional unknown inhibitor of TNF α induced NF- κ B activation. Of interest to this project, VV encoded B4R is on the list of proteins that is absent from MVA but present in VV811 and potentially represents the unknown VV encoded NF- κ B inhibitor. B4R is the VV ortholog of EVM154, a protein that we have shown inhibits NF- κ B activation in an F-box-dependent manner (Figure 6.1 to 6.6). It will be interesting to construct and characterize a

VV811 virus devoid of B4R to determine if this ankyrin/F-box protein is the unknown NF- κ B inhibitor encoded by VV811.

Regulation of NF- κ B signalling is mediated by many cellular and viral ankyrin repeat containing proteins (9, 18, 54). The large family of regulatory proteins consisting of I κ B α , I κ B β , I κ B ϵ , I κ B γ , Bcl-3, I κ B ζ , p100 and p105, utilize ankyrin repeats to bind various NF- κ B dimers, sequestering them in the nucleus (18). The VV encoded ankyrin repeat protein K1L is an inhibitor of NF- κ B activation (54). K1L is one of the few poxvirus encoded ankyrin repeat proteins that does not encode a C-terminal F-box domain, yet, it still inhibits I κ B α degradation (54). However, the mechanism through which K1L inhibits I κ B α degradation remains unclear.

The large number of NF- κ B inhibitors encoded by poxviruses highlights the importance of this anti-viral pathway, but also leads to the question of why so many inhibitors are needed. It is clear that NF- κ B can be triggered through a variety of intracellular and extracellular stimuli, and that each signalling cascade follows a unique path to trigger nuclear accumulation of NF- κ B dimers and transcriptional activation (21, 31). At this point, the mechanism with which these NF- κ B pathways sense poxvirus infection is unclear. The poxvirus encoded inhibitors of NF- κ B activation do not appear redundant, and instead are likely complimentary to each other, and potentially serve to inhibit NF- κ B activation through a variety of stimuli. Poxviruses infect a variety of cell types in each individual host, and perhaps these inhibitors serve roles that are specific to certain cells or specific stimuli. Some inhibitors are specific for the IL-1 β pathway

(A46R and A52R), while others inhibit downstream of IKK activation, suggesting that these proteins should inhibit all NF- κ B pathways that converge at IKK β phosphorylation. Additionally, some inhibitors may have acquired their inhibitory activity through regulation of other essential cellular mechanisms. This may be the case for the ECTV encoded ankyrin/F-box proteins (Figure 7.2). It remains possible that the ECTV encoded ankyrin/F-box proteins ubiquitylate substrates located within the NF- κ B activation cascade. However, if substrates for the ECTV encoded ankyrin/F-box proteins are not within the NF- κ B signalling cascade, inhibition of signalling is likely due to redirection of the SCF complex, and therefore a beneficial side effect of manipulating the host ubiquitin-proteasome system. Some of the poxvirus proteins that have been characterized as inhibitors of NF- κ B activation serve roles in the regulation of additional cellular pathways as well as NF- κ B. For example, CP77 and K1L both serve functions as host range factors (9, 54, 68). Notably, the C-terminal F-box domain of CP77 is not required for its host range function. This suggests that the ankyrin repeats of other poxviral ankyrin/F-box proteins may also be serving functions independent of interactions with the SCF complex.

7.5 Substrate Identification for ECTV Encoded Ankyrin/F-box Proteins

Although many poxvirus ankyrin/F-box proteins have now been characterized as regulators of the SCF complex through interactions between Skp1 and the viral F-box domain, substrate identification has remained elusive. Of the sixty-nine cellular F-box proteins encoded in the human genome, only nine have identified

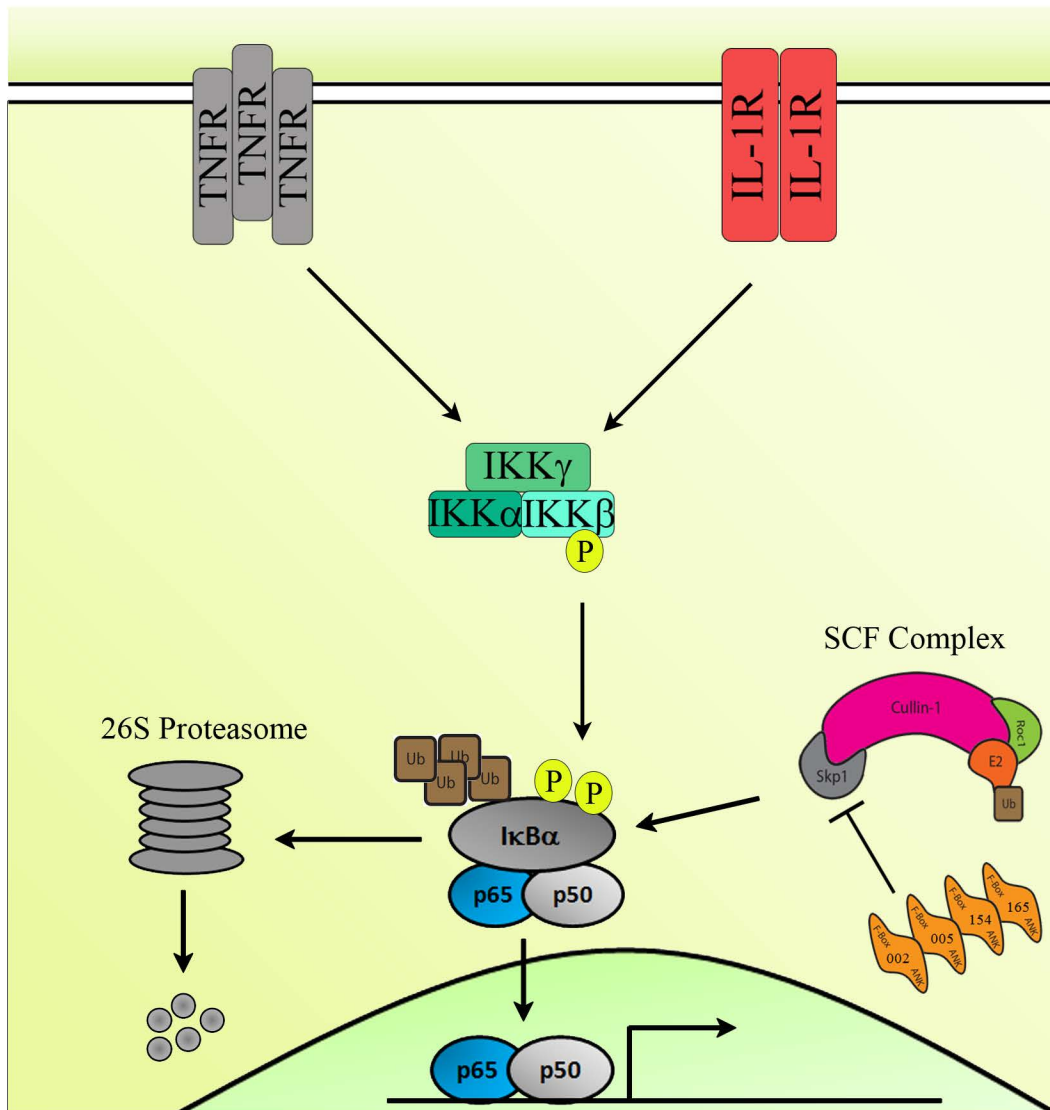


Figure 7.2. The ECTV encoded ankyrin/F-box proteins inhibit NF-κB activation through manipulation of the SCF ubiquitin ligase. Our data demonstrate that EVM002, EVM005, EVM154 and EVM165 all inhibit TNF α and IL-1 β induced p65 nuclear accumulation when over-expressed. This inhibition was shown to be dependent on the C-terminal F-box domain of each of these proteins, as mutants lacking the F-box domain failed to inhibit p65 nuclear accumulation. Further characterization of EVM002 and EVM005 demonstrated that these proteins were capable of inhibiting the degradation of I κ B α . Again, this inhibition was dependent on the C-terminal F-box domain. ECTV devoid of either EVM002 or EVM005 were still able to inhibit TNF α induced NF- κ B activation. This is likely due to the presence of additional inhibitors of the NF- κ B signalling cascade encoded by ECTV. We attempted to render ECTV susceptible to TNF α induced NF- κ B activation through the deletion of both EVM002 and EVM005, but this virus still inhibited I κ B α degradation. We will likely need to delete all four ECTV encoded ankyrin/F-box proteins and potentially additional NF- κ B inhibitors to render ECTV susceptible to NF- κ B activation.

targets (16). The poxviral F-box proteins are suspected to function as substrate adaptor molecules for the SCF complex, a process involving unique protein-protein interactions between the ankyrin repeat domains and unidentified cellular or viral target proteins (Figure 7.1). Although binding partners other than Skp1 have been identified for several of the poxvirus ankyrin/F-box proteins, none of these identified proteins have been characterized as bona fide substrates for ubiquitylation (22, 24, 40). Substrate identification for poxvirus ankyrin/F-box proteins will provide insight into the role of this family of proteins in virulence and the viral life cycle.

Throughout the course of this project, many attempts were made to identify cellular or viral proteins that interact with EVM005 which may be substrates for ubiquitylation. Preliminary attempts were made by infecting HeLa cells with VV-Flag-EVM005, followed by immunoprecipitation of Flag-EVM005. The Flag-EVM005 complexes were separated on a large Hoeffer SDS-PAGE apparatus followed by silver staining. We excised a large number of bands for identification by mass spectrometry in an attempt to identify unique proteins associated with EVM005. Our primary hit was cullin-1, the molecular scaffold for the SCF complex, but no potential substrates were identified (Figure 3.3). This was perhaps due to the EVM005 induced degradation of substrate proteins during infection. These experiments were not carried out in the presence of MG132, which could prevent proteasomal degradation of ubiquitylated proteins. A second method involved infection of HeLa cells with VV-Flag-EVM005(1-593) followed by immunoprecipitation, SDS-PAGE and mass spectrometry as

before. Flag-EVM005(1-593) contains all of the N-terminal ankyrin repeats, which we hypothesize are responsible for substrate binding. However, this construct lacks the C-terminal F-box domain, required for interaction with Skp1 and the SCF complex. We hypothesized that this construct could serve as a substrate “trap”, binding substrates through the ankyrin repeats, but these proteins would not be ubiquitylated by the SCF complex. This is a technique that requires a significant affinity between the ankyrin repeats of EVM005 and potential substrate proteins. Potentially, our inability to pull down substrates with this complex lies in the weak affinity between EVM005 and its substrates, or that these interactions may only be transient in nature, making protein binding assays difficult.

The identification of substrate proteins that are ubiquitylated by the ankyrin/F-box proteins will likely come from advanced proteomic techniques. Stable isotope labelling of amino acids in cell culture (SILAC) provides the most sensitive technique available, and has recently been used to identify nearly 1000 potential substrates for the cellular E3 ligase HRD1 (29). In this technique, cells are passaged in the presence of radio labelled amino acids several times to ensure that all cellular proteins are labelled with heavy amino acids. In conjunction, a separate sample is grown in regular media. The cells grown in the presence of labelled amino acids were then treated with siRNA to knock down HRD1 E3 ligase expression. Protein samples from mock treated cells, and siRNA treated cells grown with radio labelled amino acids were then collected and analysed by quantitative mass spectrometry. Potential substrates appear in higher quantity in

the sample in which HRD1 was knocked down. For the purpose of our viral ankyrin/F-box proteins, we could infect the unlabelled cells with wild type ECTV and the labelled cells with ECTV devoid of a single ankyrin/F-box protein. This should lead to increase levels of substrate proteins in the labelled cell sample infected with our knockout ECTVs lacking one ankyrin/F-box protein. These proteins of increased abundance would represent potential substrate proteins for the ECTV encoded ankyrin/F-box proteins.

One caveat of SILAC is that only potential “cellular” substrate proteins would be identified, as all viral substrates would remain unlabelled. To identify potential viral target proteins we could use differential in gel expression (DIGE) coupled with mass spectrometry. In this technique we would infect samples with either wild type ECTV or a knockout ECTV devoid of a single ankyrin/F-box protein. Each sample would then be harvested and labelled individually with either a fluorescent green or red dye. The samples would then be mixed, run on a 2-dimensional SDS-PAGE, and spots would be analysed by fluorescence. All spots that fluoresce yellow would represent proteins that are in equal levels in both samples. Spots that fluoresced green or red would represent proteins that are up or down regulated in the absence of the ankyrin/F-box protein. These spots can be picked and identified by mass spectrometry as candidate substrate proteins. As all proteins in the infected samples are labelled with the dyes, both cellular and viral proteins can be identified by this technique. Identification of these target proteins will be critical to the overall characterization of poxvirus encoded ankyrin/F-box proteins.

7.6 Conclusion

This thesis outlines the identification of a novel family of ankyrin/F-box proteins encoded by ECTV. We used bioinformatics to identify seven ankyrin repeat containing proteins encoded by ECTV, and analysis of each of their C-termini yielded four genes with putative F-box domains. We have shown that each of these proteins interact with the cellular SCF ubiquitin ligase complex through association of their C-terminal F-box domains with the SCF linker protein Skp1. Additionally, we have shown that the ankyrin/F-box proteins associate with polyubiquitylated proteins, suggesting that the ankyrin/F-box proteins are part of a functional SCF ubiquitin ligase (Figure 7.1). Potentially, each of the four ECTV encoded ankyrin/F-box proteins is recruiting a unique subset of substrate proteins to the SCF complex for ubiquitylation during ECTV infection. These substrates would be ubiquitylated with K48-linked polyubiquitin chains and degraded through the 26S proteasome, as the E3 ligase component, Roc1, is associated with EVM005 complexes, and mediates the formation of K48-linked polyubiquitin chains in uninfected cells. Identification of these target substrates will be essential to prove our hypothesis that the ECTV encoded ankyrin/F-box proteins function as viral substrate adaptor proteins for the cellular SCF ubiquitin ligase complex. Alternatively, the ankyrin/F-box proteins could strictly be inhibiting the SCF complex to prevent degradation of cellular targets such as the NF- κ B regulatory protein I κ B α .

We have shown that all four of the ECTV encoded ankyrin/F-box proteins inhibit the activation of the proinflammatory NF- κ B signaling cascade (Figure 7.2). These proteins require their C-terminal F-box domains to mediate this inhibition. Inhibition of NF- κ B activation by these proteins is likely, at least in part, due to the high-jacking and redirection of the cellular SCF complex during infection. This manipulation of the SCF complex inhibits the degradation of I κ B α by the cellular F-box protein β -TRCP. However, we cannot rule out the possibility that the ECTV encoded ankyrin/F-box proteins mediate the ubiquitylation of substrate proteins within the NF- κ B signaling cascade.

Through the construction of ECTV strains devoid of each of the four ankyrin/F-box proteins using a novel SEM system, we have shown that deletion of either EVM005 or EVM002 does not render ECTV susceptible to TNF α induced NF- κ B activation. ECTV- Δ 002 and ECTV- Δ 005 still inhibit I κ B α degradation, p65 nuclear accumulation and the synthesis of NF- κ B regulated transcripts. Additionally, ECTV- Δ 005 was attenuated in both the resistant C57BL/6 and susceptible A/NCR mouse strains, demonstrating that EVM005 is an essential virulence factor. Together, these data suggest a function in virulence that is independent from EVM005-mediated NF- κ B inhibition. Identification of potential substrate proteins could provide insight in the mechanism by which EVM005 contributes to ECTV virulence.

7.7 References

1. **Afonso, C. L., E. R. Tulman, G. Delhon, Z. Lu, G. J. Viljoen, D. B. Wallace, G. F. Kutish, and D. L. Rock.** 2006. Genome of crocodilepox virus. *J Virol* **80**:4978-91.
2. **Baines, A. J.** 2010. The spectrin-ankyrin-4.1-adducin membrane skeleton: adapting eukaryotic cells to the demands of animal life. *Protoplasma* **244**:99-131.
3. **Barry, M., N. van Buuren, K. Burles, K. Mottet, Q. Wang, and A. Teale.** 2010. Poxvirus exploitation of the ubiquitin-proteasome system. *Viruses* **2**:2356-80.
4. **Beinke, S., and S. C. Ley.** 2004. Functions of NF-kappaB1 and NF-kappaB2 in immune cell biology. *Biochem J* **382**:393-409.
5. **Bejon, P., E. Ogada, T. Mwangi, P. Milligan, T. Lang, G. Fegan, S. C. Gilbert, N. Peshu, K. Marsh, and A. V. Hill.** 2007. Extended follow-up following a phase 2b randomized trial of the candidate malaria vaccines FP9 ME-TRAP and MVA ME-TRAP among children in Kenya. *PLoS One* **2**:e707.
6. **Bowie, A., E. Kiss-Toth, J. A. Symons, G. L. Smith, S. K. Dower, and L. A. O'Neill.** 2000. A46R and A52R from vaccinia virus are antagonists of host IL-1 and toll-like receptor signaling. *Proc Natl Acad Sci U S A* **97**:10162-7.
7. **Bradley, R. R., and M. Terajima.** 2005. Vaccinia virus K1L protein mediates host-range function in RK-13 cells via ankyrin repeat and may interact with a cellular GTPase-activating protein. *Virus Res* **114**:104-12.
8. **Cadoz, M., A. Strady, B. Meignier, J. Taylor, J. Tartaglia, E. Paoletti, and S. Plotkin.** 1992. Immunisation with canarypox virus expressing rabies glycoprotein. *Lancet* **339**:1429-32.
9. **Chang, S. J., J. C. Hsiao, S. Sonnberg, C. T. Chiang, M. H. Yang, D. L. Tzou, A. A. Mercer, and W. Chang.** 2009. Poxvirus host range protein CP77 contains an F-box-like domain that is necessary to suppress NF-kappaB activation by tumor necrosis factor alpha but is independent of its host range function. *J Virol* **83**:4140-52.
10. **Chen, R. A., G. Ryzhakov, S. Cooray, F. Randow, and G. L. Smith.** 2008. Inhibition of IkappaB kinase by vaccinia virus virulence factor B14. *PLoS Pathog* **4**:e22.
11. **Chen, W., R. Drillien, D. Spehner, and R. M. Buller.** 1993. In vitro and in vivo study of the ectromelia virus homolog of the vaccinia virus K1L host range gene. *Virology* **196**:682-93.
12. **Chung, C. S., C. H. Chen, M. Y. Ho, C. Y. Huang, C. L. Liao, and W. Chang.** 2006. Vaccinia virus proteome: identification of proteins in vaccinia virus intracellular mature virion particles. *J Virol* **80**:2127-40.
13. **Dasgupta, S., M. Bhattacharya-Chatterjee, B. W. O'Malley, Jr., and S. K. Chatterjee.** 2006. Recombinant vaccinia virus expressing interleukin-2 invokes anti-tumor cellular immunity in an orthotopic murine model of head and neck squamous cell carcinoma. *Mol Ther* **13**:183-93.

14. **DiPerna, G., J. Stack, A. G. Bowie, A. Boyd, G. Kotwal, Z. Zhang, S. Arvikar, E. Latz, K. A. Fitzgerald, and W. L. Marshall.** 2004. Poxvirus protein N1L targets the I-kappaB kinase complex, inhibits signaling to NF-kappaB by the tumor necrosis factor superfamily of receptors, and inhibits NF-kappaB and IRF3 signaling by toll-like receptors. *J Biol Chem* **279**:36570-8.
15. **Fagan-Garcia, K., and M. Barry.** 2011. A vaccinia virus deletion mutant reveals the presence of additional inhibitors of NF-kappaB. *J Virol* **85**:883-94.
16. **Frescas, D., and M. Pagano.** 2008. Deregulated proteolysis by the F-box proteins SKP2 and beta-TrCP: tipping the scales of cancer. *Nat Rev Cancer* **8**:438-49.
17. **Gedey, R., X. L. Jin, O. Hinthong, and J. L. Shisler.** 2006. Poxviral regulation of the host NF-kappaB response: the vaccinia virus M2L protein inhibits induction of NF-kappaB activation via an ERK2 pathway in virus-infected human embryonic kidney cells. *J Virol* **80**:8676-85.
18. **Ghosh, S., and M. S. Hayden.** 2008. New regulators of NF-kappaB in inflammation. *Nat Rev Immunol* **8**:837-48.
19. **Guerin, J. L., J. Gelfi, S. Boullier, M. Delverdier, F. A. Bellanger, S. Bertagnoli, I. Drexler, G. Sutter, and F. Messud-Petit.** 2002. Myxoma virus leukemia-associated protein is responsible for major histocompatibility complex class I and Fas-CD95 down-regulation and defines scrapins, a new group of surface cellular receptor abductor proteins. *J Virol* **76**:2912-23.
20. **Harrop, R., N. Drury, W. Shingler, P. Chikoti, I. Redchenko, M. W. Carroll, S. M. Kingsman, S. Naylor, A. Melcher, J. Nicholls, H. Wassan, N. Habib, and A. Anthoney.** 2007. Vaccination of colorectal cancer patients with modified vaccinia ankara encoding the tumor antigen 5T4 (TroVax) given alongside chemotherapy induces potent immune responses. *Clin Cancer Res* **13**:4487-94.
21. **Hayden, M. S., and S. Ghosh.** 2008. Shared principles in NF-kappaB signaling. *Cell* **132**:344-62.
22. **Hsiao, J. C., C. C. Chao, M. J. Young, Y. T. Chang, E. C. Cho, and W. Chang.** 2006. A poxvirus host range protein, CP77, binds to a cellular protein, HMG20A, and regulates its dissociation from the vaccinia virus genome in CHO-K1 cells. *J Virol* **80**:7714-28.
23. **Huang, J., Q. Huang, X. Zhou, M. M. Shen, A. Yen, S. X. Yu, G. Dong, K. Qu, P. Huang, E. M. Anderson, S. Daniel-Issakani, R. M. Buller, D. G. Payan, and H. H. Lu.** 2004. The poxvirus p28 virulence factor is an E3 ubiquitin ligase. *J Biol Chem* **279**:54110-6.
24. **Johnston, J. B., G. Wang, J. W. Barrett, S. H. Nazarian, K. Colwill, M. Moran, and G. McFadden.** 2005. Myxoma virus M-T5 protects infected cells from the stress of cell cycle arrest through its interaction with host cell cullin-1. *J Virol* **79**:10750-63.
25. **Kanagasabaphy, P., G. J. Morgan, and F. E. Davies.** 2007. Proteasome inhibition and multiple myeloma. *Curr Opin Investig Drugs* **8**:447-51.

26. **Kim, J. H., J. Y. Oh, B. H. Park, D. E. Lee, J. S. Kim, H. E. Park, M. S. Roh, J. E. Je, J. H. Yoon, S. H. Thorne, D. Kirn, and T. H. Hwang.** 2006. Systemic armed oncolytic and immunologic therapy for cancer with JX-594, a targeted poxvirus expressing GM-CSF. *Mol Ther* **14**:361-70.
27. **Lang, V., J. Janzen, G. Z. Fischer, Y. Soneji, S. Beinke, A. Salmeron, H. Allen, R. T. Hay, Y. Ben-Neriah, and S. C. Ley.** 2003. betaTrCP-mediated proteolysis of NF-kappaB1 p105 requires phosphorylation of p105 serines 927 and 932. *Mol Cell Biol* **23**:402-13.
28. **Lazarides, E., and C. Woods.** 1989. Biogenesis of the red blood cell membrane-skeleton and the control of erythroid morphogenesis. *Annu Rev Cell Biol* **5**:427-52.
29. **Lee, K. A., L. P. Hammerle, P. S. Andrews, M. P. Stokes, T. Mustelin, J. C. Silva, R. A. Black, and J. R. Doedens.** 2011. Ubiquitin ligase substrate identification through quantitative proteomics at both the protein and peptide levels. *J Biol Chem.*
30. **Li, Y., X. Meng, Y. Xiang, and J. Deng.** 2010. Structure function studies of vaccinia virus host range protein k1 reveal a novel functional surface for ankyrin repeat proteins. *J Virol* **84**:3331-8.
31. **Liu, S., and Z. J. Chen.** 2011. Expanding role of ubiquitination in NF-kappaB signaling. *Cell Res* **21**:6-21.
32. **Lun, X., T. Alain, F. J. Zemp, H. Zhou, M. M. Rahman, M. G. Hamilton, G. McFadden, J. Bell, D. L. Senger, and P. A. Forsyth.** 2010. Myxoma virus virotherapy for glioma in immunocompetent animal models: optimizing administration routes and synergy with rapamycin. *Cancer Res* **70**:598-608.
33. **Lux, S. E., W. T. Tse, J. C. Menninger, K. M. John, P. Harris, O. Shalev, R. R. Chilcote, S. L. Marchesi, P. C. Watkins, V. Bennett, and et al.** 1990. Hereditary spherocytosis associated with deletion of human erythrocyte ankyrin gene on chromosome 8. *Nature* **345**:736-9.
34. **Lynch, H. E., C. A. Ray, K. L. Oie, J. J. Pollara, I. T. Petty, A. J. Sadler, B. R. Williams, and D. J. Pickup.** 2009. Modified vaccinia virus Ankara can activate NF-kappaB transcription factors through a double-stranded RNA-activated protein kinase (PKR)-dependent pathway during the early phase of virus replication. *Virology* **391**:177-86.
35. **Mansouri, M., E. Bartee, K. Gouveia, B. T. Hovey Nerenberg, J. Barrett, L. Thomas, G. Thomas, G. McFadden, and K. Fruh.** 2003. The PHD/LAP-domain protein M153R of myxomavirus is a ubiquitin ligase that induces the rapid internalization and lysosomal destruction of CD4. *J Virol* **77**:1427-40.
36. **McCart, J. A., J. M. Ward, J. Lee, Y. Hu, H. R. Alexander, S. K. Libutti, B. Moss, and D. L. Bartlett.** 2001. Systemic cancer therapy with a tumor-selective vaccinia virus mutant lacking thymidine kinase and vaccinia growth factor genes. *Cancer Res* **61**:8751-7.
37. **Mercer, A. A., S. B. Fleming, and N. Ueda.** 2005. F-box-like domains are present in most poxvirus ankyrin repeat proteins. *Virus Genes* **31**:127-33.

38. **Mo, M., S. B. Fleming, and A. A. Mercer.** 2009. Cell cycle deregulation by a poxvirus partial mimic of anaphase-promoting complex subunit 11. *Proc Natl Acad Sci U S A* **106**:19527-32.
39. **Mohamed, M. R., and G. McFadden.** 2009. NFkB inhibitors: strategies from poxviruses. *Cell Cycle* **8**:3125-32.
40. **Mohamed, M. R., M. M. Rahman, J. S. Lanchbury, D. Shattuck, C. Neff, M. Dufford, N. van Buuren, K. Fagan, M. Barry, S. Smith, I. Damon, and G. McFadden.** 2009. Proteomic screening of variola virus reveals a unique NF-kappaB inhibitor that is highly conserved among pathogenic orthopoxviruses. *Proc Natl Acad Sci U S A* **106**:9045-50.
41. **Mohamed, M. R., M. M. Rahman, A. Rice, R. W. Moyer, S. J. Werden, and G. McFadden.** 2009. Cowpox virus expresses a novel ankyrin repeat NF-kappaB inhibitor that controls inflammatory cell influx into virus-infected tissues and is critical for virus pathogenesis. *J Virol* **83**:9223-36.
42. **Nerenberg, B. T., J. Taylor, E. Bartee, K. Gouveia, M. Barry, and K. Fruh.** 2005. The poxviral RING protein p28 is a ubiquitin ligase that targets ubiquitin to viral replication factories. *J Virol* **79**:597-601.
43. **Neyts, J., P. Leyssen, E. Verbeken, and E. De Clercq.** 2004. Efficacy of cidofovir in a murine model of disseminated progressive vaccinia. *Antimicrob Agents Chemother* **48**:2267-73.
44. **Oie, K. L., and D. J. Pickup.** 2001. Cowpox virus and other members of the orthopoxvirus genus interfere with the regulation of NF-kappaB activation. *Virology* **288**:175-87.
45. **Pedersen, K., E. J. Snijder, S. Schleich, N. Roos, G. Griffiths, and J. K. Locker.** 2000. Characterization of vaccinia virus intracellular cores: implications for viral uncoating and core structure. *J Virol* **74**:3525-36.
46. **Perkus, M. E., S. J. Goebel, S. W. Davis, G. P. Johnson, E. K. Norton, and E. Paoletti.** 1991. Deletion of 55 open reading frames from the termini of vaccinia virus. *Virology* **180**:406-10.
47. **Quenelle, D. C., R. M. Buller, S. Parker, K. A. Keith, D. E. Hruby, R. Jordan, and E. R. Kern.** 2007. Efficacy of delayed treatment with ST-246 given orally against systemic orthopoxvirus infections in mice. *Antimicrob Agents Chemother* **51**:689-95.
48. **Rahman, M. M., and G. McFadden.** 2011. Modulation of NF-kappaB signalling by microbial pathogens. *Nat Rev Microbiol* **9**:291-306.
49. **Rintoul, J. L., J. Wang, D. B. Gammon, N. J. van Buuren, K. Garson, K. Jardine, M. Barry, D. H. Evans, and J. C. Bell.** 2011. A selectable and excisable marker system for the rapid creation of recombinant poxviruses. *PLoS One* **6**:e24643.
50. **Roccaro, A. M., A. Vacca, and D. Ribatti.** 2006. Bortezomib in the treatment of cancer. *Recent Pat Anticancer Drug Discov* **1**:397-403.
51. **Schroder, M., M. Baran, and A. G. Bowie.** 2008. Viral targeting of DEAD box protein 3 reveals its role in TBK1/IKKepsilon-mediated IRF activation. *EMBO J* **27**:2147-57.

52. **Sedgwick, S. G., and S. J. Smerdon.** 1999. The ankyrin repeat: a diversity of interactions on a common structural framework. *Trends Biochem Sci* **24**:311-6.
53. **Seet, B. T., J. B. Johnston, C. R. Brunetti, J. W. Barrett, H. Everett, C. Cameron, J. Sypula, S. H. Nazarian, A. Lucas, and G. McFadden.** 2003. Poxviruses and immune evasion. *Annu Rev Immunol* **21**:377-423.
54. **Shisler, J. L., and X. L. Jin.** 2004. The vaccinia virus K1L gene product inhibits host NF-kappaB activation by preventing IkappaBalpha degradation. *J Virol* **78**:3553-60.
55. **Skowyra, D., K. L. Craig, M. Tyers, S. J. Elledge, and J. W. Harper.** 1997. F-box proteins are receptors that recruit phosphorylated substrates to the SCF ubiquitin-ligase complex. *Cell* **91**:209-19.
56. **Smith, C. A., T. Davis, J. M. Wignall, W. S. Din, T. Farrah, C. Upton, G. McFadden, and R. G. Goodwin.** 1991. T2 open reading frame from the Shope fibroma virus encodes a soluble form of the TNF receptor. *Biochem Biophys Res Commun* **176**:335-42.
57. **Sonnberg, S., S. B. Fleming, and A. A. Mercer.** 2009. A truncated two-alpha-helix F-box present in poxvirus ankyrin-repeat proteins is sufficient for binding the SCF1 ubiquitin ligase complex. *J Gen Virol* **90**:1224-8.
58. **Sonnberg, S., B. T. Seet, T. Pawson, S. B. Fleming, and A. A. Mercer.** 2008. Poxvirus ankyrin repeat proteins are a unique class of F-box proteins that associate with cellular SCF1 ubiquitin ligase complexes. *Proc Natl Acad Sci U S A* **105**:10955-60.
59. **Sperling, K. M., A. Schwantes, B. S. Schnierle, and G. Sutter.** 2008. The highly conserved orthopoxvirus 68k ankyrin-like protein is part of a cellular SCF ubiquitin ligase complex. *Virology* **374**:234-9.
60. **Sperling, K. M., A. Schwantes, C. Staib, B. S. Schnierle, and G. Sutter.** 2009. The orthopoxvirus 68-kilodalton ankyrin-like protein is essential for DNA replication and complete gene expression of modified vaccinia virus Ankara in nonpermissive human and murine cells. *J Virol* **83**:6029-38.
61. **Stack, J., I. R. Haga, M. Schroder, N. W. Bartlett, G. Maloney, P. C. Reading, K. A. Fitzgerald, G. L. Smith, and A. G. Bowie.** 2005. Vaccinia virus protein A46R targets multiple Toll-like-interleukin-1 receptor adaptors and contributes to virulence. *J Exp Med* **201**:1007-18.
62. **Teale, A., S. Campbell, N. Van Buuren, W. C. Magee, K. Watmough, B. Couturier, R. Shipclark, and M. Barry.** 2009. Orthopoxviruses require a functional ubiquitin-proteasome system for productive replication. *J Virol* **83**:2099-108.
63. **Tulman, E. R., C. L. Afonso, Z. Lu, L. Zsak, G. F. Kutish, and D. L. Rock.** 2004. The genome of canarypox virus. *J Virol* **78**:353-66.
64. **Upton, C., J. L. Macen, M. Schreiber, and G. McFadden.** 1991. Myxoma virus expresses a secreted protein with homology to the tumor necrosis factor receptor gene family that contributes to viral virulence. *Virology* **184**:370-82.

65. **van Buuren, N., B. Couturier, Y. Xiong, and M. Barry.** 2008. Ectromelia virus encodes a novel family of F-box proteins that interact with the SCF complex. *J Virol* **82**:9917-27.
66. **Wang, G., J. W. Barrett, M. Stanford, S. J. Werden, J. B. Johnston, X. Gao, M. Sun, J. Q. Cheng, and G. McFadden.** 2006. Infection of human cancer cells with myxoma virus requires Akt activation via interaction with a viral ankyrin-repeat host range factor. *Proc Natl Acad Sci U S A* **103**:4640-5.
67. **Werren, J. H., S. Richards, C. A. Desjardins, O. Niehuis, J. Gadau, J. K. Colbourne, L. W. Beukeboom, C. Desplan, C. G. Elsik, C. J. Grimmelikhuijzen, P. Kitts, J. A. Lynch, T. Murphy, D. C. Oliveira, C. D. Smith, L. van de Zande, K. C. Worley, E. M. Zdobnov, M. Aerts, S. Albert, V. H. Anaya, J. M. Anzola, A. R. Barchuk, S. K. Behura, A. N. Bera, M. R. Berenbaum, R. C. Bertossa, M. M. Bitondi, S. R. Bordenstein, P. Bork, E. Bornberg-Bauer, M. Brunain, G. Cazzamali, L. Chaboub, J. Chacko, D. Chavez, C. P. Childers, J. H. Choi, M. E. Clark, C. Claudianos, R. A. Clinton, A. G. Cree, A. S. Cristino, P. M. Dang, A. C. Darby, D. C. de Graaf, B. Devreese, H. H. Dinh, R. Edwards, N. Elango, E. Elhaik, O. Ermolaeva, J. D. Evans, S. Foret, G. R. Fowler, D. Gerlach, J. D. Gibson, D. G. Gilbert, D. Graur, S. Grunder, D. E. Hagen, Y. Han, F. Hauser, D. Hultmark, H. C. t. Hunter, G. D. Hurst, S. N. Jhangian, H. Jiang, R. M. Johnson, A. K. Jones, T. Junier, T. Kadowaki, A. Kamping, Y. Kapustin, B. Kechavarzi, J. Kim, B. Kiryutin, T. Koevoets, C. L. Kovar, E. V. Kriventseva, R. Kucharski, H. Lee, S. L. Lee, K. Lees, L. R. Lewis, D. W. Loehlin, J. M. Logsdon, Jr., J. A. Lopez, R. J. Lozado, D. Maglott, R. Maleszka, A. Mayampurath, D. J. Mazur, M. A. McClure, A. D. Moore, M. B. Morgan, J. Muller, M. C. Munoz-Torres, D. M. Muzny, L. V. Nazareth, et al.** 2010. Functional and evolutionary insights from the genomes of three parasitoid *Nasonia* species. *Science* **327**:343-8.
68. **Willis, K. L., S. Patel, Y. Xiang, and J. L. Shisler.** 2009. The effect of the vaccinia K1 protein on the PKR-eIF2alpha pathway in RK13 and HeLa cells. *Virology* **394**:73-81.
69. **Wilton, B. A., S. Campbell, N. Van Buuren, R. Garneau, M. Furukawa, Y. Xiong, and M. Barry.** 2008. Ectromelia virus BTB/kelch proteins, EVM150 and EVM167, interact with cullin-3-based ubiquitin ligases. *Virology* **374**:82-99.
70. **Wyatt, L. S., P. L. Earl, L. A. Eller, and B. Moss.** 2004. Highly attenuated smallpox vaccine protects mice with and without immune deficiencies against pathogenic vaccinia virus challenge. *Proc Natl Acad Sci U S A* **101**:4590-5.
71. **Zheng, N., B. A. Schulman, L. Song, J. J. Miller, P. D. Jeffrey, P. Wang, C. Chu, D. M. Koepp, S. J. Elledge, M. Pagano, R. C. Conaway, J. W. Conaway, J. W. Harper, and N. P. Pavletich.** 2002. Structure of the Cull1-Rbx1-Skp1-F boxSkp2 SCF ubiquitin ligase complex. *Nature* **416**:703-9.

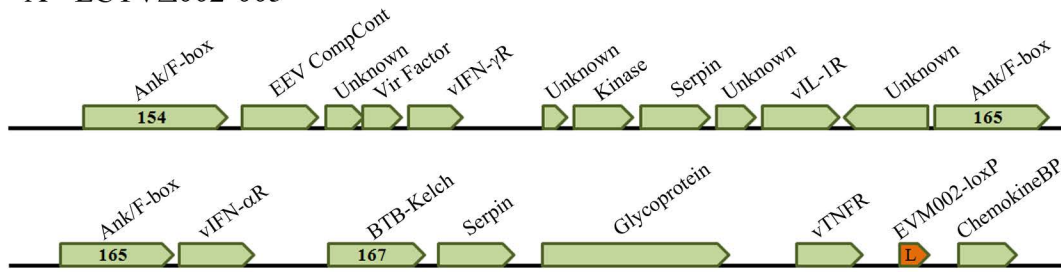
**Appendix A: Construction of a Large Deletion
ECTV Lacking 17 ORFs at the Right-hand
End of the Genome**

A.1 Deletion of Multiple Genes from the Right-End of the ECTV Genome

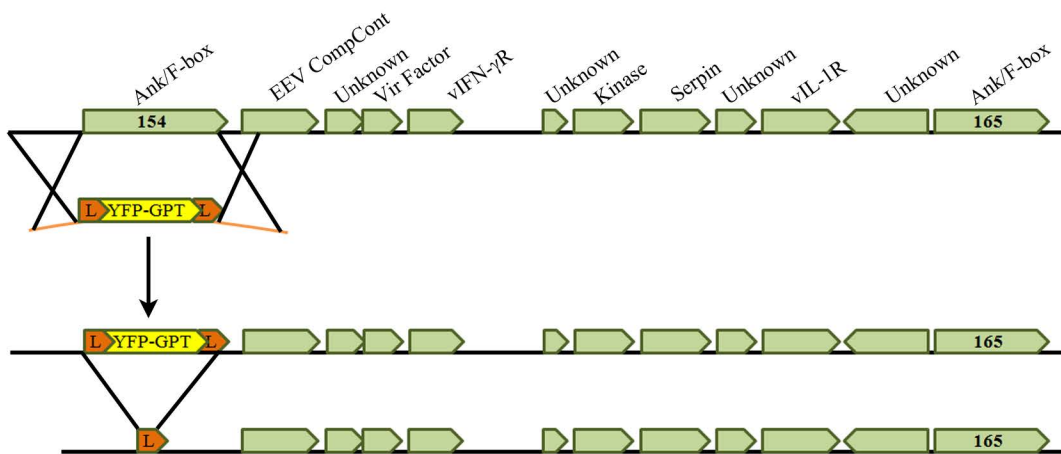
Encouraged by our results at the left-hand end of the genome, we attempted a more ambitious goal of deleting 17 ORFs from the right-hand end of the ECTV genome. It is important to note that EVM002 is located in the inverted terminal repeat (ITR) region of the ECTV genome, therefore containing two copies, EVM002 at the left-hand end of the genome, and EVM171, an identical gene at the right-hand end of the genome. Therefore, ECTV- Δ 002-005, lacking EVM002, EVM003, EVM004 and EVM005, also contains a loxP site in the EVM171 locus at the right-hand end of the genome (Appendix A.1A). To construct our large deletion ECTV, we infected BGMK cells with ECTV- Δ 002-005, and transfected in linearized pDGloxP-EVM154KO (Appendix A.1A). We then purified recombinant virus based on resistance to MPA and YFP fluorescence and confirmed the virus identity and purity by PCR (Appendix A.1A and A.2). ECTV- Δ 002-005/154-YFP-GPT contains the *yfp-gpt* cassette in the EVM154 locus as shown by a slightly smaller band on the agarose gel (Appendix A.2 lane iii). Similar to the construction of ECTV- Δ 002-005, we expected one of two possible results upon infection of U20S-Cre cells with ECTV- Δ 002-005/154-YFP-GPT. The first possibility was that only the *ypt-gpt* cassette was excised resulting in a single EVM154 deletion on the right-hand end of the genome (Appendix A.1B). The second would be the creation of an ECTV strain missing all 17 ORFs between EVM154 and EVM171 (Appendix A.1C). Our PCR data indicate that we actually obtained a mixed population of viruses following the three passages on ECTV- Δ 002-005/154-YFP-GPT on U20S-Cre cells. We

obtained PCR products corresponding to one loxP site within the EVM154 locus, representing a virus lacking only the *yfp-gpt* cassette from the EVM154 locus (Appendix A.1B and A.2 lane iii). We also obtained a PCR product of 350bp with a forward primer from the EVM154 locus and a reverse primer from the EVM171 locus, representing our large deletion virus (Appendix A.1C and 3 lane iv). At this point, we are attempting to separate these two white viruses from each other, with the goal of purifying both strains.

A - ECTV Δ 002-005



B - ECTV- Δ 002-005/154

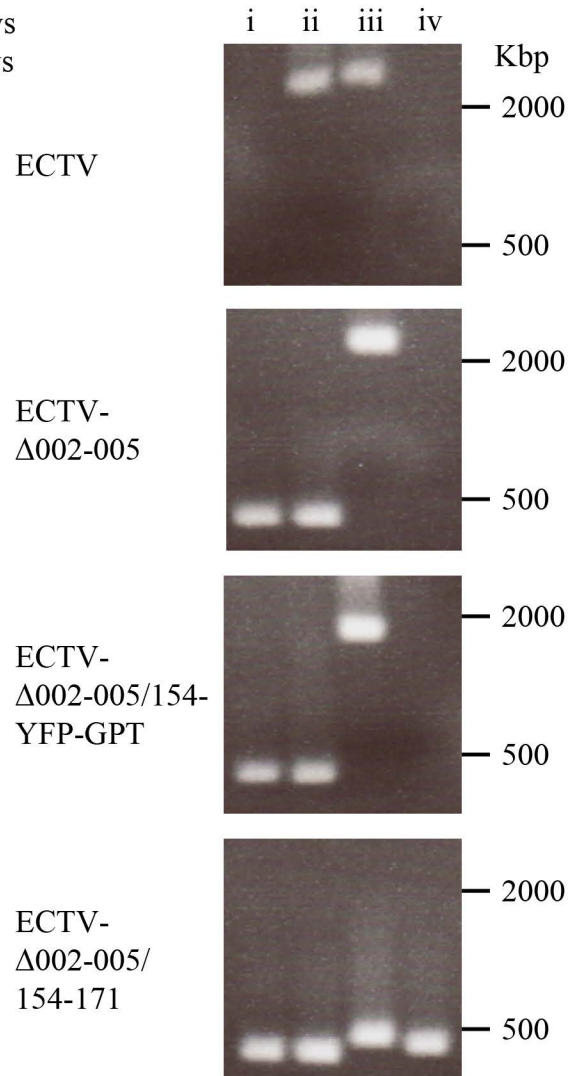


C - ECTV- Δ 002-005/154-171



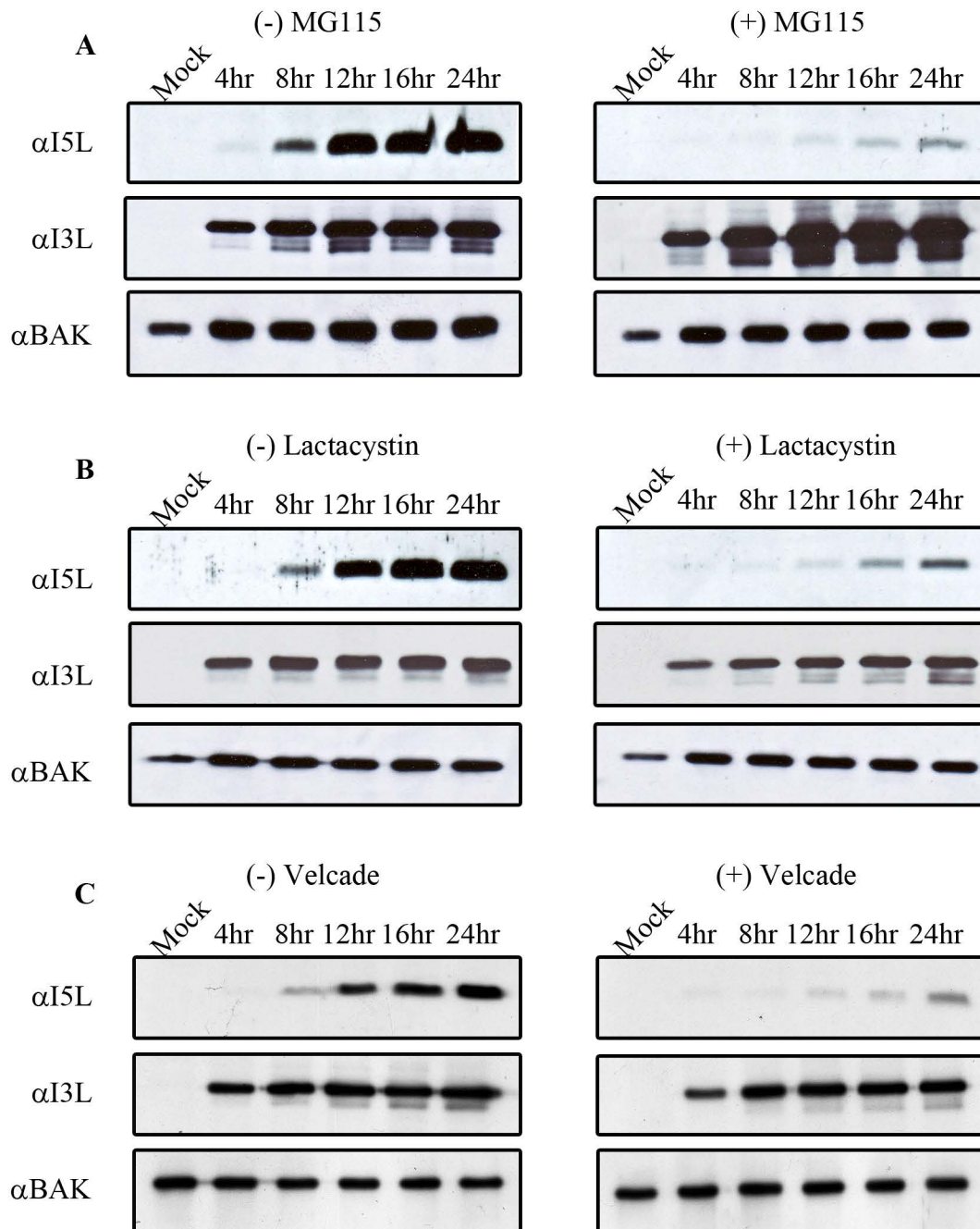
Appendix A.1. Schematic for construction of ECTV large deletion virus. **A.** ECTV- Δ 002-005 was used as a parental strain for creation of an ECTV large deletion virus. ECTV- Δ 002-005 lacks four genes at the left-hand end of the genome and EVM171 at the right-hand end. **B.** The *yfp-gpt* cassette was inserted into the EVM154 locus by transfecting linearized pDGloxP-EVM154KO. YFP-GPT positive virus was purified followed by infection of U2OS-Cre cells. Cre recombination of ECTV- Δ 002-005/154-YFP-GPT resulted in a mixed population of two viruses. The first virus had only the *yfp-gpt* cassette excised from the EVM154 locus and was named ECTV- Δ 002-005/154. **C.** The second virus had all intergenic material from EVM154 to EVM171 deleted and was named ECTV- Δ 002-005/154-171.

- i - EVM002 Fwd - EVM005 Rvs
- ii - EVM171 Fwd - EVM171 Rvs
- iii - EVM154 Fwd - EVM154 Rvs
- iv - EVM154 Fwd - EVM171 Rvs



Appendix A.2. PCR analysis of ECTV large deletion viral genomes. BGMK cells were infected with ECTV, ECTV- Δ 002-005, ECTV- Δ 002-005/154-YFP-GPT, or ECTV- Δ 002-005/154-171 for 48 hours. Viral genomes were subjected to PCR analysis for the presence of large genomic deletions spanning EVM002 to EVM005 at the left-hand end of the genome (i), of the EVM154 (ii) and EVM002/171 (iii) loci, as well as for the presence of a large deletion from EVM154 to EVM171 at the right-hand end of the genome (iv). PCR products near 500bp in length represent excision of the *yfp-gpt* cassette and/or intergenic DNA from the amplified locus. PCR products near 1700bp represent insertion of the *yfp-gpt* cassette into the amplified locus. PCR products larger than 2000bp represent full length EVM154 or EVM002/171. The presence of Cre products running at ~500bp in lanes ii, iii, and iv for ECTV- Δ 002-005/154-171 suggests an impure population following infection of U20S-Cre cells with ECTV- Δ 002-005/154-YFP-GPT.

Appendix B: Supplementary Data



Appendix B.1. Multiple proteasome inhibitors block late protein expression in vaccinia virus. HeLa cells were infected with VVCop at an MOI of 5 in the presence of 10 μ M MG115 (A), 10 μ M lactacystin (B), or 1 μ M Velcade (C). HeLa cells were pretreated with the indicated proteasome inhibitor for 1 hour pre-infection. The proteasome inhibitors were removed during infection, and added back at 1 hour post-infection. At the indicated times post-infection, protein samples were collected. Samples were separated by SDS-PAGE and subjected to western blot analysis with anti-I5L (a late protein), anti-I3L (an early protein), and anti-Bak (a loading control).